OSTEOLOGY, RELATIONSHIPS AND PALEOECOLOGY OF A NEW ARCTIC HADROSAURID (DINOSAURIA: ORNITHOPODA) FROM THE PRINCE CREEK FORMATION OF NORTHERN ALASKA

By

Hirotsugu Mori

RECOMMENDED:

Dr. Sarah Fowell

Dr. Matthew Wooller

Dr. Kris Hundertmark

Dr. Patrick Druckenmiller, Advisory Committee Chair

Dr. Sarah Fowell
Chair, Department of Geology and Geophysics

APPROVED:

Dr. Paul Layer
Dean, College of Natural Science and Mathematics

Dr. John Eichelberger
Dean of the Graduate School

4/24/14

Date

OSTEOLOGY, RELATIONSHIPS AND PALEOECOLOGY OF A NEW ARCTIC HADROSAURID (DINOSAURIA: ORNITHOPODA) FROM THE PRINCE CREEK FORMATION OF NORTHERN ALASKA

A

DISSERTATION

Presented to the Faculty

of the University of Alaska Fairbanks

in Partial Fulfillment of the Requirements

for the Degree of

DOCTOR OF PHILOSOPHY

By

Hirotsugu Mori, B.S., M.S.

Fairbanks, Alaska

May 2014

Abstract

The Liscomb Bonebed (LBB), found in the early Maastrichtian Prince Creek Formation of northern Alaska, is the single most productive site for the Arctic dinosaurs in either hemisphere. From the LBB, thousands of bones representing at least hundreds of individuals of a saurolophine hadrosaur have been collected, but they have not been previously described and their taxonomic status remains unresolved. In part, this stems from the fact that most material comes from individuals approximately one-half to one-fourth of adult size. Another long-standing question concerns whether dinosaurs in the Prince Creek Formation overwintered in the paleo-Arctic or migrated elsewhere (presumably south) to escape prolonged darkness and cold. Here, I attempt to determine the taxonomic status of the LBB hadrosaurs using three semi-independent methods: 1) geometric morphometric analysis; 2) comparative morphological analysis; and 3) cladistic analysis. An important component of this work also includes an ontogenetic study of the growth patterns of the genus *Edmontosaurus*, to which this material has been previously referred, in order to better understand ontogenetic variation within the Alaskan taxon. My results indicate the Alaskan taxon is a new species of the widespread genus *Edmontosaurus*. For the first time, the Alaskan taxon is described in detail, making it the best known polar dinosaur to date. My cladistic analysis suggests a possible biogeographic scenario in which the common ancestor of *Edmontosaurus* and *Shantungosaurus* originated in eastern Eurasia and then dispersed by the Campanian to North America via a land corridor in the area of present day Alaska. Finally, I used a novel method involving strontium isotope geochemistry to test the migration hypothesis of the new species of Alaskan *Edmontosaurus*. I measured strontium in tooth enamel of *Edmontosaurus* and a putative non-migratory species (*Troodon*) using LA-MC-ICP-MS. My results suggest diagenesis had not significantly altered the signal and that Alaskan *Edmontosaurus* likely did not migrate during approximately the last four months of life. My results lend further support for the existence of a distinct, early Maastrichtian polar dinosaur fauna known as the Paaŋaqtat Province.

Table of Contents

Page

Signature Page i

Title Page iii

Abstract v

Table of Contents vii

List of Figures xiii

List of Tables xix

Acknowledgements xxi

Introduction 1

References 4

Chapter 1 Ontogeny of *Edmontosaurus* and its implications for the taxonomic status of *Edmontosaurus* from the Prince Creek Formation (lower Maastrichtian) northern Alaska 9

1.1 Abstract 9

1.2 Introduction 10

1.2.1 Geological setting 11

1.2.2 Taxonomy of *Edmontosaurus* 12

1.2.3 Institutional abbreviations 13

1.3 Material and methods 14

1.3.1 Materials 14

1.3.2 Geometric morphometric analysis 16

1.3.3 Comparative morphological analysis 17

1.3.4 Cladistic analysis 20

1.4 Results 21

1.4.1 Geometric morphometric analysis 21

1.4.2 Comparative morphological analysis 22

Pages

1.4.2.1 Skull 23
1.4.2.2 Premaxilla 23
1.4.2.3 Nasal 24
1.4.2.4 Prefrontal 25
1.4.2.5 Frontal 25
1.4.2.6 Lacrimal 26
1.4.2.7 Jugal 26
1.4.2.8 Quadratojugal 27
1.4.2.9 Postorbital 27
1.4.2.10 Squamosal 28
1.4.2.11 Quadrate 28
1.4.2.12 Maxilla 29
1.4.2.13 Basisphenoid 29
1.4.2.14 Parietal 29
1.4.2.15 Basioccipital 30
1.4.2.16 Exoccipital-Opisthotic 30
1.4.2.17 Pterygoid 31
1.4.2.18 Predentary 31
1.4.2.19 Dentary 32
1.4.2.20 Surangular 33
1.4.2.21 Teeth 33
1.4.2.22 Splenial 34
1.4.2.23 Scapula 34
1.4.2.24 Humerus 35
1.4.2.25 Ulna 35
1.4.2.26 Pubis 36
1.4.2.27 Calcaneum 36
1.4.2.28 Metatarsal III 37
1.4.2.29 Metatarsal IV 37

Page

1.4.3 Cladistic analysis 37
1.5 Discussion 41
1.5.1 Growth patterns of *Edmontosaurus* 41
1.5.2 Taxonomic status of the PCF material 41
1.5.3 Systematic Paleontology 44
1.5.3.1 Revised diagnosis 45
1.5.3.2 Holotype 45
1.5.3.3 Paratype 45
1.5.3.4 Referred specimens 46
1.5.3.5 Type locality 46
1.5.3.6 Type horizon 46
1.5.3.7 Differential diagnosis 46
1.6 Acknowledgements 46
1.7 Figures 47
1.8 Tables 82
1.9 References 88
1.10 Appendix 99

Chapter 2 Osteology of the Arctic hadrosaurid *Edmontosaurus* sp. nov. (Dinosauria: Ornithopoda) from the Prince Creek Formation of northern Alaska 185
2.1 Abstract 185
2.2 Introduction 185
2.2.1 Institutional abbreviations 187
2.2.2 Geological setting 187
2.2.3 Material and methods 188
2.2.4 Systematic paleontology 189
2.3 Description 190
2.3.1 Skull 190
2.3.1.1 Premaxilla 190

Page
2.3.1.2 Nasal 191
2.3.1.3 Prefrontal 192
2.3.1.4 Frontal 193
2.3.1.5 Lacrimal 194
2.3.1.6 Jugal 195
2.3.1.7 Quadratojugal 196
2.3.1.8 Quadrate 197
2.3.1.9 Postorbital 198
2.3.1.10 Squamosal 199
2.3.1.11 Parietal 200
2.3.1.12 Supraoccipital 201
2.3.1.13 Maxilla 203
2.3.1.14 Maxillary teeth 205
2.3.2 Braincase 206
2.3.2.1 Laterosphenoid 206
2.3.2.2 Prootic 206
2.3.2.3 Basisphenoid 207
2.3.2.4 Basioccipital 209
2.3.2.5 Exoccipital-opisthotic 210
2.3.3 Palate 211
2.3.3.1 Ectopterygoid 211
2.3.3.2 Palatine 212
2.3.3.3 Pterygoid 212
2.3.4 Mandible 213
2.3.4.1 Predentary 213
2.3.4.2 Dentary 214
2.3.4.3 Dentary tooth 215
2.3.4.4 Surangular 216
2.3.4.5 Angular 217

Page
2.3.4.6 Splenial 217
2.3.5 Axial postcranium....218
2.3.5.1 Cervical vertebrae 218
2.3.5.2 Dorsal vertebrae....219
2.3.5.3 Dorsal ribs....220
2.3.5.4 Sacrum 221
2.3.5.5 Caudal vertebrae 222
2.3.6 Appendicular skeleton 222
2.3.6.1 Sternal 222
2.3.6.2 Scapula....223
2.3.6.3 Coracoid....224
2.3.6.4 Humerus....224
2.3.6.5 Ulna 225
2.3.6.6 Radius 226
2.3.6.7 Metacarpals....227
2.3.6.8 Ilium....228
2.3.6.9 Pubis 229
2.3.6.10 Ischium 230
2.3.6.11 Femur....231
2.3.6.12 Tibia....232
2.3.6.13 Fibula 232
2.3.6.14 Astragalus 233
2.3.6.15 Calcaneum 233
2.3.6.16 Metatarsals....234
2.4 Discussion....235
2.4.1 Biogeography of *Edmontosaurus* 235
2.4.2 Paaŋaqtat Province 237
2.5 Acknowledgements....238
2.6 Figures 239

Page
2.7 Tables....287
2.8 References....289
Chapter 3 Testing the migratory hypothesis for Alaskan *Edmontosaurus* using strontium isotope analysis of their teeth....297
3.1 Abstract....297
3.2 Introduction....298
3.2.1 Background....298
3.2.2 Isotope analysis....301
3.3 Material and methods....303
3.3.1 Tooth age....303
3.3.2 Materials....305
3.3.3 LA-MC-ICP-MS....305
3.4 Results....306
3.4.1 Tooth age....306
3.4.2 LA-MC-ICP-MS measurements....307
3.5 Discussion....307
3.5.1 Migration hypothesis....307
3.5.2 Diagenesis....310
3.6 Conclusion....312
3.7 Acknowledgements....312
3.8 Figures....313
3.9 Table....319
3.10 References....319
Conclusion....329

List of Figures

Page

Figure 1-1 (A) Location of the Liscomb Bonebed and (B) paleogeographic reconstruction map of North America at 70 Ma 47

Figure 1-2 Composite cranial reconstruction in left lateral viw of the Prince Creek Formation taxon 48

Figure 1-3. Histogram of hadrosaur bones from the Liscomb Bonebed 49

Figure 1-4. Location of landmarks and semi-landmarks 50

Figure 1-5. Principal component biplot of geometric morphometric analysis 51

Figure 1-6. Transformation grids 52

Figure 1-7. Biplot of skull length versus skull height 53

Figure 1-8. Comparison of premaxillae in dorsal view 54

Figure 1-9. Comparison of premaxillae in lateral view 55

Figure 1-10. Biplots of (A) the premaxilla versus dentary length, and (B) premaxilla versus premaxillary reflected margin length 56

Figure 1-11. Biplots of (A) nasal curvature height versus dentary length, and (B) nasal curvature versus dentary length 57

Figure 1-12. Comparison of prefrontals 58

Figure 1-13. Comparisons of frontals 59

Figure 1-14. Comparison of lacrimals 60

Figure 1-15. Biplots of (A) the jugal length versus caudal constriction, and (B) the jugal caudal constriction versus rostral constriction. 61

Figure 1-16. Biplot of the lateral exposure width of the quadratojugal versus dentary length 62

Figure 1-17. Biplot of the width of the jugal process versus dentary length 63

Page

Figure 1-18. Comparison of postorbitals 64

Figure 1-19. Comparison of squamosals 65

Figure 1-20. Biplot of the quadrate height versus its curvature 66

Figure 1-21. Comparison of lacrimal processes of the maxilla 67

Figure 1-22. Comparison of parietals 68

Figure 1-23. Comparison of basioccipitals 69

Figure 1-24. Comparison of exoccipital-opisthotics 70

Figure 1-25. Comparison of pterygoids 71

Figure 1-26. Biplots of (A) dentary deflection (in radians) versus dentary length and (B) posterior edentulous process length versus dental battery length 72

Figure 1-27. Biplot of dental deflection length versus dental battery length 73

Figure 1-28. Biplot of the dentary tooth height versus width 74

Figure 1-29. Comparison of splenials 75

Figure 1-30. Biplots of (A) coronoid process length versus scapular blade length and (B) scapular maximum width versus scapular blade width 76

Figure 1-31. Biplot of humerus versus deltopectoral process lengths 77

Figure 1-32. Biplots of (A) constriction of the ulnar diaphysis versus olecranon process thickness and (B) ulna length versus diaphysis width 78

Figure 1-33. Biplots of (A) pubic neck height versus femur length and (B) pubic neck length versus femur length 79

Figure 1-34. Biplot of the length versus width of metatarsal III 80

Figure 1-35. Result of the cladistic analyses, showing the phylogenetic position of the Prince Creek Formation taxon. 81

Page

Figure 2-1 (A) Location of the Liscomb Bonebed and (B) paleogeographic reconstruction map of North America at 70 Ma 239

Figure 2-2 Composite cranial reconstruction of *Edmontosaurus* sp. nov. in left lateral view 240

Figure 2-3 Premaxilla 241

Figure 2-4 Nasal 242

Figure 2-5 Prefrontal 243

Figure 2-6 Frontal 244

Figure 2-7 Lacrimal 245

Figure 2-8 Jugal 246

Figure 2-9 Quadratojugal 247

Figure 2-10 Quadrate 248

Figure 2-11 Postorbital 249

Figure 2-12 Squamosal 250

Figure 2-13 Parietal 251

Figure 2-14 Supraoccipital 252

Figure 2-15 Maxilla 253

Figure 2-16 Laterosphenoid 254

Figure 2-17 Prootic 255

Figure 2-18 Basisphenoid 256

Figure 2-19 Basioccipital 257

Page
Figure 2-20 Exoccipital-ophisthotic 258
Figure 2-21 Ectopterygoid 259
Figure 2-22 Palatine 260
Figure 2-23 Pterygoid 261
Figure 2-24 Predentary 262
Figure 2-25 Dentary 263
Figure 2-26 Surangular 264
Figure 2-27 Angular and splenial 265
Figure 2-28 Cervical vertebral neural arch 266
Figure 2-29 Dorsal vertebra 267
Figure 2-30 Dorsal ribs 268
Figure 2-31 Sacrum 269
Figure 2-32 Caudal vertebra 270
Figure 2-33 Sternal 271
Figure 2-34 Scapula 272
Figure 2-35 Coracoid 273
Figure 2-36 Humerus 274
Figure 2-37 Ulna and radius 275
Figure 2-38 Metacarpals 276

Page

Figure 2-39 Ilium 277

Figure 2-40 Pubis 278

Figure 2-41 Ischium 279

Figure 2-42 Femur 280

Figure 2-43 Tibia 281

Figure 2-44 Fibular 282

Figure 2-45 Astragalus 283

Figure 2-46 Calcaneum 284

Figure 2-47 Metatarsals 285

Figure 2-48 Paleobiogeography of Edmontosaurini 286

Figure 3-1 Location of the Liscomb Bonebed and paleogeographic reconstruction map of North America 312

Figure 3-2 Specimens samples in this study 313

Figure 3-3 Temporal resolution and tooth replacement rates of *Edmontosaurus* teeth 314

Figure 3-4 Box plots of $^{87}Sr/^{86}Sr$ values 315

Figure 3-5 Biplot of $_{Enamel}\ ^{87}Sr/^{86}Sr$ and $\Delta Enamel - Dentine\ ^{87}Sr/^{86}Sr$ 316

Figure 3-6 Change in $_{enamel}\ ^{87}Sr/^{86}Sr$ values for *Edmontosaurus* over time 317

List of Tables

Page
Table 1-1 Number of specimens examined in the study 82

Table 1-2 *Edmontosaurus* specimens observed for this study 83

Table 1-3 Summary of growth patterns of *Edmontosaurus* 84

Table 1-4 Morphology of the three *Edmontosaurus* taxa 88

Table 2-1 Number of specimens examined in the study 286

Table 2-2 Comparison of the length of the femur, humerus, and fibula 287

Table 3-1 Results of the $^{87}Sr/^{86}Sr$ measurements 319

Acknowledgements

This thesis was supported in part by NSF awards EAR 1226730 (co-PI's P. Druckenmiller and G. Erickson) and DBI-1057426 (PI P. Druckenmiller), a Geist Fund scholarship, and the UAF Graduate School. I kindly acknowledge the help of the Bureau of Land Management Arctic Field Office for logistical support in the excavation of the Alaskan material. I appreciate my graduate committee members, Sarah Fowell, Kris Hundertmark, Matthew Wooller, and Patrick S. Druckenmiller for their support, and David Evans and Nicolás Campione for providing me with photos of *Edmontosaurus*. I am grateful to Ron Blakey, Kieran Shepherd, Margaret Beckel, Kevin Seymour, Jack Horner, Alana Gihlick, Carl Mehling, Don Brinkman, and Hiroaki Kikkawa. I also thank H. David Sheet, Daniel Falster, Davit Warton, Ian Wright, and Pablo A. Goloboff, James S. Farris, Kevin Nixon, and Willi Henning Society for their software (Coordgen, MorphoJ, SMATR, TNT). I also appreciate Dr. Gregory Erickson for determining replacement ages of *Edmontosaurus* teeth from the PCF and Dr. Petrus le Roux for conducting the strontium isotope analysis.

Introduction

Compared to today, northern Alaska hosted a rich terrestrial vertebrate fauna during the Late Cretaceous, including a diverse array of dinosaurs [1-15], despite being located in high Arctic latitudes, at an estimated 67-85° N [16]. Most of the body fossil evidence for Alaskan dinosaurs is derived from a relatively small number of sites in the Prince Creek Formation (PCF). The PCF represents interbedded fluvial and marginal marine sediment deposited on a low gradient Arctic coastal plain that existed on the north side of the then-forming Brooks Range [17,18]. Although the age of the entire PCF ranges from the Upper Cretaceous to Eocene [19-22], the age of the dinosaur-bearing portion of the section is early Maastrichtian based on both biostratigraphic and radiometric methods [23,24]. The paleobotanical records of the PCF show that northern Alaska was much warmer than today, with a mean annual temperature of 5-6 °C during the Maastrichtian. However, during the coldest month, the temperature could have dropped to sub-freezing temperatures [25-27].

From the Prince Creek Formation, fossils of several major dinosaurian clades are known, including herbivorous species of Hadrosauridae, Ceratopsidae, Pachycephalosauridae, and basal ornithopods, as well as small to large-bodied theropod (carnivorous) taxa such as Troodontidae, Dromaeosauridae and Tyrannosauridae [3,4,15]. To date, two species, *Alaskacehpale gangloffi* [7,8] and *Pachyrhinosaurus perotorum* [13] are known from the PCF, which may be endemic taxa. Currently no single taxon of dinosaur identified in the PCF is known from any other site in North America, giving rise to the hypothesis that the early Maastrichtian dinosaurian fauna of the PCF represents a distinctive polar assemblage named the “Paaŋaqtat Province“ [12,15], although this idea is controversial [13].

An important component of the Prince Creek Formation is the Liscomb Bonebed (LBB), which is the most productive site for polar dinosaurs in either hemisphere [4]. From the LBB, isolated bones of at least hundreds of individuals of hadrosaurs have been

collected. No other polar dinosaur species is as completely known from skeletal remains as this hadrosaur, which has previously been referred to the widespread, Late Cretaceous taxon *Edmontosaurus*. For this reason, understanding the relationships and ecology of this keystone species is important in understanding broader issues regarding the Paaŋaqtat Province fauna and ecosystems in the Late Cretaceous paleo-Arctic.

There are several questions regarding these hadrosaur materials. First, the taxonomic status of this hadrosaur is unclear, and the specimens, although abundantly represented, have not been previously described. This is due in large part because most of the remains come from individuals approximately one-half to one-fourth of adult size (based on full grown specimens of *Edmontosaurus* from Alberta and Montana). Typically, juvenile remains are perceived as being less informative than adult material, which is particularly true in taxonomic studies where most diagnostic features are present only in ontogenetically mature individuals. Conversely, juvenile material is critical for understanding morphological development within a given taxon and has the potential to be taxonomically informative if the nature and degree of ontogenetic variation is understood. In most studies of juvenile dinosaur material, the juvenile specimens of a known taxon are described in the context of assessing ontogenetic change for that genus or species [29-34]. In a few cases new taxa are erected based on an assessment of ontogenetically invariable characters observed in juvenile materials [34,35].

Another problem of long-standing interest concerns how dinosaurs coped with this apparently challenging winter environment [12,36-40]. Hotton [41] put forth a migration hypothesis proposing that northern dinosaurs could have migrated to the south and more hospitable and resource-rich environments during the winter. A few studies have attempted to address the migration hypothesis for the PCF hadrosaurs. Fiorillo and Gangloff [38] argued that the PCF juvenile hadrosaurs are too small compared to adult size and thus could not have migrated like modern caribou (*Rangifer tarandus*). A histological study of the PCF hadrosaurs revealed that they experienced periodic stress [40], possibly due to over-wintering in the Arctic. Oxygen isotopic studies by Suarez et

al. [42] found that the $\delta^{18}O$ preserved in the PCF dinosaur's tooth enamel are within the possible $\delta^{18}O$ range of meteoric water in the region. All of these studies suggest the PCF dinosaurs were not migratory.

The goal of this dissertation is to address several long-standing questions regarding the PCF hadrosaur material. I have organized this dissertation into three chapters. In the first chapter, I attempt to determine the taxonomic status of the PCF hadrosaurs, using three semi-independent methods: 1) geometric morphometric analysis; 2) comparative morphological analysis; and 3) cladistics analysis. An important component of this work also includes an ontogenetic study of the growth patterns of the genus *Edmontosaurus* in order to better understand which juvenile characters of the Alaskan taxon are potentially ontogenetically variable. To compare the PCF specimens with other *Edmontosaurus* specimens, which are larger than the PCF specimens, I employed a new method using hypothetical growth trend lines.

The second chapter provides a detailed description of the PCF hadrosaur taxon. The description is based on multiple, well-preserved specimens for nearly every element, making it one of the best-understood hadrosaurid taxa known in North America. The Alaskan taxon is also compared in detail to *Edmontosaurus* from lower latitudes and other related taxa based primarily on personal observations of original material. In this chapter I also discuss the biogeographical and faunal implications of PCF hadrosaurs.

In the last chapter, I use strontium isotope geochemistry of tooth enamel from the PCF taxon and a probable non-migratory species (*Troodon*) as a wholly independent method to test the migration hypothesis for PCF hadrosaurs. Collectively, these studies provide important new insight into the faunal composition and paleoecology of an ancient polar ecosystem.

References

1. Brouwers EM, Clemens, WA, Spicer, RA, Ager, T. A., Carter LD, et al. (1987) Dinosaurs on the North Slope, Alaska: High latitude, latest Cretaceous environments. Science 237: 1608-1610.
2. Davies KL (1987) Duck-bill dinosaurs (Hadrosauridae, Ornithischia) from the North Slope of Alaska. Journal of Paleontology 61: 198-200.
3. Nelms LG (1989) Late Cretaceous dinosaurs from the North Slope of Alaska. Journal of Vertebrate Paleontology, Abstracts of Papers 9: 34A.
4. Gangloff RA (1998) Arctic dinosaurs with emphasis on the Cretaceous record of Alaska and the Eurasian-North American connection. New Mexico Museum of Natural History and Science Bulletin 14: 211-220.
5. Fiorillo AR, Gangloff RA (2000) Theropod teeth from the Prince Creek Formation (Cretaceous) of Northern Alaska, with speculations on Arctic dinosaur paleoecology. Journal of Vertebrate Paleontology 20: 675-682.
6. Fiorillo AR (2004) The dinosaur of arctic Alaska. Scientific American 291: 84-91.
7. Gangloff RA, Fiorillo AR, Norton DW (2005) The first pachycephalosaurine (Dinosauria) from the paleo-Arctic of Alaska and its paleogeographic implications. Journal of Paleontology 79: 997-1001.
8. Sullivan RM (2006) A taxonomic review of the Pachycephalosauridae (Dinosauria: Ornithischia). New Mexico Museum of Natural History and Science Bulletin 35: 347-365.
9. Fiorillo AR (2008) On the occurrence of exceptionally large teeth of *Troodon* (Dinosauria: Saurischia) from the Late Cretaceous of northern Alaska. Palaios 23: 322-328.
10. Fiorillo AR, Tykoski RS, Currie PJ, McCarthy PJ, Flaig P (2009) Description of two partial *Troodon* braincases from the Prince Creek Formation (Upper Cretaceous), North Slope Alaska. Journal of Vertebrate Paleontology 29: 178-187.

11. Brown CM, Druckenmiller P (2011) Basal ornithopod (Dinosauria: Ornithischia) teeth from the Prince Creek Formation (early Maastrichtian) of Alaska. Canadian Journal of Earth Sciences 48: 1342-1354.
12. Erickson GM, Druckenmiller PS (2011) Longevity and growth rate estimates for a polar dinosaur: a *Pachyrhinosaurus* (Dinosauria: Neoceratopsia) specimen from the North Slope of Alaska showing a complete developmental record. Historical Biology 23: 327-334.
13. Fiorillo AR, Tykoski RS (2012) A new Maastrichtian species of the centrosaurine ceratopsid *Pachyrhinosaurus* from the North Slope of Alaska. Acta Palaeontologica Polonica 57: 561-573.
14. Mannion PD, Benson RBJ, Upchurch P, Butler RJ, Carrano MT et al. (2012) A temperate palaeodiversity peak in Mesozoic dinosaurs and evidence for Late Cretaceous geographical partitioning. Global Ecology and Biogeography 21: 898-908.
15. Druckenmiller P, Erickson G, Brinkman D, Brown C, Mori H (2013) Evidence for a distinct, early Maastrichtian polar dinosaur fauna from the Prince Creek Formation of northern Alaska. Journal of Vertebrate Paleontology, Program and Abstracts 2013: 117.
16. Witte, W.K., Stone, D. B., Mull CG (1987) Paleomagnetism, paleobotany, and paleogeography of the Cretaceous, North Slope, Alaska. In: Tailleur, I.L., Weimer P, editors. Alaska North Slope Geology. Bakersfield, CA: Pacific Section, Society of Economic Paleontologists and Mineralogists. pp. 571-579.
17. Mull CG, Houseknecht DW, Bird KJ (2003) Revised Cretaceous and Tertiary stratigraphic nomenclature in the Colville Basin, northern Alaska. US Gelogical Survey Professional Paper 1673: 1-51.

18. Flaig PP, McCarthy PJ, Fiorillo AR (2011) A tidally influenced, high-latitude coastal-plain: The upper Cretaceous (Maastrichtian) Prince Creek Formation, North Slope, Alaska. In: Davidson SK, Leleu S, North. CP, editors. From river to rock record: The Preservation of fluvial sediments and their subsequent interpretation. pp. 233-264.
19. Frederiksen NO, Ager TA, Edwards LE (1988) Palynology of Maastrichtian and Paleocene rocks, lower Colville River region, North Slope of Alaska. Canadian Journal of Earth Sciences 25: 512-527.
20. Frederiksen NO (1991) Pollen zonation and correlation of Maastrichtian marine beds and associated strata, Ocean Point dinosaur locality, North Slope, Alaska. United States Geological Survey Bulletin 1990-E: E1-E24.
21. Brouwers EM, Deckker PD (1993) Late Maastrichtian and Danian ostracode faunas from Northern Alaska; reconstructions of environment and paleogeography. Palaios 8: 140-154.
22. Frederiksen NO, Mclntyre DJ, Sheehan TP (2002) Palynological dating of some Upper Cretaceous to Eocene outcrop and well samples from the region extending from the easternmost part of NPRA in Alaska to the western part of Arctic National Wildlife Refuge, North Slope of Alaska. US Geological Survey Open-File Report 02-405: 1-37.
23. McKee E, Conrad JE, Tuin BD (1989) Better dates for arctic dinosaurs. Eos 70: 74.
24. Conrad JE, Mackee EH, Turrin BD (1992) Age of tephra beds at the Ocean Point Dinosaur Locality, North Slope, Alaska, based on K-Ar and 40Ar/39Ar analyses. Washington DC: United States Government Printing Office. 12 p.
25. Spicer RA, Parrish JT (1990) Late Cretaceous-early Tertiary palaeoclimates of northern high latitudes: a quantitative view. Journal of the Geological Society, London Journal of the Geological Society 147: 329-341.

26. Fiorillo AR, McCarthy PJ, Brandlen E, Flaig PP, Norton D et al. (2007) Paleontology, sedimentology, paleopedology, and palynology of the Kikak-Tegoseak Quarry (Prince Creek Formation, Late Cretaceous), Northern Alaska. In: Braman DR, editor. Ceratopsian Symposium: Short papers, abstracts and programs. Drumheller, AB: pp. 48-49.
27. Spicer RA, Herman AB (2010) The Late Cretaceous environment of the Arctic: A quantitative reassessment based on plant fossils. Palaeogeography, Palaeoclimatology, Palaeoecology 295: 423-442.
28. Horner JR, Currie PJ (1994) Embryonic and neonatal morphology and ontogeny of a new species of *Hypacrosaurus* (Ornithischia, Lambeosauridae) from Montana and Alberta. In: Carpenter KH, Karl F., Horner JR, editors. Dinosaur eggs and babies. Cambridge, UK: Cambridge University Press. pp. 312-336.
29. Currie PJ (2003) Allometric growth in tyrannosaurids (Dinosauria: Theropoda) from the Upper Cretaceous of North America and Asia. Canadian Journal of Earth Science 40: 651-665.
30. Goodwin MB, Clemens WA, Horner JR, Padian K (2006) The smallest known *Triceratops* skull: new observations on ceratopsid cranial anatomy and ontogeny. Journal of Vertebrate Paleontology 26: 103-112.
31. Evans DC, Reisz RR (2007) Anatomy and relationships of *Lambeosaurus magnicristatus*, a crested hadrosaurid dinosaur (Ornithischia) from the Dinosaur Park Formation, Alberta. Journal of Vertebrate Paleontology 27: 373-393.
32. Whitlock JA, Wilson JA, Lamanna MC (2010) Description of a nearly complete juvenile skull of *Diplodocus* (Sauropoda: Diplodocoidea) from the Late Jurassic of North America. Journal of Vertebrate Paleontology 30: 442-457.
33. Tsuihiji T, Watabe M, Tsogtbaatar K, Tsubamoto T, Barsbold R et al. (2011) Cranial osteology of a juvenile specimen of *Tarbosaurus bataar* (Theropoda, Tyrannosauridae) from the Nemegt Formation (Upper Cretaceous) of Bugin Tsav, Mongolia. Journal of Vertebrate Paleontology 31: 497-517.

34. Bell PR, Brink KS (2013) *Kazaklambia convincens* comb. nov., a primitive juvenile lambeosaurine from the Santonian of Kazakhstan. Cretaceous Research 45: 265-274.
35. Choiniere JN, Clark JM, Forster CA, Norell MA, Eberth DA et al. (2013) A juvenile specimen of a new coelurosaur (Dinosauria: Theropoda) from the Middle-Late Jurassic Shishugou Formation of Xinjiang, People's Republic of China. Journal of Systematic Palaeontology 12: 177-215.
36. Clemens WA, Nelms LG (1993) Paleoecological implications of Alaskan terrestrial vertebrate fauna in latest Cretaceous time at high paleolatitudes. Geology 21: 503-506.
37. Chinsamy A, Rich T, Vickers-Rich P (1998) Polar Dinosaur Bone Histology. Journal of Vertebrate Paleontology 18: 385-390.
38. Fiorillo AR, Gangloff RA (2001) The caribou migration model for Arctic hadrosaurs (Dinosauria: Ornithischia): A reassessment. Historical Biology 15: 323-334.
39. Bell PR, Snively E (2008) Polar dinosaurs on parade: a review of dinosaur migration. Alcheringa: An Australasian Journal of Palaeontology 32: 271-284.
40. Chinsamy A, Thomas DB, Tumarkin-Deratzian AR, Fiorillo AR (2012) Hadrosaurs were perennial polar residents. Evolutionary Biology 295: 610-614.
41. Hotton III, N. (1980) An alternative to dinosaur endothermy. In: Thomas RDK, Olson EC, editors. A cold look at the warm-blooded dinosaurs. Boulder, CO.: Westview Press. pp. 311-350.
42. Suarez CA, Ludvigson GA, Gonzalez LA, Fiorillo AR, Flaig PP et al. (2013) Use of multiple oxygen isotope proxies for elucidating Arctic Cretaceous palaeo-hydrology. Geological Society, London, Special Publications 382: 185-202.

Chapter 1

Ontogeny of *Edmontosaurus* and its implications for the taxonomic status of *Edmontosaurus* from the Prince Creek Formation (lower Maastrichtian) northern Alaska[1]

1.1 Abstract

The taxonomic classification of juvenile fossil vertebrate remains can be problematic, due to a strong ontogenetic bias in their morphology. This problem is exemplified by undescribed juvenile hadrosaur remains from the Liscomb Bonebed in the Prince Creek Formation of northern Alaska. Although the Liscomb Bonebed has produced thousands of individual bones of a saurolophine hadrosaurid similar to *Edmontosaurus*, the species-level identity of this taxon has been unclear because the vast majority of remains are from an immature growth stage. In this study, I address the taxonomic status of the Alaskan material by first characterizing the morphological changes that occur during ontogeny in *Edmontosaurus*. I then conducted three independent analyses to compare the Alaskan material with other species of *Edmontosaurus*: 1) a geometric morphometric analysis; 2) a comparative morphological analysis; and 3) a cladistic analysis. The geometric morphometric analysis used three-dimensionally preserved skulls of *Edmontosaurus* and a new composite reconstruction of the Alaskan material. After the removal of size effects, the Alaskan material clustered with *Edmontosaurus annectens* but outside of *Edmontosaurus regalis.* In the comparative morphological analysis, I found that the Alaskan material possesses unique characters that distinguish it from *Edmontosaurus annectens* and *Edmontosaurus regalis*, including a premaxillary circumnarial septum that projects posterolaterally and the absence of a postorbital pocket. Through the geometric morphometric analysis and bivariate plots performed in the comparative morphometric analysis, the general growth pattern of *Edmontosaurus* is characterized, most features of which relate to anteroposterior elongation of the skull. Finally, in the cladistic analysis the Alaskan material was

[1]Mori H, Druckenmiller PS, and Erickson GM. Prepared for submission to PLoS One.

recovered as the sister taxon to *Edmontosaurus annectens* + *Edmontosaurus regalis,* even when ontogenetically variable characters were accounted for. These results suggest that the Alaskan material is congeneric with *Edmontosaurus*, but it cannot be readily referred to either valid species of the genus and therefore represents a new taxon.

1.2 Introduction

Juvenile dinosaurian remains are not uncommon but are frequently perceived as being less informative than adult material, particularly in taxonomic studies where most diagnostic features are present in ontogenetically mature individuals. Evans et al. [1] warns that erecting a new taxon without comparing it to specimens of similar sizes can lead to erroneous conclusions, because dinosaurs experienced strong morphological change during ontogeny. Despite these drawbacks, juvenile material is critical for understanding morphological development within a given species and has the potential to be taxonomically informative if the nature and degree of ontogenetic variation is understood. In most studies of juvenile dinosaur material, the juvenile specimens of a known taxon are described in the context of assessing ontogenetic change for that genus or species [2-6]. In some cases, juvenile or sub-adult material is part of a taxonomic revision, which may result in taxa based on immature specimens being synonymized with other taxa [7-10]. In other cases but less frequently, new taxa are erected based on an assessment of ontogenetically invariable characters observed in juvenile materials [11,12].

An abundance of juvenile hadrosaurid remains are known from the early Maastrichtian Prince Creek Formation (PCF) of northern Alaska (Figure 1-1). The material is primarily derived from a single well-known horizon known as the Liscomb Bonebed (LBB), from which thousands of disarticulated cranial and postcranial remains have been excavated [10,13-24]. While it is generally accepted that the material can be assigned to the saurolophine hadrosaurid *Edmontosaurus* [16,18,19,23,25], a species-level assignment has not been previously established given that most of the remains come

from individuals approximately one-third adult size. Here, I attempt to determine the species-level classification of this taxon using three semi-independent methods: 1) geometric morphometric analysis; 2) comparative morphological analysis; and 3) cladistics analysis. An important component of this work also includes an ontogenetic study of the growth patterns of the genus *Edmontosaurus* in order to better understand which juvenile characters of the Alaskan taxon are potentially ontogenetically variable.

1.2.1 Geological setting

The PCF (formerly referred to as the Kogosukuruk Tongue of the PCF [26]) is characterized by nonmarine sandstone, conglomerate, coal and mudstone, and is interpreted to represent interbedded fluvial (meandering channels and floodplains) and marginal marine sediments deposited on a low gradient Arctic coastal plain [27,28]. The age of the entire PCF ranges from the Upper Cretaceous to Eocene based on palynological [29-31] and biostratigraphic data [32]. The numerical age of the dinosaur-bearing section of the formation, where it is exposed along the lower Colville River and including the LBB, is 71-68 Ma based on $^{40}Ar/^{39}Ar$ methods [33,34]. The age of LBB is further constrained by an $^{40}Ar/^{39}Ar$ age of 69.2 ± 0.5 Ma from a stratigraphically underlying tuff at Sling Point and by palynological analyses [35] which are consistent with an early Maastrichtian age for the LBB [22]. This age estimate is entirely consistent with the known stratigraphic range of *Edmontosaurus*, but interestingly it falls between the specific ranges for the two valid species of the genus, *E. regalis* (late Campanian) and *E. annectens* (late Maastrichtian).

Witte et al. [36] estimated the Albian-Cenomanian paleolatitude of northern Alaska at 67-82°N. Thus northern Alaska was well within the paleo-Arctic in the Late Cretaceous. However, paleobotanical evidence indicates a mean annual temperature for Maastrichtian northern Alaska of 5-6 °C, with a cold month mean warmer than 2.0 ± 3.9 °C [20,34,37]. From pedogenic and paleobotanical evidence, Flaig et al. [38] concluded that the Arctic coastal plain had polar woodlands with an angiosperm understory and

experienced intensified dry and wet seasons. In addition to hadrosaurid remains, the PCF preserves a modestly diverse assemblage of ornithischian and saurischian dinosaurs and mammals [14-17,21,24,39-42]. However, no ectothermic vertebrates have ever been recovered [16]. Therefore, it is interpreted that the temperature during the winter was too cold for most terrestrial ectothermic amniotes, including crocodilians, squamates and turtles.

Taphonomically, the LBB occurs in a trunk channel on a distributary channel splay complex and flood plain [22,23]. The bonebed is interpreted to represent a mass mortality event associated with overbank floods deposits [24]. The flood could have resulted from snowmelt from the ancient Brooks Range [23]. The dinosaur remains from the bonebed are overwhelmingly dominated by juvenile specimens of hadrosaurids referred to *Edmontosaurus* [24]. These remains are almost entirely disarticulated, but they show little evidence of weathering, predation, or trampling and are typically preserved in three dimensions without any permineralization [23, 24].

1.2.2 Taxonomy of *Edmontosaurus*

The genus *Edmontosaurus* has a complicated history. Lambe [43] first erected *Edmontosaurus* in his description of the type species *E. regalis* from the Horseshoe Canyon Formation [43]. However, some specimens now considered to be synonymous with *Edmontosaurus* had been named prior to 1917. In 1942, Lull and Wright [44] erected a new genus *Anatosaurus*, with which they synonymized *Trachodon longiceps* (Marsh 1890) [45]*, Diclonius mirabilis* (Cope 1883) [46], *Claosaurus annectens* (Marsh 1892) [47], *Thespesius edmontoni* (Gilmore 1924) [48], and *Thespesius saskatchewanensis* (Sternberg 1926) [49]. Later, Hopson [50] argued that *Anatosaurus edmontoni* is a junior synonym of *E. regalis.* Citing Estes and Berberian [51], Hopson also proposed that all specimens of *Anatosaurus* from the Late Maastrichtian belong to a single species, *Anatosaurus annectens.* Brett-Surman [52] interpreted *Anatosaurus* to be a junior synonym of *Edmontosaurus,* with the exception of *Anatosaurus copei*, which he

referred to a new genus, *Anatotitan.* Horner et al. [53] synonymized all species of *Anatosaurus* with *Edmontosaurus annectens*, except *Anatosaurus saskatchewanensis*, which they referred to *Edmontosaurus saskatchewanensis.* Subsequently, Prieto-Márquez [25] interpreted *E. saskatchewanensis* to be a junior synonym of *E. annectens.* Based on a morphometric analysis of many specimens previously referred to *Edmontosaurus,* Campione and Evans [10] recognized only two species, *E. regalis* and *E. annectens.* Their conclusion is consistent with the statements by Hopson [50] that *Anatosaurus edmontoni* is a junior synonym of *E. regalis* and all late Maastrichtian specimens belong to a single species, *E. annectens*. My study follows the taxonomy of Hopson [50] and Campione and Evans [10] in recognizing only two species of *Edmontosaurus*: *E. regalis* from the late Campanian of the Horseshoe Canyon and Wapiti [54] Formations, and *E. annectens*, from the late Maastrichtian of the Hell Creek, Frenchman, Laramie and Lance Formations.

1.2.3 Institutional abbreviations

AENM, Amur Natural History Museum, Blagoveschensk, Russia; AMNH, American Museum of Natural History, New York City, New York, USA; BHI, Black Hills Institute of Geological Research, Hill City, South Dakota, USA; BMNH, British Museum of Natural History, London, UK; CM, Carnegie Museum of Natural History, Pittsburgh, Pennsylvania, USA; CMN, Canadian Museum of Nature, Ottawa, Ontario, Canada (formerly National Museums of Canada, NMC); DMNH, Denver Museum of Nature and Science, Denver, Colorado, USA; FMNH, Florida Museum of Natural History, Gainesville, Florida, USA; GMV, National Geological Museum of China, Beijing, China; MACN, Museo Argentino de Ciencias Naturales Bernardino Rivadavia, Buenos Aires, Argentina; RAM, Raymond M. Alf Museum of Palaeontology, Claremont, California, USA; ROM, Royal Ontario Museum, Toronto, Ontario, Canada; SM, Senckenberg Museum, Frankfurt, Germany; TMNH, Toyohashi Museum of Natural History, Toyohashi, Aichi, Japan; UMMP, University of Michigan Museum of Paleontology, Ann Arbor, Michigan, USA; UAMES, University of Alaska Museum Earth

Science, Fairbanks, Alaska, USA; USNM, United States National Museum, Washington DC, USA; YPM, Yale Paleontology Museum, New Heaven, Connecticut, USA.

1.3 Material and methods

1.3.1 Materials

More than 300 individual hadrosaur bones collected from the LBB and its vicinity and housed in University of Alaska Museum in Fairbanks were examined in the course of this study (see Table 1-1 for a complete list). Based on my own observations and the work of previous authors [10,16,18,19,24,25], my study began with the working hypothesis that the PCF taxon is congeneric with *Edmontosaurus*, or a very closely related taxon. Among five autapomorphies of *Edmontosaurus* listed by Campione and Evans [10], the PCF taxon possesses two; (1) the premaxillary margin is folded dorsoventrally, and (2) the frontal is widely exposed laterally in the reconstructed skull (Figure 1-2). Further, the PCF taxon is similar to *Edmontosaurus* in that its nasal does not show any evidence of ornamentation, as seen in some genera of Saurolophinae. Finally, being early Maastrichtian in age, the PCF taxon overlaps in stratigraphically with *Edmontosaurus* but not geographically. Specimens of the PCF taxon are known only from the Laramidian landmass, while the other members of the genus occupied lower latitudes of the same landmass.

The PCF material does not appear referable to other closely related Asian taxa, such as *Shantungosaurus*, *Kerberosaurus*, and *Kundurosaurus*, which have been variably recovered as closely related to *Edmontosaurus* in recent phylogenetic analyses [55,56]. The PCF taxon and *Edmontosaurus* differ from *Shantungosaurus* [57] in that the anterior part of the scapula is smaller, the suprailiac crest of the ilium is less developed, and they lack an ischial peduncle. The PCF taxon and other species of *Edmontosaurus* differ from *Kundurosaurus* [55] in that they lack a ridge on the lateral side of the nasal, the caudal buttress of scapula projects ventrally, and they have a ventrally curved preacetabular

process of the ilium. Finally, the PCF taxon and other species of *Edmontosaurus* differ from *Kerberosaurus* [58] in that they lack all of the following features: a pocket on the basisphenoid process; a narrow groove for ophthalmic nerve on lacrimal; a crest on the lateral side of the nasal; and a prominent palatine process on maxilla. For these reasons, I assume the PCF taxon is referable to *Edmontosaurus.*

Most PCF specimens are conspicuously small compared to adult-sized *Edmontosaurus annectens* and *E. regalis*. Because of their small size, the disarticulation of skull bones, highly porous periosteal surfaces and little to no evidence of histological remodeling, I interpret that these individuals are immature and not a dwarf Arctic hadrosaurid species.

To understand the size distribution of the PCF individuals, I prepared a histogram showing size on the X-axis and the number of specimens on the Y-axis. First, bones for which at least 10 specimens are known were selected (dentary, frontal, humerus, ulna, radius, tibia, metatarsal II, III, and IV) and their lengths measured. Then, the length of each bone was divided by the "average" length of its bone type. When calculating the average, specimens that are more than twice as large as the smallest specimens are removed. By dividing each length by average length, it is possible to compare the lengths of different bone types. Normality distribution is tested using the Shapiro-Wilk test in PAST 3.0 [59]. The results are presented in Figure 1-3. The hypothesis of normal distribution is rejected ($p << 0.001$). The histogram shows PCF individuals can be classified into three ontogenetic stages. Approximately 85 % of the specimens examined are categorized as size class 1. A reconstructed skull from these specimens (Figure 1-2) is approximately 30 cm long, which is one third of the length of the adult paratype specimen of *E. annectens*, YPM 2182 (91 cm, when measured from the anterior end of the premaxilla and the mid point of the quadrate). Size class 2 accounts for about 10 % of the examined specimens, which are approximately 30 % longer than size class 1 specimens, equivalent to 40 % of the skull length of YPM 2182. Size class 3 represents less than 5 % of the total specimens, which are approximately 80-100 % longer than the

size class 1 specimens, corresponding to 60 % of the in size of YPM 2182. Operationally, the specimens binned into size classes 2 and 3 were primarily based on their size relative to the most abundant size class 1 specimens of each bone type; thus specimens assigned to size classes 2 and 3 may not always guarantee that they are from the individuals of exactly the same growth stage due to possible allometric growth of *Edmontosaurus*. However, because specimens of size class 1 represent the majority of the specimens for most type of bones collected from the PCF, it is likely that size class 1 specimens are from individuals of the same size. Size classes 1 to 3 of the PCF material are all interpreted to be three different juvenile stages of growth. The consistency in size of each size class, particularly within size class 1, is possibly attributable to a mass mortality event among different yearly cohorts [24].

Because the premaxilla probably experienced strong allometric growth (discussed later), overall morphology and comparison with other specimens of *Edmontosaurus* is also taken into account when determining the size class. Size class 2 premaxillae are about 70 % larger than size class 1 premaxillae, but are smaller than size class 3 premaxillae of *E. annectens* (ROM 53526 and ROM 53534).

In this paper, comparative materials from other specimens of *Edmontosaurus* species are categorized according to the same size definitions. *E. regalis* specimens range from subadult (CMN 8399, BMNH 8937) to adult (ROM 801, USNM 12711). *E. annectens* has a better growth record, ranging from approximately size class 2 (LACM 23504) and size class 3 (e.g., ROM 53530) to subadult (CMN 8509) and adult (ROM 57100, MOR 003) specimens.

1.3.2 Geometric morphometric analysis

Following the morphometric analysis by Campione and Evans [10], I conducted a 2D geometric morphometric analysis of *Edmontosaurus* and the PCF taxon. Through this analysis, complex shapes can be expressed numerically. I first reconstructed a composite skull of a size class 1 PCF individual (total length = 30 cm) from casts of isolated but

well preserved, three-dimensional bones (Figure 1-2). Comparative data was acquired from photographs of eight skulls of *E. regalis* and 13 skulls of *E. annectens* housed in several museums (Table 1-2). 25 landmarks were then designated on lateral views of the skull (Figure 1-4). In order to incorporate shape change along the curves, such as the orbit and the infratemporal fenestra, 50 semi-landmarks were also designated. Semi-landmarks were assigned on curves between landmarks with constant intervals. Since there is no guarantee that these semi-landmarks are put on homologous points, they are allowed to slide on specific lines between the landmarks, so that their influence is reduced.

Most specimens are incomplete in certain areas. For landmarks and semi-landmarks that are to be assigned to missing parts, their coordinates are first approximated. Then, sets of coordinates of landmarks and semi-landmarks are aligned by Procrustes superimposition, using Coordgen 7 in IMP7, Integrated Morphometric Package [60]. Thereafter, coordinates of missing landmarks and semi-landmarks are estimated using the thin-plate spline method, implemented in an R package, Geomorph [61].

Because the PCF specimen is much smaller than other specimens of *Edmontosaurus*, size influence had to be removed. I applied a regression to the dataset against the log scaled centroid size using MorphoJ [62]. In this way, the shape information of the each specimen is divided into two components: a component that is proportional to the size, and a residual component, which is independent of size. The Principal Component Analysis (PCA) is conducted on the residual component in MorphoJ. The principal components that correlate with the size are also visualized. This corresponds to average growth change of *Edmontosaurus.*

1.3.3 Comparative morphological analysis

I compared each skeletal element from different size classes of the PCF material with comparable material of *Edmontosaurus regalis* and *E. annectens*. In addition to the

specimens included in the morphometric analysis, disarticulated specimens were also examined (Table 1-2). Whenever possible, I attempted to compare the PCF material to other immature individuals of known species to better understand ontogenetic changes that occur for each element and among each taxon.

Because the PCF material is much smaller than other material of *Edmontosaurus*, I also relied on quantitative methods to compare many elements. Quantitative data on specimens not personally observed were taken from the literature [44,52] or from photographs. Bivariate plots are employed to test if a given feature observed in the PCF material is potentially a juvenile condition of a feature seen in adult *Edmontosaurus annectens* or *E. regalis,* and to analyze the growth patterns of *Edmontosaurus.* This method partially overlaps with the geometric morphometric analysis, but it is better in that a greater number of specimens can be used for statistical testing and different elements from various regions of the skeleton can be analyzed separately. Dodson [7,63,64] showed that among the same species, log-transformed lengths of various parts show high correlations against body size, except for morphologies that related to sex. This method was later employed by other workers [3,65-67] to assess ontogeny and test the hypothesis that a given specimen is a juvenile form of a known taxon. However, because the correlation coefficient is not reliable when the data include outliers [68], a rigorous test of whether a small specimen represents a juvenile of a known specimen is difficult.

In order to address this problem, I employed a new method in this study. The analysis employed here is based on the assumption that the growth trend line of *Edmontosaurus*, from juvenile to adult, can be expressed by the following equation:

$$\text{Length} = A \times (\text{body length})^{B} \quad \text{.....(1)}$$

A and B are constants. In some cases (dentary deflection and quadrate), an angle

substitutes for “length”. By logarithmic transformation, the equation above can be transformed as

$$\text{Log (length)} = B \times \text{Log (body length)} + \log (A) \quad \text{.....(2)}$$

If the log-transformed length of any body part correlates with the log-transformed body length, any sets of log-transformed body lengths would also correlate to each other. With this assumption, I null-hypothesized that the character condition of the PCF materials is similar to a putative juvenile of *Edmontosaurus regalis* or *E. annectens* each, or both species combined when the growth trend lines of *E. annectens* and *E. regalis* are indistinguishable. With this null-hypothesis, growth trend lines of other *Edmontosaurus* species + PCF materials combined (“hypothetical growth line”) are prepared. If these hypothetical growth lines are statistically different ($p < 0.05$) from the growth trend lines of other *Edmontosaurus* specimens alone or PCF materials alone each, I conclude that the PCF materials represent a different ontogenetic trajectory for that feature. For premaxillary, nasal, postorbital and quadratojugal length, the length of the dentary is used as a proxy of the body size. Because the specimens excavated from the LBB are all disarticulated, only size class 1 PCF materials are compared against the average size of the dentary of size class 1. Because size class 1 dentaries represent the majority of the PCF materials, other size class 1 material also likely belongs to individuals of the same size. A reduced major axis (RMA) regression line was chosen to calculate the growth trend line, because it minimizes the effects of error in the both variables [69]. Only regression lines that show significant correlation are compared ($p < 0.1$). In some cases, a sufficient amount of material of the PCF taxon is available to draw regression lines with statistical significance. In that case, the hypothetical growth line is compared twice, against the regression lines of other *Edmontosaurus* species and against regression lines of PCF materials. In such cases, I applied a Bonferroni correction to reduce the

possibility of type-I error. SMATR ver. 2.0 [70] was used to prepare the RMA regression lines, R^2 and P values, and to assess whether two regression lines are statistically different. By log-transformation, the slope of the growth line becomes indicative of either positive or negative allometric growth: for length compared against length, when the slope is more than 1, it indicates positive allometric growth, and when the slope is less than 1, it indicates negative allometric growth. I assessed this growth pattern based on the 95 % CI of the slope.

Gould [71] explained that the growth trend is constant because an organism attempts to retain some physical trait constants throughout growth. A notable exception is characters possibly related to sexual display. In a case of the comb of a cassowary, the comb shows a negative allometric growth trend during juvenile stages, followed by very strong positive allometric growth trend after sexual maturity [7]. With this in mind, if the growth trend of other *Edmontosaurus* species is too steep to be an adult form of the PCF taxon, I also considered whether the compared elements could be sex-related morphology.

1.3.4 Cladistic analysis

As a basis for my phylogenetic analysis, I used a modified version of the Prieto-Márquez ([56], see Appendix 1) character matrix, consisting of 35 taxa and 266 equally weighted and unordered characters. Character data was input using Mesquite [72]. I added one new character concerning the shape of circumnarial septum (see Appendix 1). When Prieto-Márquez prepared his character matrix, he classified *Edmontosaurus edmontoni* (e.g., CMN 8399, CMN 8744, ROM 867) as either *E. annectens* or *Edmontosaurus* sp. Campione and Evans [10] later synonymized *E. edmontoni* as a juvenile form of *E. regalis*. Assuming *E. annectens* in Prieto-Márquez [25,56,73] is scored based on both *E. annectens* and "*E. edmontoni*", I re-scored *E. annectens* based on specimens which are certainly recognized as *E. annectens* (AMNH 5730, AMNH 5886, YPM 2182, CMN 8509, DMNH 1493 and TMNH 00001).

Three versions of the data matrix were prepared. In the first matrix, the characters of the PCF materials are input as-is, without considering possible ontogenetic change (Matrix 1). In the second matrix, possible ontogenetic changes are taken into account based on the results of the comparative morphological analysis (Matrix 2), whereby characters interpreted to change through ontogeny are scored as missing in the PCF taxon. After the second analysis, the putative autapomorphies for the PCF taxon, and synapomorphies of *E. regalis* and *E. annectens,* are again examined critically for their validity. Characters that are not regarded as valid are then scored as missing in matrix 3 and reanalyzed.

Because the ultimate purpose of the paper is to determine the taxonomic status of the Alaskan *Edmontosaurus* to the species level*,* quantitative characters that possibly distinguish *E. regalis* from *E. annectens* are assessed by their mean scores.

The cladistic analysis was conducted using TNT [74]. *Equijubus normani* was designated as the outgroup, following the cladistic analysis of Prieto-Márquez [73]. The most parsimonious trees were sought by the "New Technology search" option with "Sectional search" and "Tree fusing options" checked. The minimal length was searched for 100 times, with 100 random seeds. In a preliminary analysis, *Kerbosaurus manakini*, whose position on the tree is unstable, was pruned by the reduced consensus method, using Redcon 3.0 [75]. Bremer support values were calculated using a Bremer Support Script made by Goloboff [76] with the default setting (1000 replicates). Bootstrap values were calculated using the resampling function of TNT, with the standard (sample with replacement) and traditional search options and 1000 replicates, and the results were output as absolute frequencies.

1.4 Results

1.4.1 Geometric morphometric analysis

Principal component analysis is conducted against the components that are

independent of size, and *Edmontosaurus regalis* and *E. annectens* are separated by the first (PC1) and second (PC2) principal components (Figure 1-5). PC1 explains 29.2 % of the variance, and PC2 explains 15.8 %. Primarily in PC2, *E. annectens* and *E. regalis* are separated with some overlap of 95 % CIs. The PCF taxon is plotted within the 95 % CI of *E. annectens.* AMNH 5730, plotted outside the 95 % CI of *E. annectens*, was once considered to be a different genus because its skull is dorsoventrally flattener compared to other species of *Edmontosaurus* [52]; however, this was later attributed to postmortem dorsoventral crushing [10,25].

Figure 1-6A shows the shape change along the centroid size, which can be regarded as a general growth trend of *Edmontosaurus.* Notable changes include relative elongation of the premaxilla, contraction of the orbit and infratemporal fenestra, widening of the jugal process of the postorbital, and dorsoventral shortening of the quadrate. Figure 1-6B shows the shape change along PC1, which is primarily related to relative dorsoventral contraction. However, because AMNH 5730 (a dorsoventrally crushed specimen) is an outlier in the PC1 score, it is likely that other PC1 scores are influenced by post-mortem damage. Therefore, I consider PC2 to be more informative in distinguishing *E. regalis* and *E. annectens* (Figure 1-6C). The most noteworthy changes along PC2 (*E. annectens* to *E. regalis*) is the contraction in premaxillary length, a larger postnarial curvature relative to the posterior-most point of the narial opening, contraction between the posterior-most point of the predentary to the anterior-most tooth row of the dentary, and a narrower laterally exposed area of the quadratojugal.

1.4.2 Comparative morphological analysis

In this section, morphological characters that distinguish the PCF material from *Edmontosaurus annectens* and *E. regalis*, as well as ontogenetic changes observed in *Edmontosaurus* as a whole, are summarized. A more complete and detailed description of the PCF material is presented in the Chapter 2.

1.4.2.1 Skull

Although the overall skull height to length ratio is known to change through ontogeny [53], this ratio in adults is used in other cladistic analyses [25,56,73]. Relative elongation of the skull is suggested in the geometric morphometric analysis, but here it is also confirmed in the regression analysis. The regressions for *Edmontosaurus annectens* and *E. regalis* are indistinguishable, and that drawn for *E. regalis* + *E. annectens* is statistically indistinguishable from the hypothetical growth trend lines of *E. regalis* + *E. annectens* + PCF reconstruction skull (Figure 1-7). The regression line for the latter shows a negative allometric growth of the skull height relative to the skull length at the 95 % CI, supporting the observation that the skulls of edmontosaurs would become relatively elongate as they grew.

1.4.2.2 Premaxilla

In size class 1 of the PCF material, the circumnarial septum projects posterolaterally and is triangular in coronal section (Figure 1-8). In *Edmontosaurus regalis* and *E. annectens,* the septum is fan-shaped in dorsolateral view, expanding both anteriorly and posteriorly. Its dorsolateral wall is flat and is nearly parallel to the medial wall of the premaxilla in the coronal plane (Figure 1-8). In the PCF material, the circumnarial septum divides the rostral part of the premaxilla into two fossae; the anterior premaxillary cavity and the circumnarial depression. *E. annectens* and *E. regalis* also have a lateral premaxillary cavity not found in the PCF material. Some *E. annectens* premaxillae (AMNH 5046, LACM 23504, ROM 53534), which are comparable to the PCF materials in size, also have the fan-shaped septum, suggesting that this is not an ontogenetically variable feature (Figure 1-9). None of the PCF material, including a crushed specimen of size class 2 (UAMES 4184) has a circumnarial septum morphology similar to *E. regalis* or *E. annectens*. In addition, the Alaskan material has a shallow groove lateral to the posterodorsal premaxillary foramen (Figure 1-9). This groove is also seen in other *Edmontosaurus*; however, in *E. annectens,* this groove is more recessed anteriorly and is dorsoventrally much taller, resulting in a conspicuously C-shaped posterior outline of the circumnarial septum, even in size class 2 and adult specimens

(e.g., CMN 8509, ROM 53526, LACM 23502, UCMP 128374, AMNH 5046). For these reasons, I believe that these taxonomically informative characters are not ontogenetically variable.

As shown in the geometrtic morphometric analysis (see above), proportional length of the premaxilla (the distance between the anterior oral margin and anterior point of the narial fossa) is the most critical character that distinguishes adult *E. annectens* and *E. regalis,* as was noted by Campione and Evans [10]. The regression analysis indicates that PCF materials could be similar to juveniles of either of *E. regalis* or *E. annectens* (Figure 1-10A).

In *Edmontosaurus,* the premaxillary margin is reflected dorsomedially, which is also seen in the PCF materials. The dorsoventral depth of the premaxillary margin is another character that distinguishes adult *E. regalis* and *E. annectens* [10]. The regression analysis indicates that PCF materials could be similar to juveniles of either *E. annectens* or *E. regalis* (Figure 1-10B).

1.4.2.3 Nasal

In *Edmontosaurus*, the posterodorsal corner of the circumnarial ridge of the nasal forms a sigmoidal curve, accompanied by an excavation. The excavation is more developed in *E. regalis* than in *E. annectens* [10], thus it can be used to distinguish among species. In the PCF material, the nasal curvature and excavation is relatively weak. To test whether the nasal curvature is an ontogenetically variable character, the length and height of the nasal curvature are plotted against the dentary length. In terms of both the nasal curvature length and height, *E. annectens* has a less pronounced nasal curvature than *E. regalis*. The regression analysis (Figure 1-11A, B) shows this nasal curve would be more pronounced as *Edmontosaurus* grew, because all slopes are higher than 1 at 95 % CI, except the nasal curvature length of *E. regalis* (Figure 1-11B). The regression analyses suggest that the PCF material does not represent a juvenile condition of *E. annectens*, but the PCF material could be similar to a juvenile of *E. regalis*. However, considering the steep growth trend of other *Edmontosaurus,* this character

could represent a character that accelerated its growth after sexual maturity. The hollow nasal cavity of *Edmontosaurus* could have accommodated a diverticulum for sexual display purpose [50], and if so, the growth trend line of the nasal curvature would not be constant even within a single species.

1.4.2.4 Prefrontal

In adult *Edmontosaurus,* the orbital surface of the prefrontal forms a fossa [77], but no such excavation exists in size class 1 of the PCF material (e.g., UAMES 18618, 4305, UAMES 17077, UAMES 13250) or in size class 3 of *E. annectens* (ROM 53499, ROM 53500) (Figure 1-12). These specimens and PCF specimens of size class 1 and 2 are also mediolaterally narrower than those of adult *E. annectens* (CMN 2289, ROM 64076). Therefore, it is likely that during the growth of *Edmontosaurus* the prefrontal widened and the prefrontal fossa became more strongly excavated after size class 3 had been reached.

1.4.2.5 Frontal

The lateral ridge of the frontal in the PCF material is moderately (e.g., UAMES 4289) to highly (e.g., UAMES 13216) pronounced. Although it is well developed in *Edmontosaurus regalis* (CMN 2289, ROM 801, USNM 12711, BMNH 8937), this character is variable in *E. annectens*, in which some specimens (LACM 23502, AMNH 5046, ROM 57100) also have a moderately pronounced lateral ridge while others have a flat dorsal surface of the frontal (YPM PU 618, AMNH 427).

Frontals collected from the LBB are similar in anteroposterior length (7.4 ± 0.66 cm, n = 6) but show greater variation in width (3.9 ± 0.52 cm, n = 6). They are anteroposteriorly longer than wide, although the frontals of adult *Edmontosaurus* specimens are nearly as wide as long. The width to length ratio of size class 2 and 3 frontals in *E. annectens* (ROM 53501, ROM 53502) is almost the same as that of the widest frontal of the PCF material (Figure 1-13A-E). The regression analysis (Figure 1-13F) indicates the anteroposteriorly long frontal of the PCF material could be similar to a juvenile condition of edmontosaur, although an allometric growth trend could not be

determined at the 95 % CI.

1.4.2.6 Lacrimal

The lacrimal of the PCF materials differs from both *Edmontosaurus regalis* and *E. annectens* in that the anterodorsal part of the PCF material is dorsoventrally narrower. Apparently the dorsoventral depth of this part does not differ proportionally in adult *E. regalis* (CMN 2289) and size class 3 of *E. annectens* (ROM 53511 and ROM 53512) (Figure 1-14). CMN 8509 (*E. annectens*) also has a narrow lacrimal, but this can be attributed to damage. Therefore, the narrow lacrimal could be an apomorphy of the PCF taxon, or it could represent an ontogenetically variable character.

1.4.2.7 Jugal

The jugal of the PCF material has a well developed ridge on the medial surface of the rostral process, and the posterior border of the rostral process bends anteriorly near the level of the rostral spur by about 25°, which is a character not seen in other *Edmontosaurus* species (*E. regalis*, CMN 2289; *E. annectens*, ROM64076, ROM 53518). Also, the jugal is relatively more gracile than other species of *Edmontosaurus*, as measured by the ratio between the caudal constriction depth and the distance between the lower-most points of the infratemporal fenestra and orbit (jugal length, Figure 1-15). The PCF taxon has a much shallower caudal constriction to jugal dorsal length ratio (0.56 ± 0.05) than other *Edmontosaurus* specimens (0.76 ± 0.06). The regression analysis shows that the PCF materials could not represent a juvenile condition of *E. annectens* + *E. regalis* (Figure 1-15). Therefore, the gracileness of the jugal in the PCF taxon is taxonomically informative, even when ontogeny is taken into account.

The ratio between the caudal and rostral constrictions of the jugal is a character previously used in cladistic analyses [25,55,56,73]. The regression analysis of the rostral and caudal constriction depths, however, failed to reject the null hypothesis that the PCF material is a juvenile condition of *Edmontosaurus annectens* or *E. regalis*.

1.4.2.8 Quadratojugal

The quadratojugal of the PCF taxon has two depressions on the medial side of its posterior edge, where it articulates with the dorsal and ventral border of the quadratojugal notch of the quadrate. In adult *Edmontosaurus* specimens (e.g., ROM 64076, CMN 2289), these depressions are continuous. Apparently, this is an ontogenetically variable character, because size class 2 of *E. annectens* (ROM 53516) also has two weak depressions. The posterior area of the quadratojugal, where it is not covered by the jugal laterally and thus is slightly elevated, is narrower in *E. regalis* (e.g., CMN 2289, CMN 8744, and ROM 658) than *E. annectens* (e.g., CMN 8509, ROM 57100, UMMP 20000), as shown in the geometric morphometric analysis. The regression analysis shows that the PCF material has a wider lateral exposure area, as in *E. annectens*, and could not be similar to a putative juvenile of *E. regalis* (Figure 1-16). Considering that the quadratojugal is likely not associated with sexual display, there is no reason to assume that the growth trend of this element is not constant. Therefore, the regression analysis is valid.

1.4.2.9 Postorbital

Several postorbitals of size class 1 are known from the LBB. In addition, an isolated size class 3 postorbital (UAMES 33308) was collected near the LBB from nearly the same stratigraphic layer. UAMES 33308 lacks the dorsal promontorium on the frontal process commonly seen in lambeosaurines [25,73] and is nearly identical in morphology, although larger, than the size class 1 materials from the LBB. For these reasons, I regard this material as conspecific with the LBB edmontosaur. In size class 1 of the PCF specimens, the jugal process is both anteroposteriorly short and mediolaterally narrow. The regression analysis shows *E. regalis* has a wider jugal process than *E. annectens*. The narrow jugal process of the PCF materials could be similar to that of *E. annectens* but much narrower than a putative juvenile *E. regalis* (Figure 1-17). The jugal process shows positive allometric growth patterns in both *E. annectens* and *E. regalis.* This is likely true in the PCF taxon too, because the single PCF specimen (UAMES 33308) of size class 3 has a wider jugal process than size class 1 of the PCF materials.

In both size classes 1 and 3 of the PCF taxon, the posterodorsal wall of the orbital rim (the anterior surface of the jugal process) is only moderately concave anteriorly and completely lacks a deep posterior orbital pocket (Figure 1-18). Significantly, the posterior orbital socket is present even in *E. annectens* specimens of size classes 2 and 3 (ROM 53513, ROM 53514), indicating that this feature was present very early in ontogeny.

The postorbital morphology also differs from *Kundurosaurus,* which is morphologically similar and phylogenetically close to *Edmontosaurus* [55]. Size class 3 of the PCF material has a large concave anterior surface of the jugal process and the anterolateral rim of the jugal process is more extensive than in size class 1 or in *K. nagornyi* (AENM 2/921-6) [55]. Unlike *K. nagornyi*, the depression on the dorsal surface of the postorbital dorsal to the jugal process is not seen in the PCF materials. The articular surface with the frontal in the PCF materials is identical to that of size class 1 and 2 of *E. annectens* (ROM 53513, ROM 53514). Dorsal to the laterosphenoid facet on the medial surface of the postorbital is an anteroposteriorly-elongated groove, which anteriorly ends on the dorsal surface of the orbits. The postorbital of *K. nagornyi* has a corresponding groove, but it is anteroposteriorly shorter and isolated from the anterior surface of the jugal process (Figure 1-18).

1.4.2.10 Squamosal

In adult *Edmontosaurus* and other adult saurolophines, the squamosal articulates with the postorbital dorsal to or slightly posterior to the prequadratic process. Size class 1 material of the PCF taxon has a long postorbital process, so that the squamosal articulates with the postorbital well anterior to the prequadratic process (Figure 1-19). Size class 2 of the PCF material (UAMES 4361) and *E. annectens* (ROM 53510) have a relatively short postorbital process, but it is longer than that of subadult *E. annectens* (CMN 8059). Thus, I conclude this is an ontogenetically variable character, whereby the postorbital process would shorten relatively as *Edmontosaurus* grew.

1.4.2.11 Quadrate

The quadrate of the PCF material is straighter than other *Edmontosaurus*

specimens. The regression analysis (Figure 1-20) indicates that the quadrates of the PCF taxon could be similar to juvenile quadrates of other *Edmontosaurus* specimens, although its growth trend could not be determined at the 95 % CI.

1.4.2.12 Maxilla

The maxillary foramina of the PCF material are relatively larger compared to *Edmontosaurus annectens* specimens (MOR 723, ROM 64083, MOR 1609, ROM 53527, ROM 53528) but comparable to *E. regalis* (CMN 2289, AMNH 5445). In size class 2 of *E. annectens* (ROM 53527, ROM 52528), the anterior-most maxillary foramen is large, but the posterior ones are small. A canal located on the medial face of the dorsal process opens dorsomedially in the PCF material and in *E. regalis* (CMN 8744, CMN 2289); however, in size class 3 materials of *E. annectens* (ROM 53527, ROM 53528) this canal is located on the shelf ventromedial to the dorsal process and opens dorsally (Figure 1-21). In these respects, the PCF material is more similar to *E. regalis* than to *E. annectens*, although the degree to which this feature varies ontogenetically is not clear.

1.4.2.13 Basisphenoid

The interbasipterygoid ridge, a ridge between the anteroventral and posteroventral surfaces is, well developed in adult *Edmontosaurus* (CMN 2289, YPM 618, ROM 59786). In size class 1 of the PCF specimens (UAMES 13107, UAMES 12777, UAMES 6631), this ridge is not conspicuous, but it is more developed in a size class 3 specimen (UAMES 18882). Therefore, this is an ontogenetically variable character in the PCF taxon.

1.4.2.14 Parietal

The impressions of the cerebrum and cerebellum are divided by bulges on the lateral wall of the braincase. These bulges are less developed in the PCF taxon than in size class 3 of *Edmontosaurus annectens* (ROM 53493) (Figure 1-22). In ROM 53493, the lateral bulges are much more pronounced than in the PCF taxon, and the cerebellum impression tapers posteriorly. Due to a small sample size, it is not certain if this difference is attributable to either ontogenetic or taxonomic variation.

1.4.2.15 Basioccipital

The basioccipital of the PCF material is hexagonal in ventral view, unlike other *Edmontosaurus* specimens in which the basioccipital is mediolaterally constricted along its lateral margin (Figure 1-23). However, the degree to which it is constricted is more pronounced in larger specimens (Figure 1-23). In size classes 2 and 3 of *E. annectens* (ROM 53538 and AMNH 427), the ratio of basioccipital constriction width to basioccipital posterior width is 1.01 and 0.90, respectively, and in adult *E. regalis* (CMN 2289) and *E. annectens* (CMN 8509) it is 0.86 and 0.79. Because the number of comparative specimens is limited, it is difficult to assess whether the hexagonal basioccipital of the PCF material is ontogenetically variable. As a comparative context, the hexagonal basioccipital of the PCF taxon resembles that of embryonic *Hypacrosaurus stebingeri* (RTMP 87.79.157, [2]), while the basioccipitals of adult and nestling *H. stebingeri* (MOR 548) and *H. altispinus* (CMN 8675) are not hexagonal, similar to that of adult *Edmontosaurus*. Thus, the morphology of the PCF material possibly represents an immature growth stage in *Edmontosaurus*.

1.4.2.16 Exoccipital-Opisthotic

In the PCF material and *Edmontosaurus annectens* (ROM 53503, ROM 53504, 64076, ROM 64077, ROM 59786, YPM 618), the lateral surface of the exoccipital condyloid is flat, in contrast to *E. regalis* (CMN 2289), in which it expands laterally, ventral to the cranial nerve foramina. In addition, in the PCF material, these foramina are located well within the body of the exoccipital condyloid, more similar to *E. annectens* than to *E. regalis* (CMN 2289), in which they are located immediately dorsal to the exoccipital condyloid.

In a relatively small size class 1 specimens of the PCF material (UAMES 4279), the middle body of the exoccipital-opisthotic lies vertically dorsal to the exoccipital condyloid, and the apex of the paraoccipital process is located more anteriorly than the posterior-most point of the exoccipital condyloid (Figure 1-24). In contrast, in adult *Edmontosaurus* specimens (ROM 59786, *E. annectens*; CMN 2289, *E. regalis*), the

dorsal portion of the exoccipital-opisthotic complex is inclined posteriorly. As a result, the apex of the paraoccipital process is located more posteriorly than the posterior-most point of the exoccipital condyloid and the inclination of the anterodorsal margin of the exoccipital-opisthotic body is not as steep. Specimens whose sizes are intermediates of UAMES 4279 and ROM 59786 (PCF taxon, UAMES 4095, UAMES 4236; *E. annectens,* ROM 64077) are intermediate in shape in these respects (Figure 1-24). Therefore, I interpret that the dorsal half of the exoccipital-opisthotic tilted increasingly posteriorly as *Edmontosaurus* grew.

This ontogenetic change would also affect the orientation of the ventral end of the paraoccipital process, which is a character often used for phylogenetic analysis [25,55,56,73]. During ontogeny, as the opisthotic becomes increasingly inclined posteriorly, the ventral end of the paraoccipital process is directed more anteroventrally. In addition, this change is likely related to the changes seen in quadrate morphology during ontogeny, whereby the posterior-shift of the dorsal end of the quadrate would push the squamosal and paraoccipital process posteriorly.

1.4.2.17 Pterygoid

The lamina between the ectopterygoid process and ventral quadrate process in size class 1 PCF materials is less extensive than in a specimen of size class 2 of *Edmontosaurus annectens* (ROM 53539). In subadult *E. annectens* (CMN 8509) and adult *E. regalis* (CMN 2289), this bony lamina is more extensive than in these juvenile specimens (Figure 1-25). Therefore, th less extensive lamina of the PCF specimen and ROM 53539 is an ontogenetic feature, although the differences between *E. annectens* specimens ROM 53539 and CMN 8509 could also bedue to variation within the species.

1.4.2.18 Predentary

Predentary size classes 1 and 2 are present in the LBB and have at least three denticles lateral to the median denticle. The size of the denticles shows negative allometric growth, and in larger specimens (UAME 4928) the denticles are more sparsely positioned than in the smallest specimen (UAMES 4437). Although Prieto-Márquez [73]

suggests the number of denticles on the anterior margin would increase slightly through ontogeny, the PCF specimens do not show such a trend within size classes 1 and 2.

Judging from the outline of the medial side of the lateral process, the posterodorsal median process is likely relatively small in the large size class 1 specimen (UAMES 4437) than in the size class 1 specimen (UAMES 4947). Adult *E. regalis* (CMN 2289) also has a relatively small posterodorsal medial process. Therefore, this is likely an ontogenetically variable character in *Edmontosaurus.*

1.4.2.19 Dentary

The edentulous process of the dentary of the PCF taxon is strongly deflected ventrally, and it is relatively short compared to adult *Edmontosaurus annectens*. For dentaries larger than 40 cm (dentaries larger than size class 3), the mean deflection angles of *E. annectens* and *E. regalis* are significantly different, and this is one character that distinguishes *E. regalis* and *E. annectens.* In *E. annectens*, the dentary deflection shows good correlation with size, and slope is less than 0 at the 95 % CI, indicating this is an ontogenetically variable character. However, in *E. regalis* the dentary deflection does not show statistically significant correlation with the dentary length ($p = 0.16$), due to the lack of smaller specimens. Thus, a rigorous test of whether the strong deflection of the PCF materials represents a juvenile condition of *E. regalis* is not possible (Figure 1-26A). Therefore, I compared the deflection of the PCF materials and *E. annectens*. The regression analysis failed to reject the null hypothesis that the PCF material is similar to juvenile *E. annectens,* although its P value is not very high ($p = 0.07$).

The length of the posterior part of the edentulous process (distance between the posterior-most articulation point with the predentary and the anterior-most tooth socket), relative to the dental battery length is another character traditionally employed in cladistic analyses [25,55,56,73]. The geometric morphometric analysis shows this length changed as edmontosaurs grew and is longer in *E. annectens* than in *E. regalis* (Figure 1-26B). This is confirmed in the regression analysis, and *E. annectens* shows a positive allometric growth pattern. A size class 2 dentary of the PCF taxon (UAMES 4946) has a markedly

shorter edentulous process than *E. annectens* of comparable size (ROM 53530, BHI-6218). This is also reflected in the regression analysis, ruling out the possibility that the PCF materials are similar to juveniles of *E. annectens* in this respect (Figure 1-26B). However, the PCF materials could not be distinguished from *E. regalis* in this regard.

The location of the origin of the ventral deflection of the dentary along the ventral margin of the dentary is also used in cladistic analyses [25,73]. Compared to *Edmontosaurus annectens* and *E. regalis,* the ventral deflection originates more posteriorly in the PCF material (Figure 1-27). The regression analysis indicates the PCF materials could be similar to juveniles of other species of *Edmontosaurus*. The 95 % CI slope value of the *E. regalis* + *E. annectens* + PCF materials regression line suggests that if the PCF material is similar to the juvenile condition of *E. regalis* + *E. annectens*, then this character displays positive allometry, although the growth trend of *E. regalis* + *E. annectens* is not clear.

1.4.2.20 Surangular

The coronoid process of the surangular in the PCF taxon is more laterally oriented than the condition seen in *E. regalis* (CMN 2289). This would bring the convex (ventral) side of the surangular more laterally when articulated with the dentary, which is closer to a plesiomorphic feature and therefore typical of basal hadrosauroids, in which the convex side of the surangular faces more laterally than ventrally [25,73]. In the PCF material the convex side of the surangular still faces more ventrally than dorsally as in other saurolophines and lambeosaurines. This feature might be attributable to the immature growth stage of the PCF specimens. The lateral margin of the surangular, between the coronoid process and the lateral bulge, is only slightly concave medially in both size class 1 and size class 3 specimens, in contrast to the stronger curve seen in size class 2 of *E. annectens* (ROM 53535, ROM 53536) and adult *E. regalis* (CMN 8744).

1.4.2.21 Teeth

Dentary teeth from size classes 1 to 3 of the PCF taxon are known. The height to width ratios of these dentary teeth are around 1.4-2.2, which is lower than in other species

of *Edmontosaurus* [49,73,77]. The height and width ratios of the PCF material, adult (DMNH 1493) and juvenile (BHI-6218) *E. annectens*, and *E. regalis* (CMN 2288) are plotted separately, and all of them show significant correlation in the width and height. All of the regression lines, however, are statistically different from the regressions calculated from all samples. Thus, this character is highly variable. Also, an adult (DMNH 1493) and juvenile (BHI-6218) *E. annectens* show significantly different regression lines, indicating this is an ontogenetically variable character, as suggested by Brett-Surman [52] (Figure 1-28).

1.4.2.22 Splenial

On the lateral and anterior part of the splenial (Figure 1-29) is an indentation that receives the splenial process of the dentary. In adult *Edmontosaurus regalis*, this indentation is anteroposteriorly long, as its posterior end is located more posteriorly than the inflection point of the dorsal edge of the splenial. In the PCF taxon (UAMES 4246, UAMES 4275), and size class 3 (ROM 53531, ROM 53532) and adult (ROM 64076) *E. annectens*, the splenial process indentation is short, as it does not extend more posteriorly than the inflection point.

1.4.2.23 Scapula

Hadrosaur juveniles often have a shorter scapula and a narrower scapular neck than adults [2,52,78]. These differences are also observed in the scapulae of size class 1 of the PCF taxon when compared to other species of adult *Edmontosaurus*. In the PCF size class 1 specimens (e.g., UAMES 12711, UAMES 14061), the coronoid process is relatively well developed and has a coronoid process length to scapula blade length ratio of 0.13, while the ratio ranges from 0.10-0.12 in other *Edmontosaurus* specimens and 0.15 is in LACM 23504, a size class 2 specimen of *E. annectens*. The regression analysis shows the scapulae of the PCF material could be reasonably considered similar to that of juveniles of other *Edmontosaurus* species, although no clear allometric growth trend is observed (Figure 1-30A). In size classes 1 and 2 of the PCF material (UAMES 12711, UAMES 15729), and size class 2 of *E. annectens* (LACM 23504), the scapular neck is

more strongly constricted than in adults (including a size class 3 PCF scapula, UAMES 29996). The regression analysis clearly shows a trend of positive allometric widening of the neck depth as *Edmontosaurus* grew, and PCF materials are indistinguishable from other *Edmontosaurus* in this respect (Figure 1-30B).

In size classes 1 and 2 of the PCF materials, the caudal buttress extends only ventrally and less laterally than in adult scapulae (e.g., CMN 8509 and 2289), and its glenoid margin is not expanded as in *E. annectens* (CMN 8509). This condition contrasts with the scapula of *E. regalis* (CMN 2289), in which the caudal buttress faces more laterally. PCF specimens of size classes 1 and 2 (UAMES 7341) do not differ in this respect.

1.4.2.24 Humerus

The deltopectoral crest length relative to the entire humerus length differs in adult *Edmontosaurus regalis* (56 %) and *E. annectens* (49-53 %). In the PCF specimens, this ratio ranges from 47-54 % (Figure 1-31), within the range of *E. annectens*. However, in the PCF taxon and *E. regalis*, the deltopectoral crest length shows a positive allometric growth trend, and the regression analysis suggests that an adult of the PCF taxon could have a well developed deltopectoral crest as in *E. regalis.* This is not surprising, given that the deltopectoral crest is known to increase in prominence and length throughout ontogeny in other hadrosaurs [79,80]. In *E. annectens*, the deltopectoral crest does not show a clear allometric growth trend, although a significant difference is not observed by the regression analysis between the PCF taxon and *E. annectens*, after Bonferroni adjustment (Figure 1-31). Therefore, the adult PCF taxon could be similar to *E. annectens* in this respect.

1.4.2.25 Ulna

The reconstruction and orientation of the forelimb follows Senter [81]. The ontogenetic changes observed in the ulna of hadrosaurs are unclear. Brett-Surman [52] and Brett-Surman and Wagner [78] note that the juvenile ulna is shorter relative to circumference, and that the olecranon process is more gracile than in adults. In juvenile

Telmatosaurus transsylvanicus, the ulna is slightly more gracile than in the adult [82], and in *Bactrosaurus johnsoni* the ulna became shorter relative to width as it grew [80]. However, Horner and Currie [2] describe neonate *Hypacrosaurus* as having a "massive" ulna. The juvenile PCF material differs from other adult *Edmontosaurus* specimens in that its diaphysis is more strongly constricted anteroposteriorly. A plot of diaphyseal width against olecranon process ridge thickness indicates that the strong diaphyseal constriction can be reasonably considered as a juvenile condition of *Edmontosaurus* (Figure 1-32A). When diaphyseal width is plotted against length (Figure 1-32B), the PCF taxon is more similar to *E. annectens* than to *E. regalis.* Diaphyseal width shows positive allometric growth in the PCF taxon and in *E. annectens* + PCF taxon. Thus, a juvenile ulna could be described as both "massive", when you refer the thickness of the olecranon process ridge, and "gracile" when you refer the width of the diaphysis.

1.4.2.26 Pubis

Regression analysis of the dorsoventral height of the pubic neck against femoral length (Figure 1-33A) indicates the PCF taxon has a proportionally taller neck than other species of *Edmontosaurus*. In *E. annectens* + *E. regalis*, the pubic neck dorsoventral height shows positive allometric growth.

Because the anterior end of the pubis is incomplete in the PCF materials, I measured the length of the pubic neck as the distance from the iliac peduncle to the mid point of the pubic neck. The regression analysis shows *Edmontosaurus annectens* has a more elongated pubic neck than in *E. regalis*. Also, it reveals that the PCF material has a proportionally longer pubic neck than *E. regalis*, but it is proportionally indistinguishable from *E. annectens* (Figure 1-33B). Therefore, it is concluded that the PCF taxon has as long a pubis as *E. annectens.*

1.4.2.27 Calcaneum

In the PCF taxon, the articular surfaces for the tibia and fibula are more deeply concave in a size class 3 specimen (UAMES 18059) than in size class 1 specimens (e.g., UAMES 21884). Adult *Bactrosaurus johnsoni* also have more deeply concave articular

surfaces than juveniles [80]. Therefore, deeply concave articular surfaces are likely attributable to ontogenetic variation in *Edmontosaurus* too. Size class 1 PCF specimens also differ from the size class 3 specimen in that their articular surfaces are smooth.

The most unique character of the PCF taxon, present in both size class 1 and 3 specimens, is that the tibial and fibular articular surfaces are equal in size. In other saurolophines, the fibular facet is larger than the tibial facet. However, whether this is attributable to immature growth stages is unclear.

1.4.2.28 Metatarsal III

The growth pattern of the metatarsal is not clear among Hadrosauroidea, as juvenile *Bactrosaurus johnsoni* have a more slender metatarsal III than adults [80], but juveniles of *Hypacrosaurus stebingeri* and *Maiasaura peeblesorum* have a more robust metatarsal III than adults [2,79]. In the PCF taxon, a plot of proximodistal length against diaphyseal width shows a positive allometric growth pattern for the PCF taxon (Figure 1-34), similar to that of *Bactrosaurus johnsoni.*

1.4.2.29 Metatarsal IV

Metatarsal IV of all three size classes of the PCF taxon are known. In a size class 3 specimen (UAMES 6656, 12454), the medial tuberosity is more pronounced and the dorsal surface is more strongly concave than in size classes 1 (e.g., UAMES 6505) and 2 (UAMES 7344). These intraspecific differences are likely attributable to ontogeny, because similar changes are observed in in *Brachylophosaurus canadensis* (MOR 1071 8-7-99-459, MOR 1071 8-1-99-328-B), *Maiasaura peeblesorum*, (MOR 4470, MOR 1071), *Corythosaurus* sp. (CMN 34825), and *Bactrosaurus johnsoni* [80].

1.4.3 Cladistic analysis

Three equally parsimonious trees were recovered from the analysis of Matrix 1, in which possible ontogenetically variable characters of the PCF axon are input as-is (Figure 1-35). For the PCF taxon, 33 out of 266 characters are scored as missing. In all equally

parsimonious trees, the Alaskan material was recovered as the sister group to *Edmontosaurus annectens* + *E. regalis*. The strict consensus tree of these MPTs is presented Figure 1-35. The clade including the PCF taxon + other *Edmontosaurus* species is supported by fairly high bootstrap (87) and Bremer support values (5) and five synapomorphies, including: 34(1), dorsal projection of the coronoid process of the dentary; 179(0), relative widths of the skull across the postorbitals and squamosals; 196(1), the degree of the expansion of the scapular blade; 219(1), moderately developed suprailiac crest of the ilium; and 242(0), lack of the protuberance on the proximal region of the pubis ischial peduncle (Appendix 1).

In matrix 2, 13 possible ontogenetically variable characters are scored as missing. In the reanalysis, only one parsimonious tree (cladogram 2) was recovered. The tree is completely resolved, except that relationships inside the clade of Brachylophosaurini (*Brachylophosaurus* + *Maiasaura* + *Acristavus*) [83] could not be determined. The topology of the tree is congruent with the strict consensus tree recovered from Matrix 1. In the second cladogram, *Edmontosaurus regalis* + *E. annectens* are united by two synapomorphies (characters 119(2) and 266(2)), *E. regalis* has a single autapomorphy (249(1)), and *E. annectens* has none.

The PCF taxon has five autapomorphies (12(0), 13(1), 24(0), 101(1), and 265(0); Appendix 1). Character 12 relates to the increase in the number of tooth positions (alveoli) in maxilla relative to the dentary. In the size class 1 of the PCF material the number of tooth positions in the maxilla and dentary are the same (26), while adult *Edmontosaurus* species have more tooth positions in the maxilla than in the dentary. However, the numbers of tooth positions in the dentary and the maxilla are known to increase as hadrosaurs grew [25,53]. Consequently, the relative numbers of teeth would also change as they grew. Therefore, this character is not strong evidence that distinguishes the PCF taxon from other *Edmontosaurus* specimens.

Character 13 describes the maximum number of functional teeth per alveolus in the maxillary occlusal plane. As discussed above, the relative number of teeth, as well as

tooth shape, undergoes considerable ontogenetic change (Figure 1-28). Thus, without a juvenile of comparable size, the ontogenetic variation of this character is hard to determine.

Character 24 concerns the prominent ridge on the dorsal and lingual face of the predentary. Adult *Edmontosaurus regalis* (CMN 2289) has a well-developed ridge. Although weak, size class 1 of the PCF specimens do have a ridge on the process. It is not clear if the size class 2 specimen of the PCF material has such a ridge because it is damaged. Therefore, whether this weak ridge on the PCF materials would develop as they grew is not certain.

Character 101 describes the lateral profile of the quadratojugal flange of the jugal. The difference of the states is subtle, based on whether the posterodorsal line of the quadratojugal flange is convex or concave. The status of the character in the PCF taxon is based on a single specimen (UAMES 4213) that best preserves the quadratojugal flange, and its posterior border is convex. However, its quadratojugal has evidence of slight damage on its posterodorsal edge. The posterodorsal end of the quadratojugal flange could have been abraded in UAMES 4213. Therefore, this character does not seem to be strongly supported as an autapomorphy of the PCF taxon.

Character 119 describes the morphology of the central body of the postorbital. The pocket of the postorbital is regarded as an autapomorphy of *Edmontosaurus* [10]. The size class 3 postorbital of the PCF taxon (UAMES 33308) does not have the pocket seen in other *Edmontosaurus* species, while even size classes 2 and 3 of *E. annectens* (ROM 53513, ROM 53514) postorbitals have well developed pockets (Figure 1-18). The bivariate plot of the postorbital jugal process (Figure 1-17) shows that *E. regalis* has a wider jugal process than *E. annectens*. This suggests juvenile *E. regalis* would also have a wider jugal process than juvenile *E. annectens*, and it is hard to imagine that the wider jugal process of juvenile *E. regalis* lacked the pocket. Therefore, I assume this character is valid in distinguishing the PCF taxon from other *Edmontosaurus* species.

Character 249 describes the length/width of the pubic peduncle of the ischium. The ischium peduncle is not complete in the PCF materials, and the character status of other species is determined from adult materials. Therefore it is difficult to comment further regarding this character.

Character 265 relates to the ridge on the plantar surface of pedal unguals. PCF materials have a very weak ridge on the plantar surface, which is not very noticeable visually and can only be discerned by touch. Therefore, I assume this character should be scored as missing in matrix 3.

Character 266 describes the morphology of the circumnarial septum of the premaxilla. The circumnarial septum of the PCF materials projects posterolaterally, whereas in *Edmontosaurus annectens* and *E. regalis* the circumnarial septum is fan-shaped (Figure 1-8). Size classes 2 and 3 of *E. annectens* also have fan-shaped circumnarial septa (Figure 1-9). Therefore, I assume this is not an ontogenetically variable character, and that this character is valid to use in the cladistic analysis.

Because of uncertainties regarding several putative autapomorphies discovered from the analysis of Matrix 2, I scored characters 12, 13, 24, 101, and 265 as missing for the PCF taxon in the Matrix 3, and a cladistic analysis was conducted again. In the third cladogram, only one parsimonious tree was recovered, the relationship of *Edmontosaurus* + PCF taxon is identical with cladogram 2, and the clade of *E. annectens* + *E. regalis* is still supported. Additionally, in cladograms 2 and 3, the two saurolophines discovered in East Eurasia, *Kundurosaurus* and *Shantungosaurus*, clustered as successive sister taxa of *Edmontosaurus* + PCF taxon, although the decay indices and the bootstrap values were not high. Indeed, *Kundurosaurus* becomes a wild card taxon in the cladogram 1.

1.5 Discussion

1.5.1 Growth patterns of *Edmontosaurus*

Based on the comparative morphological analysis, growth trends of *Edmontosaurus* are assessed. Table 1-3 summarizes the growth changes for each element. The overall cranial growth change is characterized in terms of anteroposterior elongation of the skull. In *Edmontosaurus annectens,* elongation of the premaxilla and dentary edentulous processes are also observed. Widening of the jugal process of the postorbital and relative shortening of the postorbital process of the squamosal result from change in shape of the infratemporal fenestra. The posterodorsal part of the skull also shifts posteriorly, as seen in the shape change of the exoccipital-opisthotic and the curvature of the quadrate. Postcranial ontogenetic changes can be characterized as more robust overall, as seen in the enlargement of the deltopectoral process of the humerus, the increase in of the width of the ulna shaft, and the enlargement of the pubis.

1.5.2 Taxonomic status of the PCF material

In this study, three independent methods are employed to test the taxonomic status of the PCF material. Each method attempts to assess and/or account for the possible biases introduced due to differences in ontogenetic status of the comparative material. Results of the geometric morphometric analysis and comparative morphological analysis generally suggest that the PCF material is more similar to *Edmontosaurus annectens* than to *E. regalis*, but some notable differences with *E. annectens* are also observed (summarized in Table 1-4). The cladistic analysis reveals that the PCF taxon is neither referable to *E. annectens* nor *E. regalis*.

The results of the cladistic analyses indicate that PCF taxon is the sister taxon to *Edmontosaurus regalis* + *E. annectens*. Even when ontogenetically variable characters are scored as-is (cladogram 1), the PCF taxon clustered as a sister taxon of *E. annectens* + *E. regalis*, and the clade PCF taxon + *E. annectens* + *E. regalis* is well supported by

high Bremer support and bootstrap values. In the cladistic analyses, the character status of the PCF taxon was prepared mainly from juvenile (size class 1) specimens, but late juvenile (size class 3) specimens are preferentially scored when available. Including a juvenile species in a cladistic analysis is problematic, because species-specific characters tend not to appear until later stages of development [84-86], and therefore the phylogenic position of juvenile specimens tends to be recovered in a more basal position than may actually be the case [1]. However, there is no reason to believe that juvenile material would falsely result in a more derived position in a cladistics analysis. Therefore, it is very likely that the phylogenetic position of the PCF taxon is more derived than *Shantungosaurus.* Additionally, the basal position of the PCF taxon relative to *Edmontosaurus annectens* + *E. regalis* is supported by unambiguous characters, such as the shape of the circumnarial septum of the premaxilla and the lack of the postorbital jugal process pocket, as discussed above. These results support my interpretation that the PCF taxon is congeneric with *Edmontosaurus.*

The geometric morphometric analysis reveals differences between *E. annectens* and *E. regalis* (Figure 1-6C) that are consistent with the results of Campione and Evans [10], but this analysis provides additional data on morphological disparity between the two species, including the shorter edentulous process of the dentary and a smaller laterally exposed area of the quadratojugal in *E. regalis*, which were not previously reported. In the geometric morphometric analysis, all of these differences are analyzed together, and as a result, the PCF material plots with *E. annectens* and it is clearly distinguished from *E. regalis*.

Although the geometric morphometric results are intuitively satisfactory, there are potential sources of error that could be introduced by using this method. First, removal of size effects in the analysis is not necessarily the same thing as removing effects attributable to ontogeny, particularly if all individuals do not experience the same growth pattern. Due to different growth trajectories or heterochrony, ontogenetic effects could not be removed completely. For example, one possible byproduct would be that

paedomorphic adult forms would cluster with juveniles, even after the removal of the size effect. With these caveats in mind, I interpret the results of the geometric morphometric analysis in two possible ways: either the PCF material is conspecific with *E. annectens*, or the Alaskan material is a distinct species and *E. annectens* is a paedomorphic form of *Edmontosaurus*. Here, whether *E. annectens* or *E. regalis* can be considered as paedomorphic forms is assessed on the assumption that the reconstruction of the PCF juvenile skull is approximately similar to the juvenile condition seen in all edmontosaurs. *E. annectens* has a less pronounced posterior nasal curvature and narrower jugal process than *E. regalis.* Since these characters show positive allometric growth patterns in edmontosaurs (Figure 1-11 and 1-17), it can be said that *E. annectens* is similar to juveniles in these characters. However, *E. regalis* also has paedomorphic characters in that it has a shorter premaxilla and edentulous process, which shows a positive allometric growth pattern only in *E. annectens* (Figure1-10A and 26B). Therefore, both *E. regalis* and *E. annectens* have characters that can be considered paedomorphic of edmontosaurs in general. I assume that heterochrony of edmontosaurs does not influence the results of this analysis to a significant degree. However, Juan et al. [87] show that removal of size effects could obscure the power of a geometric morphometric analysis and that a species-level classification could be problematic. The geometric morphometric analysis results suggest the PCF material is not *E. regalis*, but it does not necessarily mean it is *E. annectens.*

The comparative morphological analysis reveals that the PCF taxon possesses a unique suite of characters, some of which are shared with *Edmontosaurus annectens* and others with *E. regalis*. Collectively, these characters distinguish the PCF taxon from both species of *Edmontosaurus*. In most comparative and regression analyses, the PCF taxon is found to be more similar to *E. annectens* than to *E. regalis,* which is consistent with the geometric morphometric analysis. For example, both *E. annectens* and the PCF taxon have a wide lateral exposure of the quadratojugal, a narrow jugal process of the postorbital, a short splenial process indentation of the dentary, a well developed olecranon process ridge, and a long pubic neck length. However, the PCF taxon clearly

differs from *E. annectens* in the length of the posterior portion of the edentulous process of the dentary. In addition, *E. annectens* has proportionally more developed nasal curvature than the PCF taxon (Figure 1-11), although it could be a character that accelerates its development after sexual maturity, similar to the comb of cassowary.

The regression analyses also reveal that the PCF taxon has some unique characters that are not seen in other species of *Edmontosaurus*. In the PCF taxon, the jugal is more gracile (Figure 1-15) and the pubis is deeper at its neck (Figure 1-33) than in other species of *Edmontosaurus.* Specifically, the juvenile material of the PCF taxon differs from juvenile *E. annectens* of similar size in that the former has a posterolaterally projected circumnarial septum of the premaxilla and lacks the postorbital pocket. Because there is not an equally juvenile *E. regalis* specimen known, the juvenile conditions of these characters in *E. regalis* is unknown. However, because *E. regalis* has a much wider jugal process than *E. annectens* (Figure 1-17), it is very likely that juvenile *E. regalis* had an even wider jugal process and deeper orbital pocket than *E. annectens*. Similarly, although the circumnarial septum of *E. regalis* is narrower than that of *E. annectens,* juvenile and adult *E. annectens* have a fan-shaped circumnarial septum, so this condition is not likely ontogenetically variable. Therefore, I conclude that the lack of the pocket in the postorbital and the shape of the circumnarial septum are unique characters of the PCF taxon. The lack of the postorbital pocket, the presence of which is regarded as a particularly diagnostic character of *Edmontosaurus* [10,43] is conspicuous and taxonomically significant, strongly indicating that the PCF material cannot be referred to either *E. annectens* or *E. regalis.* In summary, available data on the PCF material warrants erection of a new species of *Edmontosaurus*.

1.5.3 Systematic Paleontology

Ornithischia Seeley [88]

Ornithopoda Marsh [89]

Hadrosauridae Cope [90]

Saurolophinae Brown [91] *sensu* Prieto-Márquez [73]

Genus *Edmontosaurus* Lambe [77]

1.5.3.1 Revised diagnosis (modified from Campione and Evans [10])

A saurolophine hadrosaurid possessing the following autapomorphies: dorsally directed reflected anterolateral margin of premaxilla; strongly excavated posterodorsal corner of the naris in adults; a fossa or wide depression around the orbital margin in adults; a large contribution of the frontal to the orbital margin; a sharp projection on the dorsal margin of the coronoid process of the dentary; suprailiac crest of the ilium extends approximately 25-50 % the depth of the ilium; absence of a ventrolateral protuberance of the proximal region of the ischial peduncle of the pubis.

Edmontosaurus sp. nov.

1.5.3.2 Holotype

UAMES 12995, rostral portion of a size class 1 right premaxilla

1.5.3.3 Paratype

All paratypes are of size class 1, unless specified otherwise. UAMES 4271, posterior portion of the right nasal; UAMES 13250, left prefrontal; UAMES 4245, left lacrimal; UAMES 4189, right jugal; UAMES 4272, left quadratojugal; UAMES 4286, right quadrate; UAMES 33308, size class 3 right postorbital; UAMES 4361, size class 2 right squamosal; UAMES 4327, right maxilla; UAMES 15284, left laterosphenoid; UAMES 4357, right prootic; UAMES 4301, basisphenoid; UAMES 4276, basioccipital; UAMES 4309, parietal; UAMES 4291, supraoccipital; UAMES 4095, right exoccipital-opisthotic; UAMES 4240, right ectopterygoid; UAMES 4331, left palatine; UAMES 4215, left pterygoid; UAMES 4437, predentary; UAMES 4946, size class 2 left dentary; UAMES 4457, right surangular; UAMES 6646, size class 3 dorsal vertebra; UAMES 23071, size class 3 sacrum; UAMES 4873, right coracoid; UAMES 12711, right scapula; UAMES 21596, right humerus; UAMES 12525, right ulna; UAMES 6272, left radius;

UAMES 6637, left ilium; UAMES 22058, pubis; UAMES 12955, left ischium; UAMES 12515, femur; UAMES 12715, left tibia; UAMES 15553, left fibula; UAMES 21950, astragalus; UAMES 21884, right calcaneum; UAMES 12545, size class 3 right metatarsal IV.

1.5.3.4 Referred specimens

See Table 1-1.

1.5.3.5 Type locality

Liscomb Bonebed (70° 5' N, 151° 33' W), west bank of the Colville River, North Slope, Alaska.

1.5.3.6 Type horizon

Upper portion of the Prince Creek Formation, Late Cretaceous (early Maastrichtian).

1.5.3.7 Differential diagnosis

A species of *Edmontosaurus* that differs from other species of the genus in possessing the following unique character combinations: a circumnarial septum that projects posterolaterally; absence of a postorbital pocket; relatively gracile jugal; short posterior portion of the edentulous process of the dentary (relatively longer in *E. annectens*); wide lateral exposure of the quadratojugal (relatively narrow in *E. regalis*); relatively deep pubic neck.

1.6 Acknowledgements

This work was supported in part by NSF awards EAR 1226730 (co-PI's P. Druckenmiller and G. Erickson) and DBI-1057426 (PI P. Druckenmiller), a Geist Fund scholarship, and the UAF Graduate School. I kindly acknowledge the help of the Bureau of Land Management Arctic Field Office for logistical support in the excavation of the Alaskan material. I appreciate my graduate committee members, Sarah Fowell, Kris Hundertmark, Matthew Wooller, and Patrick S. Druckenmiller for their support, and

David Evans and Nicolás Campione for providing me with photos of *Edmontosaurus*. I am grateful to Ron Blakey, Kieran Shepherd, Margaret Beckel, Kevin Seymour, Jack Horner, Alana Gihlick, Carl Mehling, Don Brinkman, and Hiroaki Kikkawa. I also thank H. David Sheet, Daniel Falster, Davit Warton, Ian Wright, and Pablo A. Goloboff, James S. Farris, Kevin Nixon, and Willi Henning Society for their software (Coordgen, MorphoJ, SMATR, TNT).

1.7 Figures

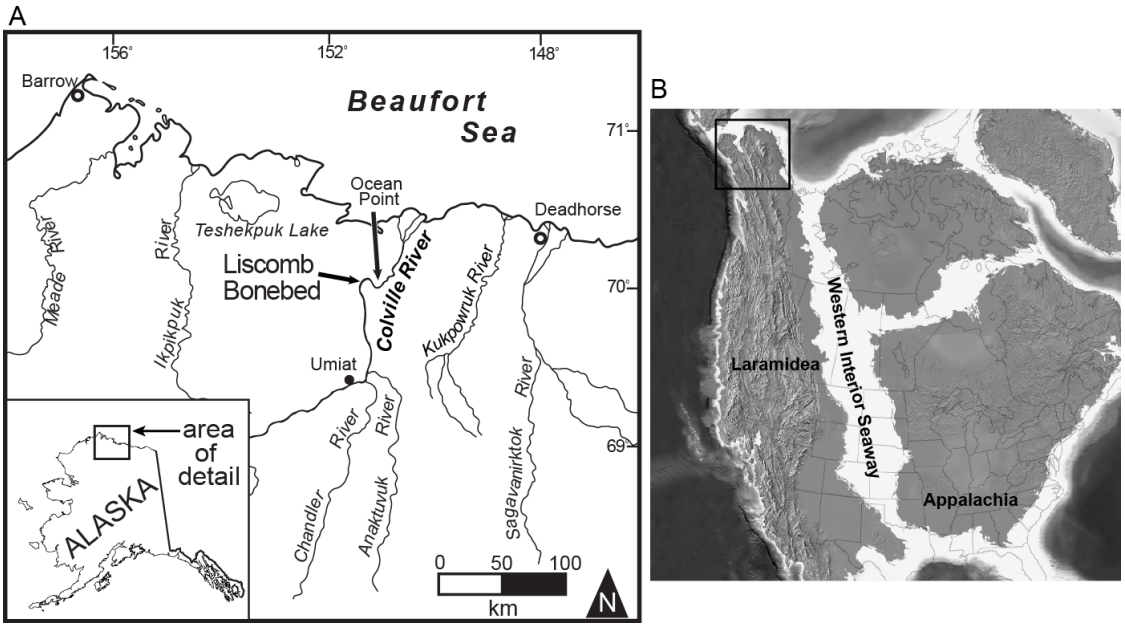

Figure 1-1. (A) Location of the Liscomb Bonebed, and (B) paleogeographic reconstruction of North America at 70 Ma [92]. The inset box indicates the location of present-day Alaska.

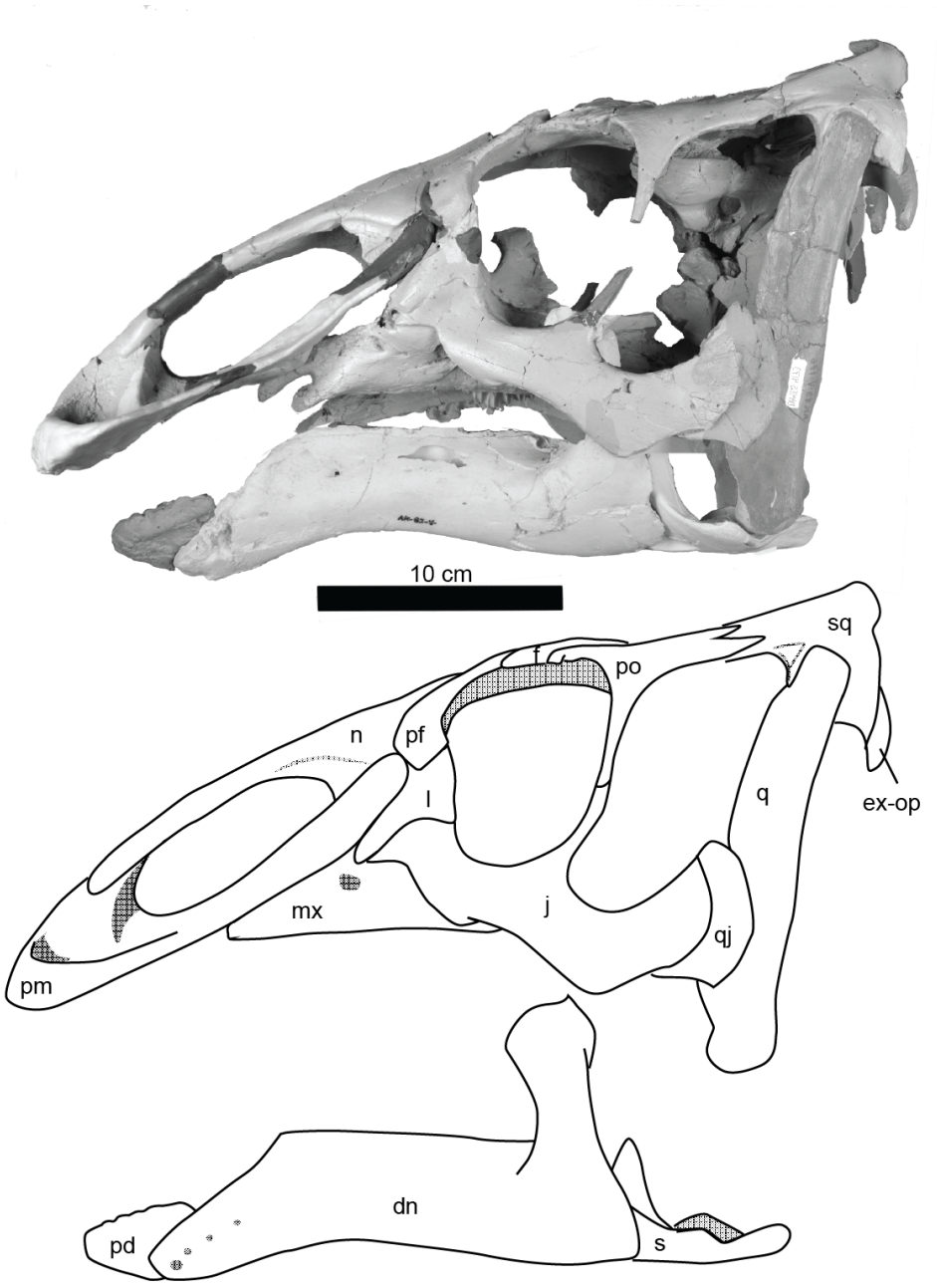

Figure 1-2. Composite cranial reconstruction in left lateral view of the Prince Creek Formation taxon. Abbreviations: dn, dentary; f, frontal; j, jugal; l, lacrimal; mx, maxilla; n, nasal; pd, predentary; pf, prefrontal; pm, premaxilla; po, postorbital; q, quadrate; qj, quadratojugal; s, surangular; sq, squamosal.

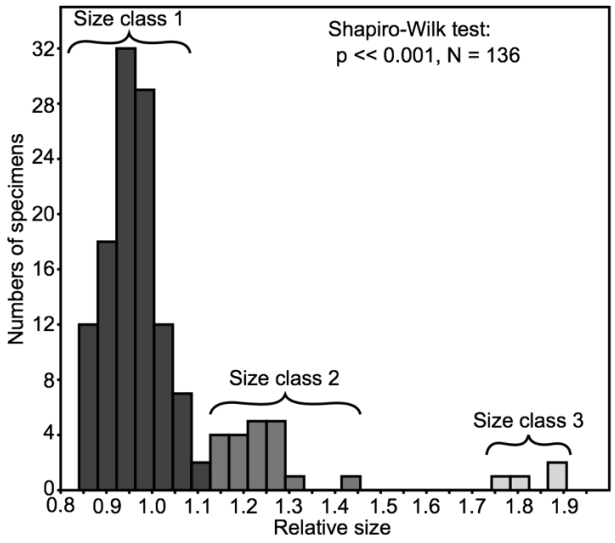

Figure 1-3. Histogram of hadrosaur bones from the Liscomb Bonebed (Prince Creek Formation) for which at least 10 specimens are known. Size is standardized by the mean of size class 1 and 2 specimens for each bone.

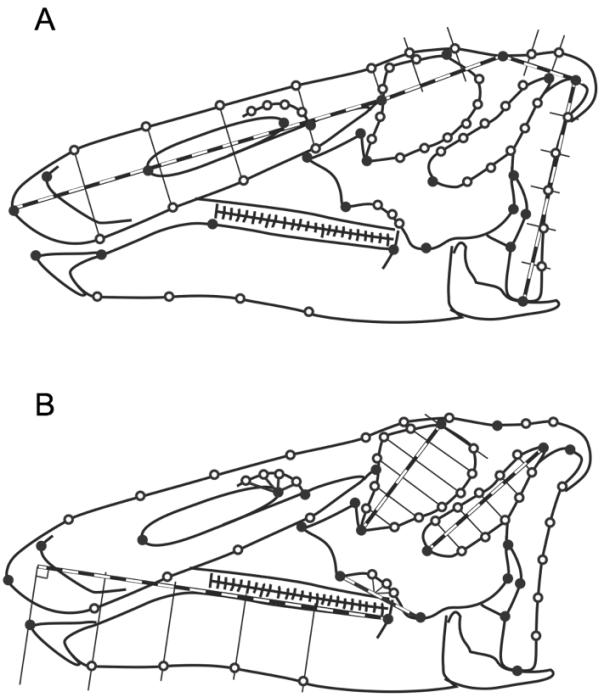

Figure 1-4. Location of landmarks and semi-landmarks used in the geometric morphometric analysis. Closed circles represent landmarks, and open circles represent semi-landmarks. Semi-landmarks are defined with the certain intervals or angles along the broken lines. Figure 1-4A shows how semi-landmarks are defined on the dorsal border of the skull, posterior border of the quadrate, and ventrolateral edge of the premaxilla. Figure 1-4B shows how semi-landmarks are defined on the edges of the orbit, infratemporal fenestra ventral edge of the jugal, and ventral border of the dentary.

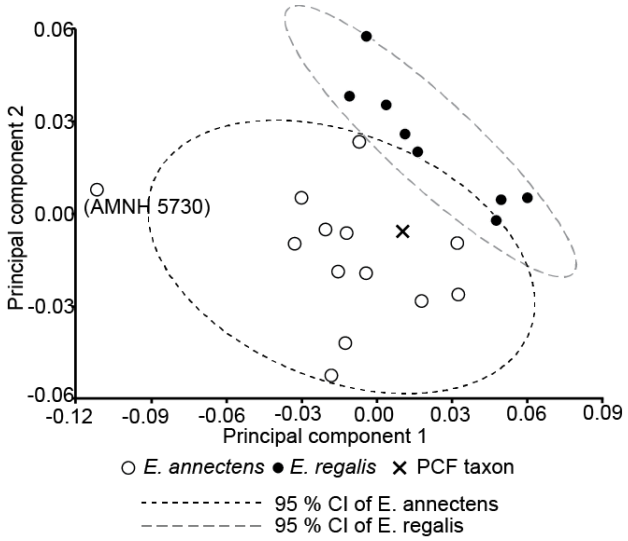

Figure 1-5. Principal component biplot of the geometric morphometric analysis. The Prince Creek Formation taxon clusters with *Edmontosaurus annectens,* outside the 95 % confidence interval of *E. regalis.*

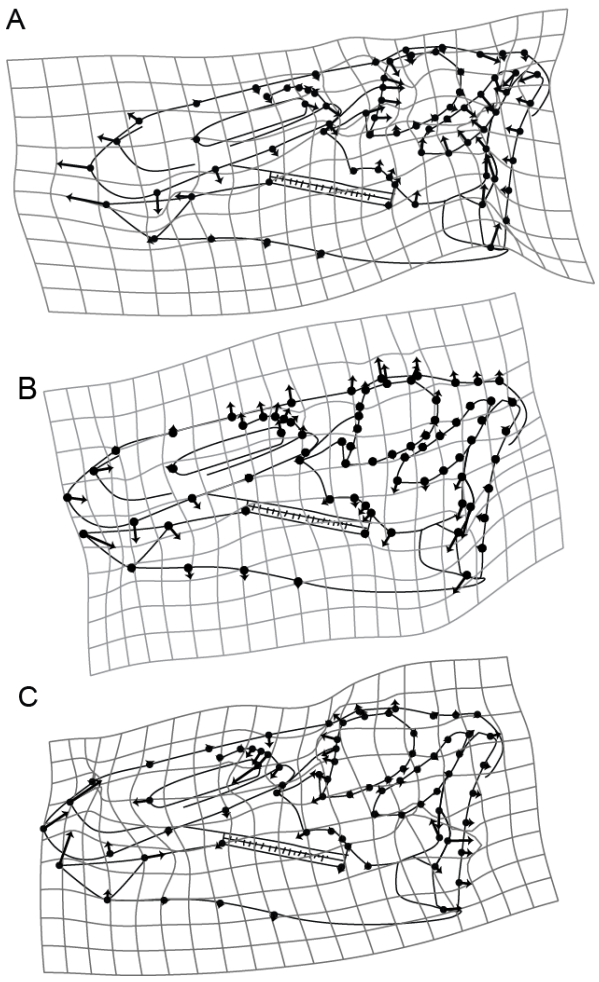

Figure 1-6. Transformation grids. (A) Shape change along the centroid size, which shows a growth pattern change in *Edmontosaurus*. (B) Shape change along PC1, which likely reflects deformation. (C) Shape changes along PC2, which distinguishes *E. regalis* and *E. annectens.*

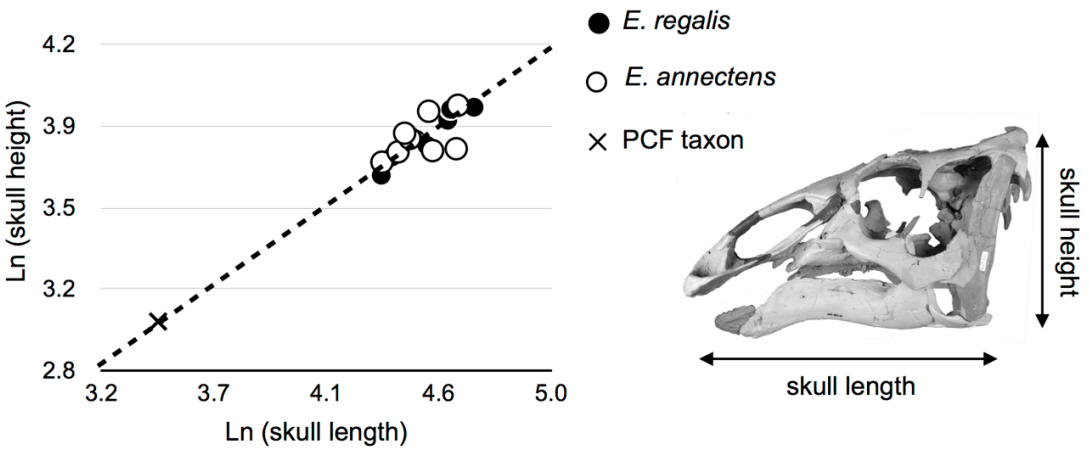

	Group	N	P value (correlation)	Slope (95 % CI)	R^2	P value *E.* a.+ E. *r.*
----	*E.a* + *E. r.*	15	0.00	0.56 to 1.16	0.60	-
	E.a + *E. r.* + PCF	16	0.00	0.65 to 0.88	0.93	0.72

Figure 1-7. Biplot of skull length versus skull height. Because the regression lines are statistically and visually indistinguishable, only one line is shown. Abbreviations: *E. r.*, *Edmontosaurus regalis*; *E. a.*, *Edmontosaurus annectens*; PCF, Prince Creek Formation taxon.

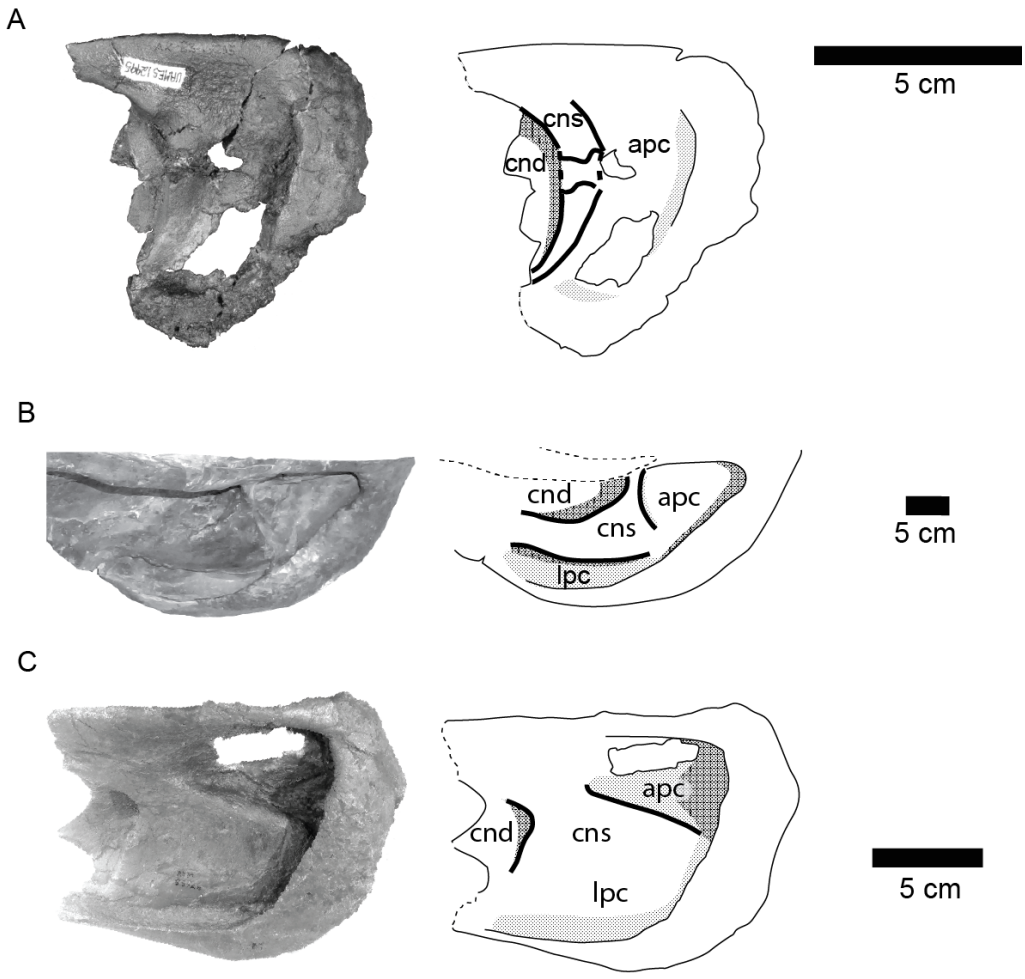

Figure 1-8. Comparison premaxillae in dorsal view. Rostral portion of right premaxillae in dorsal view of (A) size class 1 of the Prince Creek Formation taxon (UAMES 12995), (B) adult *Edmontosaurus regalis* (CMN 2289), and (C) size class 3 *E. annectens* (ROM 53526). Abbreviations: apc, anterior premaxillary cavity; cnd, circumnarial depression; cns, circumnarial septum; lpc, lateral premaxillary cavity; pmfg, premaxillary foramina groove. The circumnarial septum of the PCF taxon projects only posterolaterally, while those of *E. regalis* and *E. annectens* project both anteriorly and posteriorly.

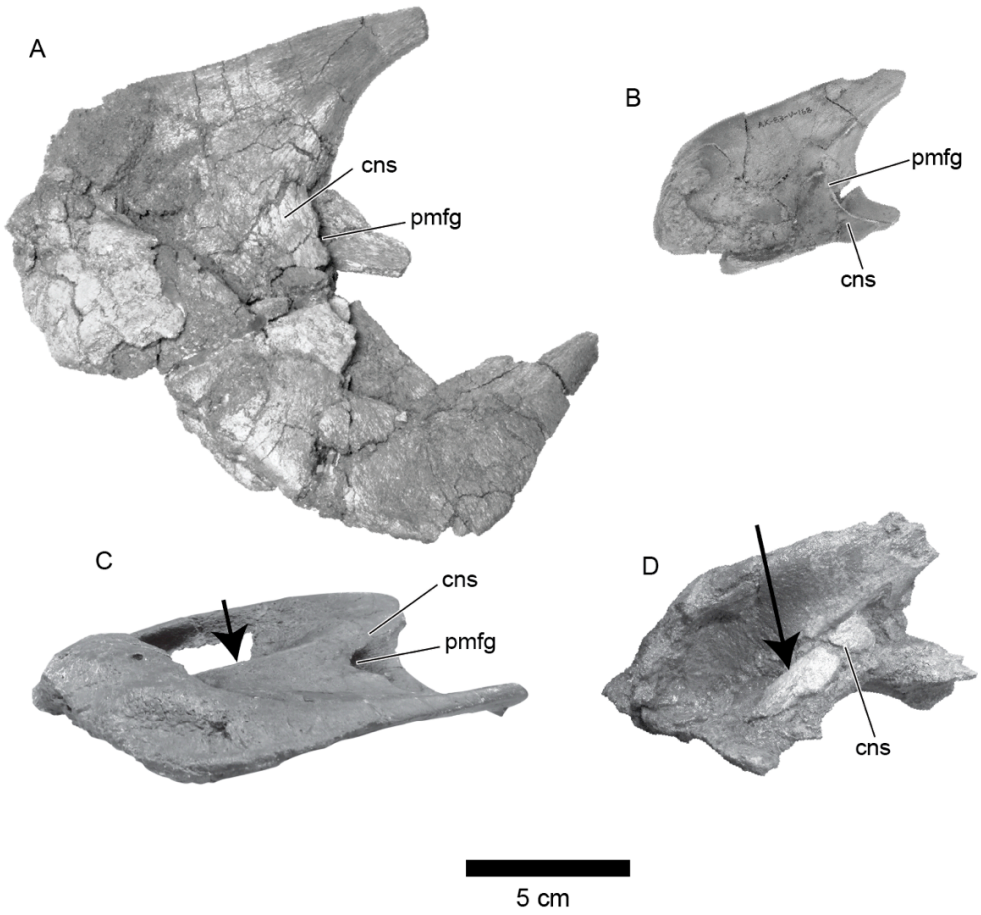

Figure 1-9. Comparison of premaxillae in lateral view. Left premaxillae in lateral view of (A) Size class 2 of the Prince Creek Formation taxon (UAMES 4184), (B) size class 1 of the Prince Creek Formation taxon (UAMES 4955), (C) size class 3 of *Edmontosaurus annectens* (ROM 53526), and (D) size class 2 of *E. annectens* (LACM 23504). Note that the circumnarial septum of *E. annectens* has a fan-shaped circumnarial septum that extends both anteriorly (as shown by the arrows) and posteriorly. In PCF specimens of similar sizes, the circumnarial septum extends only posteriorly. Abbreviations: cns, circumnarial septum; pmfg, premaxillary foramina groove.

Figure 1-10 (facing page). Biplots of (A) the premaxilla versus dentary length, and (B) premaxilla versus premaxillary reflected margin length. When the compared regressions have statistically indistinguishable slopes but statistically significant differences in elevations, the P values are marked with an asterisk. The Prince Creek Formation taxon could not be distinguished from other species in these lengths. When two lines are statistically and visually indistinguishable, only one line is shown. Abbreviations: *E. r., Edmontosaurus regalis*; *E. a., Edmontosaurus annectens*; PCF, Prince Creek Formation taxon.

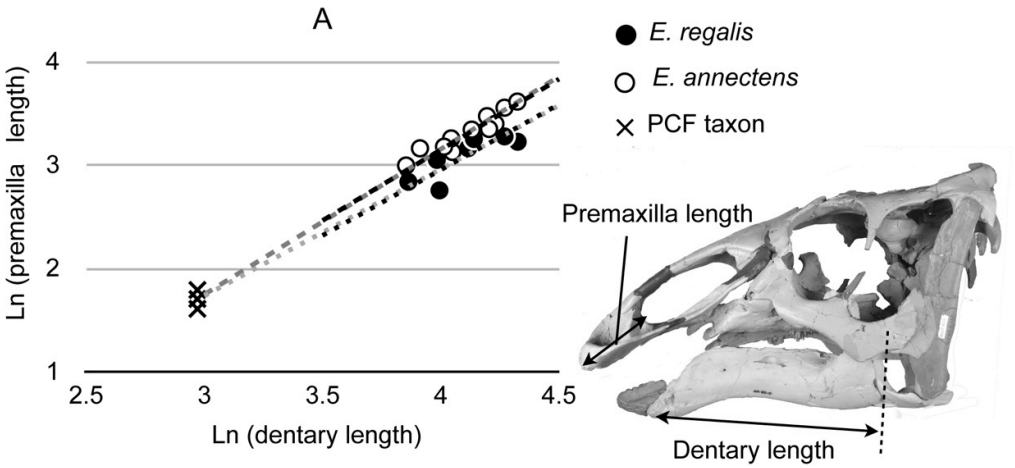

Group	N	P value (correlation)	Slope (95 % CI)	R^2	P value *E.r.*	P value *E.a.*+PCF
E. annectens	11	0.00	1.11 to 1.69	0.92	**0.00***	0.37
E. a. + PCF	14	0.00	1.32 to 1.50	0.99	-	-
					E. a.	*E. r.* + PCF
E. regalis	7	0.02	0.69 to 2.34	0.68	**0.00***	0.90
E. r. + PCF	10	0.00	1.08 to 1.40	0.90	-	-

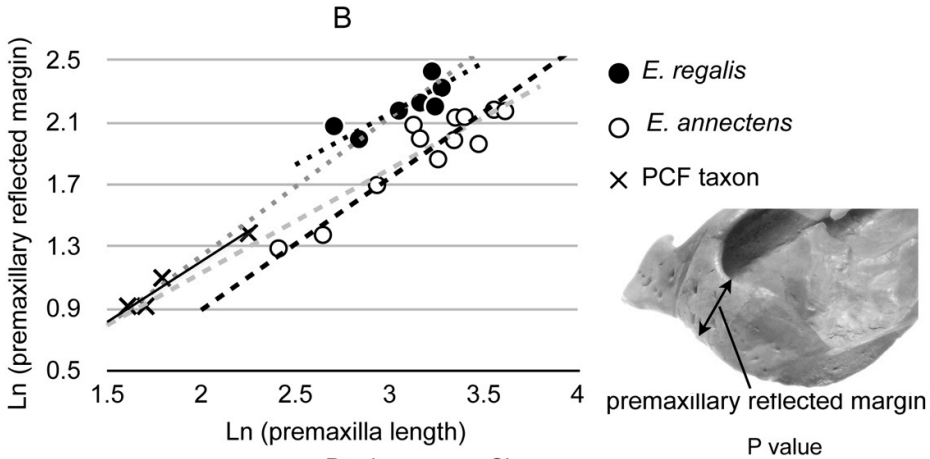

Group	N	P value (correlation)	Slope (95 % CI)	R^2	P value *E. r.*	P value *E.a.* + PCF
E. annectens	12	0.00	0.67 to 1.10	0.87	**0.00***	0.11
E. a. + PCF	16	0.00	0.59 to 0.76	0.95	-	-
PCF material	4	0.02	0.42 to 1.44	0.95	-	0.52
					E. a.	*E.r.* + PCF
E. regalis	7	0.01	0.39 to 1.18	0.75	**0.00***	0.30
E. r. + PCF	11	0.00	0.79 to 1.01	0.97	-	-
PCF material	4	0.02	0.42 to 1.44	0.95	-	0.46

Figure 1-11 (facing page). Biplots of (A) nasal curvature height versus dentary length, and (B) nasal curvature versus dentary length. When the compared regressions have statistically indistinguishable slope values but statistically significant differences in elevation, the P values are marked with an asterisk. Abbreviations: *E. r., Edmontosaurus regalis*; *E. a., Edmontosaurus annectens*; PCF, Prince Creek Formation taxon.

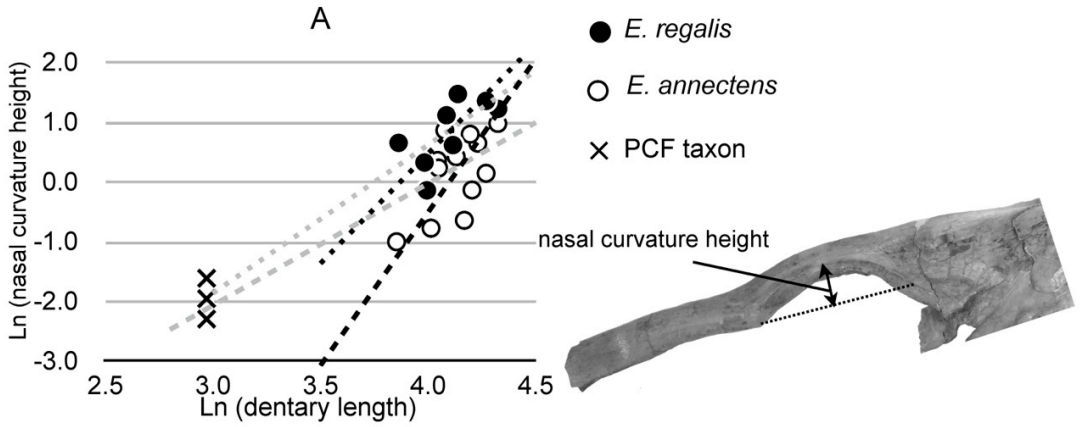

Group	N	P value (correlation)	Slope (95 % CI)	R^2	P value *E.r.*	P value *E.a.*+PCF
E. annectens	12	0.04	3.00 to 8.80	0.35	**0.00***	**0.00**
E. a. + PCF	16	0.00	1.57 to 2.65	0.79	-	-
					E. a.	*E.r.* + PCF
E. regalis	8	0.07	1.85 to 7.32	0.44	**0.00***	0.24
E. r. + PCF	12	0.00	2.07 to 2.99	0.93	-	-

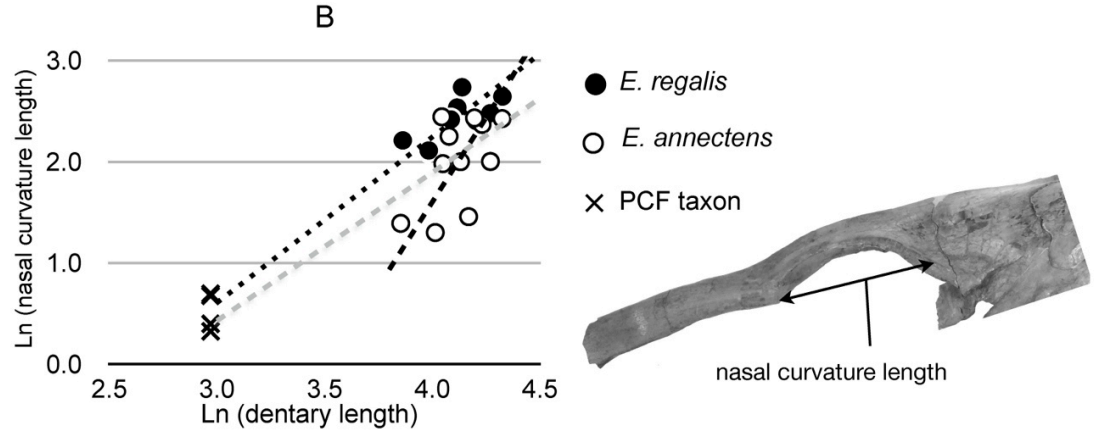

Group	N	P value (correlation)	Slope (95 % CI)	R^2	P value *E.r.*	P value *E.a.*+PCF
E. annectens	12	0.05	1.73 to 5.00	0.30	**0.00***	**0.01**
E. a. + PCF	16	0.00	1.17 to 1.86	0.83	-	-
					E. a.	*E.r.* + PCF
E. regalis	8	0.03	0.86 to 2.97	0.56	**0.00***	0.87
E. r. + PCF	12	0.00	2.07 to 2.99	0.97	-	-

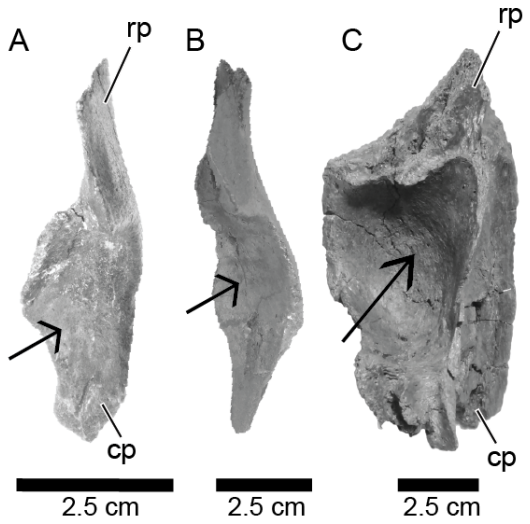

Figure 1-12. Comparison of prefrontals. Left squamosals in ventral view of (A) size class 1 of the Prince Creek Formation taxon (UAMES 13250), (B) size class 3 of *Edmontosaurus annectens* (ROM 53499, reversed), and (C) adult *E. annectens* (ROM 64076, reversed). The arrows point the orbital surface. The prefrontal fossa is only observed in adult specimens. Abbreviations: rp, rostral plate; cp, caudal plate.

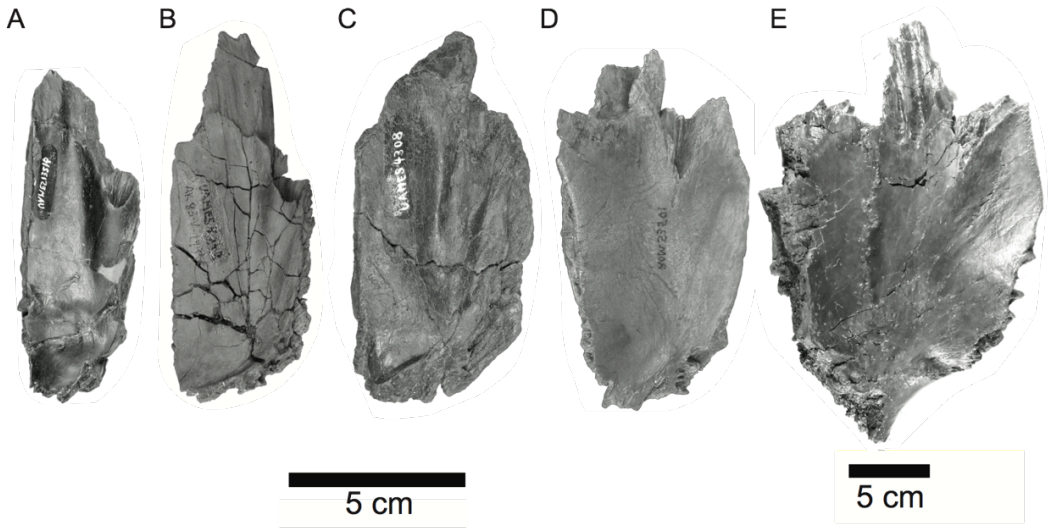

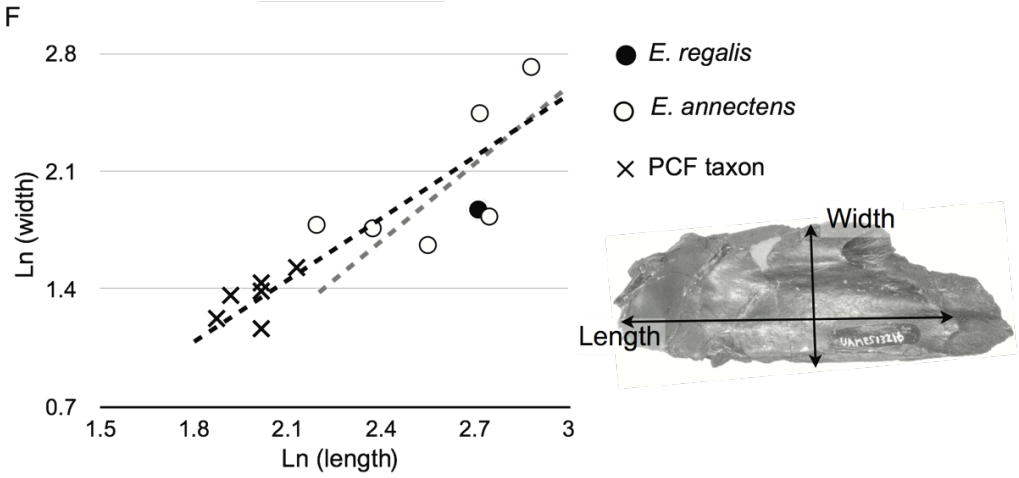

Group	N	P value (correlation)	Slope (95 % CI)	R^2	P value *E. a.* + *E. r.*
E. a. + *E. r.*	7	0.054	0.76 to 3.10	0.56	-
E. a. + *E.r.* + PCF	13	0.000	0.91 to 1.65	0.79	0.53

Figure 1-13. Comparisons of frontals. Left frontals in dorsal views of (A) size class 1 of the Prince Creek Formation taxon (UAMES 13216, reversed), (B) size class 1 of the Prince Creek Formation taxon (UAMES 4242), (C) size class 2 of the Prince Creek Formation taxon (UAMES 4308), (D) size class 3 of *Edmontosaurus annectens* (ROM 53501, reversed), (E) adult *E. annectens* (ROM 64076). (F) Biplot of the frontal lengths versus widths. The length is defined as the portion of the frontal not covered by the nasal anteriorly. Abbreviations: *E. r.*, *Edmontosaurus regalis*; *E. a.*, *E. annectens.* Figure A to D are equally scaled. Scale bar equals 5 cm; PCF, Prince Creek Formation taxon.

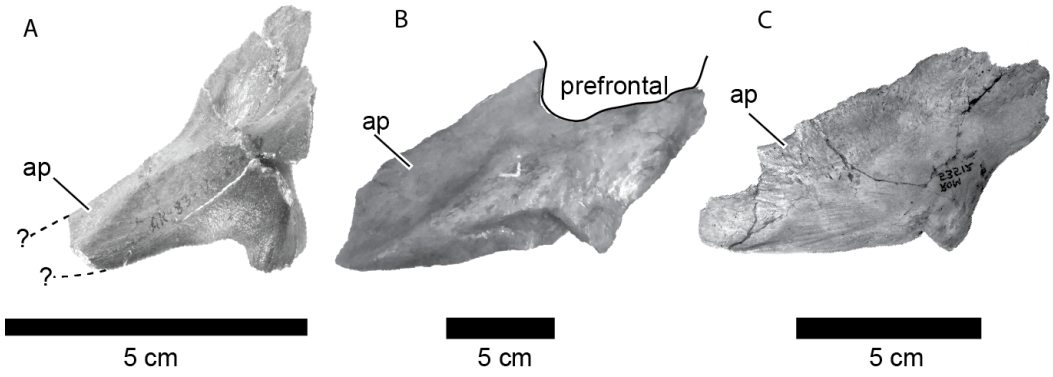

Figure 1-14. Comparison of lacrimals. Lateral views of (A) size class 1 left lacrimal of the Prince Creek Formation taxon (UAMES 4245), (B) adult left lacrimal of *Edmontosaurus regalis* (CMN 2289) and (C) size class 3 right lacrimal of *E. annectens* (ROM 53512, reversed). Note that the anterior process of the lacrimal of the Prince Creek Formation taxon is dorsoventrally narrower than in other specimens. Scale bar represents 5 cm. Abbreviations: ap, anterior process.

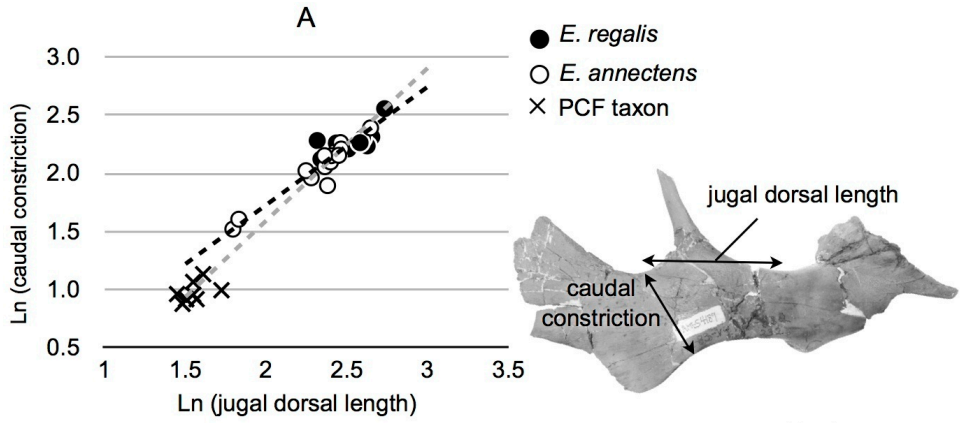

Group	N	P value (correlation)	Slope (95 % CI)	R	P value: *E. a.* + *E. r.*	P value: *E. a.* + *E. r.* + PCF
E. a. + *E. r.*	23	0.00	0.87 to 1.22	0.90	-	**0.01**
E. a. + *E. r.* + PCF	31	0.00	1.22 to 1.42	0.96	**0.01**	-

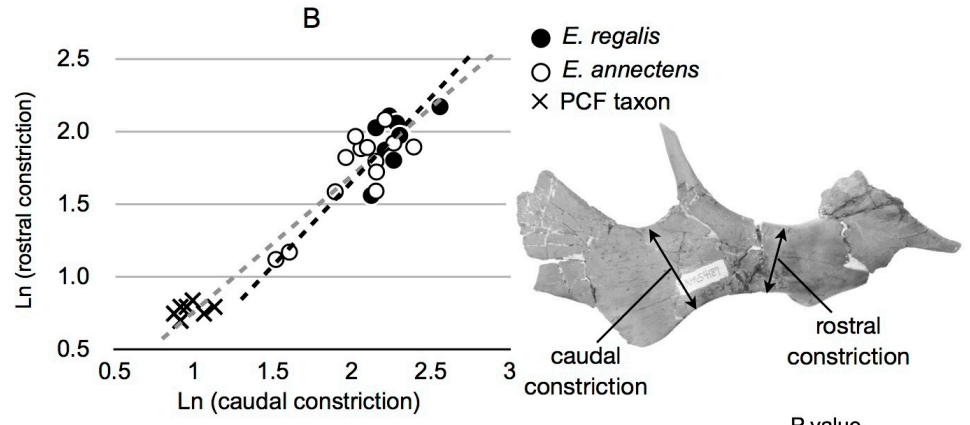

Group	N	P value (correlation)	Slope (95 % CI)	R	P value: *E. a.* + *E. r.*	P value: *E. a.* + *E. r.* + PCF
E. a. + *E. r.*	22	0.00	0.90 to 1.51	0.69	-	0.11
E. a. + *E. r.* + PCF	30	0.00	0.85 to 1.03	0.94	0.11	-

Figure 1-15. Biplots of (A) the jugal length versus caudal constriction, and (B) the jugal caudal constriction versus rostral constriction. The jugal length is defined as the distance between the lower-most points of the infratemporal fenestra and orbit. The Prince Creek Formation taxon has relatively shallower caudal constriction than other species of *Edmontosaurus.* Abbreviations: *E. r.*, *Edmontosaurus regalis*; *E. a.*, *Edmontosaurus annectens*; PCF, Prince Creek Formation taxon.

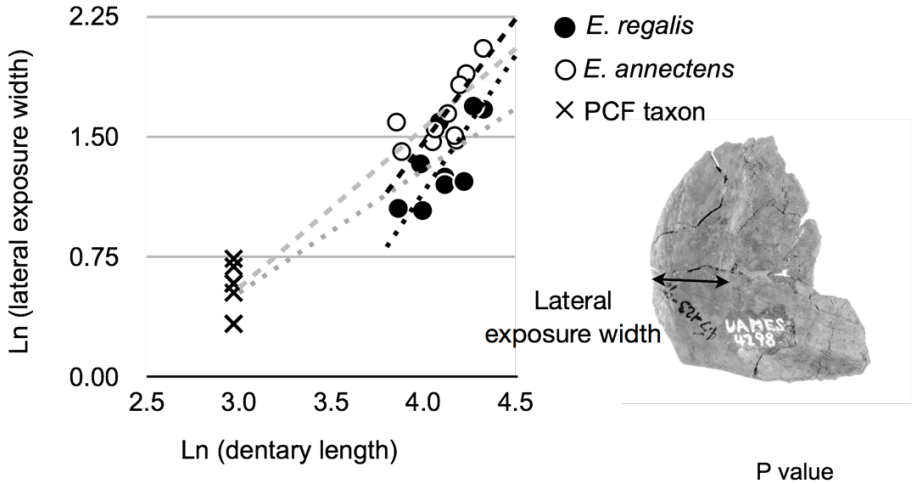

	Group	N	P value (correlation)	Slope (95 % CI)	R^2	P value: *E. r.*	P value: *E. a.* + PCF
- - - -	*E. annectens*	9	0.08	0.80 to 2.98	0.78	**0.00***	0.18
- - - -	*E. a.* + PCF	17	0.00	0.87 to 1.14	0.94	-	-

	Group	N	P value (correlation)	Slope (95 % CI)	R^2	P value: *E. a.*	P value: *E. r.* + PCF
·····	*E. regalis*	9	0.03	0.95 to 3.08	0.51	**0.00***	**0.02**
·····	*E. r.* + PCF	17	0.00	0.63 to 0.94	0.86	-	-

Figure 1-16. Biplot of the lateral exposure width of the quadratojugal versus dentary length. The Prince Creek Formation taxon is similar to *Edmontosaurus annectens* in the lateral exposure width of the quadratojugal. Abbreviations: *E. r.*, *Edmontosaurus regalis*; *E. a.*, *Edmontosaurus annectens*; PCF, Prince Creek Formation taxon. When the compared regressions have a statistically indistinguishable slope values but statistically significant different elevations, the P values are marked with an asterisk. Abbreviations: *E. r.*, *Edmontosaurus regalis*; *E. a.*, *Edmontosaurus annectens*; PCF, Prince Creek Formation taxon.

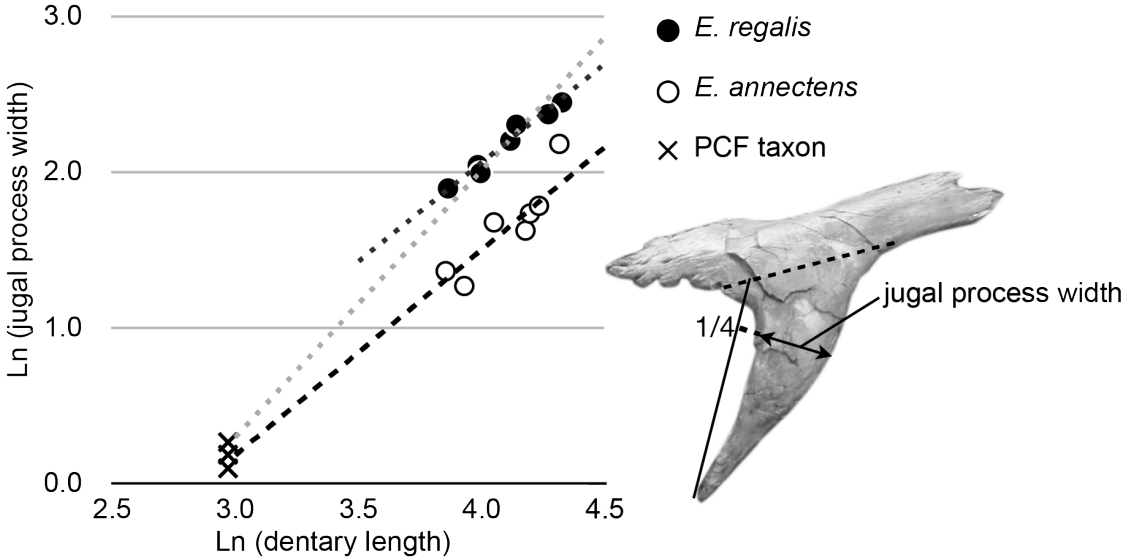

	Group	N	P value (correlation)	Slope (95 % CI)	R^2	P value *E. r.*	P value *E. a.* + PCF
- - - -	*E. annectens*	7	0.01	1.09 to 2.88	0.81	**0.00***	0.22
- - - -	*E. a.* + PCF	11	0.00	1.19 to 1.49	0.98	-	-

	Group	N	P value (correlation)	Slope (95 % CI)	R^2	P value *E. a.*	P value *E. r.* + PCF
·····	*E. regalis*	7	0.00	1.02 to 1.57	0.96	**0.00***	**0.01**
·····	*E. r.* + PCF	11	0.00	1.65 to 1.86	0.99	-	-

Figure 1-17. Biplot of the width of the jugal process versus dentary length. The jugal process width is measured at one-quarter distance from its dorsal end. The Prince Creek Formation taxon has a narrower jugal process than *Edmontosaurus regalis.* When two lines are statistically and visually indistinguishable, only one line is shown. When compared regression lines have statistically indistinguishable slope values but have statistically significant differences in elevation, the P values are marked with an asterisk. Abbreviations: *E. r.*, *Edmontosaurus regalis*; *E. a.*, *Edmontosaurus annectens*; PCF, Prince Creek Formation taxon.

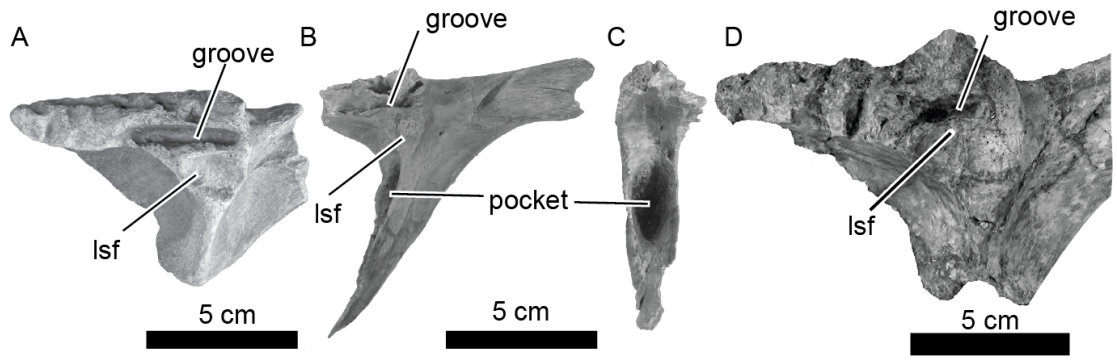

Figure 1-18. Comparison of postorbitals. Right postorbitals of (A) size class 3 of the Prince Creek Formation taxon (UAMES 33308) in medial view, (B, C) size class 2 left postorbital of *Edmontosaurus annectens* (ROM 53513, reversed), in medial and anterior view, and (D) adult left postorbital of *Kundurosaurus nagornyi* (AENM 2/921-6), from Godefroit et al., 2012, Fig. 6 [55] in medial view. Note that the size class 3 specimens of the Prince Creek Formation taxon do not have a deep posterior orbital pocket seen in the size class 2 specimens of *E. annectens*, but the articulation surface with the frontal is identical. Abbreviation: lsf, laterosphenoid facet.

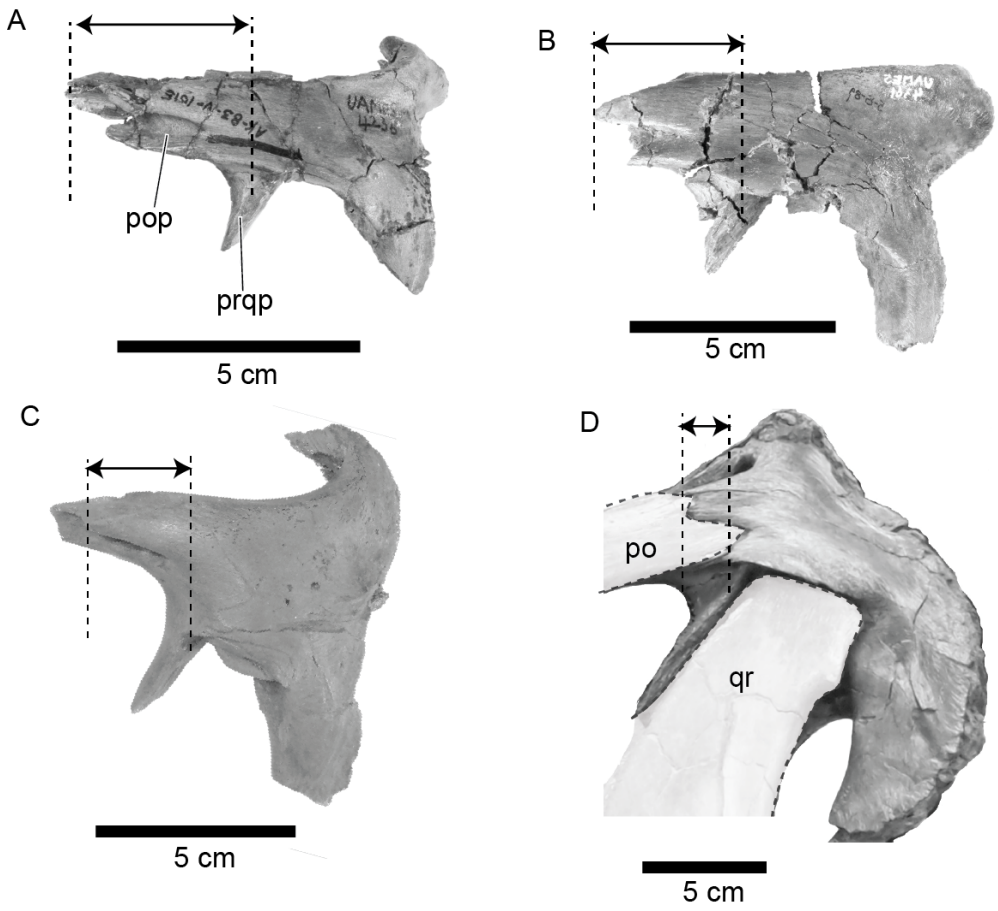

Figure 1-19 Comparison of squamosals. Left squamosals in lateral view of (A) size class 1 of the Prince Creek Formation taxon (UAMES 4236), (B) size class 2 of the Prince Creek Formation taxon (reversed, UAMES 4361), (C) size class 2 of *E. annectens* (reversed, ROM 53510), (D) subadult *E. annectens* (CMN 8509). Larger specimens have shorter postorbital processes anterior to the prequadratic processes. Scale bars represent 5 cm. Abbreviations: po, postorbital; pop, postorbital process; prqp, prequadratic process; qr, quadrate.

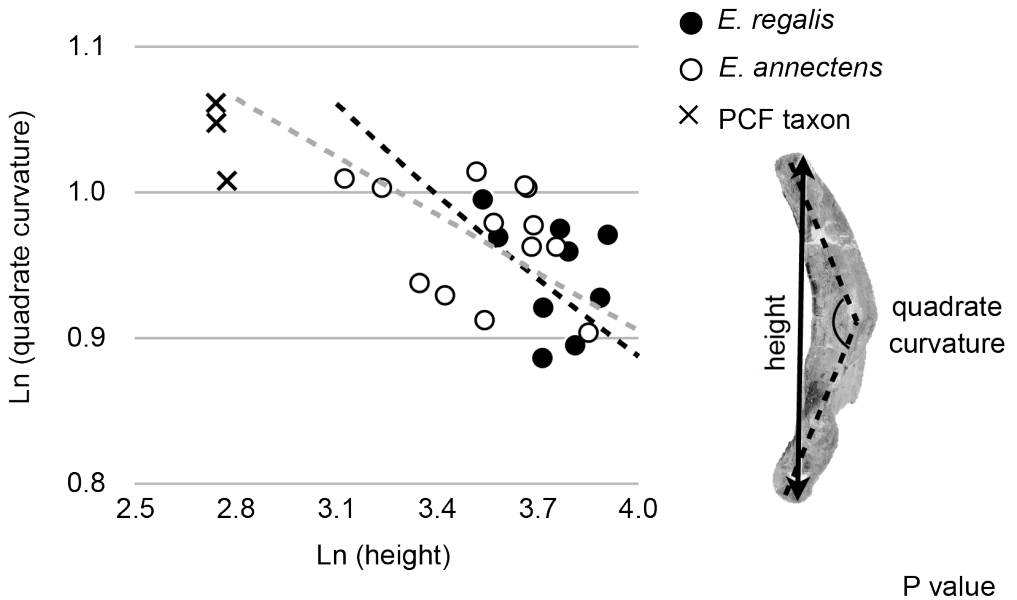

Group	N	P value (correlation)	Slope (95 % CI)	R^2	P value: E. a. + E. r.	P value: E. a. + E. r. + PCF
E. a. + *E. r.*	22	0.06	-0.24 to -0.11	0.17	-	0.15
E. a. + *E. r.* + PCF	25	0.00	-0.15 to 0.08	0.44	0.15	-

Figure 1-20. Biplot of the quadrate height versus its curvature in radian. Abbreviations: *E. r.*, *Edmontosaurus regalis*; *E. a.*, *Edmontosaurus annectens*; PCF, Prince Creek Formation taxon.

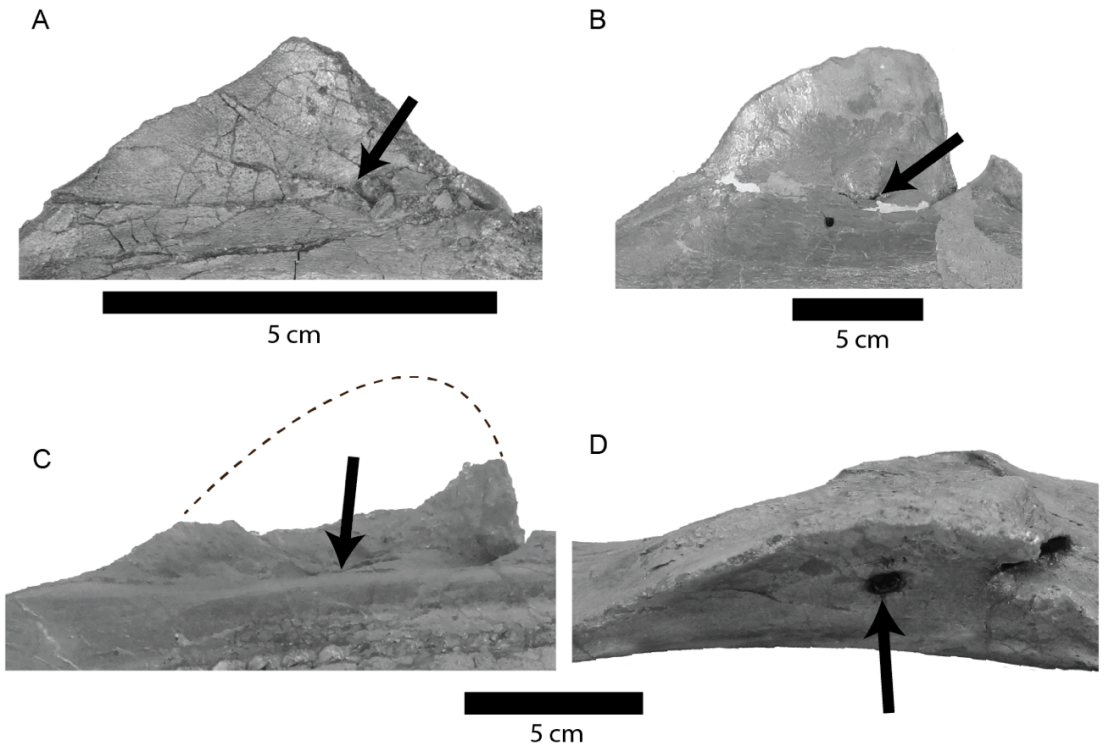

Figure 1-21. Comparison of lacrimal processes of the maxilla. Right lacrimal processes of the maxilla of (A) size class 1 of the Prince Creek Formation taxon (UAMES 4327) in medial view, (B) adult *Edmontosaurus regalis* (CMN 2289: B) in medial view, (C, D) size class 3 of *E. annectens* (ROM 53528) in medial and dorsal view. In the PCF taxon and *E. regalis*, the canal opens medially, while in *E. annectens* the canal opens dorsally.

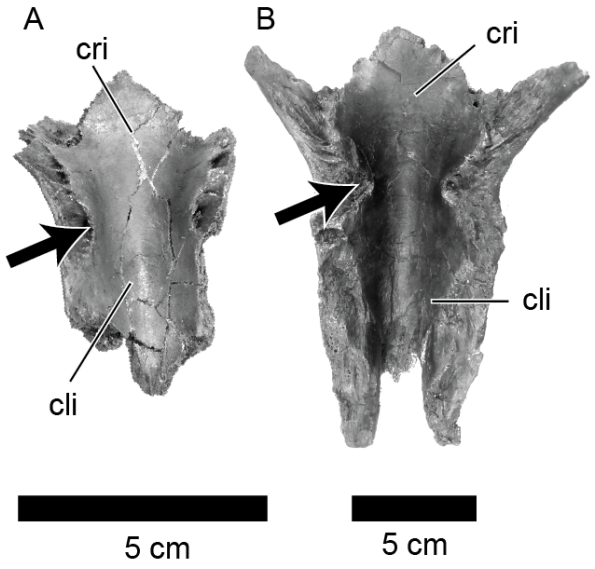

Figure 1-22. Comparison of parietals. Parietal in ventral view of (A) size class 1 of the Prince Creek Formation taxon (UAMES 4309) and (B) size class 3 of *Edmontosaurus annectens* (ROM 53493). The bulge between cerebral and cerebellar impressions (pointed by arrows) is less developed in the Prince Creek Formation taxon than in *E. annectens.* Abbreviations: cli, cerebellum impression; cri, cerebrum impression.

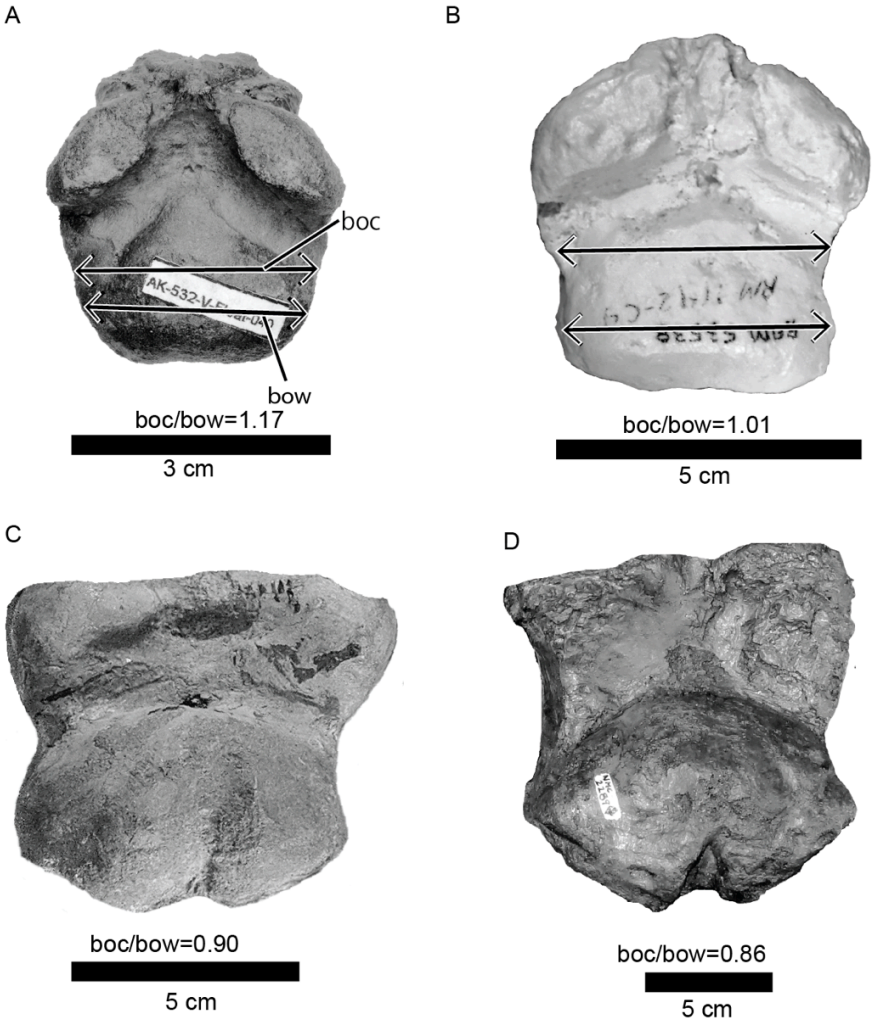

Figure 1-23. Copmarison of basioccipitals. Basioccipitals in ventral view of (A) size class 1 of the Prince Creek Formation taxon (UAMES 4276), (B) size class 2 of *E. annectens* (ROM 53583), (C) size class 3 of *E. annectens* (AMNH 427), and (D) adult *E. regalis* (CMN 2289). Abbreviations: boc, basioccipital constriction; bow, basioccipital posterior width.

Figure 1-24 (facing page). Comparison of exoccipital-opisthotics. Right exoccipital-opisthotic of (A, B) a relatively small size class 1 of the Prince Creek Formation taxon (UAMES 4279) in lateral and dorsal view, (C, D) large size class 1 of the Prince Creek Formation taxon (UAMES 4095) in lateral and dorsal view, (E, F) size class 2 of the PCF taxon (UAMES 4263) in lateral and dorsal view (G), subadult *E. annectens* (ROM 64077) in lateral view, and (H) adult *E. annectens* (ROM 59786) in lateral view. The auxiliary line "i" is drawn so that it crosses cranial nerves IX to XII. Line "ii" is orthogonal to line "i" and contacts with the posterior-most part of the exoccipital condyloid. Auxiliary line "iii" is drawn on the lateral suture of the exoccipital-opisthotic and the supraoccipital. Note that the apex of the opisthotic (indicated by the arrows) shifts posteriorly relative the line "ii" in larger specimens, and that the angles between lines "i" and "iii" are more acute in larger specimens. In posterodorsal view (B, D, F), the angles between the paraoccipital processes and the exoccipital condyloids are more obtuse. Scale bars equal 5 cm. Abbreviations: eoc; exoccipital condyloid; mbeo, middle body of the exoccipital-opisthotic; pocp, paraoccipital process.

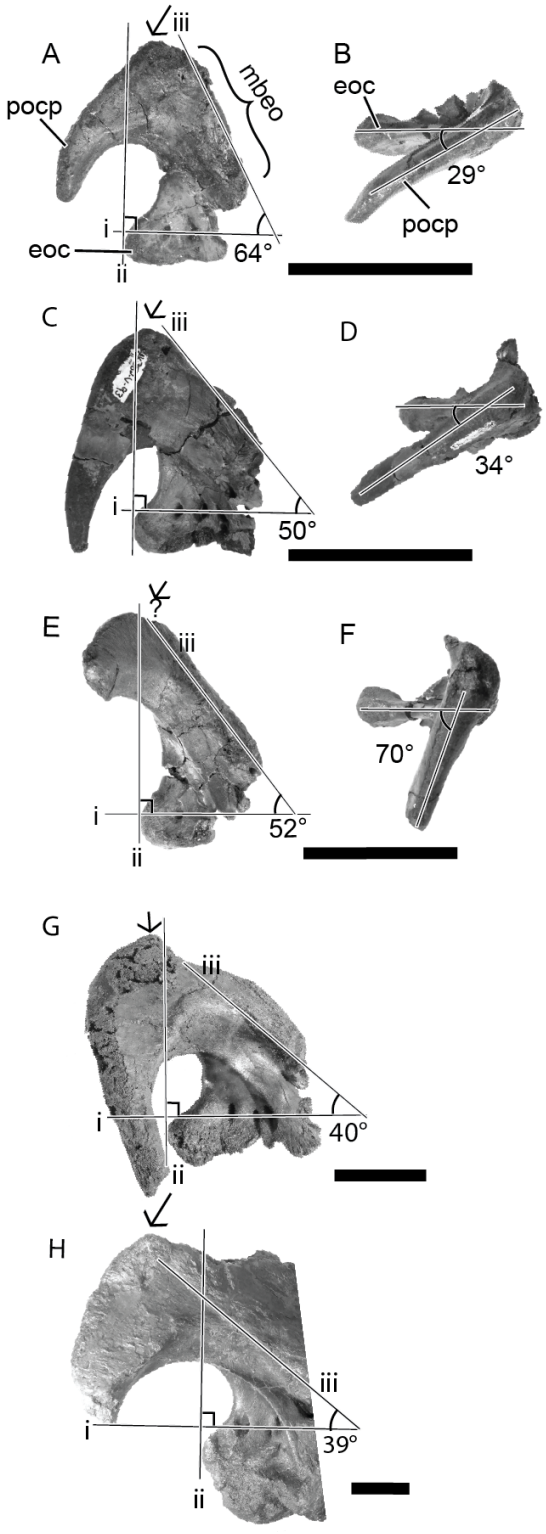
A
iii
mbeo
pocp
i
eoc
ii
64°
B
eoc
29°
pocp
C
iii
i
50°
D
34°
E
?
iii
i
ii
52°
F
70°
G
iii
i
ii
40°
H
iii
i
ii
39°

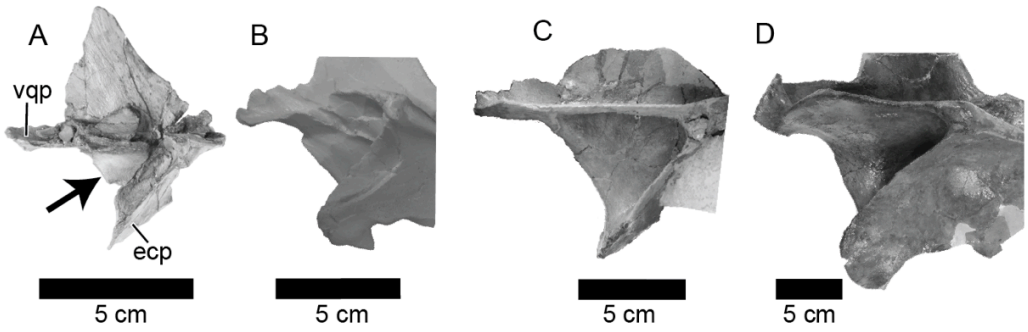

Figure 1-25. Comparison of pterygoids. Left pterygoids in medial view of (A) size class 1 of the PCF specimen (UAMES 4215), (B) size class 2 of *E. annectens* (ROM 53539, reversed), (C) subadult *E. annectens* (CMN 8509), and (D) adult *E. regalis* (CMN 2289). The arrow indicates the position of the bony lamina between the ventral quadrate process and ectopterygoid process. Abbreviations: ecp, ectopterygoid process; vqp, ventral quadrate process.

Figure 1-26 (facing page). Biplots of (A) dentary deflection (in radians) versus dentary length and (B) posterior edentulous process length versus dental battery length. Abbreviations: *E. r., Edmontosaurus regalis; E. a., Edmontosaurus annectens*; PCF, Prince Creek Formation taxon.

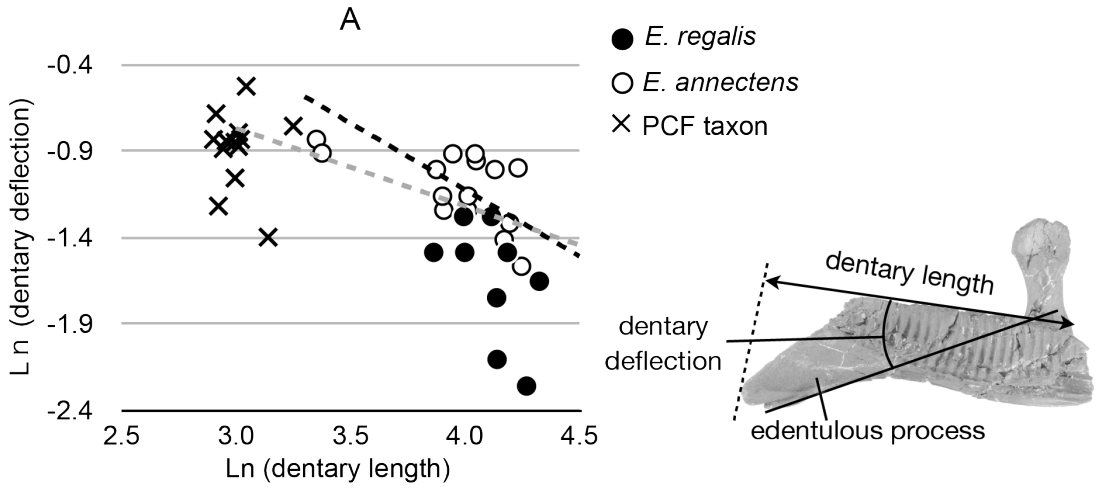

Group	N	P value (correlation)	Slope (95 % CI)	R^2	P value *E. a.*	P value *E. a.* + PCF
E. annectens	15	0.03	-1.23 to -0.47	0.32	-	0.07
E. annectens + PCF	28	0.00	-0.62 to -0.32	0.32	0.07	-

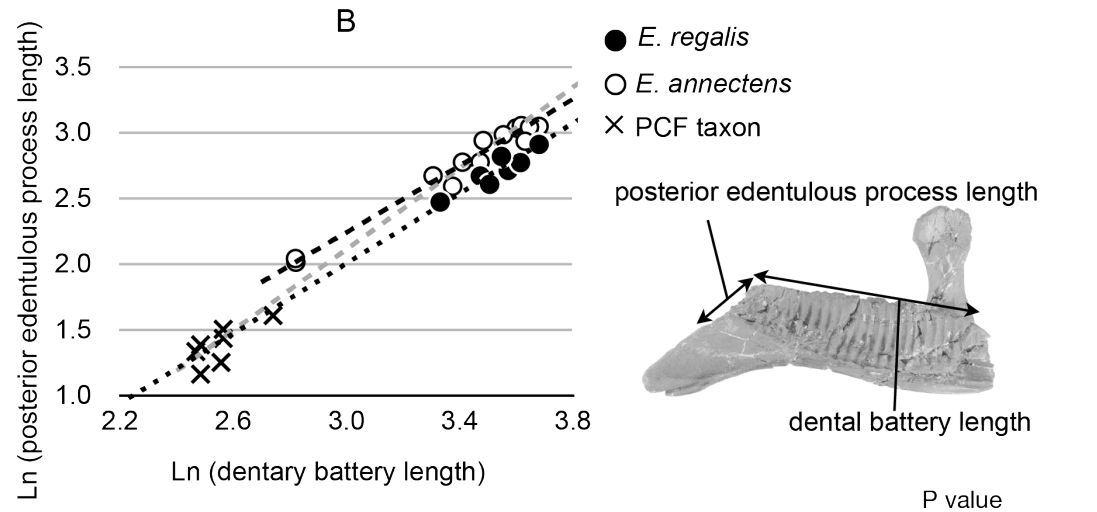

Group	N	P value (correlation)	Slope (95 % CI)	R^2	P value *E. r.*	P value *E.a.* + PCF
E. annectens	13	0.00	1.11 to 1.40	0.97	**0.00***	**0.01**
E. a. + PCF	20	0.00	1.42 to 1.64	0.98	-	-
					E. a.	*E.r.* + PCF
E. regalis	8	0.00	0.93 to 1.82	0.88	**0.00***	0.79
E. r. + PCF	15	0.00	1.27 to 1.45	0.99	-	-

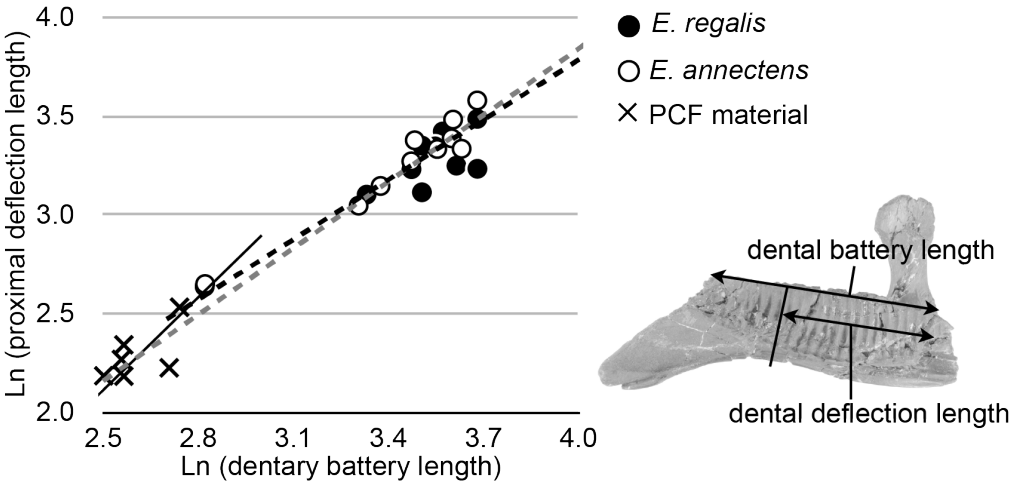

Group	N	P value (correlation)	Slope (95 % CI)	R^2	P value: *E. a.* + *E. r.* + PCF
- - - - *E. a.* + *E. r.*	20	0.00	0.84 to 1.20	0.86	0.28
- - - - *E. a.* + *E. r.* + PCF	28	0.00	1.03 to 1.21	0.96	-
——— PCF material	8	0.02	0.87 to 2.82	0.61	0.23

Figure 1-27. Biplots of dental deflection length versus dental battery length. Abbreviations: *E. r.*, *Edmontosaurus regalis*; *E. a.*, *Edmontosaurus annectens*; PCF, Prince Creek Formation taxon.

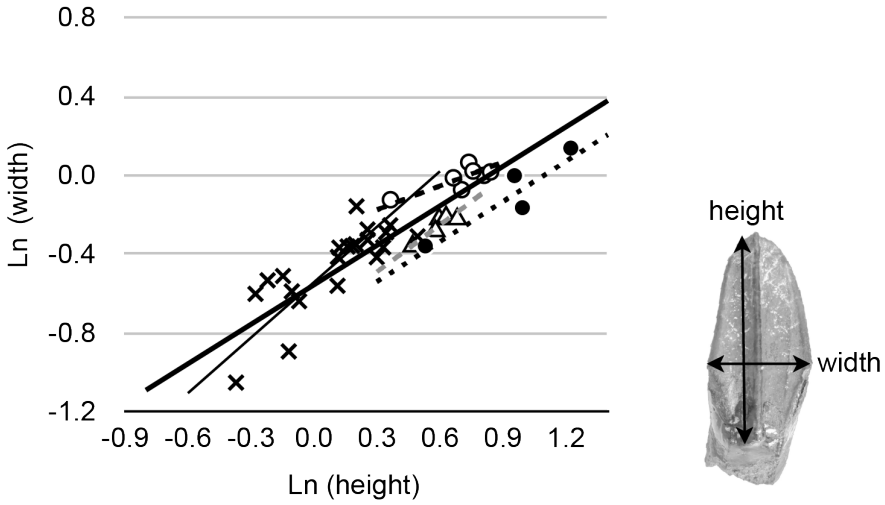

	Group	N	P value (correlation)	Slope (95 % CI)	R^2	p value: All samples	p value: DMNH 1493
	All samples	38	0.00	0.57 to 0.79	0.76	-	**0.03***
○	DMNH 1493 (*E. a.*)	7	0.04	0.21 to 0.78	0.62	**0.03***	-
△	BHI-6218 (*E. a.*)	5	0.03	0.39 to 1.60	0.83	**0.00***	**0.00***
●	CMN 2289 (*E.r.*)	5	0.01	0.41 to 1.25	0.90	**0.00***	-
×	PCF taxon	21	0.00	0.46 to 0.86	0.78	0.06	**0.04**

Figure 1-28. Biplot of the dentary tooth height versus width. Abbreviations: *E. r.*, *Edmontosaurus regalis*; *E. a.*, *Edmontosaurus annectens*.

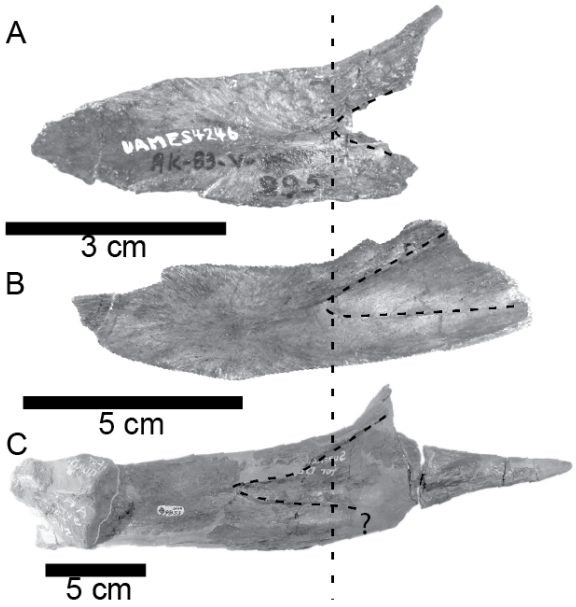

Figure 1-29. Comparison of splenials. Right splenials in lateral view of (A) the Prince Creek Formation taxon (UAMES 4246), (B) size class 3 of the *Edmontosaurus annectens* (ROM 53532, reversed), and (C) adult *E. regalis* (CMN 2289, reversed.) The broken line is drawn on the inflection points of the dorsal lines of the splenials, and broken curves indicate the dentary process indentation on the splenial.

Figure 1-30 (facing page). Biplots of (A) coronoid process length versus scapular blade length, and (B) scapular maximum width versus scapular blade width. Abbreviations: *E. r.*, *Edmontosaurus regalis*; *E. a.*, *Edmontosaurus annectens*; PCF, Prince Creek Formation taxon.

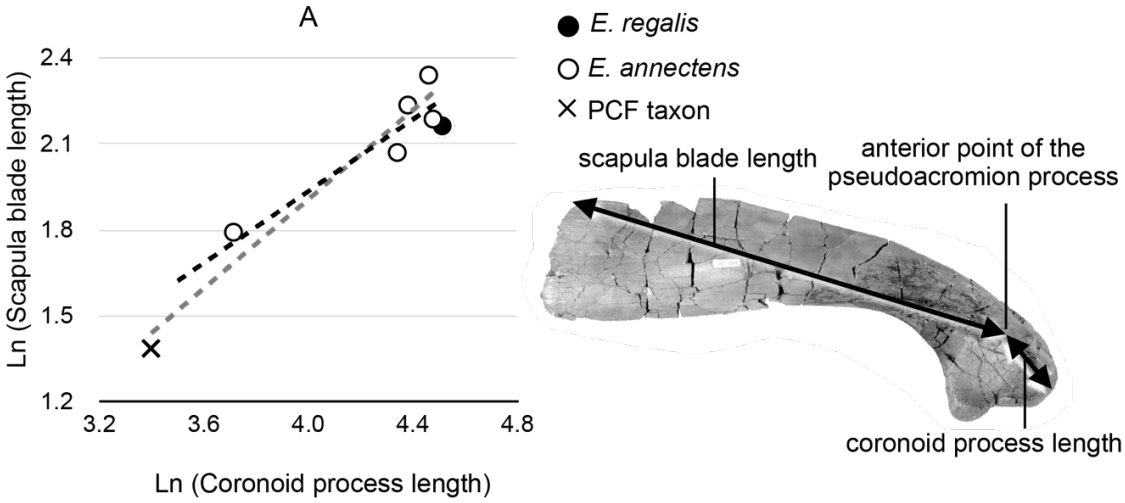

Group	N	P value (correlation)	Slope (95 % CI)	R	P value *E. a.* + *E.r.* + PCF
E.a + *E. r.*	6	0.02	0.35 to 1.11	0.81	0.55
E.a + *E. r.* + PCF	7	0.00	0.54 to 1.02	0.92	-

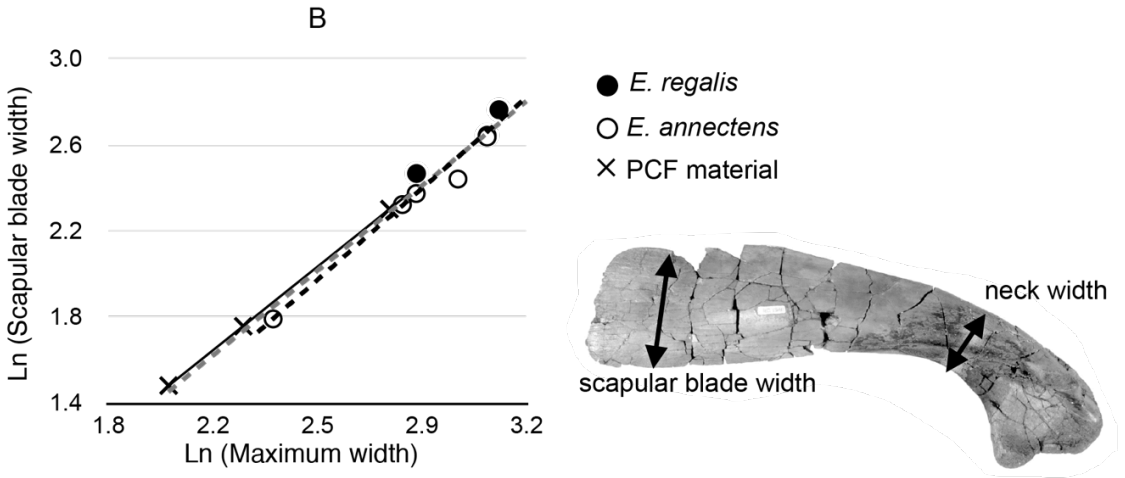

Group	N	P value (correlation)	Slope (95% CI)	R	P value *E. a.* + *E. r.* + PCF
E.a + *E. r.*	8	0.00	1.01 to 1.47	0.96	0.40
E.a + *E. r.* + PC	11	0.00	1.03 to 1.24	0.98	-
PCF	3	0.00	1.09 to 1.13	1.00	0.74

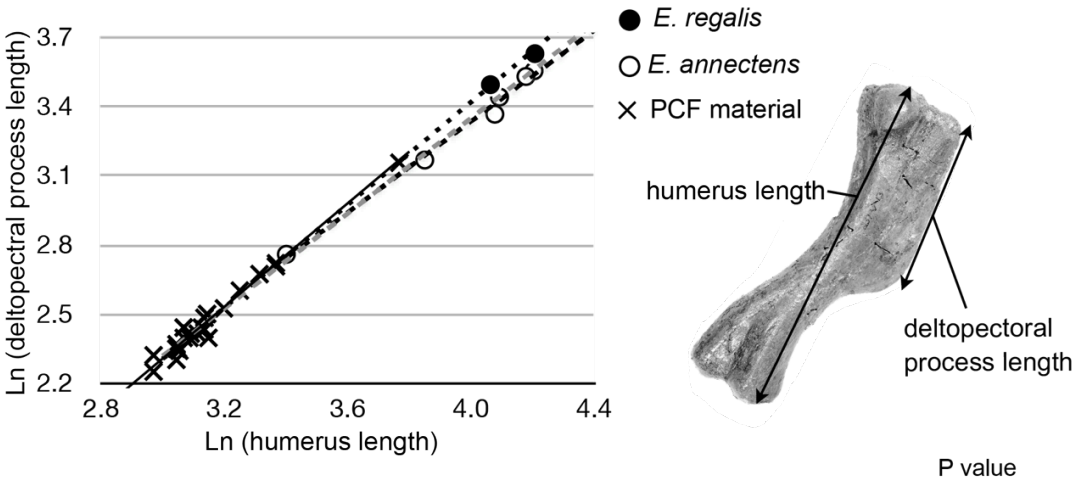

	Group	N	P value (correlation)	Slope (95 % CI)	R^2	P value: *E. r.*	P value: *E.a.* + PCF
- - - -	*E. annectens*	6	0.00	0.87 to 1.16	0.99	**0.00***	0.44
- - - -	*E. a.* + PCF	30	0.00	1.00 to 1.07	0.99	-	-
———	PCF material	24	0.00	1.04 to 1.20	0.97	-	0.03
						E. a.	*E.r.* + PCF
·····	*E. r.* + PCF	26	0.00	1.07 to 1.15	0.99	**0.00***	-
———	PCF material	24	0.00	1.06 to 1.22	0.93	-	0.61

Figure 1-31. Biplot of humerus versus deltopectoral process lengths. A statistically significant difference is not observed after Bonferroni adjustment. Abbreviations: *E. r.*, *Edmontosaurus regalis*; *E. a.*, *Edmontosaurus annectens*; PCF, Prince Creek Formation taxon.

Figure 1-32 (facing page). Biplot of (A) constriction of the ulnar diaphysis versus olecranon process thickness and (B) ulna length versus diaphysis width. Abbreviations: *E. r., Edmontosaurus regalis; E. a., Edmontosaurus annectens*; PCF, Prince Creek Formation taxon.

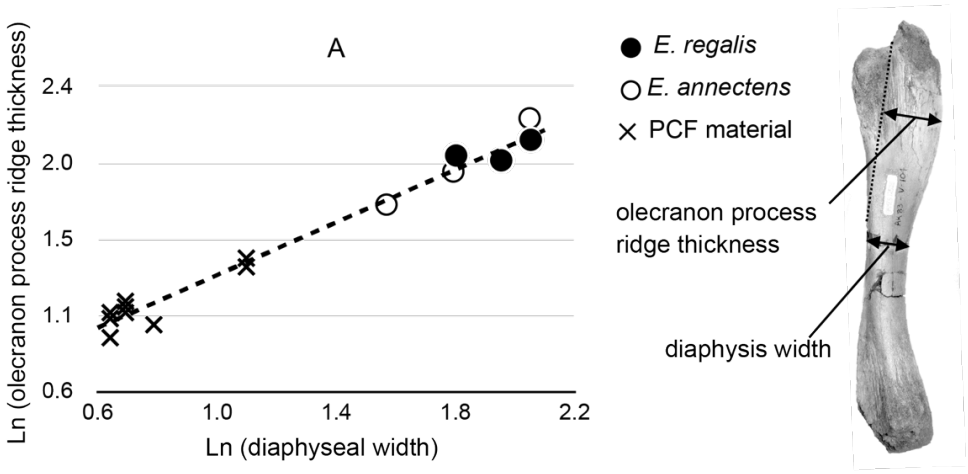

	Group	N	P value (correlation)	Slope (95 % CI)	R^2	P value *E. a.* + *E. r.* + PCF
	E. a. + *E. r.*	6	0.01	0.56 to 1.55	0.85	0.46
- - - -	*E. a.* + *E. r.* + PCF	15	0.00	0.73 to 0.87	0.98	-
	PCF material	9	0.00	0.55 to 1.22	0.79	0.88

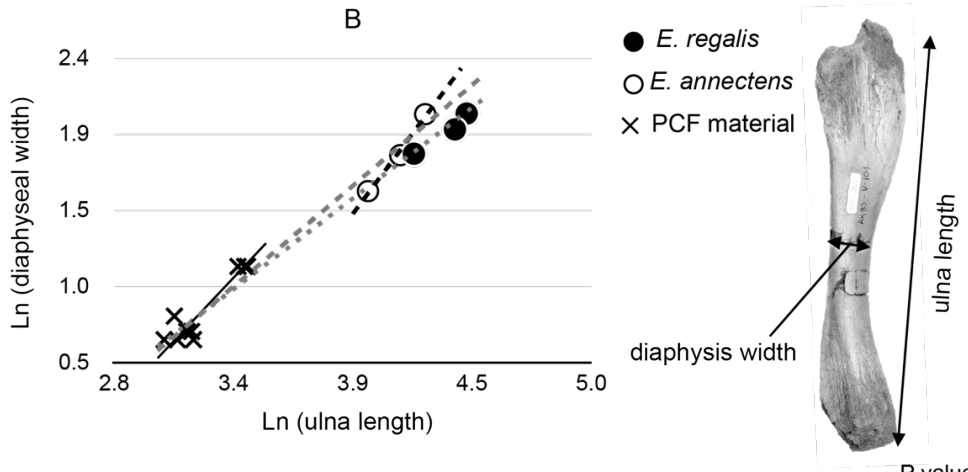

	Group	N	P value (correlation)	Slope (95 % CI)	R^2	P value *E. r.*	P value *E. a.* + PCF
- - - - -	*E. annectens*	3	0.07	0.57 to 5.71	0.99	**0.00***	0.16
- - - - -	*E. annectens* + PCF	13	0.00	1.02 to 1.27	0.97	-	-
———	PCF material	10	0.00	1.08 to 1.92	0.87	-	0.88
							E. r. + PCF
.....	*E. regalis* + PCF	13	0.00	0.94 to 1.13	0.98		-
———	PCF material	10	0.00	1.08 to 1.92	0.87		**0.03**

Figure 1-33 (facing page). Biplots of (A) pubic neck height versus femur length and (B) pubic neck length versus femur length. Abbreviations: *E. r.*, *Edmontosaurus regalis*; *E. a.*, *Edmontosaurus annectens*; PCF, Prince Creek Formation taxon.

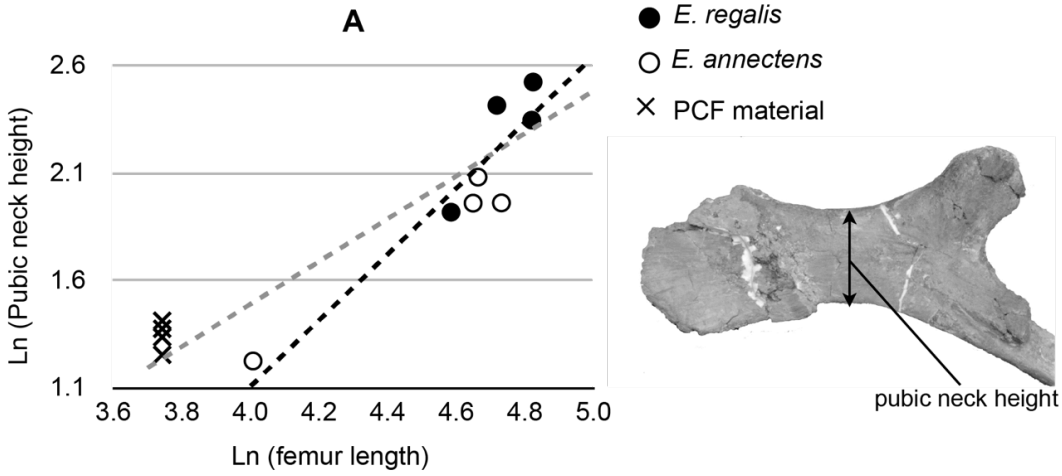

Group	N	P value (correlation)	Slope (95 % CI)	R^2	P value *E.* a.+ E. *r.*
E.a + *E. r.*	9	0.00	1.08 to 2.18	0.84	-
E.a + *E. r.* + PCF	13	0.00	0.78 to 1.26	0.87	**0.02**

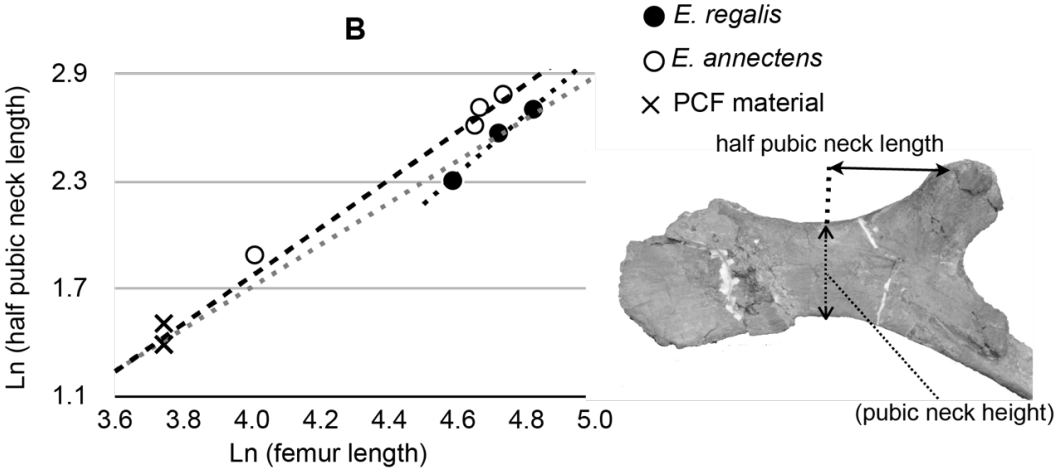

Group	N	P value (correlation)	Slope (95 % CI)	R^2	P value *E. r.*	P value *E. a.* + PCF
E. annectens	5	0.01	0.84 to 1.86	0.95	**0.00***	-
E.annectens + PCF	9	0.00	1.21 to 1.56	0.98	-	0.61
					E. a.	*E.r.* + PCF
E. regalis	4	0.01	1.23 to 2.30	0.99	**0.00***	-
E.regalis + PCF	8	0.00	1.08 to 1.30	0.99	-	**0.04**

Figure 1-33 (facing page). Biplots of (A) pubic neck height versus femur length and (B) pubic neck length versus femur length. Abbreviations: *E. r.*, *Edmontosaurus regalis*; *E. a.*, *Edmontosaurus annectens*; PCF, Prince Creek Formation taxon.

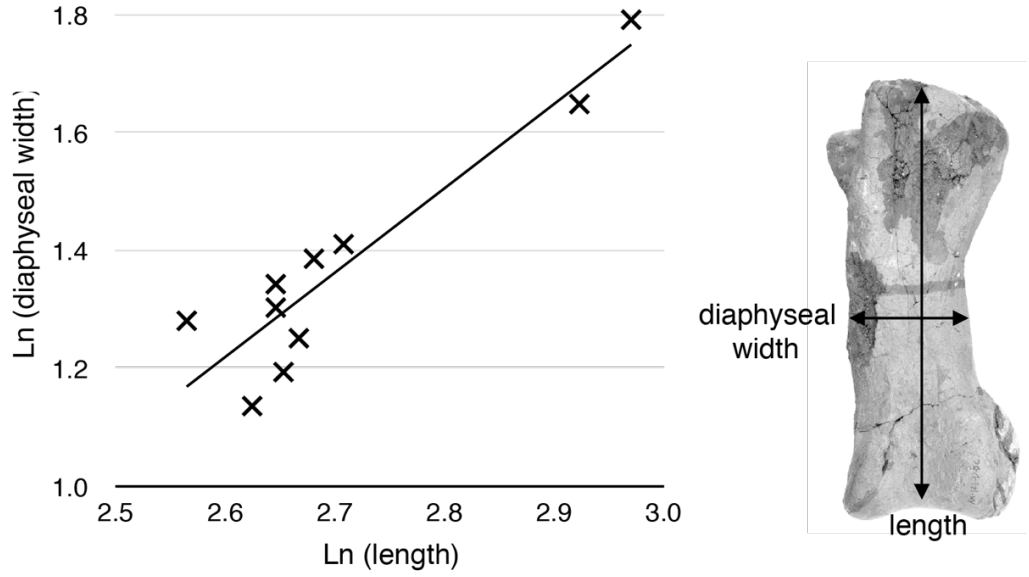

	Group	N	P value (correlation)	Slope (95 % CI)	R^2
× ———	PCF taxon	10	0.00	1.24 to 2.08	0.86

Figure 1-34. Biplot of the length versus width of metatarsal III of the Prince Creek Formation taxon. *E. r.*, *Edmontosaurus regalis*; *E. a.*, *Edmontosaurus annectens*; PCF, Prince Creek Formation taxon.

Figure 1-35 (facing page). Result of the cladistic analyses, showing the phylogenetic position of the Prince Creek Formation taxon. Matrix 1 resulted in three most parsimonious trees (MPT), and matrices 2 and 3 resulted in a single MPT each. The strict consensus tree from the three MPTs from matrix 1 and other MTPs from matrices 2 and 3 were identical in topology so all results are shown here in a single tree. Bootstrap values and Bremer support values are also shown. For the clades collapsed in the strict consensus tree from the analysis of matrix 1, these values are substituted by a dash.

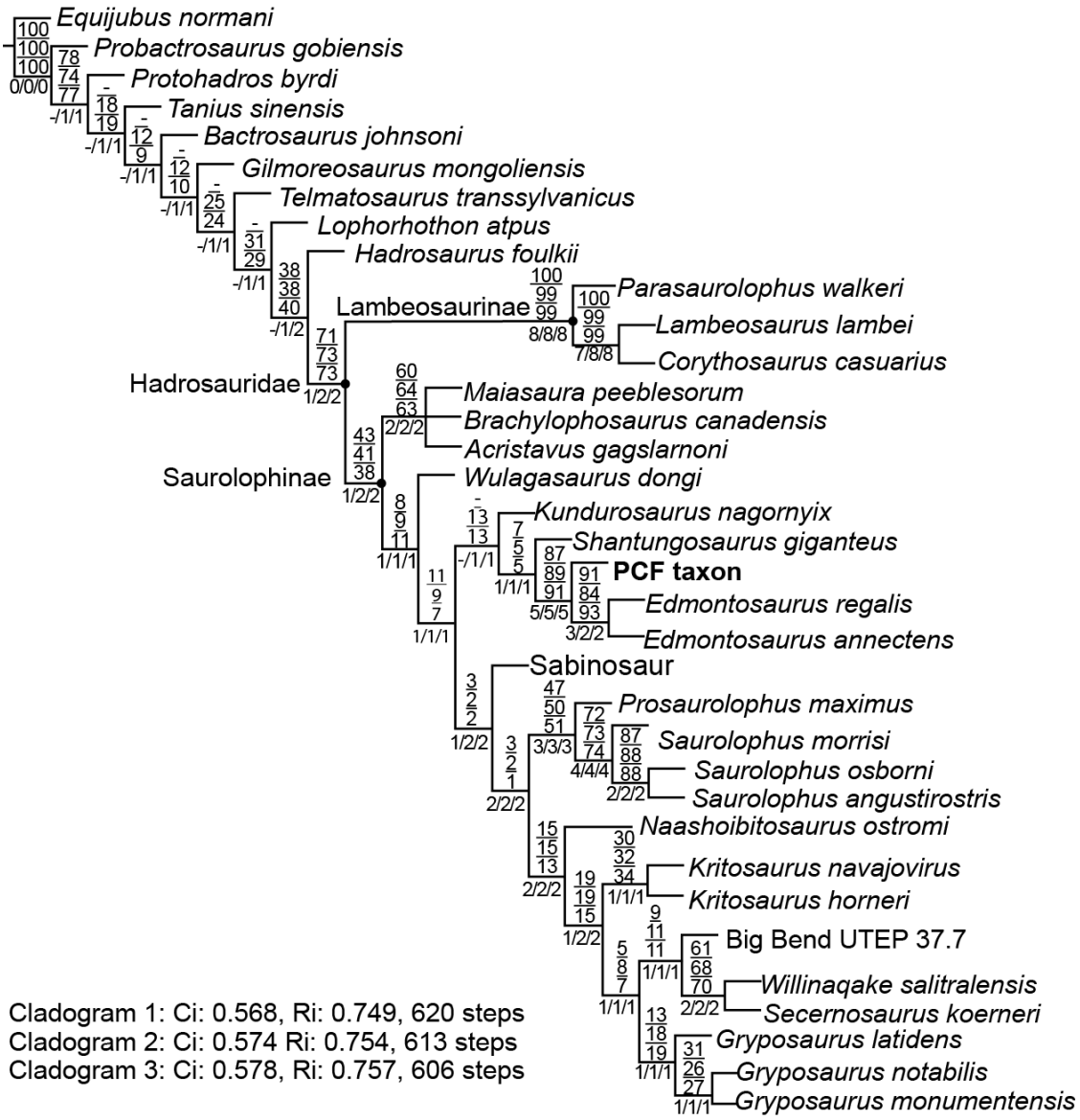

Cladogram 1: Ci: 0.568, Ri: 0.749, 620 steps
Cladogram 2: Ci: 0.574 Ri: 0.754, 613 steps
Cladogram 3: Ci: 0.578, Ri: 0.757, 606 steps

Bootstrap values: Cladogram 1 / Cladogram 2 / Cladogram 3

Bremer support values: Cladogram 1/Cladogram 2/Cladogram 3

1.8 Tables

Table 1-1. Number of specimens observed for this study

Element	Size class 1	Size class 2	Size class 3
Premaxilla	5	1	
Nasal	9		
Prefrontal	5		
Frontal	9	2	
Lacrimal	5		
Jugal	8		1
Quadratojugal	10		
Quadrate	6	2	
Postorbital	9		1
Squamosal	7	1	
Maxilla	6		
Laterosphenoid	6		
Prootic	3		
Basisphenoid	8	1	1
Basioccipital	5		
Parietal	7		
Supraoccipital	5	1	
Exoccipital-opisthotic	8	2	
Ectopterygoid	3	1	
Palatine	3		
Pterygoid	3		1
Predentary	3	1	
Dentary	12	1	
Surangular	10	1	1
Angular	2		
Splenial	2		
Cervical vertebrae	1	2 (?)	1
Dorsal vertebrae	7	2	2
Dorsal rib			
Sacrum			1
Caudal vertebrae	14	3	4
Dorsal rib	7		1
Sternum	1		
Scapula	5	3	1
Coracoid	5		
Humerus	23	3	1
Ulna	8	3	1
Radius	12	2	
Metacarpal II	2		
Metacarpal III	4		1
Metacarpal IV	3		
Metacarpal V	4		
Ilium	3		
Pubis	6	1	
Ischium	2		
Femur	6	2	
Tibia	9	2	
Fibula	6		
Calcaneum	5		1
astragalus	4		
Metatarsal II	10	1	
Metatarsal III	14	2	
Metatarsal IV	8	2	2
Sum	328	43	21

Table 1-2 *Edmontosaurus* specimens observed for this study

Edmontosaurus annectens	*Edmontosaurus regalis*
AMNH **427, 5046***, 5730, **5879**, 5886	AMNH 5224*
BHI **6218**	BMNH **8927***
CMN **8509***	CM 26258*
DMNH **1493***	CMN **2288*, 2289, 8399*, 8744**
LACM 23502*, **23504**	FMNH 15004*
MOR **003***	ROM **801*, 658, 867**
NCSM 23119*	
ROM **57100***, **64076**, **64084**, **64083**, **64076, 64077, 64078, 64079, 59786, 53492-53541**	
SM 4036*	
TMNH **00001**	
UCMP 128374*	
UMMP 20000*	
USNM 3814	
YPM **2182***	

Bold specimens are directly observed by the author. Specimens used for the geometric morphometric analysis are marked by an asterisk.

Table 1-3. Summary of growth patterns of *Edmontosaurus.*

Elements	Group	Growth pattern	Method
Skull length	*E. annectens* + *E. regalis* + PCF taxon	Positive allometric growth relative to the skull height	Regression analysis
Premaxilla length	*E. annectens* *E. annectens* + PCF taxon *E. regalis* + PCF taxon	Positive allometric growth relative to the dentary length	Regression analysis
Nasal curvature	*E. annectens* *E. regalis?* *E regalis* + PCF taxon	Height and length, relative to the dentary length	Regression analysis
Prefrontal fossa and width	*E. annectens* + PCF taxon	Prefrontal widens and a fossa would developed	Comparative morphological study
Frontal width	*E. annectens* + *E. regalis* + PCF taxon	Positive allometric growth relative to its length	Comparative morphological study, but not supported in the regression analysis
Postorbital jugal process width	*E. annectens* *E. annectens* + PCF taxon *E. regalis*	Positive allometric growth relative to the dentary length	Regression analysis
Postorbital process of the squamosal	*E. annectens* + *E. regalis* + PCF taxon	Shortens as it grows	Comparative morphological study

Table 1-3. Summary of growth patterns of *Edmontosaurus* (continued)

Quadrate	*E. annectens* + *E. regalis*	Curves as it grows	Regression analysis
Basisphenoid	*E. annectens* + *E. regalis* + PCF taxon	Interbasipterygoid ridge develop	Comparative morphological study
Basioccipital	*E. annectens* + PCF taxon	Acquires a constriction	Comparative morphological study
Exoccipital-opisthotic	*E. annectens* + PCF taxon	Opisthotic inclines posteriorly	Comparative morphological study
Predentary denticles	PCF taxon	Negative allometric growth	Comparative morphological study
Predentary posterodorsal medial process	*E. regalis* + PCF taxon	Negative allometric growth	Comparative morphological study
Dentary edentulous process	*E. annectens* *E. annectens* + PCF taxon	Straightens	Regression analysis

Table 1-3. Summary of growth patterns of *Edmontosaurus* (continued)

Dentary posterior edentulous process length	*E. annectens* *E. annectens* + PCF taxon *E. regalis* + PCF taxon	Positive allometric growth relative to the dental battery length	Regression analysis
Origination of the dentary deflection	*E. annectens* + *E. regalis* + PCF taxon	Shifts anteriorly	Regression analysis
Surangular	*E. regalis* + PCF taxon	Ventral side of the surangular faces more ventrally in adult	Comparative morphological study
Tooth	*E. annectens*	Widens	Comparative morphological study
Scapular neck width	*E. annectens* + *E. regalis* *E. annectens* + *E. regalis* + PCF taxon PCF taxon	Positive allometric growth relative to the scapular blade width	Regression analysis
Humerus deltopectoral process	*E. regalis* + PCF taxon *E. annectens* + PCF taxon PCF taxon	Positive allometric growth relative to the humerus length	Regression analysis
Ulna diaphyseal width	*E. annectens* + PCF taxon PCF taxon	Positive allometric growth relative to the ulna length	Regression analysis

Table 1-3. Summary of growth patterns of *Edmontosaurus* (continued)

Pubic neck wide	*E. annectens* + *E. regalis*	Positive allometric growth relative to the femur length	Regression analysis
Half pubic neck length	*E. annectens* + PCF taxon *E. regalis*	Positive allometric growth relative to the femur length	Regression analysis
Tibia and fibular articulation surface of the calcaneum	*E. annectens* + PCF taxon	Deepens and becomes rugose	Comparative morphological
Metatarsal III	PCF taxon	Widens relative to the length	Regression analysis

Due to the narrow size range and individual variations, the allometric growth trend could not be determined for each species at the 95 % CI (it does not rule out allometric growth patterns in each species). For some elements, only when PCF juvenile materials are grouped together with adult *Edmontosaurus annectens* or *E. regalis*, allometric growth trend could be determined. The reader is cautioned that the growth patterns of such groups are based on hypotheses that the elements of the juvenile PCF taxon resemble those of juveniles of other *Edmontosaurus*. These hypotheses were tested by the regression analyses for each element, and table 1-3 only shows growth patterns when such hypothesis was not rejected. For some elements, comparative morphological analyses are conducted on limited numbers of specimens, and even sometimes between the juvenile PCF taxon and subadult and adult *E. annectens* + *E. regalis.* Ideally, whether the differences observed really reflect ontogenetical variation have to be tested within each species. Thus, discovery of adult PCF taxon and juveniles of *E. annectens* and *E. regalis* is necessary to firmly conclude these results.

Table 1-4. Morphology of the three *Edmontosaurus* taxa

Character	PCF taxon	*E. annectens*	*E. regalis*
1. Geometric Morphometric analysis	Clustered with *E. annectens*	Mostly clustered within the 95 % CI of *E. annectens*	Clustered within the 95 % CI of *E. regalis*
2. Circumnarial septum of the premaxilla	Projects posterolaterally	Fan-shaped, anteroposteriorly wide, deep groove lateral to the posterodorsal premaxillary foramen	Fan-shaped, anteroposteriorly narrow
3. Posterodorsal corner of the circumnarial ridge of the nasal	More developed in adult than *E. annectens*?	Weakly developed	Well developed
4. Anterodorsal part of the lacrimal	Narrow	Wide	Wide
5. Jugal	Gracile	Robust	Robust
6. Lateral exposure of the quadratojugal	Wide	Wide	Narrow
7. Jugal process of the postorbital	Narrow, without a pocket	Narrow, with a pocket	Wide, with a pocket
8. A canal on the medial side of the lacrimal process of the maxilla	Opens laterally	Opens medially	Opens laterally
9. Bulge between the cerebrum and cerebellum	Weakly developed	Strongly developed	?
10. Posterior part of the dentary edentulous process	Short	Long	Short
11. Indentation of the splenial	Short	Short	Long
13. Ulna diaphysis constriction	Shows a positive allometric growth trend	Indistinguishable from the PCF materials	Too narrow to be a adult status of the PCF taxon
13. Pubis	Deeper pubic neck height, and longer pubic neck	Shallow pubic neck height, and longer pubic neck	Shallow pubic neck height, and shorter pubic neck
14. Ischium	Larger and deeper acetabular border	Smaller and shallower acetabular border	Smaller and shallower acetabular border
15. Calcaneum	The tibial and fibular articular facets are nearly equal in size	The fibular articulation facet is larger than tibial articular facet	?

1.9 References

1. Evans DC, Campione NE, Brink K, Schott R, Brown C (2013) Wasted youth: The importance of ontogenetically equivalent semaphoronts in dinosaur phylogenetic systematics. Journal of Vertebrate Paleontology, Program and Abstracts 2013: 124.

2. Horner JR, Currie PJ (1994) Embryonic and neonatal morphology and ontogeny of a new species of *Hypacrosaurus* (Ornithischia, Lambeosauridae) from Montana and Alberta. In: Carpenter KH, Karl F., Horner JR, editors. Dinosaur eggs and babies. Cambridge, UK: Cambridge University Press. pp. 312-336.

3. Currie PJ (2003) Allometric growth in tyrannosaurids (Dinosauria: Theropoda) from the Upper Cretaceous of North America and Asia. Canadian Journal of Earth Science 40: 651-665.

4. Goodwin MB, Clemens WA, Horner JR, Padian K (2006) The smallest known *Triceratops* skull: new observations on ceratopsid cranial anatomy and ontogeny. Journal of Vertebrate Paleontology 26: 103-112.

5. Whitlock JA, Wilson JA, Lamanna MC (2010) Description of a nearly complete juvenile skull of *Diplodocus* (Sauropoda: Diplodocoidea) from the Late Jurassic of North America. Journal of Vertebrate Paleontology 30: 442-457.

6. Tsuihiji T, Watabe M, Tsogtbaatar K, Tsubamoto T, Barsbold R et al. (2011) Cranial osteology of a juvenile specimen of *Tarbosaurus bataar* (Theropoda, Tyrannosauridae) from the Nemegt Formation (Upper Cretaceous) of Bugin Tsav, Mongolia. Journal of Vertebrate Paleontology 31: 497-517.

7. Dodson P (1975) Taxonomic implications of relative growth in lambeosaurine hadrosaurs. Systematic Zoology 24: 37-54.

8. Horner JR, Goodwin MB (2009) Extreme cranial ontogeny in the Upper Cretaceous dinosaur *Pachycephalosaurus*. PLoS ONE 4: e7626.

9. Scannella JB, Horner JR (2010) *Torosaurus* Marsh, 1891, is *Triceratops* Marsh, 1889 (Ceratopsidae: Chasmosaurinae): Synonymy through ontogeny. Journal of Vertebrate Paleontology 30: 1157-1168.

10. Campione NE, Evans DC (2011) Cranial growth and variation in edmontosaurs (Dinosauria: Hadrosauridae): Implications for Latest Cretaceous megaherbivore diversity in North America. PLoS ONE 6: e25186.

11. Bell PR, Brink KS (2013) *Kazaklambia convincens* comb. nov., a primitive juvenile lambeosaurine from the Santonian of Kazakhstan. Cretaceous Research 45: 265-274.

12. Choiniere JN, Clark JM, Forster CA, Norell MA, Eberth DA et al. (2013) A juvenile specimen of a new coelurosaur (Dinosauria: Theropoda) from the Middle-Late Jurassic Shishugou Formation of Xinjiang, People's Republic of China. Journal of Systematic Palaeontology 12: 177-215.

13. Davies KL (1987) Duck-bill dinosaurs (Hadrosauridae, Ornithischia) from the North Slope of Alaska. Journal of Paleontology 61: 198-200.

14. Brouwers EM, Clemens, WA, Spicer, RA, Ager, TA, Carter LD, et al. (1987) Dinosaurs on the North Slope, Alaska: High latitude, latest Cretaceous environments. Science 237: 1608-1610.

15. Nelms LG (1989) Late Cretaceous dinosaurs from the North Slope of Alaska. Journal of Vertebrate Paleontology, Abstracts of Papers 9: 34A.

16. Clemens WA, Nelms LG (1993) Paleoecological implications of Alaskan terrestrial vertebrate fauna in latest Cretaceous time at high paleolatitudes. Geology 21: 503-506.

17. Gangloff RA (1994) The record of Cretaceous dinosaurs in Alaska: an overview. In: Thurston DK, Fujita K, editors. 1992 Proceedings of the international vonference on Arctic margins. Alaska Geological Society. pp. 399-404.

18. Gangloff RA (1998) Arctic dinosaurs with emphasis on the Cretaceous record of Alaska and the Eurasian-North American connection. New Mexico Museum of Natural History and Science Bulletin 14: 211-220.

19. Fiorillo AR, Gangloff RA (2001) The caribou migration model for Arctic hadrosaurs (Dinosauria: Ornithischia): A reassessment. Historical Biology 15: 323-334.

20. Fiorillo AR, McCarthy PJ, Brandlen E, Flaig PP, Norton D et al. (2007) Paleontology, sedimentology, paleopedology, and palynology of the Kikak-Tegoseak Quarry (Prince Creek Formation, Late Cretaceous), Northern Alaska. In: Braman DR, editor. Ceratopsian Symposium: Short papers, abstracts and programs. Drumheller, AB: pp. 48-49.

21. Fiorillo AR (2008) Dinosaurs of Alaska: Implications for the Cretaceous origin of Beringia. The terrane puzzle: New perspectives on paleontology and stratigraphy from the North American cordillera 442: 313-325.

22. Flaig PP (2010) Depositional environments of the Late Cretaceous (Maastrichtian) dinosaur-bearing Prince Creek Formation: Colville River region, North Slope, Alaska. Unpublished Ph.D. thesis. Fairbanks, AK: University of Alaska Fairbanks. 311 p.

23. Fiorillo AR, McCarthy PJ, Flaig PP (2010) Taphonomic and sedimentologic interpretations of the dinosaur-bearing Upper Cretaceous Strata of the Prince Creek Formation, Northern Alaska: Insights from an ancient high-latitude terrestrial ecosystem. Palaeogeography, Palaeoclimatology, Palaeoecology 295: 376-388.

24. Gangloff RA, Fiorillo AR (2010) Taphonomy and paleoecology of a bonebed from the Prince Creek Formation, North Slope, Alaska. Palaios 25: 299-317.

25. Prieto-Márquez A (2008) Phylogeny and historical biogeography of hadrosaurid dinosaurs. Unpublished Ph.D. thesis. Tallahassee: Florida State University. 861 p.

26. Gryc G, Patton Jr WW, Payne TG (1951) Present Cretaceous stratigraphic nomenclature of northern Alaska. Journal of the Washington Academy of Sciences 41: 159-167.

27. Mull CG, Houseknecht DW, Bird KJ (2003) Revised Cretaceous and Tertiary stratigraphic nomenclature in the Colville Basin, northern Alaska. US Gelogical Survey Professional Paper 1673: 1-51.

28. Flaig PP, McCarthy PJ, Fiorillo AR (2011) A tidally influenced, high-latitude coastal-plain: The upper Cretaceous (Maastrichtian) Prince Creek Formation, North Slope, Alaska. In: Davidson SK, Leleu S, North. CP, editors. From river to rock record: The preservation of fluvial sediments and their subsequent interpretation. pp. 233-264.

29. Frederiksen NO, Ager TA, Edwards LE (1988) Palynology of Maastrichtian and Paleocene rocks, lower Colville River region, North Slope of Alaska. Canadian Journal of Earth Sciences 25: 512-527.

30. Frederiksen NO (1991) Pollen zonation and correlation of Maastrichtian marine beds and associated strata, Ocean Point dinosaur locality, North Slope, Alaska. United States Geological Survey Bulletin 1990-E: E1-E24.

31. Frederiksen NO, Mclntyre DJ, Sheehan TP (2002) Palynological dating of some Upper Cretaceous to Eocene outcrop and well samples from the region extending from the easternmost part of NPRA in Alaska to the western part of Arctic National Wildlife Refuge, North Slope of Alaska. US Geological Survey Open-File Report 02-405: 1-37.

32. Brouwers EM, Deckker PD (1993) Late Maastrichtian and Danian ostracode faunas from Northern Alaska; reconstructions of environment and paleogeography. Palaios 8: 140-154.

33. McKee E, Conrad JE, Tuin BD (1989) Better dates for arctic dinosaurs. Eos 70: 74.

34. Besse J, Courtillot V (1991) Revised and synthetic apparent polar wander paths of the African, Eurasian, North American and Indian plates, and true polar wander since 200 Ma. Journal of Geophysical Research 96: 4029-4050.

35. Flores RM, Myers MD, Houseknecht DW, Stricker GD, Brizzolara DW et al. (2007) Stratigraphy and facies of Cretaceous Schrader Bluff and Prince Creek Formations in Colville River Bluffs, North Slope, Alaska. United States Geological Survey Professional Paper 1747: 1-52.

36. Witte, WK, Stone, DB, Mull CG (1987) Paleomagnetism, paleobotany, and paleogeography of the Cretaceous, North Slope, Alaska. In: Tailleur, I.L., Weimer P, editors. Alaska North Slope Geology: The Pacific Section, Bakersfield, Society of Economic Paleontologists and Mineralogists and the Alaska Geological Society 1. Bakersfield, CA: Pacific Section, Society of Economic Paleontologists and Mineralogists. pp. 571-579.

37. Spicer RA, Herman AB (2010) The Late Cretaceous environment of the Arctic: A quantitative reassessment based on plant fossils. Palaeogeography, Palaeoclimatology, Palaeoecology 295: 423-442.

38. Flaig PP, McCarthy PJ, Fiorillo AR (2013) Anatomy, evolution, and paleoenvironmental interpretation of an ancient arctic coastal plain: integrated paleopedology and palynology from the Upper Cretaceous (Maastrichtian) Prince Creek Formation, North Slope, Alaska, USA. In: Driese SG, Nordt LC, editors. New frontiers in paleopedology and terrestrial paleoclimatology: Paleosols and soil surface analog systems. pp. 179-230.

39. Gangloff RA, Fiorillo AR, Norton DW (2005) The first pachycephalosaurine (Dinosauria) from the paleo-Arctic of Alaska and its paleogeographic implications. Journal of Paleontology 79: 997-1001.

40. Fiorillo AR, Tykoski RS, Currie PJ, McCarthy PJ, Flaig P (2009) Description of two partial *Troodon* braincases from the Prince Creek Formation (Upper Cretaceous), North Slope Alaska. Journal of Vertebrate Paleontology 29: 178-187.

41. Brown CM, Druckenmiller P (2011) Basal ornithopod (Dinosauria: Ornithischia) teeth from the Prince Creek Formation (early Maastrichtian) of Alaska. Canadian Journal of Earth Sciences 48: 1342-1354.

42. Fiorillo AR, Tykoski RS (2012) A new Maastrichtian species of the centrosaurine ceratopsid *Pachyrhinosaurus* from the North Slope of Alaska. Acta Palaeontologica Polonica 57: 561-573.

43. Lambe LM (1917) A new genus and species of crestless hadrosaur from the Edmonton Formation of Alberta. Ottawa Naturalist 31: 65-73.

44. Lull RS, Wright NE (1942) Hadrosaurian dinosaurs of North America. Geological Society of America Special Papers 40: 1-242.

45. Marsh OC (1890) Description of new dinosaurian reptiles. American Journal of Science 39: 81-87.

46. Cope ED (1883) On the characters of the skull in the Hadrosauridae. Proceedings of the Academy of Natural Sciences of Philadelphia 35: 97-107.

47. Marsh OC (1892) Notice of new reptiles from the Laramie Formation. American Journal of Science 3: 449-453.

48. Gilmore CW (1924) A new species of hadrosaurian dinosaur from the Edmonton Formation (Cretaceous) of Alberta. Bulletin of Geological Survey Canada 38: 13-26.

49. Sternberg CM (1926) A new species of *Thespesius* from the Lance Formation of Saskatchewan. Bulletin of Geological Survey Canada 44: 73-84.

50. Hopson JA (1975) The evolution of cranial display structures in hadrosaurian dinosaurs. Paleobiology 1: 21-43.

51. Estes R, Berberian P (1970) Paleoecology of a Late Cretaceous vertebrate community from Montana. Breviora 343: 1-35.

52. Brett-Surman MK (1989) A revision of the Hadrosauridae (Reptilia: Ornithischia) and their evolution during the Campanian and Maastrichtian. Unpublished Ph.D. thesis. Washington DC: George Washington University. 272 p.

53. Horner JR, Weishampel DB, Forster CA (2004) Hadrosauridae. In: Weishampel DB, Dodson P, Osmølska H, editors. The Dinosauria. Berkeley and Los Angels, California: University of California Press. pp. 438-463.

54. Bell PR, Fanti F, Currie PJ, Arbour VM (2013) A Mummified duck-billed dinosaur with a soft-tissue cock's comb. Current Biology 24: 70-75.

55. Godefroit P, Bolotsky YL, Lauters P (2012) A new saurolophine dinosaur from the Latest Cretaceous of far Eastern Russia. PLoS ONE 7: e36849.

56. Prieto-Márquez A (2013) Skeletal morphology of *Kritosaurus navajovius* (Dinosauria: Hadrosauridae) from the Late Cretaceous of the North American south-west, with an evaluation of the phylogenetic systematics and biogeography of Kritosaurini. Journal of Systematic Palaeontology 12: 133-175.

57. Hu C-C (1972) A new hadrosaur from the Cretaceous of Chucheng, Shantung. Peking, China: 29 p.

58. Bolotsky YL, Godefroit P (2004) A new hadrosaurine dinosaur from the Late Cretaceous of Far Eastern Russia. Journal of Vertebrate Paleontology 24: 351-365.

59. Harper DAT, Ryan PD (2001) PAST: paleontological statistics software package for education and data analysis. Palaeontol Electronica 4: 1-9.

60. Sheets HD, Zelditch ML, Swiderski D (2004) IMP-Integrated Morphometic Package. 7 ed. Buffalo, N.Y.: Published by the Authors.

61. Adams DC, Otárola-Castillo E (2013) Geomorph: An R package for the collection and analysis of geometric morphometric shape data. Methods in Ecology and Evolution 4: 393-399.

62. Klingenberg CP (2011) MorphoJ: an integrated software package for geometric morphometrics. Molecular Ecology Resources 11: 353-357.

63. Dodson P (1975) Functional and ecological significance of relative growth in *Alligator*. Journal of Zoology 175: 315-355.

64. Dodson P (1975) Relative growth in two sympatric species of *Sceloporus*. American Midland Naturalist 94: 421-450.

65. Evans DC (2010) Cranial anatomy and systematics of *Hypacrosaurus altispinus*, and a comparative analysis of skull growth in lambeosaurine hadrosaurids (Dinosauria: Ornithischia). Zoological Journal of the Linnean Society 159: 398-434.

66. Schott RK, Evans DC (2012) Squamosal ontogeny and variation in the pachycephalosaurian dinosaur *Stegoceras validum* Lambe, 1902, from the Dinosaur Park Formation, Alberta. Journal of Vertebrate Paleontology 32: 903-913.

67. Maxwell EE (2012) New metrics to differentiate species of *Stenopterygius* (Reptilia: Ichthyosauria) from the Lower Jurassic of southwestern Germany. Journal of Paleontology 86: 105-115.

68. Schuyler WH (2004) Reading statistics and research, 4th ed. Boston, MA: Pearson. 544 p.

69. Pearson K (1901) LIII. On lines and planes of closest fit to systems of points in space. The London, Edinburgh, and Dublin Philosophical Magazine and Journal of Science 2: 559-572.

70. Falster DS, Warton, D.I., Wright IJ (2006) SMATR: Standardized major axis tests and routines, ver 2.0. Available: http://www.bio.mq.edu.au/ecology/SMATR/.

71. Gould SJ (1966) Allometry and size in ontogeny and phylogeny. Biological Reviews 41: 587-638.

72. Maddison WP, Maddison DR (2011) Mesquite: a modular system for evolutionary analysis. Version 2.75. Available: http://mesquiteproject.org.

73. Prieto-Márquez A (2010) Global phylogeny of Hadrosauridae (Dinosauria: Ornithopoda) using parsimony and Bayesian methods. Zoological Journal of the Linnean Society 159: 435-502.

74. Goloboff PA, Farris JS, Nixon KC (2008) TNT, a free program for phylogenetic analysis. Wiley Online Library. 774 p.

75. Wilkinson M (2001) REDCON 3.0. Software and documentation. Available: http://www.nhm.ac.uk/research-curation/research/projects/software/.

76. Goloboff PA Bremer Support Script. Ver. 1.0. Available: http://tnt.insectmuseum.org/index.php/Main_Page.

77. Lambe ML (1920) The Hadrosaur *Edmontosaurus* from the Upper Cretaceous of Alberta. Canada Geological Survey Memoir 120: 1-79.

78. Brett-Surman M, Wagner JR (2007) Discussion of character analysis of the appendicular anatomy in Campanian and Maastrichtian North American hadrosaurids-variation and ontogeny. In: Carpenter K, editor. Horn and beaks: Ceratopsian and ornithopod dinosaurs. Bloomington, IN: Indiana University Press. pp. 135-169.

79. Dilkes DW (2001) An ontogenetic perspective on locomotion in the Late Cretaceous dinosaur *Maiasaura peeblesorum* (Ornithischia: Hadrosauridae). Canadian Journal of Earth Science 38: 1205-1227.

80. Prieto-Márquez A (2011) Cranial and appendicular ontogeny of *Bactrosaurus johnsoni*, a hadrosauroid dinosaur from the Late Cretaceous of northern China. Palaeontology 54: 773-792.

81. Senter P (2012) Forearm orientation in Hadrosauridae (Dinosauria: Ornithopoda) and implications for museum mounts. Palaeontologia Electronica 15: 1-10.

82. Grigorescu D, Csiki Z (2006) Ontogenetic development of *Telmatosaurus transsylvanicus* (Omitischia: Hadrosauria) from the Maastrichtian of the Hateg Basin, Romania – evidence from the limb bones. Hantkeniana 5: 20-26.

83. Gates TA, Horner JR, Hanna RR, Nelson CR (2011) New unadorned hadrosaurine hadrosaurid (Dinosauria, Ornithopoda) from the Campanian of North America. Journal of Vertebrate Paleontology 31: 798-811.

84. Baer KEv (1828) Über Entwicklungsgeschichte der Thiere. Beobachtung und Reflexion, Theil 1. Königsberg: Gebrüder Bornträger.

85. Nelson GJ (1978) Ontogeny, phylogeny, paleontology, and the biogenetic law. Systematic zoology 27: 324-345.

86. Kitching I, Forey PL, Humphries, Christopher J, Williams DM (1998) Cladistics: The theory and practice of parsimony analysis. Second edition. Oxford, UK: Oxford University Press. 228 p.

87. Juan L, Tseng ZJ, Wilson MV, Murray AM (2012) Body shape differences between North American and Asian fossil catostomids and ontogenetic change in early cypriniforms. Journal of Vertebrate Paleontology, Program and Abstracts 2012: 128.

88. Seeley HG (1887) Researches on the structure, organization, and classification of the fossil reptilia. I. On *Protorosaurus Speneri* (von Meyer). Philosophical Transactions of the Royal Society of London B 178: 187-213.

89. Marsh OC (1881) Principal characters of American Jurassic dinosaurs, IV. American Journal of Science 3: 167-170.

90. Cope ED (1870) Synopsis of the extinct Batrachia and Reptilia of North America. Transactions of the American Philosophical Society, 2nd series 14: 252.

91. Brown B (1914) *Corythosaurus casuarius*, a new crested dinosaur from the Belly River Cretaceous; with provisional classification of the family Trachodontidae. Bulletin of the American Museum of Natural History 33: 559-565.

92. Blakey RC (2009) Paleogeography and geologic evolution of North America. Available: http://cpgeosystems.com/nam.html.

1.10 Appendix

The following is a list of characters used for the phylogenic analysis in this study, after Prieto-Márquez [56]. I also show the coding of the PCF taxon, *E. annectens* and *E. regalis*.

1. Maximum number of tooth positions in the dentary dental battery (DTTH1): 30 or less (sample mean of 22 alveolar positions) (0); 31-42 (sample mean of 37 alveolar positions) (1); more than 42 (sample mean of 49 alveolar positions) (2).

PCF taxon (matrix 1)…0

PCF taxon (matrix 2 and 3)…?

E. regalis…2

E. annectens… 2

Comment: Prieto-Márquez [25] shows that the number of tooth sockets in the dentary and maxilla would increase during growth.

2. Minimum number of teeth per alveoli arranged dorsoventrally at mid length of the dental battery (DTTH3): two (0); three (1); four; (2) five or more (3).

PCF taxon (matrix 1, 2 and 3)…2 or 3

E. regalis…3

E. annectens…3

Comment: no PCF dentary is preserved with complete teeth row, so I divided the depth of the tooth socket by isolated tooth length.

3. Maximum number of functional teeth exposed on the dentary occlusal plane (DTTH4): one (0); one functional tooth rostrally and caudally, and up to two teeth at and approaching the middle of the dental battery (1); three functional teeth throughout most of the dental battery, gradually decreasing to two near the rostral and caudal ends of the dentary (2).

PCF taxon (matrix 1, 2 and 3)…?

E. regalis…2

E. annectens…2

4. Flat and steeply inclined occlusal surface in the dentary (DTTH14): absent (0); present (1).

PCF taxon (matrix 1, 2 and 3)…?

E. regalis…0

E. annectens…0

5. Height/width ratio of the dentary tooth crowns in lingual aspect (DTTH5): ratio up to 1.95 (sample mean ratio of 1.6) (0); ratio from 1.95-2.7 (sample mean ratio of 2.4) (1); ratio from 2.8-3.3 (sample mean ratio of 3.0) (2); ratio greater than 3.3 (sample mean ratio of 3.7) (3).

PCF taxon (matrix 1)…0

PCF taxon (matrix 2, 3)…?

E. regalis…2

E. annectens…1

Comment: see section 1.4.2.21. The value changes through growth (Figure 1-28)

6. Maximum number of ridges on the enameled lingual side of dentary tooth crowns (DTTH6): presence of a primary major ridge extending from the ventral to the dorsal end of the crown, a rostral and slightly shorter secondary ridge and several (three or more) subsidiary, faintly developed and short tertiary ridges (0); presence of primary, secondary, and one or two tertiary ridges (1); presence of a primary ridge and one or two faint and shorter ridges (2); loss of all but the primary ridge (3).

PCF taxon (matrix 1, 2 and 3)…3

E. regalis…3

E. annectens…3

7. Dentary tooth crowns, position of the primary ridge (DTTH7): well offset caudally from the midline (0); median for most teeth, although some teeth within the same dental battery may display a slight caudal offset of the primary ridge (1).

PCF taxon (matrix 1, 2 and 3)…1

E. regalis…1

E. annectens…1

8. Overall morphology of the dentary marginal denticles (DTTH10): wedge to tongue-shaped (0); curved and mammillated asymmetrical ledge (1); absent or very reduced to small papillae along the apical half of the dorsal half of the crown (2).

PCF taxon (matrix 1, 2 and 3)…2

E. regalis…2

E. annectens…2

9. Denticle size (DTTH12): the denticles of both mesial and distal margins are equal in size (0); the mesial margin has larger denticles than the distal one (1).

PCF taxon (matrix 1, 2 and 3)…0

E. regalis…0

E. annectens…0

10. Imbrication of dentary tooth crowns (DTTH13): absent (0); present, the mesial margin overlaps the distal one of the adjacent crown (1).

PCF taxon (matrix 1, 2 and 3)…0

E. regalis…0

E. annectens…0

11. Maximum number of tooth positions in the maxillary dental battery (MXTH1): up to 32 tooth positions (sample mean of 23 teeth) (0); from 33-44 tooth positions (sample mean of 40 teeth) (1); 45 or more tooth positions (sample mean of 49 teeth) (2).

PCF taxon (matrix 1)…0

PCF taxon (matrix 2 and 3)…?

E. regalis…2

E. annectens…2

Comment: as in the dentary teeth, maxillary teeth would increase in number throughout growth [25].

12. Increase in the number of tooth positions in the maxilla relative to the dentary (MXTH3): absent (0); present, maxillary dental battery with 5-20% more tooth positions

than the dentary one (1).

PCF taxon (matrix 1 and 2)…0

PCF taxon (matrix 3)…?

E. regalis…1

E. annectens…1

Comment: see section 1.4.3.

13. Maximum number of functional teeth per alveolus in the maxillary occlusal plane (MXTH4): one (0); one tooth for most of the dental battery, with the sporadic presence of a second tooth forming the occlusal plane (1); two functional teeth throughout most of the dental battery length, gradually changing to one near the rostral and caudal ends of the maxilla (2).

PCF taxon (matrix 1 and 2)…1

PCF taxon (matrix 3)…?

E. regalis…2

E. annectens…2

Comment: see section 1.4.3.

14. Maximum number of ridges on the enameled labial side of maxillary tooth crowns (MXTH5): presence of a primary major ridge and three or more much fainter ridges (0); loss of all but the primary ridge in all or, at least, most of the crowns (in the latter situation a few crowns show a fainter secondary ridge) (1).

PCF taxon (matrix 1, 2 and 3)…1

E. regalis…1

E. annectens…1

15. Maxillary tooth crowns, position of the primary ridge (MXTH6): the dental battery contains a mixture of teeth with primary ridge positioned caudally and teeth with the ridge at the center of the crown (0); the majority of teeth in the dental battery have a primary ridge positioned at the midline of the crown (1).

PCF taxon (matrix 1, 2 and 3)…1

E. regalis…1

E. annectens…1

16. Overall morphology of the maxillary marginal denticles (MXTH8): wedge to tongue-shaped (0); curved and mammillated asymmetrical ledge (1); absent or reduced to small papillae along the apical half of the dorsal half of the crown (2).

PCF taxon (matrix 1, 2 and 3)…2

E. regalis…2

E. annectens…2

17. Predentary. Ratio between the predentary maximum mediolateral width and the maximum rostrocaudal length along the lateral process (PDT1): up to 1.75 (0); more than 1.75 (1).

PCF taxon (matrix 1, 2 and 3)…?

E. regalis…0

E. annectens…0

18. Predentary. Orientation of the rostral surface relative to the dorsal margin of the lateral process (PDT3): angle of 75º or greater (sample mean angle of 81º) (0); angle between 56º and 74º (sample mean angle of 66º) (1); angle between 40º and 55º (sample

mean angle of 47º) (2); angle of 40º or less, gently rounded rostral surface (sample mean angle of 34º) (3).

PCF taxon (matrix 1, 2 and 3)…?

E. regalis…1

E. annectens…1

Comment: in none of the PCF materials is the lateral process is completely preserved.

19. Predentary. Shape of the denticles of the predentary oral margin (PDT4): triangular and pointed (0); subrectangular to rectangular (1).

PCF taxon (matrix 1, 2 and 3)…1

E. regalis…1

E. annectens…1

20. Predentary. Number of predentary denticles in adult individuals lateral to the median denticle (not included in the count) (PDT6): maximum of five (0); six or more (1).

PCF taxon (matrix 1, 2 and 3)…0

E. regalis…0

E. annectens…?

21. Predentary. Extension of the predentary denticulate margin (PDT7): denticles extending into the lateral process (0); denticles limited to the rostral margin (1).

PCF taxon (matrix 1, 2 and 3)…1

E. regalis…1

E. annectens…1

22. Predentary. Morphology of the predentary rostrolateral corner (PDT8): gently rounded and continuous with the lateral process, giving the predentary an arcuate dorsal profile (0); subsquared rostrolateral corner (1); subsquared, very broad and rostrolaterally projected (2).

PCF taxon (matrix 1, 2 and 3)…1

E. regalis…1

E. annectens…1

23. Predentary. Development of a lateral shelf on the dorsal side of the predentary lateral process (PDT9): absence of shelf, presence of a rostrocaudally short and shallow groove limited to the distal region of the lateral process, bounded by a tall lateral wall (0); short and shallow shelf limited to the laterocaudal region of the lateral process (1); short and well-incised shelf that is wider near the rostrolateral corner of the predentary (2); shelf extremely narrow mediolaterally and very long rostrocaudally (3); shelf rostrocaudally long, deeply incised and mediolaterally broad, forming half of the mediolateral breadth of the lateral process and becoming wider distally (4).

PCF taxon (matrix 1, 2 and 3)…3 or 4

E. regalis…4

E. annectens…4

Comment: no PCF specimen preserves the complete lateral process. UAMES 4928 partially preserves the right but it is too incomplete to determine its status.

24. Predentary. Ridge on the dorsal lingual, keel-shaped process (PDT11): the process lacks a prominent median ridge on the lingual side of the rostral region of the predentary, and, if present, the former forms and projects caudally from the caudal margin of the

predentary rostral region (0); the process has a well-developed ridge on the lingual surface of the rostral segment of the predentary, from which the former extends further caudally to lie dorsal to the dentary symphysis (1).

PCF taxon (matrix 1 and 2)…0

PCF taxon (matrix 3)…?

E. regalis…1

E. annectens…1

Comment: see section 1.4.3.

25. Predentary. Ventral median process, degree of indentation of the split of the process into two distinct lobes (PDT13): short indentation and deep undivided portion, the splitting originates at a distance from the predentary ventral margin that equals approximately half of the mediolateral width of the ventral process (0); long indentation and shallow undivided portion, the splitting originates at a distance from the predentary ventral margin that is less than the mediolateral width of the process (1).

PCF taxon (matrix 1, 2 and 3)…?

E. regalis…1

E. annectens…1

26. Dentary. Ratio between the length of the proximal edentulous slope of the dentary and the distance between the rostralmost tooth position and the caudal margin of the coronoid process (DT1): less than 0.20 (sample mean ratio of 0.11) (0); ratio between 0.20 and 0.31 (sample mean ratio of 0.27) (1); ratio between 0.32 and 0.45 (sample mean ratio of 0.35) (2); ratio greater than 0.45 (sample mean ratio of 0.54) (3).

PCF taxon (matrix 1)…1&2

PCF taxon (matrix 2, 3)…?

E. regalis…2 & 3 (contra [25,56,73])

E. annectens…3

Comment: see section 1.4.2.19. The edentulous process length experiences positive allometric growth in both *E. regalis* and *E. annectens.* The PCF materials could represent a juvenile condition of *E. regalis,* but not of *E. annectens.*

27. Dentary. Angle of deflection of the rostral ventral margin of the dentary (DT4): angle less than 17º (sample mean angle of 13º) (0); angle between 17º and 25º (sample mean angle of 22º) (1); angle greater than 25º (sample mean angle of 33º) (2).

PCF taxon (matrix 1)… 1

PCF taxon (matrix 2 and 3)…?

E. regalis…0

E. annectens…0 & 1 (contra [25,56,73])

Comment: see section 1.4.2.19. I do not know if the deflection correlation exists in *E. regalis,* but it is not statistically distinguishable from that of *E. annectens* ($p = 0.07$).

28. Dentary. Location of the origination of the ventral deflection of the dentary (measured as the ratio between the distance from the caudal margin of the coronoid process to the inflexion point of the ventral margin and the distance from the caudal margin the coronoid process to the rostralmost alveolus) (DT5): the deflection occurs near the rostral end of the dentary, ratio greater than 0.78 (sample mean ratio of 0.87) (0); ratio between 0.66 and 0.78 (sample mean ratio of 0.72) (1); deflection originating near the middle of the dental battery, ratio of 0.65 or less (sample mean ratio of 0.59) (2).

PCF taxon (matrix 1)…0, 1, 2

PCF taxon (matrix 2 and 3)…?

E. regalis…0 & 1 (contra [25,56,73])

E. annectens…0 & 1

This character is highly variable in *Edmontosaurus* and the PCF taxon. On average, the PCF material has relatively shorter ratio. However, it is an ontogenetically different character.

29. Dentary. Lingual projection symphyseal region of the dentary (measured as a ratio between the labiolingual extension of the symphyseal region and the maximum labiolingual width of the dentary) (DT6): ratio up to 2.85 (0); extremely elongated rostral end of the dentary, ratio greater than 2.85 (1).

PCF taxon (matrix 1, 2 and 3)…0

E. regalis…0

E. annectens…0

30. Dentary. Orientation of the dentary symphysis (measured as the angle formed by this surface and the lateral side of the rostral half of the dentary) (DT7): angle greater than 15º (sample mean angle of 23º) (0); angle up to 15º (sample mean angle of 10º) (1).

PCF taxon (matrix 1, 2 and 3)…1

E. regalis…1

E. annectens…1

31. Dentary. Medial or lateral profile of the dorsal margin of the rostral edentulous region of the dentary for articulation with the predentary (DT9): ranging from having a very subtle concavity (almost straight) to straight or even displaying a subtle convexity (0); having a well-pronounced concavity (1).

PCF taxon (matrix 1, 2 and 3)…0

E. regalis…0

E. annectens…0

32. Dentary. Angle between the long axis of the coronoid process and the dorsal margin of the alveolar sulci of the dental battery (DT11): coronoid process subvertical or caudally inclined (0); process rostrally inclined (1).

PCF taxon (matrix 1, 2 and 3)…1

E. regalis…1

E. annectens…1

33. Dentary. Morphology of the apex of the coronoid process (DT12): slightly expanded rostrocaudally, with very limited development of rostral and caudal expansions resulting in an apex that is taller than wider (0); well developed expansion of both the caudal and, especially, the rostral margins (1).

PCF taxon (matrix 1, 2 and 3)…1

E. regalis…1

E. annectens…1

34. Dentary. Caudodorsal margin of the coronoid process projected dorsally into a sharp point (DT13): absent (0); present (1).

PCF taxon (matrix 1, 2 and 3)…1

E. regalis…1

E. annectens…1

Comment: contra [25,56,73]. Some *Edmontosaurus* specimens have this projection (i.e.

Lambe [77]).

35. Dentary. Thick and dorsoventrally elongated ridge on the medial side of the coronoid process, located near the caudal margin of the process (DT14); present, the ridge forms the rostral boundary of a depressed facet for attachment of the rostrodorsal process of the surangular; coarse striations present rostral to the ridge (1).

PCF taxon (matrix 1, 2 and 3)…1

E. regalis…1

E. annectens…1

36. Dentary. Lateral expansion of caudal region of the dentary, ventral to the base of the coronoid process (measured as the angle between the lateral surface of the dentary and that of the region caudoventral to the coronoid process) (DT15): the lateral side of the dentary is only slightly expanded laterally ventral to the coronoid process, with an angle greater than 165º (sample mean angle of 171º) (0); well developed expansion of the lateral side of the dentary ventral to the coronoid process, with an angle up to 165º (sample mean angle of 154º) (1).

PCF taxon (matrix 1, 2 and 3)…1

E. regalis…1

E. annectens…1

37. Dentary. Orientation of the longitudinal axis of the dentary occlusal plane relative to the lateral side of the bone (as seen dorsally and caudal to the edentulous region) (DT16): diagonal axis, directed rostrolaterally and forming approximately 15º with the lateral side of the dentary (0); axis parallel to the lateral side of the dentary (1).

PCF taxon (matrix 1, 2 and 3)…1

E. regalis…1

E. annectens…1

38. Dentary. Lingual arching of the occlusal plane (DT17): present, lingually convex occlusal plane (0); absent, rostrocaudally straight occlusal plane (1).

PCF taxon (matrix 1, 2 and 3)…1

E. regalis…1

E. annectens…1

39. Dentary. Caudal extension of the dental battery (DT18): the caudal end of the dental battery is found rostral to the caudal margin of the coronoid process (0); the caudal end of the dental battery is found flush with the caudal margin of the coronoid process (1); the caudal end of the dental battery is found caudal to the caudal margin of the coronoid process (2).

PCF taxon (matrix 1)…1

PCF taxon (matrix 2 and 3)…?

E. regalis…2

E. annectens…2

Comment: in a size class 2 *E. annectens* (AMNH 5046), the status is also 1. Therefore, this is an ontogenetically variable character.

40. Dentary. Separation between the dentary tooth row and the coronoid process (DT19): the coronoid process is laterally offset (but nearly in contact) with the tooth row, lacking a platform in-between the tooth row and the base of the process (0); the coronoid process is laterally offset relative to the tooth row, with the presence of a concave platform or, in some cases, a laterodorsal concave slope separating the base of the process from the dental battery (1).

PCF taxon (matrix 1, 2 and 3)…1

E. regalis…1

E. annectens…1

41. Surangular. Morphology of the rostrodorsal process of the surangular (SA1): rostrocaudally thick process, slightly reduced in thickness rostrally, extensively exposed in lateral view (0); rostrocaudally reduced in thickness, strap-like and wedging dorsally into a thin sliver that becomes concealed in lateral view by the dorsal half of the caudal margin of the coronoid process (1).

PCF taxon (matrix 1, 2 and 3)…1

E. regalis…1

E. annectens…1

42. Surangular foramen (SA2): present (0); absent (1).

PCF taxon (matrix 1, 2 and 3)…1

E. regalis…1

E. annectens…1

43. Surangular. Accessory foramen located rostrodorsal to the main surangular foramen (SA3): present (0); absent (1).

PCF taxon (matrix 1, 2 and 3)…1

E. regalis…1

E. annectens…1

44. Surangular. Orientation of the convex side of the lateral lap and the lateroventral surface of the main body of the surangular (SA4): facing more laterally than ventrally (0);

facing more ventrally than laterally (1).

PCF taxon (matrix 1, 2 and 3)…1

E. regalis…1

E. annectens…1

45. Surangular. Lateral curvature of the caudal process of the surangular (SA5): absent, process nearly straight rostrocaudally (0); present, process laterally recurved (1).

PCF taxon (matrix 1, 2 and 3)…0

E. regalis…0

E. annectens…0

46. Angular. Position of the angular in the mandible (ANG): positioned ventrally and slightly medially, exposed in lateral view (0); positioned medially, not exposed in lateral view (1).

PCF taxon (matrix 1, 2 and 3)…1

E. regalis…1

E. annectens…1

47. Prearticular bone (PRAR): absent (0); present (1).

PCF taxon (matrix 1, 2 and 3)…?

E. regalis…0

E. annectens…0

48. Premaxilla. Mediolateral expansion of the premaxillary oral margin (measured as the ratio between the maximum mediolateral width of the premaxilla and the minimum

width at the narrowest point or post-oral constriction) (PMX1): relatively narrow, ratio less than 1.65 (mean ratio of 1.45) (0); ratio between 1.65 and 2 (mean ratio of 1.84) (1); very wide, with a ratio greater than 2 (mean ratio of 2.22) (2).

PCF taxon (matrix 1, 2 and 3)…2

E. regalis…2

E. annectens…2

Comment: for the PCF taxon, the ratio was measured from a reconstructed skull.

49. Premaxilla. Position of the premaxillary oral margin relative to the occlusal plane of the dentition (PMX2): premaxillary margin slightly ventrally offset from occlusal plane (approximately, the dorsoventral distance between the occlusal plane and the level of the premaxillary oral margin is less than the mean depth of the dentary) (0); very strongly deflected ventrally (approximately, the dorsoventral distance between the occlusal plane and the level of the premaxillary oral margin is equal to or larger than the mean depth of the dentary) (1).

PCF taxon (matrix 0, 2, 3)…0

E. regalis…0&1 (Contra [25,56,73])

E. annectens…0&1 (Contra [25,56,73])

50. Premaxilla. Degree of expansion and folding of the oral margin of the premaxilla (PMX3): moderately expanded border, dorsoventrally thicker towards the parasagittal plane of the snout, and slightly deflected ventrally (0); moderately expanded border, becoming thinner towards the parasagittal plane of the snout (1); folded caudodorsally into a thin recurved margin (2); ventrally deflected and dorsoventrally expanded, forming a very broad “lip-like” margin (3).

PCF taxon (matrix 1, 2 and 3)…3

E. regalis…3

E. annectens…3

51. Premaxilla. Premaxillary oral margin with a "double layer" morphology consisting of an external denticle-bearing layer and an internal layer of thickened bone set back slightly from the oral margin and separated from the denticular layer by a deep sulcus bearing vascular foramina (PMX5): absent (0); present (1).

PCF taxon (matrix 1, 2 and 3)…1

E. regalis…1

E. annectens…1

52. Premaxilla. Circumnarial depression including a premaxillary rostral fossa set rostral to the circumnarial fossa proper (PMX8): absent (0); present, separated from circumnarial depression by a rostrocaudally wide ridge (1).

PCF taxon (matrix 1, 2 and 3)…1

E. regalis…1

E. annectens…1

53. Premaxilla. Accessory rostral fossa located lateral to the rostral fossa and rostrolateral to the circumnarial fossa, parallel to the lateral border of the oral margin (PMX9): absent (0); present (1).

PCF taxon (matrix 1, 2 and 3)…1

E. regalis…1

E. annectens…1

54. Premaxilla. Premaxillary foramen located rostrally and ventrolateral to the rostral

margin of the narial foramen (PMX6): absent (0); present (1).

PCF taxon (matrix 1, 2 and 3)…1

E. regalis…1

E. annectens…1

55. Premaxilla. Premaxillary accessory foramen entering rostrally through the rostral fossa, located rostral to the premaxillary foramen (PMX7): absent (0); present, empties into a common chamber with the premaxillary foramen (1).

PCF taxon (matrix 1, 2 and 3)…1

E. regalis…1

E. annectens…1

56. Premaxilla. Elongation of premaxillary medial process (PMX10): the premaxillary caudodorsal process does not meet the caudoventral process caudally (0); elongate caudodorsal process that extends caudally to meet the caudoventral process, forming the caudal margin of the external naris (1).

PCF taxon (matrix 1, 2 and 3)…0

E. regalis…0

E. annectens…0

57. Premaxilla. Vertical groove on the caudoventral process of the premaxilla, located rostral to the dorsal process of the maxilla and extending ventrally from a small opening between the two premaxillary caudal processes; the groove is bounded rostrally by a triangular ventral projection of the caudolateral process of the premaxilla (PMX11): absent (0); present (1).

PCF taxon (matrix 1, 2 and 3)…0

E. regalis…0

E. annectens…0

58. Premaxilla. Elongation of the lateral process of the premaxilla (PMX12): relatively short, the caudoventral process extends caudodorsally to end dorsal to the lacrimal or mededodorsal to the rostral end of the prefrontal (0); long, the caudoventral process extends to end medial to the dorsal region of the prefrontal (1); very long, the caudoventral process extends caudodorsal to the prefrontal (2).

PCF taxon (matrix 1, 2 and 3)…0

E. regalis…0

E. annectens…0

59. Premaxilla. Morphology of the caudal region of the caudoventral process of the adult premaxilla (PMX13): mediolaterally compressed and triangular (0); dorsoventrally broad and directed caudally or caudally and slightly dorsally (1); triangular and dorsoventrally expanded, laterally convex lobe, directed rostrodorsally (2).

PCF taxon (matrix 1, 2 and 3)…0

E. regalis…0

E. annectens…0

60. Premaxilla. Premaxillary caudodorsal process has an accessory rostroventral flange that overlaps the lateral surface of the nasal in the rostral region of a supracranial crest (PMX14): absent (0); present (1).

PCF taxon (matrix 1, 2 and 3)…0

E. regalis…0

E. annectens…0

61. Premaxilla. Laterodorsal profile of the caudodorsal and caudoventral margins of the external bony naris (PMX15): subrectangular to subellipsoidal (0); triangular and very long (length/width ratio greater than 2.85), caudal constriction gradually closing caudodorsally (1); triangular and moderately long (length/width ratio greater than 2.85), caudal constriction gradually closing caudodorsally (length/width ratio between 1.85 and 2.85) (2); lacriform (length/width ratio less than 1.85), caudal constriction occurs abruptly and is primarily composed of a lateroventral expansion of the caudodorsal premaxillary process (3); lacriform (length/width ratio less than 1.85), caudal constriction occurs abruptly and is primarily composed of a dorsal expansion of the caudoventral process of the premaxilla (4).

PCF taxon (matrix 1, 2 and 3)…0

E. regalis…0

E. annectens…0

62. Premaxilla. Dorsolateral flange at approximately mid-length of the mediolaterally compressed caudoventral process of the premaxilla (PMX16): absent (0); present (1).

PCF taxon (matrix 1, 2 and 3)…0

E. regalis…0

E. annectens…0

63. Premaxilla. One or more foramina on the rostromedial surface of the premaxilla (PMX17): absent (0); present (1).

PCF taxon (matrix 1, 2 and 3)…1

E. regalis…0&1

E. annectens…0&1

64. Premaxilla. Lateral profile of the dorsal margin of the rostral rostrum (PMX18): convex (0); straight to gently concave (1); strongly concave (2).

PCF taxon (matrix 1, 2 and 3)…0

E. regalis…0

E. annectens…0

65. Premaxilla. Contour of the rostrolateral region of the thin everted oral margin (PMX19; Prieto-Márquez & Wagner in press, character 289): broad and arcuate (0); subangular (1).

This character applies to Lambeosaurine, and is therefore irrelevant to *Edmontosaurus.*

66. Premaxilla. Orientation of the medial process relative to the lateral process around the narial foramen (PMX20): subparallel (0); processes slightly converging caudally (1).

PCF taxon (matrix 1, 2 and 3)…0

E. regalis…0

E. annectens…0

67. Nasal. Location of the nasal bone and nasal cavity in the adult skull (NS1): the nasal extends from the rostral region of the skull roof to the rostrodorsal region of the snout with the nasal cavity rostromedial to the orbit (0); nasal retracted caudal to the rostrum and occupying a supracranial position in the skull, with the ventral region of the nasal meeting the prefrontal rostral to the orbit, resulting in a crest that extends supraorbitally (1); retracted caudal to the rostrum and occupying a supracranial position in the skull, with the ventral region of the nasal meeting the prefrontal caudal to the rostral margin of the orbit, resulting in a convoluted narial passage and hollow crest that extend supraorbitally (2).

PCF taxon (matrix 1, 2 and 3)…0

E. regalis…0

E. annectens…0

68. Nasal. Curvature of the caudodorsal region of the nasal (NS2): absent, nasal straight caudodorsally (0); present, nasal rotated and folded caudodorsally (1).

PCF taxon (matrix 1, 2 and 3)…0

E. regalis…0

E. annectens…0

69. Nasal. Morphology of the rostral end of the nasal dorsal process at the contact with the medial process of the premaxilla (NS3): long and wedge-shaped rostral process, gradually decreasing in width rostrally to a sharp point (0); hook-like process, it becomes abruptly deep near its rostral end and then wedges rostrally to a rostroventrally directed (1); long and subrectangular process, with slightly rounded corners (2); small rostral process of the nasal fits along the ventral edge of the premaxilla, the latter briefly overlapping the nasal (3); the nasal bifurcates to meet the premaxilla in a W-shaped interfingering suture, a long and finger-like process of the nasal has an extensive overlapping joint with the caudodorsal process of the premaxilla; and additional, more caudally located shorter process of the nasal abuts the premaxilla (4).

PCF taxon (matrix 1, 2 and 3)…?

E. regalis…2

E. annectens…2

70. Nasal. Morphology of the nasal contact with the caudodorsal region of the medial premaxillary process at the caudal margin of the narial foramen (NS4): the nasal forms a subrectangular flange exposed dorsal to the premaxillary caudoventral process (0); the nasal forms a large hook-like rostroventral process, exposed dorsal to the premaxillary

caudoventral process (1); the nasal forms a greatly shortened and dorsoventrally narrow hook-like rostroventral process, exposed dorsal to the premaxillary caudoventral process (2).

PCF taxon (matrix 1, 2 and 3)…2

E. regalis…2

E. annectens…2

71. Nasal. Location of the rostral end of the dorsal process of the nasal relative to the rostral margin of the narial foramen (NS5): the rostral end of the dorsal process of the nasal does not reach the rostral margin of the narial foramen (0); the rostral end of the rostrodorsal process of the nasal reaches the rostral margin of the narial foramen (1).

PCF taxon (matrix 1, 2 and 3)…1

E. regalis…1

E. annectens…1

72. Nasal. Caudoventral region of nasal, in hollow supracranial crest, ventrally recurved and hook-shaped, with a rostral process that inserts under the caudoventral process of the premaxilla (NS6): absent (0); present (1).

This character is irrelevant to *Edmontosaurus.*

73. Nasal. Caudal end of the nasals forming a pair of finger-like process on top of the frontals and centered around the sagittal plane of the skull roof (NS7): absent (0); present (1).

PCF taxon (matrix 1, 2 and 3)…?

E. regalis…0

E. annectens…0

74. Nasal. Caudal end of nasals forming a pair of processes that insert between the frontals at the sagittal plane of the skull roof (NS8): absent (0); present (1).

PCF taxon (matrix 1, 2 and 3)…?

E. regalis…0

E. annectens…0

75. Nasal. Mediolateral breath of caudal nasal processes that insert in between the frontals at sagittal plane of the skull (N10): processes broad and converging caudally in width, forming a V-shaped dorsal outline between the frontals (0); processes greatly compressed mediolaterally and finger-like (1).

This character is irrelevant to *Edmontosaurus.*

76. Nasal. Position of the summit of nasal arch crest relative to the caudodorsal margin of the narial foramen (NS9): summit located dorsal to the caudal margin of the narial foramen (0); summit located caudodorsal to the caudal margin of the narial foramen (1).

This character is irrelevant to *Edmontosaurus.*

77. Maxilla. Rostrodorsal process that is medially offset from the body of the maxilla and extends also medial to the caudoventral process of premaxilla to form part of medial floor of external naris (MX1): absent, the rostral end of the maxilla forms a ventrally sloping rostrodorsal shelf that underlies the premaxilla (0); present (1).

PCF taxon (matrix 1, 2 and 3)…1

E. regalis…1

E. annectens…1

78. Maxilla. Lateral exposure of the rostrodorsal process (MX2): not exposed or only

the distal tip exposed through the narial foramen in lateral view (0); large segment of the process exposed through the narial foramen in lateral view (1).

PCF taxon (matrix 1, 2 and 3)…0

E. regalis…0

E. annectens…0

79. Maxilla. Angle between the dorsal margin of the rostroventral process or shelf of the maxilla and the rostral segment of the tooth row (MX4): rostrodorsal region of the maxilla subconical in shape, dorsoventrally narrow, forming an angle of 25º or less with the rostral tooth row (mean angle of 20º) (0); dorsoventrally thicker, forming an angle greater then 25º and up to 39º with the rostral tooth row (mean angle of 31º) (1); rostroventral process dipping steeply ventrally, forming an angle of 40º or greater with the tooth row (mean angle of 43º), rostral region of the maxilla appearing dorsally "swollen" and rostrocaudally compressed (2).

PCF taxon (matrix 1, 2 and 3)…0

E. regalis…0

E. annectens…0

80. Maxilla. Lateral profile of the lateral surface of the rostrodorsal region of the maxilla (MX5): subtriangular profile with broadly arcuate dorsal margin below jugal and lacrimal (0); triangular and rostrocaudally compressed (1); trapezoid, extensive lateral exposure, with horizontal dorsal margin under lacrimal (2).

PCF taxon (matrix 1, 2 and 3)…2

E. regalis…2

E. annectens…2

81. Maxilla. Trapezoid lateral profile of rostrodorsal region of maxilla with extensive lateral exposure under lacrimal (MX18): length of exposed rostrodorsal margin is less than 40% of distance between rostral end of maxilla and caudoventral corner of orbital margin of jugal in articulated skull (0); exposed rostrodorsal margin is at least 40% of distance between rostral end of maxilla and caudoventral corner of orbital margin of jugal in articulated skull (1).

PCF taxon (matrix 1, 2 and 3)…0

E. regalis…0

E. annectens…0

82. Maxilla. Position of the dorsal process and the dorsal margin of the dorsolateral promontory of the maxilla (expressed as the ratio between the distance from its summit to the rostral end of the maxilla and the rostrocaudal length of the element) (MX7): caudally located dorsolateral promontory (with a ratio greater than 0.57; mean of 0.64), base of dorsal process positioned within the caudal third of the maxilla (0); centrally located dorsolateral promontory (with a ratio between 0.47 and 0.57; mean of 0.51), base of dorsal process positioned slightly caudal to the mid-length of the maxilla (1); dorsolateral promontory located slightly rostral to the mid-length of the maxilla (with a ratio between 0.35 and 0.46; mean of 0.42), base of dorsal process centered around the mid-length of the bone (2); the base of dorsal process and dorsolateral promontory located rostral to the mid-length of the maxilla, with a ratio less than 0.35 (mean of 0.28) for the relative position of the rostrodorsal promontory (3).

PCF taxon (matrix 1, 2 and 3)…2

E. regalis…2

E. annectens…2

83. Maxilla. Morphology of the apex of the dorsal process of the maxilla (MX8):

subtriangular, not dorsoventrally taller than it is rostrocaudally wide (0); dorsoventrally taller than it is wide, with a peaked and caudally inclined apex (1).

PCF taxon (matrix 1, 2 and 3)…0

E. regalis…0

E. annectens…0

84. Maxilla. Morphology of the jugal articulation surface (MX9): protruding lateral to the caudal third of the maxilla as a mediolaterally compressed finger-like process directed caudolaterally, separated a short distance from the lateral side of the (0); process consisting on a promontory located dorsal and rostral to the ectopterygoid shelf, bearing a concave and subtriangular, dorsolaterally-facing joint surface for the jugal, with a caudolaterally directed corner (1); subtriangular joint surface for the jugal that is more laterally than dorsally-facing, with a lateroventrally-directed pointed corner that is located adjacent and slightly dorsal to the proximal end of the lateral ridge of the ectopterygoid shelf (2); dorsally elevated jugal joint (distance between the ventral margin of the jugal joint and ectopterygoid shelf nearly equal to depth of the caudal segment of the maxilla), caudal margin of the joint flush with the caudal margin of the rostrodorsal eminence of the lateral side of the maxilla (3).

PCF taxon (matrix 1, 2 and 3)…2

E. regalis…2

E. annectens…2

85. Maxilla. Arrangement of maxillary foramina ventral and rostral to the jugal articulation (excluding large rostrodorsal or rostrolateral foramen, MX10): positioned rostrocaudally and scattered throughout the lateral side of the maxilla (0); forming either a row or cluster that is oriented rostrodorsally (1).

PCF taxon (matrix 1, 2 and 3)…1

E. regalis…1

E. annectens…1

86. Maxilla. Number of maxillary foramina ventral and rostral to the jugal articulation (excluding large rostrodorsal or rostrolateral foramen) (MX11): seven or more (0); six or less (1).

PCF taxon (matrix 1, 2 and 3)…1

E. regalis…1

E. annectens…1

87. Maxilla. Large rostral maxillary foramen (MX12): opening on the rostrolateral body of the maxilla, within the rostral half of the rostrodorsal margin of the element and exposed in lateral view (0); opening on the rostrolateral body of the maxilla, within the dorsal half of the rostrodorsal margin of the element and exposed in lateral view (1); opening on the dorsal surface of the maxilla along the maxilla-premaxilla contact, not exposed laterally (2).

PCF taxon (matrix 1, 2 and 3)…1

E. regalis…1

E. annectens…1

88. Maxilla-lacrimal contact (MX13): present externally (0); largely covered externally by the jugal-premaxilla contact (1).

PCF taxon (matrix 1, 2 and 3)…1

E. regalis…1

E. annectens…1

89. Maxilla. Length of the ectopterygoid shelf relative to the total rostrocaudal length of the alveolar margin of the maxilla (MX14): ratio between the length ectopterygoid shelf and the length of the rostrocaudal alveolar margin up to 0.25 (mean ratio of 0.20) (0); ratio greater than 0.25 and up to 0.35 (mean ratio of 0.30) (1); ratio greater than 0.35 (mean ratio of 0.45) (2).

PCF taxon (matrix 1, 2 and 3)…2

E. regalis…2

E. annectens…2

90. Maxilla. Slope of the ectopterygoid shelf, measured as the angle between this and the rostrocaudal axis of the caudal segment of the tooth row (MX15): steeply inclined caudoventrally, with an angle greater than 21º (mean angle of 29º) (0); shelf inclined with an angle greater than 10 and up to 21º (mean angle of 15º) (1); slightly inclined shelf, with an angle greater than 4º and up to 10º (mean angle of 8º) (2); horizontal shelf, with an angle up to 4º (3).

PCF taxon (matrix 1, 2 and 3)…3

E. regalis…3

E. annectens…3

91. Maxilla. Morphology of the lateral emargination of the ectopterygoid shelf (MX16): dorsoventrally thin ridge (0); faint or dorsoventrally thin rostrally, then abruptly becoming dorsoventrally thick along the caudal segment of the margin (1); dorsoventrally thick continuous ridge, gradually thicker caudally than rostrally (2).

PCF taxon (matrix 1, 2 and 3)…2

E. regalis…2

E. annectens…2

92. Maxilla. Position of the central region of the arcuate row of special foramina on the medial side of the maxilla (MX17): ventral to or at the level of the mid-dorsoventral depth of the maxilla (0); dorsal to the mid-dorsoventral depth of the maxilla (1).

PCF taxon (matrix 1, 2 and 3)…1

E. regalis…1

E. annectens…1

93. Lacrimal. General morphology of the adult lacrimal in lateral view (LC1): triangular and rostrocaudally elongated, with a rostral process that is rostrally (and slightly ventrally) directed (0); triangular, rostrocaudally abbreviated with a relatively shorter and thinner rostral process (1).

PCF taxon (matrix 1, 2 and 3)…0

E. regalis…0

E. annectens…0

94. Lacrimal. Ventral margin of the lacrimal with a prominent convexity rostral to the jugal notch (LC2): absent (0); present (1).

PCF taxon (matrix 1, 2 and 3)…0

E. regalis…0

E. annectens…0

95. Jugal. Rostral apex of the rostral process of the jugal (J1): present, wedge-shaped, elongated and sharply pointed, positioned at mid distance along the dorsoventral depth of the rostral process (0); present, wedge-shaped, pointed and less elongated than in (0), positioned within the dorsal half of the rostral process of the jugal; the dorsal margin of the apex forms a steeper angle with the horizontal than in state (0) (1); greatly reduced to

a blunt convexity (2); reduced to a short process, only slightly thinner rostrally and ending abruptly (3); absent, straight nearly vertical rostral margin (4); absent, tongue-shaped rostral margin (5).

PCF taxon (matrix 1, 2 and 3)…1

E. regalis…1

E. annectens…1

96. Jugal. Dorsoventral expansion of the caudodorsal margin of the rostral process of the jugal (J2): dorsoventrally narrow, rostrodorsally directed and forming little of the rostroventral margin of the orbital rim (0); dorsoventrally deep (about 60-90% as deep as the rostral jugal constriction), dorsally or slightly recurved caudodorsally, forming the rostroventral corner of the orbital rim (1).

PCF taxon (matrix 1, 2 and 3)…1

E. regalis…1

E. annectens…1

97. Jugal. Morphology of the triangular caudoventral margin of the rostral process of the jugal (J3): shallow and rostrocaudally wide prominence (wider than deep) (0); ventrally pointed, approximately as deep as or slightly deeper as its proximal end is wide (1); ventrally projected triangular narrow process, at least twice as deep as it is wide, sharply pointed and often recurved caudally (2).

PCF taxon (matrix 1, 2 and 3)…0

E. regalis…0

E. annectens…0

98. Jugal. Location of the caudoventral apex of the rostral process relative to the

caudodorsal articulation with the lacrimal (with longitudinal axis of the rostral process oriented horizontally) (J4): apex located caudoventral to the caudal margin of the lacrimal process (0); apex located ventral to the caudal margin of the lacrimal process (1).

PCF taxon (matrix 1, 2 and 3)…0

E. regalis…0

E. annectens…0

99. Jugal. Orientation of the medial articular surface of the rostral process of the jugal (J5): facing medioventrally, the articular surface forms a deep concavity bounded dorsally and caudally by a laterally offset rim (0); facing medially, the articular surface is bounded only caudally by a rim of bone (1).

PCF taxon (matrix 1, 2 and 3)…1

E. regalis…1

E. annectens…1

100. Jugal. Ventral expansion of the caudoventral jugal flange (measured as the ratio between the dorsoventral depth of the flange and the minimum depth of the caudal constriction of the jugal) (J8): slightly expanded flange, ratio of 1.36 or less (mean ratio of 1.29) (0); moderately expanded flange, ratio greater than 1.36 and up to 1.55 (mean ratio of 1.44) (1); greatly expanded flange, ratio greater than 1.55 (mean ratio of 1.68) (2).

PCF taxon (matrix 1, 2 and 3)…0 and 1

E. regalis…1

E. annectens…1

101. Jugal. Lateral profile of the quadratojugal flange (J9) subconical, dorsoventrally

tall and rostrocaudally narrow, with a nearly vertical caudal margin (0); auricular in shape, with subparallel concave to nearly straight dorsal and convex ventral margins that converge dorsally into a short subconical point (1); fan-like, with dorsal and ventral margins that are subparallel and diverge caudodorsally; dorsal and ventral margins can be straight or slightly bowed dorsally (2); auricular in shape, with subparallel concave to nearly straight dorsal and convex ventral margins that converge dorsally into a recurved or dorsally directed tall subconical extension (this state is similar to (1), but the dorsal region of the flange is rostrocaudally narrower and taller) (3).

PCF taxon (matrix 1 and 2)…1

PCF taxon (matrix 3)…?

E. regalis…3

E. annectens…3

Comment: see section 1.4.2.7.

102. Jugal. Morphology of the ventral margin located between the caudoventral and quadratojugal flanges (J10): relatively short and shallow concavity (0); relatively wide and well-pronounced concavity (1).

PCF taxon (matrix 1, 2 and 3)…0

E. regalis…0

E. annectens…0

103. Jugal. Relative depth of the caudal and rostral constrictions (rostral constriction region located between the rostral and postorbital processes; caudal constriction region located between the postorbital process and the caudoventral flange) (J11): deeper rostral constriction, ratio of the depth of the caudal constriction relative to the rostral of 1 or less (0); deeper caudal constriction, with a ratio greater than 1 and less than 1.35 (1);

extremely deep caudal constriction, with a ratio greater than 1.35 (2).

PCF taxon (matrix 1 and 3)…1

PCF taxon (matrix 2 and 3)…?

E. regalis…2

E. annectens…1 & 2 (contra [25,56,73])

Comment: see section 1.4.2.7.

104. Jugal. Relative width and lateral profiles of the orbital and infratemporal margins of the jugal (J13): wider orbital margin and relatively constricted ventral margin of the infratemporal fenestra (0); orbital and infratemporal margins are nearly equally wide (1); wider infratemporal margin (2).

PCF taxon (matrix 1, 2 and 3)…1

E. regalis…1

E. annectens…1

105. Quadrate. Degree of curvature of the caudal margin of the quadrate (Q1): the caudal margin of the dorsal half or third of the quadrate displays a slight curvature relative to the ventral half of the element, with an angle of 150º or greater (mean angle of 161º) (0); the caudal margin of the dorsal half or third of the quadrate is strongly curved caudally relative to the ventral half of the element, with an angle less than 150º (mean angle of 143º) (1).

PCF taxon (matrix 1, 2 and 3)…0

E. regalis…0

E. annectens…0

Comment: see section 1.4.2.11.

106. Quadrate. Position of the quadratojugal (paraquadrate) notch along the dorsoventral length of the quadrate (measured as the ratio between the distance from the mid-length of the notch to the quadrate head and the dorsoventral length of the element) (Q2): the mid point of the notch is located near the mid-length of the quadrate, ratio less than 0.60 (mean ratio of 0.54) (0); the mid point of the notch is located ventral to the mid-length of the quadrate, ratio of 0.60 or greater (mean ratio of 0.64) (1).

PCF taxon (matrix 1, 2 and 3)…1

E. regalis…1

E. annectens…1

107. Quadrate. Orientation of the dorsal margin of the quadratojugal notch of the quadrate (measured as the angle between this and the caudal margin of the element) (Q3): angle greater than 45º (mean angle of 52º) (0); angle up to 45º (mean angle of 28º) (1).

PCF taxon (matrix 1, 2 and 3)…1

E. regalis…1

E. annectens…1

108. Quadrate. Morphology of the lateral profile of the quadratojugal notch of the quadrate (Q4): subcircular, with a ventral half of the notch that is recurved and has a horizontal rostral segment (0); wide arcuate and asymmetrical, with the ventral half of the notch having a short horizontal rostral segment (1); wide arcuate and symmetrical, the ventral half of the notch being rostroventrally-directed, nearly straight as it is the dorsal half (2).

PCF taxon (matrix 1, 2 and 3)…2

E. regalis…2

E. annectens…2

109. Quadrate. Development of the squamosal buttress on the caudal margin of the dorsal end of the quadrate (Q5): absent or poorly developed as a gentle convexity (0); present, the buttress is a sharp protuberance hanging from the caudal side of the dorsal fourth of the quadrate, near the head of the element (1).

PCF taxon (matrix 1, 2 and 3)…0

E. regalis…0

E. annectens…0

110. Quadrate. Morphology of ventral surface of the quadrate (Q6): mediolaterally broad and rostrocaudally compressed, lateral condyle slightly larger than the medial one (mean ratio between the rostrocaudal width of the lateral condyle and the mediolateral width of the ventral end of the quadrate of 0.59); the ventral surface of the lateral condyle is only slightly offset ventrally relative to the ventral surface of the medial condyle (0); subtriangular in ventral view, lateral condyle rostrocaudally expanded and much larger than the medial one (mean ratio between the rostrocaudal width of the lateral condyle and the mediolateral width of the ventral end of the quadrate of 0.90); the ventral surface of the lateral condyle is well offset ventrally relative to the ventral surface of the medial condyle (1).

PCF taxon (matrix 1, 2 and 3)…1

E. regalis…1

E. annectens…1

111. Prefrontal. Dorsomedial margin of the prefrontal developed into a caudodorsally-oriented crest (PF1): absent (0); present, not extending caudal to the prefrontal-frontal articulation (1); present, the crest extends caudally over the dorsal surface of the frontal and above the prefrontal-postorbital articulation in lateral view in adults (2).

PCF taxon (matrix 1, 2 and 3)…0

E. regalis…0

E. annectens…0

112. Prefrontal. Lateral profile of the rostrodorsal margin of the prefrontal (PF2): subarcuate to smoothly curved, the rostral margin is rostroventrally oriented and forming an obtuse angle with the dorsal orbital margin (0); rostromedially broad with subsquared rostrodorsal corner (1).

PCF taxon (matrix 1, 2 and 3)…1

E. regalis…1

E. annectens…1

113. Prefrontal. Deep fossa on the ventral surface of the rostrodorsal corner of the orbit, rostrodorsal orbital margin being squared and slightly projected rostrodorsally (PF7): absent (0); present (1).

PCF taxon (matrix 1)…0

PCF taxon (matrix 2 and 3)…?

E. regalis…1

E. annectens…1

Comment: see section 1.4.2.4.

114. Prefrontal. Mediolateral breadth of the exposed rostroventral region of the prefrontal (PF3): the rostroventral region is mediolaterally expanded (0); the exposed rostroventral region is mediolaterally compressed and narrow (1).

PCF taxon (matrix 1, 2 and 3)…0

E. regalis…0

E. annectens…0

115. Prefrontal. Inclusion of the prefrontal in the circumnarial fossa (PF4): absent (0); present (1).

PCF taxon (matrix 1, 2 and 3)…0

E. regalis…0

E. annectens…0

116. Prefrontal. Exposure of the prefrontal-nasal contact in lateral and/or dorsal view (PF6): contact totally exposed in lateral and/or dorsal view (0); contact visible in lateral view along the caudal and half of the dorsal margin of the prefrontal (1); contact visible in lateral view only along the caudal region of the prefrontal in adults, due to the invasion of the premaxilla along the medial side of the prefrontal (2).

PCF taxon (matrix 1, 2 and 3)…0

E. regalis…0

E. annectens…0

117. Postorbital. Dorsal promontorium on the rostral process of the postorbital (PO1): absent, the dorsal surface of the postorbital above the jugal process is horizontal or slightly concave (0); present in adult specimens, the articular margin for the prefrontal is elevated and the dorsal surface of the postorbital above the jugal process is deeply depressed (1).

PCF taxon (matrix 1, 2 and 3)…0

E. regalis…0

E. annectens…0

118. Postorbital. Rostrocaudal constriction of the dorsal region of the infratemporal fenestra (PO2): absent, caudal (squamosal) process of the postorbital elongate over the infratemporal fenestra (broad and subrectangular dorsal region of the fenestra) (0); present and caused by the presence of a nearly straight and oblique caudoventral margin of the caudodorsal region of the postorbital (dorsal region of infratemporal fenestra typically subtriangular) (1); present and caused by rostrocaudal shortening of the caudal process of the postorbital (dorsal region of infratemporal fenestra typically oval) (2).

PCF taxon (matrix 1)…0

PCF taxon (matrix 2 and 3)…?

E. regalis…1

E. annectens…1

This character is influenced by the width of the jugal process of the postorbital (section 1.4.2.9) and the length of the postorbital process of the squamosal (section 1.4.2.10), both of which are ontogenetically variable characters.

119. Postorbital. Morphology of the central body of the postorbital (PO3): triangular, rostrocaudally broad, expanded rostroventrally to form a straight and obliquely oriented caudodorsal orbital margin (0); triangular, with a caudodorsal orbital margin that ranges in lateral profile from semicircular to subsquared (1); rostrocaudally expanded, rostromedially excavated and bulging laterally ("inflated"), containing a deep pocket (2).

PCF taxon (matrix 1, 2, and 3)…1

E. regalis…2

E. annectens…2

Comment: although the widening of the postorbital bar is an ontogenetic character (see section 1.4.2.9), the size class 3 postorbital does not have a pocket seen in other

Edmontosaurus sp., but the bony lamina of the caudodorsal orbital margin is more extensive, resulting a shallow but large depression.

120. Postorbital. Morphology of the caudal end of the caudal process of the postorbital at its articulation with the squamosal (PO5): oblong or wedge-shaped (0); bifid (1).

PCF taxon (matrix 1, 2 and 3)…1

E. regalis…1

E. annectens…1

121. Postorbital. Caudal extension of the caudal ramus of the postorbital that overlaps the laterodorsal surface of the squamosal (PO6): the caudal end of the postorbital caudal ramus extends to a point rostral to the quadrate cotylus and does not overlap the latter (0); the caudal end of the postorbital caudal ramus extends caudodorsal to the precotyloid process and over as much as the rostral half of the quadrate cotylus (1); the caudal end of the postorbital caudal ramus completely overlaps the laterodorsal side of the squamosal quadrate cotylus (2).

PCF taxon (matrix 1)…0

PCF taxon (matrix 2 and 3)…?

E. regalis…1

E. annectens…1

Comment: see section 1.4.2.10.

122. Squamosal. Length of the precotyloid process of the squamosal (measured as the ratio of its length relative to the width of the quadrate cotylus) (SQ1): very short precotyloid process, ratio less than 0.95 (mean ratio of 0.74) (0); moderately long precotyloid process, ratio between 0.95 and 1.25 (mean ratio of 1.13) (1); very long precotyloid process, ratio greater than 1.25 (mean ratio of 1.41) (2).

PCF taxon (matrix 1, 2 and 3)…1

E. regalis…1

E. annectens…1

123. Squamosal. Dorsoventral expansion of the caudolateral surface of the squamosal (SQ2): unexpanded, shallowly exposed in caudal view (0); greatly expanded dorsomedially, forming a deep, near vertical, well-exposed face in caudal view (1).

PCF taxon (matrix 1, 2 and 3)…0

E. regalis…0

E. annectens…0

124. Squamosal. Separation of the squamosals at the occipital margin of the skull roof (SQ3): completely separated by the parietal (0); the squamosal approach the sagittal plane of the skull, separated by a narrow band of parietal (1); extensive intersquamosal joint present at the midline, parietal completely excluded from the sagittal plane of the skull at that particular spot (in adults) (2).

PCF taxon (matrix 1, 2 and 3)…1

E. regalis…1

E. annectens…1

125. Squamosal. Rostromedial indenture of the medial ramus of the squamosal (SQ4): absent, medial ramus of the squamosal extends medially, forming a subsquared caudolateral border of the skull roof (0); present, medial ramus of the squamosal curves rostromedially, so that the back of the skull appears to be deeply indented rostrally when viewed dorsally (1).

PCF taxon (matrix 1, 2 and 3)…0

E. regalis…0

E. annectens…0

126. Frontal. Bifurcation of the rostromedial margin of the frontals at the sagittal plane of the skull roof, leaving a V-shaped space in between (F1): absent (0); present (1).

PCF taxon (matrix 1, 2 and 3)…1

E. regalis…1

E. annectens…1

127. Frontal fontanelle, present at least at one stage during ontogeny (F2): absent (0); present (1).

PCF taxon (matrix 1, 2 and 3)…0

E. regalis…0

E. annectens…0

128. Frontal. Nasal articulation surface of the frontal shaped into a rostroventrally-sloping platform (F3): absent (0); present (1).

PCF taxon (matrix 1, 2 and 3)…0

E. regalis…0

E. annectens…0

129. Frontal. Nasal articulation surface of the frontal shaped into a dorsoventrally thickened, tongue-like platform that projects caudodorsally to overhang the parietal in adults (F4): absent (0); present (1).

PCF taxon (matrix 1, 2 and 3)…0

E. regalis…0

E. annectens…0

130. Frontal. Median cleft separating the two striated tongues of the frontal platform (F5): absent (0); present (1).

This character is irrelevant to *Edmontosaurus.*

131. Frontal. Triangular rostrolateral projection ending into narrow apex (F10): absent (0); present (1).

PCF taxon (matrix 1, 2 and 3)…0

E. regalis…0

E. annectens…0

132. Frontal. Exposure of the frontal at the dorsal margin of the orbit (F6): frontal completely excluded from the orbital margin by an extensive articulation between the prefrontal and postorbital (0); frontal exposed, forming part of the dorsal orbital margin in between the prefrontal and postorbital (1).

PCF taxon (matrix 1, 2 and 3)…1

E. regalis…1

E. annectens…1

133. Frontal, upward doming dorsal to the braincase in subadult (and perhaps young adult) specimens (F7): absent (0); present (1).

PCF taxon (matrix 1, 2 and 3)…0

E. regalis…0

E. annectens…0

134. Frontal, length/width ratio of the ectocranial surface (F8): relatively elongated ectocranial surface, with a ratio greater than 0.8 (0); relatively short ectocranial surface, with a ratio of 0.8 or less, but greater than 0.4 (1); greatly shortened ectocranial surface, with a ratio less than 0.4 (2).

PCF taxon (matrix 1, 2 and 3)…0

E. regalis…0

E. annectens…0

135. Frontal. Morphology of the ventral annular ridge that defines the rostral extent of the cerebral fossa (F9): long, low and gently rounded in medial view (0); sharp annular ridge (1).

PCF taxon (matrix 1, 2 and 3)…0

E. regalis…0

E. annectens…0

136. Frontal platform extending caudodorsally to form a finger-shaped buttress under nasal crest (F11): absent (0); present (1).

PCF taxon (matrix 1, 2 and 3)…0

E. regalis…0

E. annectens…0

137. Parietal. Maximum length/minimum width proportions of the adult parietal (PAR1): very short, length/width ratio less than 1.40 (sample mean ratio of 1.19) (0); short, ratio between 1.40 and 2.35 (sample mean ratio of 1.98) (1); relatively long, ratio greater than 2.35 (sample mean ratio of 2.75) (2).

PCF taxon (matrix 1, 2 and 3)…2

E. regalis…2

E. annectens…2

138. Parietal. Orientation of the parietal midline crest (PAR2): straight and level with the skull roof or slightly down-warped along its length (0); the sagittal crest deepens caudally and is strongly down-warped (1).

PCF taxon (matrix 1, 2 and 3)…0

E. regalis…0

E. annectens…0

139. Parietal. Rostral extension of the sagittal crest along the dorsal surface of the parietal (PAR4): the sagittal crest extends along the entire length of the parietal and remains sharp and well defined at the rostral region (0); the sagittal crest extends along the entire length of the parietal but its sharpness fades away at the rostral region where the parietal is rostrocaudally shorter than it is wide (1); the sagittal crest only extends along the caudal half of the parietal and the rostral half of the dorsal surface of the parietal is flattened, lacking any ridge or mediolateral compression (2).

PCF taxon (matrix 1, 2 and 3)…0

E. regalis…0

E. annectens…0

140. Basioccipital. Participation of the basioccipital in the ventral margin of the foramen magnum (BO1): absent, the exoccipital condyloids nearly or completely exclude the basioccipital from the ventral margin of the foramen magnum (0); present, the exoccipitals are separated at the sagittal plane of the braincase and allow the basioccipital to become part of the ventral margin of the foramen magnum (1).

PCF taxon (matrix 1, 2 and 3)…1

E. regalis…1

E. annectens…1

141. Basioccipital. Length of basioccipital constriction (BO3): relatively long and well developed (0); poorly developed and relatively short constriction (1).

PCF taxon (matrix 1, 2 and 3)…1

E. regalis…1

E. annectens…1

142. Basisphenoid. Development of the alar process of the basisphenoid (BS2): moderately developed (0); very well developed, relatively large in size (1).

PCF taxon (matrix 1, 2 and 3)…0

E. regalis…0

E. annectens…0

143. Basisphenoid. Ventral transverse caudal ridge between the basipterygoid processes of the basisphenoid (BS3): absent or very poorly developed (0); present, sharply defined ridge (1).

PCF taxon (matrix 1, 2 and 3)…1

E. regalis…1

E. annectens…1

144. Basisphenoid. Short median ventral process located between the basipterygoid processes of the basisphenoid (BS4): absent (0); present, ventrally or rostroventrally inclined (1).

PCF taxon (matrix 1, 2 and 3)…1

E. regalis…1

E. annectens…1

145. Basisphenoid. Development of the rostral constriction of the basisphenoid, caudal to the basipterygoid processes (measured as the ratio between the minimum mediolateral width of the rostral constriction and the maximum width of the basisphenoid across the spheno-occipital tubercles) (BS5): very thick constriction, ratio less than 1.45 (sample mean ratio of 1.37) (0); moderately developed constriction, ratio between 1.45 and 1.90 (sample mean ratio of 1.72) (1); very thin constriction, ratio greater than 1.90 (sample mean ratio of 2.25) (2).

PCF taxon (matrix 1, 2 and 3)…1

E. regalis…1

E. annectens…1

146. Laterosphenoid. Complete lateral osseous closure of the ophthalmic sulcus (V_1) of the laterosphenoid (LS1): absent (0); present (1).

PCF taxon (matrix 1, 2 and 3)…0

E. regalis…0

E. annectens…0

147. Laterosphenoid. Extreme reduction of the length of the postorbital process of the laterosphenoid to 25 % or less the length of the mediodorsal flange of this element (LS2): absent (0); present (1).

PCF taxon (matrix 1, 2 and 3)…1

E. regalis…1

E. annectens…1

148. Exoccipital. Caudal extension of the exoccipital-supraoccipital shelf above the foramen magnum (EX1): very short rostrocaudal length, approximately less than half the diameter of the foramen magnum (0); moderately long, approximately more than half but less than the diameter of the foramen magnum (1); very long, substantially longer (often twice or more) than the diameter of the foramen magnum (2).

PCF taxon (matrix 1, 2 and 3)…2

E. regalis…2

E. annectens…2

149. Pterygoid. Elevation of the proximodorsal region of the quadrate wing of the pterygoid (PLT1): absent (0); present (1).

PCF taxon (matrix 1, 2 and 3)…0

E. regalis…0

E. annectens…0

150. Pterygoid. Ventral extension of the lamina located ventral to the central buttress of the pterygoid (PLT2): lamina of moderate size, a relatively large portion of the ventral quadrate process and the rostroventral process extends beyond the ventral margin of the lamina (0); extensive lamina, only a relatively small portion of the ventral quadrate process and the rostroventral process extends beyond the ventral margin of the lamina (1).

PCF taxon (matrix 1 and 2)…0

PCF taxon (matrix 3)…?

E. regalis…1

E. annectens…0 and 1

148

Comment: see section 1.4.2.17.

151. Ectopterygoid–jugal contact (PLT3): present, the ectopterygoid contacts the medial side of the jugal (0); absent, the jugal lacks an articular facet for the ectopterygoid (1).

PCF taxon (matrix 1, 2 and 3)…1

E. regalis…1

E. annectens…1

152. Angle between the dorsal margin of the rostrum parallel to the long axis of the external naris and the maxillary tooth row (adults only) (RST2): angle up to 30º (sample mean angle of 27º) (0); angle greater than 30º and up to 40º (sample mean angle of 34º) (1); angle greater than 40º (sample mean angle of 47º) (2).

PCF taxon (matrix 1, 2 and 3)…0

E. regalis…0

E. annectens…0

Comment: the result of the morphometric analysis shows the skull of *Edmontosaurus* would elongate as they grew, which would change the angle. Yet, the character status of the PCF taxon would be less than 30º.

153. Exposure of the nasal passage (NPS1): present, nasal passage open and exposed on the lateral side of the rostrum (0); absent, nasal passage nearly or completely enclosed by bone and formation of internal cavities and passages (such as lateral diverticula and a common median chamber) (1).

PCF taxon (matrix 1, 2 and 3)…0

E. regalis…0

E. annectens…0

154. Lateral profile of the narial foramen (NPS2): broad and subellipsoidal in lateral profile (0); narrow and subellipsoidal in lateral profile (1); extremely narrow, slit-like in lateral profile (2).

PCF taxon (matrix 1, 2 and 3)…1

E. regalis…1

E. annectens…1

155. Degree of closure of the nasal passage on the lateral crest surface between the caudoventral process of the premaxilla and the nasal (NPS3): present, premaxilla-nasal fontanellae persist into late ontogenetic stages (0); absent, fontanellae completely closed in adults (1).

This character is irrelevant to *Edmontosaurus.*

156. Ratio between the length of the narial foramen and the distance between the rostroventral corner of the premaxilla and the rostroventral margin of the prefrontal (NPS4): very short narial foramen, ratio up to 0.40 (sample mean ratio of 0.32) (0); moderately long narial foramen, ratio greater than 0.40 but less than 0.60 (sample mean ratio of 0.49) (1); elongated narial foramen, ratio between 0.60 and 0.65 (sample mean ratio of 0.62) (2); extremely long narial foramen, ratio greater than 0.65 (sample mean ratio of 0.72) (3).

PCF taxon (matrix 1, 2 and 3)…1

E. regalis…1

E. annectens…1

157. Nasal vestibule folded into an S-loop in the enclosed premaxillary passages rostral to the dorsal process of the maxilla (NPS5): absent (0); present (1).

150

PCF taxon (matrix 1, 2 and 3)…0

E. regalis…0

E. annectens…0

158. Location of the lateral diverticulum relative to the common median chamber (NPS6): lateral to the common median chamber (0); rostral to the common median chamber (1); caudodorsal to the common median chamber (2).

This character is irrelevant to *Edmontosaurus*.

159. Communication between the external bony naris, the lateral diverticulum and the common median chamber (NPS7): a tubular premaxillary passage extends caudodorsally from the bony naris to the lateral diverticulum, that is then connected to the common median chamber (0); a tubular premaxillary passage connects directly the bony naris to the common median chamber (1).

This character is irrelevant to *Edmontosaurus*.

160. Caudal extent of the nasal passage dorsal and/or caudal to the orbit (NPS8): absent, nasal passage restricted to the antorbital region of the skull (0); present, but not extending caudal to the occiput, with a nasal vestibule that flanks a common median chamber (1); present, nasal vestibule extending caudodorsal to the occipital region of the skull (2).

PCF taxon (matrix 1, 2 and 3)…0

E. regalis…0

E. annectens…0

161. Composition of the caudal margin of the functional external naris (NPS9): formed by the nasal dorsally and the premaxilla ventrally (0); formed entirely by the nasal (1); formed entirely by the premaxilla (2).

PCF taxon (matrix 1, 2 and 3)…1

E. regalis…1

E. annectens…1

162. Circumnarial fossa on the lateral surface of the facial region of the skull (CMN1): absent, circumnarial structure entirely enclosed (0); present (1).

PCF taxon (matrix 1, 2 and 3)…1

E. regalis…1

E. annectens…1

163. Caudodorsal extension of circumnarial fossa (homologous to the lateral diverticulum inside hollow supracranial crests) (CMN2): the fossa does not reach the caudal margin of the narial foramen and, thus, lacks a caudal margin (0); the fossa extends as far as to surround the caudal margin of the narial foramen, but does not reach the orbit (1); the fossa extends as far as the rostrodorsal region of the orbit (2); the fossa extends beyond the orbit, caudodorsal to its caudal margin (3).

PCF taxon (matrix 1, 2 and 3)…1

E. regalis…1

E. annectens…1

164. Degree of excavation of the caudal region of the circumnarial fossa (CMN3): lightly incised (0); deeply incised (1); invaginated (2).

PCF taxon (matrix 1)…0

PCF taxon (matrix 2 and 3)…?

E. regalis…2

E. annectens…2

Comment: see section 1.4.2.3.

165. Elevation of the skull roof dorsal to the ancestral lateral profile (i.e., presence of supracranial crest) (CRS1): absent (0); present (1).

PCF taxon (matrix 1, 2 and 3)…0

E. regalis…0

E. annectens…0

166. Composition of the supracranial crest (or the homologous region of the skull from which the crest forms) (excluding supporting elements) (CRS2): composed exclusively of the nasals (0); primarily composed of the nasals and frontals (1); primarily composed of the nasals and premaxillae (2).

PCF taxon (matrix 1, 2 and 3)…0

E. regalis…0

E. annectens…0

167. Relative contribution of the nasal and premaxilla in the formation of hollow supracranial crests (CRS3): the nasals constitute half or a larger portion of the crest in the form of a caudal plate-like surface (0); the nasals form a smaller portion of the crest relative to the surrounding premaxillae (1).

This character is irrelevant to *Edmontosaurus.*

168. Supracranial crest shape (CRS4): dome-like broad and low protuberance (0); mediolaterally compressed arcuate protuberance, rostral or, in adults, dorsal to the level to the orbits (1); paddle-like and caudally (as well as slightly dorsally) directed solid blade of bone (2); mediolaterally narrow and paddle-like, extending caudal to the occiput

(3); rostrally excavated and rostrally-facing protuberance, rostrodorsal to the orbit (4); nasal fold that rises dorsally or caudodorsally to form a laterally excavated promontory, with a caudal region that rests over the frontals (5); raised into a large vertical fan, formed by a solid plate-like extension of the premaxilla ("cockscomb") above the nasal passages in the rostral region of the crest (6); long and tubular, caudodorsally directed beyond the occiput and slightly arched (7).

This character is irrelevant to *Edmontosaurus.*

169. Hollow crest-snout angle along the dorsal margin of the premaxilla in lateral view (in adults) (CRS5): absent, the lateral profile of the snout is continuous with the lateral profile of the dorsal premaxillary margin of the crest (0); facial profile shallowly concave in lateral view, angle greater than 140º (1); angle between 110º and 140º (2); crest procumbent and rostrally inclined, angle less than 110º (3).

This character is irrelevant to *Edmontosaurus.*

170. Caudal extension of the hook-like nasal process on the caudoventral region of helmet-shaped hollow supracranial crests (CRS6): rostral to or at the level of the caudal margin of the occiput (0); extended caudal to the level of the caudal margin of the occiput (1).

This character is irrelevant to *Edmontosaurus.*

171. Palpebral (supraorbital) bone (PLP): absent (0); present (1).

PCF taxon (matrix 1, 2 and 3)…0

E. regalis…0

E. annectens…0

172. Length/width proportions of the orbit (ORB) nearly circular, approximately as wide as it is deep (0); elongated, dorsoventrally deeper than it is wide (1).

PCF taxon (matrix 1, 2 and 3)…1

E. regalis…1

E. annectens…1

Comment: although this is likely an ontogenic character, the status in the PCF taxon does not differ from adult *Edmontosaurus.*

173. Presence of a gap (paraquadratic foramen) between the quadratojugal and the jugal (PQF): absent (0); present (1).

PCF taxon (matrix 1, 2 and 3)…0

E. regalis…0

E. annectens…0

174. Size of the infratemporal fenestra relative to that of the orbit (ITF1): infratemporal fenestra both rostrocaudally wider and dorsoventrally deeper than the orbit (0); infratemporal fenestra rostrocaudally narrower than or approximately as wide as the orbit (1).

PCF taxon (matrix 1, 2 and 3)…1

E. regalis…1

E. annectens…1

Comment: although this is likely an ontogenic character, the status in the PCF taxon does not differ from adult *Edmontosaurus.* Because the infratemporal fenestra would narrow as they grew, it would be safe to score as 1 for the PCF taxon.

175. Shape and rostrocaudal width of the dorsal margin of the infratemporal fenestra relative to that of the dorsal orbital margin (ITF2): subrectangular, with a dorsal infratemporal margin that is approximately as wide as the ventral margin (0);

subtriangular, with a dorsal infratemporal margin that is narrower than the ventral margin (1).

PCF taxon (matrix 1)…0

PCF taxon (matrix 2 and 3)…?

E. regalis…1

E. annectens…1

This character is influenced by the width of the jugal process of the postorbital (section 1.4.2.9) and the length of the postorbital process of the squamosal (section 1.4.2.10), both of which are ontogenetically variable characters.

176. Location of the dorsal margin of the infratemporal fenestra relative to the dorsal margin of the orbit (ITF3): the dorsal margin of the infratemporal fenestra lies approximately at the same level than the dorsal margin of the orbit and the caudal region of the skull roof is subhorizontal or slightly sloping rostroventrally relative to the frontal plane (0); the dorsal margin of the infratemporal fenestra is substantially more dorsally located than the dorsal margin of the orbit and the caudal region of the skull roof is rostroventrally inclined relative to the frontal plane (1); the dorsal margin of the infratemporal fenestra lies slightly or substantially below the level of the dorsal margin of the orbit and the caudal region of the skull roof is subhorizontal or slightly sloping caudoventrally relative to the frontal plane (2).

PCF taxon (matrix 1, 2 and 3)…0

E. regalis…0

E. annectens…0

177. Morphology of the dorsal outline of the supratemporal fenestra (STF): subrectangular, with the long axis directed rostrally (0); oval, with the long axis directed

rostrolaterally (1); oval and wider mediolaterally than rostrocaudally (2).

PCF taxon (matrix 1, 2 and 3)…0

E. regalis…0

E. annectens…0

178. Depth of the skull (ratio between the skull height along caudal margin of quadrate and distance from rostral predentary tip to the level of the caudal margin of quadrate) (SK1): ratio less than 0.70 (0); relatively deep skull, ratio of 0.70 or greater (1).

PCF taxon (matrix 1, 2, and 3)…0

E. regalis…0

E. annectens…0

Comment: morphometric analysis shows the skull would elongate as *Edmontosaurus* grew, but the status of the PCF taxon is scored as 0, as in other *Edmontosaurus.*

179. Maximum transverse width of the cranium in dorsal view across the postorbitals relative to the width across the quadrate cotylus of the squamosals (SK2): the skull is more than 25 % wider across the postorbitals (sample mean ratio of 0.35) (0); the skull is up to 25 % wider across the postorbitals (sample mean ratio of 0.14) (1).

PCF taxon (matrix 1, 2 and 3)…0

E. regalis…0

E. annectens…0

Comment: the ratio for the PCF taxon is estimated from the reconstructed skull.

180. Cervical vertebrae. Morphology of the dorsal flange of the axis (CRV1): dorsally convex flange extending beyond or to the level of the cranialmost region of the

postzygapophyses (0); presence of short cranial flange separated from the postzygapophyseal region by a prominent embayment (1).

PCF taxon (matrix 1, 2 and 3)…?

E. regalis…0

E. annectens…0

181. Cervical vertebrae. Development of the postzygapophyseal processes of cranial and middle cervical vertebrae (CRV2): relatively low and relatively short, less than three times the craniocaudal breadth of the neural arch (0); relatively high and relatively long, three times or more longer than the breadth of the neural arch (1).

PCF taxon (matrix 1, 2 and 3)…1

E. regalis…1

E. annectens…1

182. Number of cervical vertebrae (CRV3): 11 or less (0); 12 or more (1).

PCF taxon (matrix 1, 2 and 3)…?

E. regalis…1

E. annectens…1

183. Height of the neural spine relative to that of the centrum of the tallest caudal dorsal or sacral vertebrae (in adults) (DRS1): short neural spine, ratio up to 2.10 (mean ratio of 1.79) (0); ratio greater than 2.10 and up to 3.25 (mean ratio of 2.57) (1); very long neural spine, ratio greater than 3.25 (mean ratio of 3.97) (2).

PCF taxon (matrix 1, 2 and 3)…?

E. regalis…0

E. annectens…0

184. Slightly elongated neural spines in the cranial dorsal vertebrae, forming a "wither-like" region above the pectoral girdle (DRS2): absent (0); present (1).

PCF taxon (matrix 1, 2 and 3)…?

E. regalis…0

E. annectens…0

185. Minimum count of co-ossified vertebrae in the sacral region (including single dorsal and caudal contributions (SCR): seven or fewer (0); eight or more (1).

PCF taxon (matrix 1, 2 and 3)…1

E. regalis…1

E. annectens…1

186. Chevron length relative to the length of the neural spines in the caudal vertebrae of the proximal half of the tail (CDL): chevrons shorter or nearly as long as the neural spines (0); chevrons longer than the neural spines (1).

PCF taxon (matrix 1, 2 and 3)…?

E. regalis…1

E. annectens…1

187. Sternum. Length of the "handle-like" caudolateral process of the sternal relative to that of the craniomedial plate (excluding the caudoventral process) (ST): caudolateral process slightly shorter or as long as the rostromedial plate (0); caudolateral process longer than the craniomedial plate (1).

PCF taxon (matrix 1, 2 and 3)…?

E. regalis…1

E. annectens…1

188. Coracoid size relative to the length of the scapula (COR1): relatively large coracoid, ratio between craniocaudal length of coracoid and length of scapula of approximately 0.2 (0); coracoid reduced in size relative to the scapula (1).

PCF taxon (matrix 1, 2 and 3)…1

E. regalis…1

E. annectens…1

189. Coracoid. Ratio between the length of the lateral margin of the facet for the scapular articulation and the length of the lateral margin of the glenoid (COR2): longer scapular facet, with a ratio greater than 1.30 (sample mean ratio of 1.48) (0); slightly longer scapular facet, ratio greater than 1 and up to 1.30 (sample mean ratio of 1.14) (1); glenoid longer than the scapular facet, with a ratio up to 1 (sample mean ratio of 0.75) (2).

PCF taxon (matrix 1, 2 and 3)…2

E. regalis…2

E. annectens…2

190. Coracoid. Angle between the lateral margins of the facet for scapular articulation and the glenoid (COR3): angle greater than 115º (sample mean angle of 124º) (0); angle up to 115º (sample mean angle of 102º) (1).

PCF taxon (matrix 1, 2 and 3)…?

E. regalis…1

E. annectens…1

191. Coracoid. Morphology of the craniomedial margin of the coracoid (COR4): convex or straight, associated to a moderate development and slight projection biceps tubercle (0); concave, associated to a relatively large and lateroventrally-projected biceps tubercle (1).

PCF taxon (matrix 1, 2 and 3)…1

E. regalis…1

E. annectens…1

192. Coracoid. Development of the "hook-like" ventral process of the coracoid, measured as the ratio between the dorsoventral depth and the breadth of the process (COR5): relatively short, ratio less than 0.65 (sample mean ratio of 0.55) (0); ratio between 0.65 and 0.80 (sample mean ratio of 0.71) (1); long process, nearly as deep as it is wide, with a ratio greater than 0.80 (sample mean ratio of 0.96) (2).

PCF taxon (matrix 1, 2 and 3)…1

E. regalis…1

E. annectens…1 & 2 (contra [25,56,73])

193. Coracoid. Curvature of the ventral "hook-like" process of the coracoid (COR6): ventrally directed (0); recurved, so that the process is caudoventrally directed (1).

PCF taxon (matrix 1, 2 and 3)…1

E. regalis…1

E. annectens…1

194. Scapula. Lateral profile of the dorsal margin of the scapula (SCP1): craniocaudally straight from the cranial margin of the coracoid facet to the distal end of the blade (0); curved, dorsally convex, curvature originating at the level of the dorsal

margin of the pseudoacromion process and is most pronounced over the dorsoventral constriction (1).

PCF taxon (matrix 1, 2 and 3)…1

E. regalis…1

E. annectens…1

195. Scapular length, ratio between the craniocaudal length of the scapula (from the cranial end of the pseudoacromion process to the distal margin of the blade) and the dorsoventral depth of the cranial end (from the cranial end of the pseudoacromion process to the ventral apex of the glenoidal facet) (SCP2): relatively short scapula, ratio up to 4 (sample mean ratio of 3.54) (0); relatively long scapula, ratio greater than 4 (sample mean ratio of 4.64) (1).

PCF taxon (matrix 1, 2 and 3)…1

E. regalis…1

E. annectens…1

196. Scapula. Dorsoventral expansion of the distal region of the scapular blade (measured as a ratio between the depth of the distal end of the blade and the depth of the proximal region) (SCP4): ratio less than 1 (sample mean ratio of 0.80) (0); ratio of 1 or greater (sample mean ratio of 1.15) (1).

PCF taxon (matrix 1, 2 and 3)…1

E. regalis…1

E. annectens…1

197. Scapula. Proximal constriction (scapular “neck”), ratio between the dorsoventral width of the proximal constriction and the dorsoventral depth of the cranial end of the

scapula (SCP5): narrow “neck”, ratio up to 0.60 (sample mean ratio of 0.53) (0); relatively broad “neck”, ratio greater than 0.60 (sample mean ratio of 0.68) (1).

PCF taxon (matrix 1, 2 and 3)…1

E. regalis…1

E. annectens…1

198. Scapula. Morphology and orientation of the pseudoacromion process (SCP6-7): recurved, so that the cranial region is dorsally or craniodorsally directed (0); horizontal, occasionally with minor and subtle dorsal or ventral curvatures, so that the cranial region is cranially or mostly cranially directed (1).

PCF taxon (matrix 1, 2 and 3)…1

E. regalis…1

E. annectens…1

199. Scapula. Degree of curvature of the dorsally oriented pseudoacromion process of the scapula (SCP6-7): strongly recurved, so that the cranial region of the process is dorsally oriented (0); slightly recurved, with concave lateral profile of the dorsal margin, so that the cranial region of the process is craniodorsally oriented (1).

This character is irrelevant to *Edmontosaurus*.

200. Scapula. Cranial extension of the craniodorsal region of the scapula (bearing the coracoid facet), measured as a ratio between the distance from the coracoid joint and the cranial end of the pseudoacromion process and the height between this and the ventral apex of the glenoidal facet (SCP8): short craniodorsal region, ratio less than 0.45 (sample mean ratio of 0.35) (0); long craniodorsal region, ratio of 0.45 or greater (sample mean ratio of 0.53) (1).

PCF taxon (matrix 1, 2 and 3)…0

E. regalis…0

E. annectens…0

201. Scapula. Development of the deltoid ridge (SCP9): dorsoventrally narrow convexity limited to the proximal region of the scapula, near the pseudoacromion process from which it develops, with a poorly demarcated ventral margin (0); dorsoventrally deep and craniocaudally long, with a well demarcated ventral margin (1).

PCF taxon (matrix 1, 2 and 3)…1

E. regalis…1

E. annectens…1

202. Humerus. Length of the deltopectoral crest of the humerus (measured as the ratio between the proximodistal length of the crest and the proximodistal length of the humerus (HM1): proximodistally short crest, ratio less than 0.48 (sample mean ratio of 0.44) (0); ratio between 0.48 and 0.55 (sample mean ratio of 0.52) (1); very long crest, ratio greater than 0.55 (sample mean ratio of 0.59) (2).

PCF taxon (matrix 1)…1

PCF taxon (matrix 2, 3)…?

E. regalis…2

E. annectens…1 (contra [25,56,73])

Comment: the absolute value of the ratio in the PCF taxon is within the range of *E. annectens,* there is not enough evidence to prove or disprove that the deltopectoral crest would change through growth, although it is not impossible.

203. Humerus. Lateroventral expansion of the deltopectoral crest of the humerus (measured as the ratio between the width of the humerus across the distal fourth of the

deltopectoral crest and the width of the distal shaft at the point of maximum curvature) (HM2): poorly expanded deltopectoral crest, ratio less than 1.65 (sample mean ratio of 1.53) (0); ratio between 1.65 and 1.90 (sample mean ratio of 1.76) (1); very expanded deltopectoral crest, ratio greater than 1.90 (sample mean ratio of 2) (2).

PCF taxon (matrix 1, 2 and 3)…1

E. regalis…1

E. annectens…1

204. Humerus. Degree of angulation of the ventral margin of the deltopectoral crest (HM3): well-rounded (0); extending abruptly from the humeral shaft to give a distinct angular profile (1).

PCF taxon (matrix 1, 2 and 3)…1

E. regalis…1

E. annectens…1

205. Humerus. Overall proportions of the humerus (measured as a ratio between the total length and the width of the lateral surface of the proximal end of the humerus) (HM4): relatively short and stocky humerus, ratio less than 4.25 (mean ratio of 3.85) (0); ratio between 4.25 and 4.90 (sample mean ratio of 4.60) (1); relatively long and thin humerus, ratio greater than 4.90 (mean ratio of 5.4) (2).

PCF taxon (matrix 1, 2 and 3)…1

E. regalis…1

E. annectens…1

206. Ulna. Length of the ulna relative to its dorsoventral thickness (measured at mid-shaft) (UL1): ratio length/width less than 10 (0); ratio length/width equal or larger than

10 (1).

PCF taxon (matrix 1)…1

PCF taxon (matrix 2&3)…?

E. regalis…1

E. annectens…0 & 1

Comment: see section 1.4.2.25.

207. Ulnar length relative to humeral length (UL2): ulna shorter than or as long as the humerus (0); longer ulna, up to 20 % longer than the humerus (1); longer ulna, being more than 20 % longer than the humerus (2).

PCF taxon (matrix 1, 2 and 3)…1

E. regalis…1

E. annectens…1

208. Composition of the carpus (MN1): presence of fused ulnare, radiale, intermedium and distal carpals (0); number of carpal bones reduced to a maximum of two unfused elements (1).

PCF taxon (matrix 1, 2 and 3)…?

E. regalis…1

E. annectens…1

209. Manual digit I (MN2): presence of metacarpal I and one ungual phalanx (0); entire digit I absent (1).

PCF taxon (matrix 1, 2 and 3)…?

E. regalis…1

E. annectens…1

210. Elongation of the manus exemplified by elongation of metacarpals II through IV, measured as the ratio between the length of metacarpal III and the width of its mid-shaft (MN3): relatively short and blocky, ratio up to 5 (sample mean ratio of 4.25) (0); relatively long and slender, ratio greater than 5 (sample mean ratio of 8.54) (1).

PCF taxon (matrix 1, 2 and 3)…1

E. regalis…1

E. annectens…1

211. Elongation of metacarpal V, so that it is more than twice as long as it is proximally wide (MN4): absent (0); present (1).

PCF taxon (matrix 1, 2 and 3)…1

E. regalis…1

E. annectens…1

212. Length/width proportions of manual phalanx III1 (MN6: proximodistally compressed, mediolaterally wider than it is long (0); slightly longer proximodistally than it is wide mediolaterally (1); very elongated, proximodistal length that is at least twice its mediolateral width at the middle of its longitudinal axis (2).

PCF taxon (matrix 1, 2 and 3)…1

E. regalis…1

E. annectens…1

213. Shape of manual ungual II (MN7): claw-like (0); hoof-like (1).

PCF taxon (matrix 1, 2 and 3)…1

E. regalis…1

E. annectens…1

214. Proximodistal length of manual phalanx II1 relative to that of II2 (MN8): phalanx II1 less than three times longer than phalanx II2 (0); phalanx II1 three times or more longer than phalanx II2 (1).

PCF taxon (matrix 1, 2 and 3)…1

E. regalis…1

E. annectens…1

215. Ilium. Angle of ventral deflection of the preacetabular process of the ilium (IL1): angle greater than 150º (sample mean angle of 162º) (0); angle of 150º or less (sample mean angle of 143º) (1).

PCF taxon (matrix 1, 2 and 3)…1

E. regalis…1

E. annectens…1

216. Ilium. Dorsoventral depth of the proximal region of the preacetabular process (measured as a ratio between this and the dorsoventral distance between the pubic peduncle and the dorsal margin of the ilium) (IL3): shallow, less than half the depth of the cranial central plate, ratio less than 0.50 (sample mean ratio of 0.42) (0); approximately as deep as the cranial central plate depth, ratio between 0.50 and 0.55 (sample mean ratio of 0.51) (1); deeper than half the depth of the cranial central plate, ratio greater than 0.55 (sample mean ratio of 0.62) (2).

PCF taxon (matrix 1, 2 and 3)…2

E. regalis…2

E. annectens…2

217. Ilium. Dorsoventral depth of the central plate of the ilium (expressed as a ratio between this and the distance between the pubic peduncle and the caudodorsal prominence of the ischial peduncle) (IL4): ratio of 0.80 or greater (sample mean ratio of 0.90) (0); ratio less than 0.80 (sample mean ratio of 0.71) (1).

PCF taxon (matrix 1, 2 and 3)…1

E. regalis…1

E. annectens…1

218. Ilium. Position of the ventral-most margin of the supraacetabular process relative to the caudoventral margin of the lateral ridge of caudal protuberance of the ischial peduncle of the ilium (IL5): apex located caudodorsally (0); apex located above caudoventral margin of protuberance (1); apex located craniodorsally (2).

PCF taxon (matrix 1, 2 and 3)…2

E. regalis…2

E. annectens…2

219. Ilium. Development of the lateroventral projection of the suprailiac crest of the ilium (IL6): forms a longitudinal and continuous “swelling” or reflected border along the dorsal margin of the central plate and the proximal region of the postacetabular process, with a depth up to 25 % the depth of the ilium (0); projected lateroventrally at least 25 % (but less than half) the depth of the ilium (1); projects lateroventrally between half and three quarters of the dorsoventral depth of the ilium (2); projects lateroventrally to overlap totally or at least half of the lateral ridge of the caudal prominence of the ischial peduncle (3).

PCF taxon (matrix 1, 2 and 3)…1

E. regalis…1

E. annectens…1

220. Ilium. Craniocaudal breadth of the supraacetabular process, measured as the ratio between the breadth of the process across its dorsal region and the craniocaudal length of the central iliac blade from the caudal ischial peduncle to the pubic one (IL7): craniocaudally wider than the central plate of the ilium, ratio greater than 0.85 (sample mean ratio of 1.16) (0); craniocaudally broad, ratio between 0.70 and 0.85 (sample mean of 0.73) (1); slightly broader than half the length of the central iliac blade, ratio between 0.55 and 0.69 (sample mean ratio of 0.62) (2); short, ratio less than 0.55 (sample mean ratio of 0.48) (3).

PCF taxon (matrix 1, 2 and 3)…3

E. regalis…3

E. annectens…3

221. Ilium. Symmetry of the lateral profile of the supraacetabular process (IL8): asymmetrical, with a caudally skewed lateral profile (0); symmetrical or with a slightly caudally skewed profile (1).

PCF taxon (matrix 1, 2 and 3)…1

E. regalis…1

E. annectens…1

222. Ilium. Morphology of the lateroventral margin of the supraacetabular process (IL9): craniocaudally sinuous (0); widely arched (1); U or V-shaped (2); subrectangular, with a shallow notch that divides the ventral margin in two poorly demarcated lobes (3).

PCF taxon (matrix 1, 2 and 3)…2

E. regalis…2

E. annectens…2

223. Ilium. Demarcation of the caudodorsal margin of the lateroventral rim of the supraacetabular process (IL10): the caudodorsal margin is poorly defined and appears discontinuous with the dorsal margin of the proximal region of the postacetabular process due to the lack of a well demarcated caudodorsal ridge (0); the caudodorsal margin is a well-defined ridge that is continuous with the dorsal margin of the proximal region of the postacetabular process (1).

PCF taxon (matrix 1, 2 and 3)…0

E. regalis…0

E. annectens…0

224. Ilium. Morphology of the pubic peduncle of the ilium (IL11): relatively large and dorsoventrally deep (longer than wide), subconical, with a proximal region that is only slightly craniocaudally wider than the distal end of the process (0); relatively shorter (wider or as wide as long) and triangular, with a proximal region that is much craniocaudally wider than the distal end (1).

PCF taxon (matrix 1, 2 and 3)…1

E. regalis…1

E. annectens…1

225. Ilium. Morphology of the ischial peduncle of the ilium (IL12): formed by a single and large, oval ventral protrusion (0); composed of a large and oval ventral protrusion and by a smaller, caudodorsally located prominence emerging from the caudodorsal ridge (1); formed by two protrusions of similar size, the caudal-most one located slightly

caudodorsally (2).

PCF taxon (matrix 1, 2 and 3)…2

E. regalis…2

E. annectens…2

226. Ilium. Ratio between the craniocaudal length of the postacetabular process and the craniocaudal length of the central plate of the ilium (IL13): short postacetabular process, ratio up to 0.80 (sample mean ratio of 0.70) (0); postacetabular process nearly as long as the central plate, ratio greater than 0.80 but less than 1.1 (sample mean ratio of 0.90) (1); postacetabular process substantially longer than the central plate, ratio of 1.1 or greater (sample mean ratio of 1.23) (2).

PCF taxon (matrix 1, 2 and 3)…1

E. regalis…1

E. annectens…1

227. Ilium. Brevis shelf at the base of the postacetabular process of the ilium (IL14): absent (0); present (1).

PCF taxon (matrix 1, 2 and 3)…0

E. regalis…0

E. annectens…0

228. Ilium. Medioventral ridge on the medial side of the postacetabular process, crossing the bone surface from the proximoventral to the caudodorsal margins and orientation of the brevis shelf (IL15): absent or presence of a faint ridge (0); well-defined ridge bounding the medial margin of the brevis shelf; the latter faces medioventrally and in medial view appears restricted to the caudal region of the postacetabular process (1);

well-defined ridge forming the medial margin of a medioventrally-facing shelf, with a postacetabular process that is progressively expanded mediolaterally towards the caudal end (2); well-developed, oblique and expanded flange forming the medial margin of an extensive brevis shelf that faces more ventrally than medially (3).

PCF taxon (matrix 1, 2 and 3)…0

E. regalis…0

E. annectens…0

229. Ilium. Craniocaudally-oriented median ridge on the laterodorsal surface of the postacetabular process (IL16): absent (0); present (1).

PCF taxon (matrix 1, 2 and 3)…0

E. regalis…0

E. annectens…0

230. Ilium. Geometry of the lateral profile of the postacetabular process of the ilium (IL17): the ventral margin converges caudodorsally to meet the horizontal dorsal margin, forming a tapering caudal end and producing a triangular lateral profile of the process (0); dorsal and ventral margins parallel or slightly convergent, forming a distinct (rectangular or subcircular) caudal margin (1).

PCF taxon (matrix 1, 2 and 3)…1

E. regalis…1

E. annectens…1

231. Ilium. Orientation of the dorsal margin of the postacetabular process relative to the acetabular margin (IL18): horizontal dorsal margin, parallel or nearly parallel to the acetabular margin (0); caudodorsally oriented dorsal margin, rising dorsally relative to

the acetabular margin (1).

PCF taxon (matrix 1, 2 and 3)…1

E. regalis…1

E. annectens…1

232. Ilium. Position of the medial sacral ridge within the medial surface of the central plate of the ilium (IL19): ridge well separated ventrally from the dorsal margin of the ilium, set between 50 % and 30 % the dorsoventral depth of the central plate (0); ridge located more dorsally, closer to the dorsal margin, within the dorsal third (less than 30 % the depth) of the central plate (1).

PCF taxon (matrix 1, 2 and 3)…1

E. regalis…1

E. annectens…1

233. Ilium. Lateral profile of the dorsal or laterodorsal margin of the ilium (IL21): straight or slightly convex (0); distinctly depressed over the supraacetabular process and dorsally bowed over the proximal region of the preacetabular process (1).

PCF taxon (matrix 1, 2 and 3)…1

E. regalis…1

E. annectens…1

234. Pubis. Orientation of the dorsoventral expansion of the prepubic process (PB1): the dorsal region of the expansion is more expanded than the ventral region, so that distally the process is dorsally-directed (0); the ventral region is more expanded than the dorsal region, so that the distal expansion is ventrally-directed (1).

PCF taxon (matrix 1, 2 and 3)…?

E. regalis…1

E. annectens…1

235. Pubis. Geometry of the dorsoventral expansion of the prepubic process of the pubis (in lateral or medial views) (PB2): circular to oval expansion, extensive and convex ventral margin (0); subsquared distal dorsal margin, expansion dorsoventrally taller than cranioventrally long, very pronounced proximal dorsal concavity and nearly straight distal ventral margin (1); ellipsoidal, expansion craniocaudally longer than dorsoventrally tall, well pronounced concavities of the dorsal and ventral proximal margins (2); oval expansion, dorsoventrally taller than craniocaudally long, well pronounced concave profiles of dorsal and ventral proximal margins (3); rectangular, craniocaudally longer than dorsoventrally tall, nearly straight profiles of the dorsal and ventral proximal margins (4).

PCF taxon (matrix 1, 2 and 3)…?

E. regalis…3

E. annectens…3

236. Pubis. Depth of the dorsoventral expansion of the distal region of the prepubic process relative to the width of the acetabular margin of the pubis (PB3): distal expansion as wide as or shallower than width of the acetabular margin (0); dorsoventral expansion deeper than the acetabular margin (1).

PCF taxon (matrix 1, 2 and 3)…?

E. regalis…1

E. annectens…1

237. Pubis. Craniocaudal length of the proximal constriction of the prepubic process of the pubis relative to length of the dorsoventral expansion (PB4): constriction longer than

the dorsoventral expansion, that is restricted to the distal region of the process (0); constriction and distal expansion have approximately the same length (1); constriction slightly shorter than the dorsoventral expansion, that begins at the proximal region of the process (2).

PCF taxon (matrix 1, 2 and 3)…?

E. regalis…0

E. annectens…0

238. Pubis. Relative position of maximum concavity of the dorsal and ventral margins of the prepubic process of the pubis (PB5): maximum ventral concavity achieved adjacent to the proximal region of the postpubic process, maximum dorsal concavity located further distally (0); maximum ventral concavity located ventral to or slightly caudal to the maximum dorsal concavity (1).

PCF taxon (matrix 1, 2 and 3)…1

E. regalis…1

E. annectens…1

239. Pubis. Morphology of the acetabular margin, ventral to the lateral edge of the iliac peduncle (PB6): the lateral margin of the iliac peduncle extends ventrally forming a prominent ridge that merges with the proximal region of the ischial peduncle (0); the lateral margin of the iliac peduncle progressively disappears ventrally into the lateral surface of the region adjacent to the acetabular margin (1).

PCF taxon (matrix 1, 2 and 3)…1

E. regalis…1

E. annectens…1

240. Pubis, obturator foramen (PB7): present, proximal postpubic ramus has a caudodorsally oriented short process that contacts totally or partially with the ischial peduncle to form the obturator foramen (0); absent, proximal postpubic ramus lacks a dorsocaudally oriented process (1).

PCF taxon (matrix 1, 2 and 3)…1

E. regalis…1

E. annectens…1

241. Pubis. Length/width ratio of the ischial peduncle of the pubis (PB8): very short ischial peduncle, ratio less than 1.85 (sample mean ratio of 1.5) (0); ratio ranging from 1.85 to less than 3 (sample mean ratio of 2.4) (1); very long, ratio of 3 or more (with a sample mean ratio of 4) (2).

PCF taxon (matrix 1, 2 and 3)…?

E. regalis…1

E. annectens…1

242. Pubis. Lateroventral protuberance on the proximal region of the ischial peduncle of the pubis (PB9): absent or very faintly developed (0); present (1).

PCF taxon (matrix 1, 2 and 3)…0

E. regalis…0

E. annectens…0

243. Pubis. Depth/width proportions of the iliac peduncle of the pubis (PB10): craniocaudally broader than dorsoventrally tall (0); taller dorsoventrally than broad craniocaudally (1).

PCF taxon (matrix 1, 2 and 3)…1

E. regalis…1

E. annectens…1

244. Pubis. Total length of the pubis, as the ratio between the craniocaudal distance from the acetabular margin to the distal margin of the prepubic process and the distance from the dorsal margin of the iliac peduncle and the ventral margin of the proximal postpubic shaft-(PB11): short, ratio less than 2.70 (sample mean ratio of 2.30) (0); long, ratio between 2.70 and 3 (sample mean ratio of 2.84) (1); very long, ratio greater than 3 (sample mean ratio of 3.53) (2).

PCF taxon (matrix 1, 2 and 3)…?

E. regalis…2

E. annectens…2

Comment: the anterior margin of the prepubic process is damaged, so its exact length is hard to determine. The ratio is at least longer than 2.3.

245. Ischium. Development of a caudal curvature of the distal margin of the iliac peduncle of the ischium (IS1): curvature absent, distal margin slightly rounded and, in some exemplars, slightly curved cranially (0); presence of a very short and slight curvature in the caudodorsal corner (1); presence of a well developed curvature in the caudodorsal corner, so that the peduncle appears “thumb-like” in lateral and medial profiles (2).

PCF taxon (matrix 1, 2 and 3)…0

E. regalis…0

E. annectens…0

246. Ischium. Elongation of the iliac peduncle of the ischium (ratio between the proximodistal length and the craniocaudal width of the distal margin) (IS3): relatively

short peduncle, ratio less than 1.5 (sample mean ratio of 1.27) (0); ratio between 1.5 and 2 (sample mean ratio of 1.78) (1); relatively long peduncle, ratio greater than 2 (sample mean ratio of 2.30) (2).

PCF taxon (matrix 1, 2 and 3)…2

E. regalis…2

E. annectens…2

247. Ischium. Relative orientation of the acetabular and caudodorsal margins of the iliac peduncle of the ischium (IS4): margins are either parallel or slightly convergent relative to each other (correlated with a greater expansion of the craniodorsal corner of the peduncle) (0); margins become slightly to greatly divergent near the proximal region of the peduncle (1).

PCF taxon (matrix 1, 2 and 3)…1

E. regalis…1

E. annectens…1

248. Ischium. Orientation of the craniocaudal axis of the pubic peduncle (perpendicular to its articular margin) relative to the ischial shaft (IS5): ventrally inclined, angle up to 130º (sample mean angle of 118º) (0); slightly inclined ventrally, angle greater than 130 and up to 170º (sample mean angle of 157º) (1); pubic peduncle parallel to the ischial shaft (2).

PCF taxon (matrix 1, 2 and 3)…2

E. regalis…2

E. annectens…2

249. Ischium. Length/width proportions of the pubic peduncle of the ischium (IS6):

proximodistally longer than the distal articular surface is wide (0); approximately as long proximodistally as the distal articular surface is dorsoventrally wide (1); proximodistally shorter than the dorsoventral width of the distal articular surface (2).

PCF taxon (matrix 1, 2 and 3)…?

E. regalis…1

E. annectens…2

250. Ischium. Relative position of the dorsal acetabular margin of the pubic peduncle (IS7): ventral to or at the same level as the dorsal margin of the ischial shaft (0); peduncular margin set dorsal to the dorsal margin of the ischial shaft (1).

PCF taxon (matrix 1, 2 and 3)…1

E. regalis…0

E. annectens…0&1

251. Ischium. Dorsoventral thickness of the mid-shaft of the ischium (measured as a ratio between this and the length of the entire shaft) (IS8): very thin shaft, up to 5 % the length of the ischial shaft (sample mean of 4.6 %) (0); thickness ranging from more than 5 % and up to 7.5 % the length of the ischial shaft (sample mean of 6.7 %) (1); very thick shaft, thickness greater than 7.5 % the length of the ischial shaft (sample mean of 8.4 %) (2).

PCF taxon (matrix 1, 2 and 3)…?

E. regalis…0

E. annectens…0

252. Ischium. Morphology of the distal region of the ischial shaft (IS9): slightly expanded into a blunt end (0); ventrally expanded forming a large “foot” or “boot-like”

process (1).

PCF taxon (matrix 1, 2 and 3)…?

E. regalis…0

E. annectens…0

253. Ischium. Degree of ventral projection of the distal expansion of the ischium (expressed as the ratio between the length of the ischial shaft and the length of the distal ventral expansion) (IS10): ratio less than 0.25 (sample mean ratio of 0.18) (0); ratio of 0.25 or greater (sample mean ratio of 0.28) (1).

Comment: as *Edmontosaurus* does not have boot-like ischial shaft, this character is irrelevant.

254. Ischium. Morphology of the cranial margin of the ventral expansion of the distal ischial shaft (IS11): slightly concave and directed caudoventrally to meet the caudal margin to nearly a point (0); strongly concave, recurved cranial margin (1).

Comment: as *Edmontosaurus* does not have boot-like ischial shaft, this character is irrelevant.

255. Ischium. Orientation of the long axis of the distal "foot" relative to the ischial shaft (IS12): straight, ventrally directed (0); cranioventrally directed, the inclination starting at the dorsal margin of the "foot" (1).

Comment: as *Edmontosaurus* does not have boot-like ischial shaft, this character is irrelevant.

256. Femur. Degree of curvature of the distal half of the femoral shaft (FM1): slightly curved caudomedially (0); absence of curvature, straight distal shaft (1).

PCF taxon (matrix 1, 2 and 3)…1

E. regalis…1

E. annectens…1

257. Femur. Lateral profile of the caudoventral margin of the fourth trochanter of the femur (FM2): triangular and ending in a caudally, and slightly ventrally, directed point (0); smooth and arcuate (1).

PCF taxon (matrix 1, 2 and 3)…?

E. regalis…1

E. annectens…1

258. Tibia. Extension of the cnemial crest of the tibia (TB): the cnemial crest is restricted to the proximal end of the tibia (0); cnemial crest further extended along the cranial surface of the proximal half of the diaphysis (1).

PCF taxon (matrix 1, 2 and 3)…1

E. regalis…1

E. annectens…1

259. Astragalus. Development of the medial platform of the astragalus (AS): it extends medially to completely underlie the medial malleolus of the tibia (0); short, wedges laterally underlying only part of the medial malleolus of the tibia (1).

PCF taxon (matrix 1, 2 and 3)…0

E. regalis…0

E. annectens…0

260. Distal tarsals II and III (DSTS): present (0); absent (1).

PCF taxon (matrix 1, 2 and 3)…?

E. regalis…1

E. annectens…1

261. Metatarsal I (PES1): absent (0); slender and splint-like element (1).

PCF taxon (matrix 1, 2 and 3)…?

E. regalis…0

E. annectens…0

262. Length/width proportions of pedal phalanx II2 (PES3): proximodistally shortened, being twice as wide mediolaterally as it is proximodistally long (0); subsquared, only slightly shorter proximodistally than it is wide mediolaterally (1).

PCF taxon (matrix 1, 2 and 3)…1

E. regalis…1

E. annectens…1

263. Length/width proportions of the disc-shaped pedal phalanx III2-III3 (PES4): up to three times (or less) wider than they are proximodistally long (0); more than three times wider than they are proximodistally long (1).

PCF taxon (matrix 1, 2 and 3)…?

E. regalis…0

E. annectens…0

264. Morphology of the pedal unguals (PES6): proximodistally elongated and arrow-shaped, with a bluntly truncated tip and prominent claw grooves (0); mediolaterally broad and proximodistally shortened, rounded shield or hoof-like shaped, with reduced or absent claw grooves (1).

PCF taxon (matrix 1, 2 and 3)…1

E. regalis…1

E. annectens…1

265. Ridge on the plantar surface of pedal unguals (PES7): absent (0); present (1).

PCF taxon (matrix 1 and 2)…0

PCF taxon (matrix 2)…?

E. regalis…1

E. annectens…1

Comment: PCF taxon has a very weak ridge on the plantar surface.

266. Morphology of the circumnarial septum (new): Does not exist (0); exists and separates the anterolateral part of the premaxilla into two fossae (1); exists, and laterally expands both anteriorly and posteriorly, separating the anterolateral part of the premaxilla into three parts (3).

PCF taxon (matrix 1, matrix 2, 3)…1

E. regalis…2

E. annectens…2

Comment: see section 1.4.2.2.

Chapter 2

Osteology of the Arctic hadrosaurid *Edmontosaurus* sp. nov. (Dinosauria: Ornithopoda) from the Prince Creek Formation of northern Alaska[2]

2.1 Abstract

Several thousand individual elements of the Arctic hadrosaurid *Edmontosaurus* sp. nov. (Hadrosauridae: Saurolophinae) have been collected from the Liscomb Bonebed in the Prince Creek Formation (Late Cretaceous) of northern Alaska. The material from the bonebed is entirely disarticulated and includes elements from individuals of three different juvenile growth stages, the majority of which are from small juveniles approximately 30 % of adult size. These specimens represent the smallest individuals known for the genus *Edmontosaurus* and are therefore important in understanding both the osteology of the new taxon and ontogenetic patterns in the genus as a whole. Here I present a detailed description of the cranial and postcranial anatomy of *Edmontosaurus* sp. nov. based on material from different growth stages and compare these data with other material from the two valid species of *Edmontosaurus*, *E. regalis* and *E. annectens*, as well as other saurolophines from North America and Asia. The osteology of the new Alaskan taxon is characterized on the basis of multiple, well-preserved specimens for nearly every element, making it one of the best-understood hadrosaurid taxa known from North America. Based on a cladistic analysis for derived saurolophines, a biogeographic scenario is presented whereby *Edmontosaurus* originated in eastern Eurasia and dispersed into North America by the Campanian via a land corridor in the area of present day Alaska, before diversifying across all of Laramidia. The recognition of another endemic dinosaur species from the Prince Creek Formation adds further support to the existence of a distinct, early Maastrichtian polar fauna known as the Paaŋaqtat Province.

2.2 Introduction

In the Late Cretaceous, the Arctic hosted a relatively rich terrestrial vertebrate

[2]Mori H, Druckenmiller PS, and Erickson GM. Prepared for submission to Zoological Journal of the Linnean Society.

fauna compared to today [1-15], likely reflecting its moderate climate. In particular, the Prince Creek Formation (PCF) of northern Alaska preserves a rich dinosaurian assemblage that is of great interest because these taxa occur as far north as land is known to have existed during the entire Mesozoic. From the PCF, two unique dinosaur species are currently known, *Alaskacephale gangloffi* Sullivan, 2006 [7,8] and *Pachyrhinosaurus perotorum* Fiorillo & Tykoski, 2012 [13]. In addition, large and morphologically distinct teeth of the small theropod cf. *Troodon* are also reported [9], along with other undescribed forms under study [11]. As currently understood, the unique faunal composition of the PCF has given rise to the hypothesis that a unique, early Maastrichtian polar dinosaur fauna, provisionally named the "Paaŋaqtat Province" existed in Alaska [12,15], although this idea is controversial [13].

Among various fossil localities discovered in the Prince Creek Formation, the Liscomb Bonebed (LBB) is the most productive and arguably the single most fossiliferous site for polar dinosaurs in either hemisphere [4]. The LBB is exposed along the lower Colville River, occurs in the upper portion of the PCF and has been excavated for over two decades (Figure 2-1). To date, thousands of disarticulated, juvenile hadrosaurid remains have been discovered. Based on geometric morphometric, comparative morphological and cladistic analyses, a new species of the Campanian to Maastrichtian dinosaur *Edmontosaurus* is now recognized (see Chapter 1). Here, I present a detailed osteological description of the cranial and postcranial remains of the new PCF *Edmontosaurus* based, in most instances, on multiple specimens of each element. Although most elements are described from juvenile remains, the well-preserved and abundant remains from the LBB make this one of the best understood hadrosaurids described to date and provide critical new information about the paleoecology of Cretaceous polar environments. Finally, phylogenetic relationships are interpreted in a biogeographic context to better understand the evolution and distribution of derived saurolophines in North America and Eurasia.

2.2.1 Institutional abbreviations

AENM, Amur Natural History Museum, Blagoveschensk, Russia; AMNH, American Museum of Natural History, New York City, New York, USA; BHI, Black Hills Institute of Geological Research, Hill City, South Dakota, USA; BMNH, British Museum of Natural History, London, UK; CM, Carnegie Museum of Natural History, Pittsburgh, Pennsylvania, USA; CMN, Canadian Museum of Nature, Ottawa, Ontario, Canada (formerly National Museums of Canada, NMC); DMNH, Denver Museum of Nature and Science, Denver, Colorado, USA; FMNH, Florida Museum of Natural History, Gainesville, Florida, USA; GMV, National Geological Museum of China, Beijing, China; MACN, Museo Argentino de Ciencias Naturales Bernardino Rivadavia, Buenos Aires, Argentina; RAM, Raymond M. Alf Museum of Palaeontology, Claremont, California, USA; ROM, Royal Ontario Museum, Toronto, Ontario, Canada; SM, Senckenberg Museum, Frankfurt, Germany; TMNH, Toyohashi Museum of Natural History, Toyohashi, Aichi, Japan; UMMP, University of Michigan Museum of Paleontology, Ann Arbor, Michigan, USA; UAMES, University of Alaska Museum Earth Science, Fairbanks, Alaska, USA; USNM, United States National Museum, Washington, USA; YPM, Yale Paleontology Museum, New Heaven, Connecticut, USA.

2.2.2 Geological setting

The Prince Creek Formation (formerly referred to as the Kogosukuruk Tongue of the Prince Creek Formation [16]) is characterized by nonmarine sandstone, conglomerate, coal and mudstone, and is interpreted to represent interbedded fluvial (meandering channels and floodplains) and marginal marine sediments deposited on a low gradient Arctic coastal plain [17,18]. The age of the entire PCF ranges from Upper Cretaceous to Eocene based on palynological [19-21] and biostratigraphic data [22]. The dinosaur-bearing section of the formation, including the LBB, has been dated to 71-68 Ma, using $^{40}Ar/^{39}Ar$ methods [23,24] based on samples from exposures along the lower Coleville River. The age of LBB is further constrained by an $^{40}Ar/^{39}Ar$ age of 69.2 ± 0.5 Ma from a stratigraphically underlying tuff at Sling Point and by palynological analyses [25], which

are consistent with an early Maastrichtian age for the LBB [26]. This age estimate falls entirely within the known stratigraphic range of *Edmontosaurus*, but interestingly falls between the ranges for the other two valid species of the genus, *E. regalis* (late Campanian) and *E. annectens* (late Maastrichtian).

Witte et al. [27] placed the paleolatitude of northern Alaska at 67-85°N. Thus the northern Alaska was well within the paleo-Arctic in the Late Cretaceous. However, paleobotanical evidence indicates mean annual temperatures of 5-6 °C for the Maastrichtian, with a cold month mean warmer than 2.0 ± 3.9 °C [28-30]. From pedogenic and paleobotanical evidence, Flaig et al. [31] concluded that the Arctic coastal plain had polar woodlands with an angiosperm understory and experienced intensified dry and wet seasons. In addition to hadrosaurid remains, the PCF preserves a modestly diverse assemblage of ornithischian and saurischian dinosaurs and mammals [1,3,7,10,11,13,32-35]. However, no ectothermic vertebrates have ever been recovered [32]. Therefore, it is inferred that the temperature during the winter was too cold for terrestrial ectothermic animals.

Taphonomically, the Liscomb Bonebed occurs in a trunk channel on a distributary channel splay complex and flood plain [26, 36]. The bonebed is interpreted to represent a mass mortality event associated with overbank flood deposits [35], which might have resulted from rapid melting of snow in the ancient Brooks Range that was located to the south [36]. The dinosaur remains from the bonebed are overwhelmingly dominated by juvenile specimens of hadrosaurs (*Edmontosaurus*) [35]. These remains are almost entirely disarticulated, but show little evidence of weathering or trampling and are typically preserved in three dimensions, often without any permineralization [35, 36].

2.2.3 Material and methods

More than 300 individual hadrosaur bones collected from Liscomb Bonebed (Figure 2-1) and housed in Earth Sciences Collection at the University of Alaska Museum were examined in the course of this study (Table 2-1). Additionally, a small number of other specimens collected from nearly the same stratigraphic interval within

the PCF and within 3 km of the LBB quarry were also included in the study. As described further below, these specimens are consistent in morphology and preservation with the LBB material but also include specimens from larger size classes so they are expand our understanding of the ontogenetic variation of the species.

Individual remains of the Alaskan edmontosaur can be classified into three ontogenetic stages. Approximately 85 % of the specimens examined are categorized into size class 1. A reconstructed skull from these specimens (Figure 2-2) is approximately 30 cm long, which is one third of the length of the paratype adult specimen of *Edmontosaurus annectens* Horner et al., 2004 [37] (YPM 2182; 91 cm, when measured from the anterior end of the premaxilla and the mid point of the quadrate). Size class 2 accounts for about 10 % of the examined specimens that are approximately 30 % longer than size class 1 specimens, which is equivalent to 40 % of the skull length of YPM 2182. Size class 3 represents less than 5 % of the total specimens. These are approximately 80-100 % longer than the size class 1 specimens, corresponding to 60 % of the in size of YPM 2182. Definition of the size classes 2 and 3 are primarily based on relative size compared to the size class 1 specimens for each bone type, thus there is no guarantee that specimens categorized into size classes 2 and 3 are from the individuals of the same sizes, due to possible allometric growth of *Edmontosaurus*.

2.2.4 Systematic paleontology

Ornithischia Seeley, 1887 [38]

Ornithopoda Marsh, 1881 [39]

Hadrosauridae Cope, 1870 [40]

Saurolophine Brown, 1914 [41] *sensu* Prieto-Márquez [42]

Genus *Edmontosaurus* Lambe, 1917 [43]

Edmontosaurus sp. nov.

2.3 Description

2.3.1 Skull

All bones discovered from Liscomb Bonebed are disarticulated. The skull (Figure 2-2) was assembled from several bones of size class 1, which are described in detail below. Descriptions of each bone are based on multiple specimens except the sternum and sacrum (see table 2-1). For the premaxilla, nasal, quadrate, parietal and ischium, composite images derived from two specimens are provided.

2.3.1.1 Premaxilla

All premaxillae are incompletely preserved. From size class 1, UAMES 12995 preserves the nearly complete laterally expanded rostral region while UAMES 4283 preserves the nearly complete posterolateral process. UAMES 4184 is from size class 2, but it is mediolaterally crushed and not well-preserved. Figures 2-3A-D show a composite reconstruction based on the two size class 1 specimens.

The anterodorsal outline of the premaxilla in lateral view is rounded. As in other hadrosaurs, the oral margin of the premaxilla is ventrolaterally expanded. Judging from the reconstructed juvenile skull (Figure 2-2), the anteroventral oral margin of the premaxilla would not be positioned far ventral to the occlusal plane. The anterolateral portion of the oral margin is sub-squared. The oral margin of the premaxilla is reflected dorsally. The surface of the rostral margin is rugose and bears at least three denticles approximately 5-7 mm wide, although the exact number is not known due to damage in this region. Along the dorsolateral margin of the premaxillary fold are at least four accessory premaxillary foramina, while in most saurolophines (except a size class 3 of *Edmontosaurus annectens*; ROM 53526) only one premaxillary foramen is known. Posterior to the premaxillary fold is the anterior premaxillary cavity. This cavity slightly excavates the lateral wall of premaxilla. The circumnarial septum separates the anterior premaxillary cavity and the circumnarial depression. This septum is penetrated by an anterodorsal premaxillary foramen anteriorly and a posterodorsal premaxillary foramen posteriorly. These foramina connect in the septum and open ventrally as a ventral

premaxillary foramen. This condition is the same as that in *E. annectens* (AMNH 5046) [44]. The circumnarial septum projects posterolaterally and is triangular in the coronal section; its anterior surface smoothly merges with the medial wall of the premaxilla, and its posterior surface forms a right angle with the sagittal plane. This morphology is commonly seen in saurolophines, but it contrasts with the circumnarial septum of *E. annectens* and *E. regalis* Lambe, 1917 [43], in which the circumnarial septum diverges both anteriorly and posteriorly, has a flat dorsolateral wall, and is nearly parallel to the medial wall of the premaxilla in the coronal plane (see Chapter 1). On the posterior surface of the circumnarial septum and lateral to the posterodorsal premaxillary foramen is a shallow groove. Although mediolaterally crushed, size class 2 (UAMES 4184) does not differ from the PCF size class 1 specimens in the morphology of the circumnarial septum.

Ventrally, the posterior surface of the ventral premaxillary foramen is slightly depressed. Medially, on the anteroventral corner of the premaxilla, is a slight depression along the sagittal plane. Because of this depression, the right and left premaxilla would not meet completely anteromedially. This depression is also present in a size class 2 specimen (UAMES 4184). The isolated posterolateral process (UMAES 4283) can be articulated firmly with the maxilla (UAMES 4327), apparently limiting room for pleurokinetic movement. The posterolateral process has a groove that receives the anteromedial process of the maxilla on its medial side. The medial margin of the posterolateral process dorsal to the groove is thick and rounded. Below this groove is a ridge that inserts between the anteromedial and anteroventral process. This configuration is also seen in *Prosaurolophus maximus* Brown, 1916 [45] (MOR 446 [46]), and *Brachylophosaurus canadensis* Sternberg, 1953 [47] (CMN 8893 [48]).

2.3.1.2 Nasal

The overall shape of the nasal (Figure 2-4) is similar to *Kundurosaurus nagornyi* Godefroit et al., 2012 [49] (AENM 2/58 [49]), *Kerberosaurus manakini* Bolotsky & Godefroit, 2004 [50] (AENM 1/318 [50]), and other species of *Edmontosaurus* in that the

anterodorsal process (frontal process of Horner [46], anterior process of Gates and Sampson [51]) is slim and rod-like, being much narrower than the caudal plate. The profile of the nasal along its dorsal margin from the caudal plate to the anterodorsal process is nearly straight. Among saurolophine taxa, the nasal often curves ventrally anterior to the posterior end of the external nares. In adult *Edmontosaurus*, this curvature is weak and it is almost straight, as in the Alaskan *Edmontosaurus*. The length of the anterodorsal process accounts for at least half of the entire bone length, being much longer than the anteroventral process. UAMES 4265 preserves the most complete anterodorsal process but still shows evidence of damage at its distal end. The circumnarial ridge, which marks the rim of the circumnarial depression and is conspicuously developed in *Edmontosaurus*, begins in the proximal part of the anterodorsal process and forms a weak sigmoidal curve to meet with the dorsal border of the posterolateral process of the premaxilla. In adult *Edmontosaurus*, especially in *E. regalis* (e.g., CMN 2289, BMNH 8927), this sigmoidal curvature is pronounced, but in the Alaskan edmontosaur this curvature is very weak to negligible, which is attributable to ontogeny (see Chapter 1). Thus, the circumnarial opening ends well anterior to the orbit. Laterally, the nasal is faintly invaginated by the circumnarial ridge. On the anteroventral corner of the caudal plate is a short wedge-like anteroventral process. On the lateral surface of the anteroventral process is a sutural boundary for the ventral process of the premaxilla, which continues to the posteroventral border of the caudal plate. This sutural line cuts the circumnarial ridge, which projects posteriorly near its posterior end. The ventral border of the anteroventral process extends posterodorsally to contact the premaxillary ventral process medially.

2.3.1.3 Prefrontal

The prefrontal (Figure 2-5) is an “L” shaped element in lateral view, which is composed of a short and sub-squared rostral plate and an elongated caudal ramus forming an angle of 90° to the rostral plate. Compared to adult *Edmontosaurus regalis* (e.g., BMNH 8927, CMN 2289) and *E. annectens* (CMN 8509, SM 4036), the prefrontal of the Alaskan edmontosaur is narrower mediolaterally, due to the lack of a pocket seen in adult

E. annectens (see Chapter 1).

The rostral plate is thin mediolaterally, and it becomes progressively thinner anteriorly. The lateral surface of the rostral plate is flat. On the lateral surface of the rostral plate are two foramina that may penetrate the prefrontal and open on the anterodorsal surface of the orbit. The caudal ramus is more elongated posteriorly relative to the rostral plate. The dorsal orbital rim of the prefrontal is straight but rugose. The dorsomedial border of the prefrontal is straight, except at the posterior end of the caudal ramus, where it tapers mediolaterally, and its ventral surface is excavated to articulate with the frontal.

Medially, the prefrontal articulates with the nasal at the anterodorsal part of the rostral plate and caudal ramus. Posterior to the rostral plate, the anteroventral part of the caudal ramus projects a plate ventrally to receive the posterodorsal process of the lacrimal. Unlike in adult *Edmontosaurus* [52,53], the orbital margin of the prefrontal is nearly flat and there is no fossa, but this is likely due to the ontogeny (see Chapter 1). Dorsal to this plate is a groove that receives the anterolateral border of the frontal. This groove is continuous with the articular surface of the nasal.

2.3.1.4 Frontal

The frontal (Figure 2-6) of size class 1 of the Alaskan edmontosaur material is anteroposteriorly longer than wide. Comparisons with other juvenile and adult specimens indicate that in *Edmontosaurus* the frontal likely becomes proportionately wider as it grows (see Chapter 1). Some frontals of the Alaskan edmontosaur (e.g., UAMES 4242, UAMES 4308) are proportionally wider compared to the smallest ones and are assumed to represent size class 2 specimens.

UAMES 13216 preserves the articular surface for the nasal. Although it is difficult to estimate its original size and shape due to damage, the articular surface appears to taper anteriorly and accounts for only a small portion of the frontal. Laterally, the frontal has a socket that receives the posterior end of the prefrontal. Dorsal to this

socket is a pronounced lateral ridge along the orbital margin, and the frontal is notched by the prefrontal in front of this socket and ridge. This lateral ridge is also pronounced in *E. regalis* (CMN 2289, ROM 801, USNM 12711, BMNHR 8927) and variably so in *E. annectens* (see Chapter 1). In size class 2 materials, this lateral ridge is less pronounced. Ventral to the lateral ridge and socket is an orbital depression. The orbital depression is strongly excavated dorsally, so that the frontal is V-shaped in the transverse plane. The posterior part of the dorsal surface of the frontal is raised to the level of the height of the lateral ridge as in other immature hadrosaurids [54]. The posterior border of the roof is rimmed with a small ridge. The lateral part of the rim is rugose and it has a crescent-shaped groove to articulate with postfrontal, but this groove shallows anteriorly and does not continue to the anterior end of the lateral ridge. The frontal attains maximum thickness at its posterolateral corner wall. Posteriorly, the frontal interdigitates with the parietal, where the wall is less thick than the posterolateral wall. Ventrally, the cerebral cavity is separated from the orbital depression and the olfactory depression by a rugose ridge. This ridge is less pronounced than that of *E. annectens* specimens of size class 2 (ROM 53501).

2.3.1.5 Lacrimal

The lacrimal (Figure 2-7) is sub-triangular in lateral view, mediolaterally thin anteriorly and mediolaterally thick posteriorly. The tip of the anterior process is dorsoventrally narrow and pointed. The anterodorsal half of the anterior process is covered by the posterolateral process of the premaxilla; this articular surface is gently concave in outline and is much narrower than in other size class 3 or adult *Edmontosaurus* specimens (*E. regalis*, CMN 2289; *E. annectens,* ROM 53511, ROM 53512, see Chapter 1). The posterodorsal process is covered by the prefrontal in lateral view. Ventrolateral to the posterodorsal process is a groove that receives the ventral border of the prefrontal. This groove is extensive anteriorly, indicating that the posterolateral process of the premaxilla and the prefrontal were in contact. A large portion of the posterolateral border of the lacrimal is gently flared laterally. The degree of the flare is comparable to some *Edmontosaurus* specimens (e.g., *E. regalis*, CMN 2289,

CMN 2288; *E. annectens*, AMNH 5730) but not to other specimens (*E. regalis*, CMN 8399; *E. annectens*, ROM 53511, CMN 8509). In contrast to the lateral surface of the lacrimal, the posteromedial border is flat. The lacrimal foramen, which penetrates the lacrimal, resembles a short ellipse in posterior view. The medial wall of the lacrimal foramen is closed in the posterior half of the foramen, but open in the anterior half, resulting in a groove. The prefrontal contributes to the dorsal part of the posterior exit of the lacrimal foramen. The posteroventral process covers the posterior surface of the lacrimal process of the jugal. Its distal end is anterolaterally and posteromedially extensive and bears a serrated ventral margin in the best preserved specimen, UAMES 4356. The anterior end of the palatine might contact the lacrimal anteromedially on the posteroventral process, but it is hard to tell due to the disarticulated nature of the specimens. Anterior to the posteroventral process, the lacrimal has a groove on its ventral surface, which articulates with the groove in the lacrimal process of the jugal. This groove is variably developed among the specimens of the Alaskan edmontosaur, being well developed in UAMES 4245 but weak in UAMES 4254.

2.3.1.6 Jugal

Overall, the jugal of the Alaskan edmontosaur (Figure 2-8) is gracile in that its depth at the caudal constriction (the minimum distance between the ventral border of the temporal fossa and ventral border arch between the ventral apex and posteroventral flange) is shallower than that of other *Edmontosaurus* species, even when ontogeny is taken into account (see Chapter 1). The medial surface of the rostral process is divided by the rostral process medial ridge that leads to the rostral spur. This ridge and spur rest on the jugal shelf of the maxilla and are more pronounced in the Alaskan edmontosaur specimens than other size class 2 or adult *Edmontosaurus* specimens (e.g., *E. regalis,* CMN 2289; *E. annectens,* ROM 53518, ROM 64076). The rostral spur of the jugal is an elongated asymmetrically-shaped triangle, which points anteriorly and slightly ventrally. The jugal articulates with the lacrimal along a groove on the anterodorsal edge of the lacrimal process. Medially, the posterior border of the rostral process is marked by a ridge, which runs obliquely dorsally and posteroventrally. This ridge bends anteriorly by

about 25° near the level of the rostral spur, which is a character not seen in other *Edmontosaurus* species. The ventral apex is wider than deep and is caudally offset from the dorsocaudal margin of the rostral process. The anteroventral edge of the lacrimal process is sigmoidal. The ventral margin of the orbit is wider than that of the infratemporal fenestra. The postorbital process tilts slightly posteriorly. The quadratojugal flange (jugal flange of Bell [55], quadratojugal process of Cuthbertson and Holmes [48]) is often damaged, but it is well preserved in UAMES 4213. It is wing-shaped, the anterodorsal and posteroventral borders are sub-parallel around its proximal part, its anterodorsal border is straight, and the posteroventral border is moderately concave, unlike in many saurolophines, including other *Edmontosaurus* species (*E. annectens*, ROM 64076, CMN 8509; *E. regalis,* CMN 2288). However, there is some damage on the posterodorsal edge of the quadratojugal flange; thus, whether it preserves its original shape is equivocal. Medially, the quadratojugal flange has a slight groove that articulates with the quadratojugal. In other *Edmontosaurus* species, this articulation surface is separated by a small ridge (e.g., *E. annectens*; ROM 64076, ROM 53518; *E. regalis,* CMN 2288). Such a structure is not seen in the Alaskan edmontosaur.

2.3.1.7 Quadratojugal

The quadratojugal (Figure 2-9) is trapezoidal in outline, as in most saurolophines, with the possible exceptions of *Maiasaura peeblesorum* Horner & Currie, 1994 [56] (MOR 547 and YPM-PU 22405) and *Acristavus gagslarsoni* Gate et al., 2011 [57] (MOR 1155). Laterally, the anterior half of the quadratojugal is mediolaterally compressed where it articulates with the jugal, and therefore the posterior half is thicker than the anterior half. This thickened posterior area is variable in the Alaskan edmontosaur, but on average it is proportionally as wide as in *E. annectens* and narrower than in *E. regalis* (see Chapter 1). Posterodorsally and ventrally on the medial side, there are two shallow depressions to articulate with the dorsal and ventral border of the quadratojugal notch of the quadrate. Slightly anteriorly to the posteroventral depression is a posterior ridge, by which the quadratojugal attains its maximum thickness. The ventral border of the quadratojugal is gently sigmoidal.

2.3.1.8 Quadrate

Overall, the quadrate of the Alaskan edmontosaur (Figure 2-10) is only slightly curved posteriorly. The degree of the curvature is weaker than in other adult *Edmontosaurus* specimens, and it is likely an ontogenetically variable character in *Edmontosaurus* (see Chapter 1). The quadrate shaft is anteromedially narrower than some adult saurolophines, including some adult *E. regalis* (CMN 2289, ROM 658) and *E. annectens* (MOR 003). However, other individuals of *E. annectens* (ROM 53521, ROM 64076) have as narrow a quadrate shaft as that seen in the Alaskan edmontosaur, suggesting considerable variation of this character in *Edmontosaurus.* Anteromedial to the quadrate head is a shallow groove that receives the prequadrate process of the squamosal. Because of this groove, this portion of the quadrate head appears narrower in lateral view, which is also seen in some other specimens of *Edmontosaurus* (*E. regalis*, AMNH 5254, CMN 2289, CMN 8744, CMN 8399, FMNH 15004; *E. annectens,* CMN 8509), but not in some other *E. annectens* (ROM 53521, ROM 64076). The squamosal buttress (quadrate buttress of Gates and Sampson [51]) is very weakly developed. The quadratojugal notch is arcuate, and nearly symmetrical. The top of the notch is located near the midpoint of the quadrate shaft. Compared to other specimens of *Edmontosaurus* (*E. regalis*, CMN 8744, CMN 2288; *E. annectens,* ROM 53521, ROM 64076), the quadratojugal notch is anteroposteriorly deeper, rather close to the condition seen in *Gryposaurus monumentensis* Gate & Sampson, 2007 [51] (RAM 6797 [51]), *Saurolophus osborni* Brown, 1912 [58] (AMNH 5221), and *Shantungosaurus giganteus* Hu, 1972 [59] (GMV V.1780 [59]). None of the PCF specimens preserve a complete pterygoid wing, but judging from incomplete specimens (UAMES 4286 and UAMES 4235), it is dorsoventrally more extensive than in *Saurolophus osborni* (AMNH 5221) but less so than in *G. monumentensis* (RAM 6797 [57]), and thus it resembles adult *Edmontosaurus* specimens (*E. regalis*, CMN 2289; *E. annectens,* ROM 64076). The posterolateral margin of the pterygoid wing is asymmetrical in outline. This shape is more similar to the semi-right scalene triangular pterygoid wing of adult *Edmontosaurus* specimens (*E. regalis*, CMN 2289; *E. annectens,* ROM 64076) than to the semi-

symmetrical triangular pterygoid wing of *G. monumentensis* (RAM 6797 [57]) and *Shantungosaurus giganteus* (GMV V.1780 [59]). The lower anterior flange is symmetrically triangular. The medial condyle is much smaller than the lateral condyle. The reflection of the medial surface of the medial condyle is more pronounced than in adult *E. regalis* (CMN 2289).

2.3.1.9 Postorbital

Several size class 1 postorbitals are known from the LBB (Figure 2-11). Additionally, a size class 3 postorbital (UAMES 33308) was also collected near the LBB from nearly the same stratigraphic layer. UAMES 33308 lacks the dorsal promontorium on the frontal process commonly seen in lambeosaurines [42,60] and is nearly identical in morphology, although larger, than the size class 1 materials from the LBB. For these reasons, I regard this material as conspecific with the LBB materials. The postorbital is composed primarily of three processes: the frontal process (frontal facet of Godefroit et al. [49]), the jugal process (medial ramus of Godefroit et al. [49]), and the squamosal process (caudal ramus of Godefroit et al. [49]). The frontal process is shorter than the squamosal process and its lateral surface is rugose, suggesting the existence of palpebrals, as in *Saurolophus maximus* [46]. Anteriorly, the process is roughly triangular in cross section in the transverse plane, with its apex pointing dorsally. There is no penetrating foramen as reported in subadult *Prosaurolophus maximus* (MOR 454) [46] and *Brachylophosaurus canadensis* (MOR 1071-7-13-99-87-G) [61]. The dorsal profile of the postorbital is nearly straight. The jugal process is both anteroposteriorly and mediolaterally much narrower than that of other *Edmontosaurus regalis*, although not narrower than that of *E. annectens* (See Chapter 1). In *E. regalis* and *E. annectens*, including a size class 2 specimen of *E. annectens* (ROM 53513), the posterior wall of the jugal process has a deep fossa. In both the size class 1 and size class 3 postorbitals of the Alaskan edmontosaur, the posterior wall of the orbital rim (the anterior surface of the jugal process) is only moderately concave anteriorly and does not have deep posterior orbital fossa. The fossa in the postorbital is present in both *E. annectens* and *E. regalis* [62]; thus, lack of the postorbital fossa in the Alaskan edmontosaur indicates the Alaskan

edmontosaur is not referable to either species (see Chapter 1). The size class 3 postorbital differs from that of the size class 1 specimens in that the bony shelf of the posterodorsal corner of the orbit is anteroventrally more extensive. The dorsal profile of the postorbital is nearly straight, with a very weak depression, as in other *Edmontosaurus* species. Medially and dorsal to the laterosphenoid facet is an anteroposteriorly-elongated groove, which ends anteriorly on the dorsal surface of the orbit. This pattern is consistent in both the size class 1 and size class 3 postorbitals, as well as in size class 2 and 3 specimens of *E. annectens* (see Chapter 1). At the posterior end of the squamosal process is a large V-shaped indentation where it interdigitates with the postorbital process of the squamosal. A similar articular morphology is also seen in subadult *Prosaurolophus maximus* (MOR 454), *Saurolophus osborni* (AMNH 5220 [55]) and many specimens of *Edmontosaurus* species (*E. regalis,* CMN 8399, BMNHR 8927, CM 26258; *E. annectens*, UMMP 20000, UCMP 128374, MOR 003, CMN8509), but not in some other *E. regalis* (CMN 2288 and CMN 2289). In the PCF specimens, the position of the indentation is variable among individuals. For example, the indentation is located more ventrally in UAMES 4983 than in UAMES 12965. On the medial side of the postorbital of the PCF specimens, the anterior end of the indentation reaches nearly to the root of the squamosal process. This is much deeper than in a size class 2 specimen of *E. annectens* (ROM 53513).

2.3.1.10 Squamosal

The dorsal profile of the squamosal (Figure 2-12) is straight in lateral view. The anterior end of the postorbital process (rostral process of Godefroit et al. [49]) is marked with two postorbital grooves that interdigitate with the postorbital. The postorbital process is relatively gracile and longer than that of other adult saurolophines. It articulates with the postorbital well anterior to the prequadratic process (precotyloid process of Gates and Sampson [51], Prieto-Márquez [42,63], and Godefroit et al. [49]), unlike in adult *Edmontosaurus* and other adult saurolophines, in which the squamosal articulates with the postorbital dorsal to or slightly posterior to the prequadratic process. The relative length of the postorbital processes of *Edmontosaurus* specimens of size class 2 and 3 (Alaskan edmontosaur, UAMES 4361; and *E. annectens*, ROM 53510) are

intermediate between size class 1 and adult *Edmontosaurus* specimens, suggesting this is an ontogenetically variable character (see Chapter 1). The prequadratic process extends anteroventrally, making an angle of 60-70° with the shaft of the postorbital process. The length of the process is nearly as long as the thickness of the main shaft above the quadrate cotylus. The postquadratic process (postcotyloid process of Gates and Sampson, [51] and Godefroit et al. [49]) extends nearly vertically from the main body (61°-103°) and is compressed anterolaterally and posteromedially. Between these processes is the quadrate cotylus that accommodates the head of the quadrate and opens ventrally. The lateral border of the cotylus forms a gentle curve to contact the postquadratic process. Posteriorly, the parietal process extends posteromedially and ends in a thick bulge to joint the parietal. The ventromedial part of the parietal process is excavated to form the supraoccipital foramen, which is well preserved in UAMES 4234 and UAMES 17763.

2.3.1.11 Parietal

In the PCF parietal (Figure 2-13) specimens, the postorbital process and supraoccipital process are not preserved, and only the anteromedial half of the parietal and an isolated sagittal process are present. The anterior margin of the parietal is deeply rugose. Anteriorly, the parietal has a crenulated and triangular (in dorsal view) anteromedial process (central anterior process of Prieto-Márquez [61], rostromedial process of Bolotsky and Godefroit [50], Bell [55], and Prieto-Márquez [42]). The dorsal surface of the anteromedial process is narrow, but it expands laterally at its ventral portion to form an upside-down T-shape in anterior view. Posterior and dorsal to this process is a triangular depression, which narrows further posteriorly to form the sagittal crest. Such a triangular depression is also seen in other species of *Edmontosaurus* (e.g., *E. regalis,* CMN 2289; *E. annectens*, CMN 8509, ROM 53493), *Shantungosaurus giganteus* (GMV V. 1780 [59]), *Prosaurolophus maximus* (MOR 447-8-13-7-13 [46]), *Gryposaurus notabilis* Lambe, 1914 [64] (AMNH 5350), and *Saurolophus osborni* (AMNH 5221 [55]). *Kudurosaurus nagornyi* (AEHN 2/921-8, Godefroit et al. [49]) and *Kerberosaurus manakini* (AENM 1/319, Bolotsky and Godefroit [50]) are reported to have a similar depression, but it is not conspicuous in their figures. *Brachylophosaurus*

canadensis (MOR 1071) has much smaller depression, and juvenile *B. canadensis* (MOR 1071 7-13 99-87-I) lacks it completely. Within the triangular depression, some PCF specimens (UAMES 4309 and UAMES 13167) have a central ridge that runs anteroposteriorly, while other specimens (UAMES 4210 and UAMES 12957) do not. CMN 2289 (*E. regalis*) and CMN 8509 (*E. annectens*) have the former, and ROM 53493 (*E. annectens*) has the latter pattern. The outline of the lateral margin, posterior to the postorbital process where the parietal articulates with the laterosphenoid, is smooth, without a depression in dorsal view, as in *K. nagornyi* (AEHN 2/921-8, Godefroit et al. [49]). A similar depression is seen in the juvenile specimen of *E. annectens* (ROM 53493), subadult *P. maximus* (MOR 447-8-13-7-13) and *B. canadensis* (MOR 1071). Due to poor preservation, the dorsal outline along the sagittal crest in lateral view is not known. However, based on a partially preserved sagittal process (UAMES 12975), it appears to curve gently in a posterodorsal direction, as in many saurolophines. The anteroventral portion of the isolated sagittal process (UAMES4256) is compressed mediolaterally, although the ventral margin of the sagittal process is wider and grooved to receive the central ridge of the supraoccipital. The posterodorsal portion of the sagittal process, presumably where it articulates with squamosal, is striated. Ventrally, impressions of the cerebrum and cerebellum are preserved. The cerebral impression is wide and shallow, and cerebellar impression is narrow and deep. These impressions are separated by weak bulges expanding medially from the lateral wall of the braincase. This bulge is less developed than in *E. annectens* of size class 3 (ROM 53493, see Chapter 1) and is rather close to that of *K. nagornyi* (AEHN 2/921-8 [49]).

2.3.1.12 Supraoccipital

In other saurolophines, the supraoccipital is anteroposteriorly much longer than wide, as in subadult *Prosaurolophus maximus* (MOR 447-8-8-7-14[46], *Edmontosaurus annectens*, ROM 53444, and *Secernosaurus koerneri* Prieto-Márquez, 2010 [65] (MACN-RN144 [65]), while in *Lambeosaurus* sp. (NMC 0170), the width and length are more equal. Specimens of the Alaskan edmontosaur (Figure 2-14) are anteroventrally shorter than other saurolophines, with the length/width ratio being closer to that of

Lambeosaurus sp. (CMN 0170) It is unclear whether this variation is attributable to taxonomic difference or to ontogeny. Anterolaterally, the prootic process on each side projects anteriorly and articulates with the prootic anteriorly. Between these processes is a V-shaped notch in dorsal view. In ventral view, this notch is Ω shaped due to the medial expansions near the middle to distal portion of the prootic processes. This is true in hadrosaurids in general, but in the PCF specimens such an expansion is only weakly developed. Ventrally, the prootic processes are rugose and articulate with the dorsal surfaces of the prootics and anterior end of the exoccipitals. On the ventral surfaces of the prootic processes are foramina that appear to have communicated with complementary foramina of the prootics. Posterior to these foramina on the prootic processes are other foramina, which appear to open into the braincase. The aforementioned expansions near the middle to distal part of the prootic processes correspond to these canals and foramina. On its ventrolateral side the supraoccipital attaches to the dorsal parts of the opisthotic processes of the prootics. Dorsal to these articulation surfaces are ridges that seemingly separate the articulation surfaces for the processes of the prootic and exoccipital. Dorsally there is an ascending ridge (ascending process of Horner [46]), surrounded laterally by the articulation grooves for the supraoccipital processes of the parietal. The dorsal profile of the ascending ridge is gently convex and it has a groove to underpin the sagittal process of the parietal. In posterior view, the base of the ascending ridge is transversely wide and trapezoidal, likely to increase the surface area for the insertion of M. rectus. The articular grooves for the supraoccipital processes of the parietal are triangular. On the posterolateral sides of the supraoccipital are shallow grooves by which the supraoccipital articulates with the anterodorsal edges of the exoccipital-opisthotics. Anterodorsally to these grooves are exoccipital wings (exoccipital process in Horner [46]) that project laterally. The exoccipital wings are not well developed in a size class 1 specimen (UAMES 4291), possibly due to either poor preservation or ontogeny, because UAMES 12727, a size class 2 specimen, possesses larger exoccipital wings. Nevertheless, the exoccipital wings are anteroposteriorly less developed than in subadult *P. maximus* (MOR 447-8-8-7-14 [46]). At its posteroventral surface, the supraoccipital contacts the

supraoccipital wings of the exoccipital-opisthotics. This articular surface with the supraoccipital wings is mostly flat, trapezoidal, and bears low and sub-parallel multiple ridges. Compared to other saurolophines (*P. maximus*, MOR 447-8-8-7-14; *S. koerneri*, MACN-RN 144; *E. annectens,* ROM 53444), this trapezoidal structure of the Alaskan edmontosaur is more rectangular and anteroposteriorly short. This is also true in size class 2 of *E. annectens* (ROM 53444). This contributes to the overall proportion of the supraoccipital mentioned earlier. At the center of the surface is a small ridge indicating where the medial borders of the supraoccipital wings meet. Apparently, the surapoccipital is excluded from the foramen magnum by the exoccipital-opisthotics. The posterior border of the supraoccipital is more weakly concave than in *P. maximus* (MOR 447-8-8-7-14 [46]).

2.3.1.13 Maxilla

Overall, the maxilla (Figure 2-15A-E) is triangular in lateral view, with its anterodorsal margin shorter than the posterodorsal margin, as in most specimens of *Edmontosaurus* species (*E. regalis,* CMN 2289, CMN 8744; *E. annectens* ROM 53527, ROM 53528,). Anteriorly, the maxilla bifurcates into anteromedial (anterodorsal process of Horner [46]) and anteroventral processes (rostrodorsal and rostroventral processes of Prieto-Márquez [42,60]). In some saurolophines, the anteromedial process is longer and more conspicuous in lateral view than the anteroventral process (e.g., *Brachylophosaurus canadensis*, MOR 1071 7-6-98-79; *E. annectens*. ROM 53527 and MOR 723). None of the PCF specimens preserve complete anteromedial and anteroventral processes, but the anteromedial process is dorsoventrally narrower than that of *B. canadensis* and *E. annectens* specimens noted above, as in other *Edmontosaurus* species (*E. regalis*, CMN 2289; *E. annectens*, MOR 1609). The anteroventral process curves only slightly ventrally, lying at an angle of 25° (UAMES 4327) to 30° (UAMES 4186) with respect to the tooth row (horizontal plane).

The apex of the dorsal lacrimal process (lacrimal flange of Horner [46]) is pointed and forms an angle of 102° (n = 6, 99-106°). It is shaped like an isosceles triangle in

lateral view. A similar-shaped dorsal lacrimal process is also seen in *Kerberosaurus manakini* (AENM 1/32 and 323, according the a reconstruction by Bolotsky and Godefroit [50]), *Brachylophosaurus canadensis* (MOR 1071 7-6-98-79), and size class 2 *Edmontosaurus annectens* (ROM 53527). Some other saurolophines, adult *Edmontosaurus* specimens (*E. regalis*, CMN 2289; *E. annectens*, MOR 1609), and a size class 3 *E. annectens* (ROM 53528) differ in that the posterior edge of the dorsal lacrimal process is nearly vertical relative to the tooth row in lateral view. The shape of the dorsal lacrimal process is unique in *E. regalis* (CMN 2289) in that its apex is rounded rather than pointed, but it is likely that this morphology is attributable to incorrect reconstruction, as such a shape is not seen in other saurolophines. The dorsal lacrimal process of the Alaskan edmontosaur is dorsoventrally shorter than in the other specimens of *Edmontosaurus* species noted above. Anterolateral to the lacrimal process is the jugal shelf (jugal sulcus of Godefroit et al [49]), on which the rostral process medial ridge of the jugal rests. The jugal shelf is nearly horizontal and laterally more pronounced than in other *Edmontosaurus* (*E. regalis,* CMN 8744, CMN 2289; *E. annectens,* ROM 53527, MOR 723, MOR 1609). In the Alaskan edmontosaur and other juvenile *E. annectens* (MOR 723, ROM 53527 and ROM 53528), the height of the jugal shelf is lower compared to the adult specimens (*E. regalis,* CMN 2289, CMN 8744; *E. annectens*, MOR 1609). Posterolateral to the jugal shelf is the jugal facet that receives the main body of the rostral process of the jugal, which mostly covers the contact between maxilla and lacrimal. The jugal facet faces dorsolaterally. The posterior margin of the jugal facet is marked with a crescentic rim that projects posteriorly (palatine process, palatine projection of Prieto-Márquez [42]). Posteromedial to this projection is an elongated and narrow indentation, which might receive the ventral margin of the palatine, although it appears to be too deep to be an articular groove. Five maxillary foramina, the anterior-most being largest, are aligned ventral to the jugal facet. These foramina are occur in a straight line. The foramina are more conspicuous than those of *E. annectens* but comparable to some *E. regalis* (see Chapter 1). A canal, located on the posteroventral part of the medial side of the dorsal process (lacrimal process canal), opens medially.

This condition is closer to *E. regalis* than to *E. annectens* (see Chapter 1). The ectopterygoid shelf lies posterior to the jugal facet, at the same height as the posterior-most maxillary foramen, and it is almost horizontally oriented. A short posterior process (pterygoid process of Prieto-Márquez [42,60]) projects posteriorly from the medial wall of the ectopterygoid shelf. The dorsal margin of the process is horizontal (UAMES 4327) to slightly oblique (UAMES 4250). The distance between the occlusal plane and the row of dental foramina is relatively narrow, contributing to the overall narrowness of the maxilla. The ventral border of the maxilla is slightly concave. There are 26 tooth positions (UAMES 4327 and 7662), with 1 to 2 teeth on the occlusal plane and 3 to 4 teeth per tooth family.

2.3.1.14 Maxillary teeth

The maxillary teeth (Figure 2-15F-I) are roughly diamond-shape in buccal view. The primary ridge alone runs dorsoventrally on the buccal side; no secondary ridge exists. The primary ridge is nearly straight and does not expand anteroposteriorly near its base. A strong offset of the primary ridge caudally, seen in some hadrosaurs [42,60], was not observed in the Alaskan edmontosaur. The marginal denticles are reduced in size, and only exist in the apical half of the tooth. They are more densely packed near the apex. In UAMES 4185 the marginal denticles are in a line, but in UAMES 4250, 4278 and 22699, maxillary teeth have more denticles and they are more dense and more randomly located than in UAMES 4185. This variation in the marginal denticles is likely attributable to individual difference, not to position in the tooth row.

2.3.2 Braincase

2.3.2.1 Laterosphenoid

The laterosphenoid (Figure 2-16) is roughly triangular in lateral view and is composed of the medial dorsal flange, the postorbital process, the prootic process, and the basisphenoid processes. The medial dorsal flange curves gently laterally. The postorbital process extends from the anterior end of the medial dorsal flange, is reduced in length and width as in other *Edmontosaurus* specimens [60,66], and points laterally to

contact with the postorbital via a ball joint. The dorsal margin of the laterosphenoid folds medially at a right angle and contacts with the parietal. The posterior half of this flange, where it articulates with the parietal, is inflated medially. Ventrally, the medial dorsal flange curves gently in the sagittal section, so that the lateral surface of the laterosphenoid is concave. The prootic process, which attaches to the prootic anterodorsally to cranial nerve V, is square-shaped, short, and does not extend over the exit for cranial nerve V. The posterior facet of this process is rugose where it firmly articulates with the prootic. The foramen for cranial nerve V does not notch the laterosphenoid in lateral view, but the groove for the ophthalmic branch of trigeminal nerve notches the lateral surface transversely. The groove is deep and wide posteriorly, but shallower and narrower anteriorly. The basisphenoid process is bifurcated into medial and lateral basisphenoid processes ventrally. The lateral basisphenoid process articulates with the prootic and basisphenoid, and the medial basisphenoid process articulates with its counterpart. On the anteroventral margin, dorsal to the lateral basisphenoid process, is a slight concavity, which may be a foramen for cranial nerve II, as in subadult *Prosaurolophus maximus* (MOR 447-7-14-7-6 [46]). Ventral to this medial basisphenoid process is the pituitary cavity. Medially, near the level of the groove for the ophthalmic branch of trigeminal nerve on the lateral side, is a short small groove that opens anteriorly.

2.3.2.2 Prootic

The overall shape of the prootic (Figure 2-17) is similar to that of *Prosaurolophus maximus* (MOR 447-8-3-7-2 [46]) and a size class 2 specimen of *Edmontosaurus annectens* (ROM 53537) in that the anterior border of the prootic is deeply notched by the foramen ovale (cranial nerve V). The posterior border of the prootic is straight to only slightly concave posteriorly and articulates with the exoccipital-opisthotic. Lambe [52] assumed that in *E. regalis* (CMN 2289) a greater portion of the foramen ovale is not in the prootic, but in the alisphenoid. Considering the close relationship of *E. regalis* and *E. annectens* + Alaskan edmontosaur, I assume Lambe misinterpreted a crack as a suture line. Cranial nerve VII penetrates the prootic, and on the lateral side, a groove possibly

for VII is located ventral to its exit. This groove is apparently continuous with the groove on the bifurcated alar process. Ventral to the foramen ovale is the prootic depression that might be the origin of *M. levator bulbi* [67]. The depression is continuous onto the anterolateral surface of the alar process. This depression is also seen in *Kundurosaurus nagornyi* (AENM 2/121 [49]), *Kerberosaurus manakini* (AENM 1/319 [50]), and *Brachylophosaurus canadensis* (MOR 1071-7-7-98-86). In *Edmontosaurus*, this depression exists in YPM 618, ROM 53537, ROM 59786 (*E. annectens*), but not conspicuously in CMN 8509, AMN 427 (*E. annectens*), and CMN 2288 (*E. regalis*). On the posterior edge of the depression is a ridge that projects posterolaterally and is continuous to the alar process of the basisphenoid. As is often true in other saurolophines, the groove for cranial nerve VII bifurcates the alar process longitudinally. On the medial side, the ventrally facing opening for cranial nerve VIII is located dorsally to the opening to for cranial nerve VII, which also faces ventrally. Posterior to the exit for cranial nerve VIII is another foramen, possibly the fenestra rotunda. These three openings share the same depression on the medial side. The opening for cranial nerve VIII and the fenestra rotunda merge in the prootic and open to the fenestra ovalis posteriorly. Dorsally, there is a canal that is continuous with the supraoccipital. The opisthotic process (supraoccipital process of Horner [46] and caudodorsal ramus of Godefroit et al. [49]) curves dorsally and projects posterodorsally to cover the suture of the anterior border of the exoccipital-opisthotic complex and ventral border of the supraoccipital.

2.3.2.3 Basisphenoid

The basisphenoid (Figure 2-18) attaches to the laterosphenoid anterodorsally, the prootic dorsally, and the basioccipital posterodorsally. However, unlike *Prosaurolophus maximus* (MOR 447-7-14-7-6 [46]) the basisphenoid does not contact the exoccipital-opisthotic. The parasphenoid process, which projects anterodorsally from the basisphenoid and contacts the laterosphenoid dorsally, is not preserved. At its root is the pituitary cavity, or sella turcica. This cavity is penetrated by the right and left internal carotid canals from the posterior wall of the cavity. Two foramina enter the cavity obliquely from its dorsal part. The corresponding foramen in *Prosaurolophus maximus*

(MOR 447-7-14-7-6) is interpreted as cranial nerve III by Horner [46], but Godefroit et al. [49] interpret it as cranial nerve VI in *Kundurosaurus manakini* (AENM 2/121, 2/921-1, 2/928). Dorsolaterally along the contact with the prootic are two gaps that probably correspond to cranial nerve IV. Only the base of the alar process is preserved. However, the alar process of the basisphenoid appears to be dorsally continuous to the flange posterior to the prootic depression, which is also found in other hadrosaurids. The alar process is bifurcated by cranial nerve II. Posterior to the base of the alar process is the anterior portion of the sphenooccipital tubera, by which the basisphenoid attaches to the basioccipital. Left and right sphenooccipital tubera are separated by an anteroposterior groove to receive the median mound of the basioccipital (see Figure 2-17). The basipterygoid processes (pterygoid process of Lambe [52], Horner [46], Bell [55], and Cuthbertson and Holmes [48]) ventral to this groove project ventrolaterally. The basisphenoid processes are shorter and stouter than those in adult saurolophines, and the anteroventral edge of the basisphenoid process is parallel to the posterodorsal surface of the basisphenoid. Since these characters are also found in subadult *E. annectens* (ROM 53492), this is not a unique character of the Alaskan edmontosaur. In many saurolophines, including adult *Edmontosaurus* specimens (*E. regalis*, CMN 2289; *E. annectens,* YPM 618, ROM 64076, and ROM 59786), the anteroventral and posteroventral surfaces are separated by the interbasipterygoid ridge. The interbasipterygoid ridge of brachylophosaurines (*Brachylophosaurus canadensis*, *Acristavus gagslarsoni*, *Maiasaura peeblesorum*) projects prominently ventrally [57], but this is not so in *Edmontosaurus* specimens. In size class 1 Alaskan edmontosaurs (UAMES 13107, UAMES 12777, UAMES 6631, and possibly in UAMES 4301), due to the depressions on the anteroventral and posteroventral surfaces, there is a blunt edge between the basipterygoid processes, which might be an immature form of the interbasipterygoid ridge. The size class 3 specimen (UAMES 18882) preserves a weakly developed interbasipterygoid ridge. Therefore, this is an ontogenetically variable character in the Alaskan edmontosaur (see Chapter 1). This ridge also has an interbasipterygoid median process in the Alaskan edmontosaur. Gates et al. [57] report

that this process is narrower in brachylophosaurines than other saurolophines. Among species of *Edmontosaurus*, this character is variable, as CMN 2289 (*E. regalis*), ROM 53492 (*E. annectens*) and size class 1 PCF specimens also have narrow interbasipterygoid median process, while ROM 64076 (*E. annectens*) and the size class 3 specimen of the PCF edmontosaur (UAMES 18882) have wider interbasipterygoid median processes.

2.3.2.4 Basioccipital

Only size class 1 basioccipitals have been recovered. The basioccipital (Figure 2-19) is hexagonally-shaped in dorsal view and its width and anteroposterior length are nearly equal. It is relatively thicker dorsoventrally than other hadrosaur basioccipitals, such as *Prosaurolophus maximus* (MOR 447-7-14-7-6 [46]) and size class 2 *Edmontosaurus annectens* (ROM 53538). Anterodorsally, there is one rounded depression on each side that receives the posteroventral portion of the prootic. On the dorsal side is a V-shaped sulcus that served as the floor of the braincase. Posteriorly this sulcus narrows mediolaterally and extends only three quarters of the total length of the basioccipital. The dorsolateral surfaces, where the basioccipital articulates with exoccipital-opisthotic, are rugose. Posteriorly to this groove is a trace of the posterior medial groove (medial vertical cleft of Prieto-Márquez [42,60]), which runs dorsoventrally on the posterior surface of the basioccipital. The development of this groove appears to be much weaker than in *E. annectens* (AMNH 427, CMN 8509)*, E. regalis* (CMN 2289) and *Gryposaurus notabilis* (AMNH 5350), but it is comparable to size class 2 *E. annectens* (ROM 53538), although PCF specimens have evidence of some abrasion. Anteroventrally the basisphenoid interlocks with the basioccipital via the posterior sphenooccipital tubera and the median mound. The posterior sphenooccipital tubera are much wider than the anterior sphenooccipital tubera of the basisphenoid. The posterior sphenooccipital tubera are well pronounced, as the basioccipital attains its maximum dorsoventral height and mediolateral width at this point. Medial and posterior to the tubera is a Y-shaped basioccipital medial cleft, which separates the tubera and the basal portion of the occipital condyle. The surfaces of the tubera are smooth, unlike in

other hadrosaur specimens, but this could be due to abrasion. In other hadrosaurs, including *E. regalis* (CMN 2289), the basioccipital is constricted by this cleft mediolaterally. This constriction is weaker in size class 2 and subadult *E. annectens* (ROM 53538, CMN 8509), and the Alaskan edmontosaur lacks a constriction, resulting in a hexagonal shape. A hexagonal shaped basioccipital is also observed in an embryonic *Hypacrosaurus stebingeri* Horner & Currie, 1994 (RTMP 87.79.206 [54]). Thus, this can be an ontogenetically variable character (See Chapter 1).

2.3.2.5 Exoccipital-opisthotic

The exoccipital and opisthotic (Figure 2-20) are fused to form a single complex, as in other hadrosaurs [68]. The paraoccipital process is hook-shaped, and projects ventrolaterally, more posteriorly than laterally in dorsal view. Its ventral end points ventrally and barely reaches the level of the exoccipital condyloid in small size class 1 specimens. The supraoccipital wing extends from the middle portion of the exoccipital-opisthotic to medially underpin the supraoccipital. Anteroventrally, this wing folds 90°. This 90° fold is not seen in *Prosaurolophus maximus* (MOR 447-7-14-7-5 [46]). In smaller size class 1 specimens, the middle portion of the exoccipital-opisthotic lies vertically dorsal to the exoccipital condyloid. In larger specimens of *Edmontosaurus*, including larger size class 1 material of the PCF taxon (UAMES 4095), the dorsal half of the exoccipital-opisthotic tilts posteriorly, the paraoccipital process is located more posterodorsally and the apex of the paraoccipital process is located more anteriorly than in the size class 1 PCF material. As a result, in a large size class 1 specimen, the ventral-most portion of the paraoccipital process reaches near the level of the exoccipital-basioccipital contact. This difference is attributable to ontogenetic variation (see Chapter 1).

The lateral surface of the exoccipital condyloid is flat, in contrast to *Edmontosaurus regalis* (CMN 2289), in which the portion of the exoccipital condyloid ventral to the cranial nerve foramina expands laterally. This expansion is also not seen in *E. annectens* (e.g., ROM 53503, 64076, AMNH 427, see Chapter 1). The condyloid has

four foramina, interpreted as cranial nerves IX-XII and the jugal vein (best preserved in UAMES 13764, Figure 2-20). In the Alaskan edmontosaur, these foramina are located well within the body of the exoccipital condyloid. In *E. annectens* (ROM 64076, ROM 53503, YPM 618, and AMNH 427), these are located more dorsally, and in *E. regalis* (CMN 2289) they are located dorsal to the condyloid. The exit for the jugal vein is much smaller than the other three foramina, and the foramen for cranial nerve XI is slightly smaller than other cranial nerve foramina. The jugal vein apparently penetrates the exoccipital condyloid. In CMN 2289 (*E. regalis*) and YPM 618 (*E. annectens*), exits for cranial nerves IX, X, XI, and the jugal vein are included in a relatively deep depression in the lateral side, but such a feature is not seen in other specimens of *E. annectens* (ROM 64076, ROM 64077, and AMNH 427). In most Alaskan edmontosaur specimens, exits for the cranial nerves IX to XI and the jugal vein are not included in a depression, except in UAMES 4279. Anterior to the exists for cranial nerves IX-X is an oblique ridge along the anterolateral side of the condyloid, which is seen in other specimens of *Edmontosaurus,* but not in some saurolophines, such as *Kerberosaurus manakini* (AENM 1/319, Godefroit et al. [49]), and subadult *P. maximus* (MOR 447-7-14-7-5 [46]). This ridge is less developed than it is in adult *Edmontosaurus* specimens (e.g., *E. annectens,* ROM 64077; *E. regalis,* CMN 2288). Anterior to this ridge are a groove and the fenestra ovalis. The ventral groove of the foramen magnum on the dorsal side of the basioccipital extends three quarters of the basioccipital. This indicates that the ventromedial border of the exoccipital condyloid did not meet with its counterpart to exclude the basioccipital from the foramen magnum.

2.3.3 Palate

2.3.3.1 Ectopterygoid

The ectopterygoid (Figure 2-21) of size class 1 Alaskan edmontosaurs does not differ from that of adult *Edmontosaurus regalis* (CMN 2289). Whether it differs from that of *E. annectens* is difficult to assess, due to poor preservation of the element in the latter species. In the ectopterygoid of the Alaskan edmontosaur, the maxillary process

forms a gentle sigmoidal curve in medial or lateral views and articulates on the ectopterygoid shelf of the maxilla. The pterygoid flange extends posterolaterally and attaches to the pterygoid on its posterior side. On the anterior side, the pterygoid flange wraps around the posterior edge of the posterior process of the maxilla.

2.3.3.2 Palatine

The overall proportions of the palatine (Figure 2-22) are typical of saurolophines. The pterygoid process and the ventral border of the palatine form a nearly right angle, while in other saurolophines the pterygoid process tilts anteriorly. As a result, and the jugal process extends more anteriorly than the anterodorsal end of the pterygoid process and the concave margin of the anterior edge of the palatine is wider and shallower. The pterygoid process is more robust than that of *Brachylophosaurus canadensis* (MOR 1071 8-15-98-567), and the anterodorsal margin of the pterygoid process is hooked. The anterior end of the jugal process is not hooked.

2.3.3.3 Pterygoid

The pterygoid (Figure 2-23) has two wings, the dorsal quadrate wing and palatine wings, and two processes, the ventral quadrate and ectopterygoid processes. It also has a short medial process which projects posteromedially. The palatine process, ectopterygoid process, and ventral quadrate process are buttressed by ridges from this medial process.

A size class 1 specimen (UAMES 4215) preserves the base of the palatine wing. The palatine wing forms an angle of 135° to the dorsal quadrate wing and the bony lamina between the ectopterygoid process and the ventral quadrate process (quadrate ramus of Prieto-Márquez [61]), which are on the same plane. A size class 3 specimen (UAMES 4252) preserves a flange that extends anteriorly to the ridge that buttresses the palatine wing. This flange is highest posteriorly and narrows anteriorly. The lateral side of the flange is excavated posteriorly. Around the center of the excavated area is a small foramen. From where this flange ends distally, the palatine wing begins to expand laterally to contact the vomer and palatine.

The ectopterygoid process of UAMES 4215 projects posteroventrally, while that of UAMES 4252 projects anteroventrally. This difference is likely attributable to poor preservation of UAMES 4252. The lamina between the ectopterygoid process and ventral quadrate processes is less extensive than it is in adult *Edmontosaurus* specimens (see Chapter 1), reaching only about half the length between the medial process and the ventral quadrate process.

The ridges that buttress the ectopterygoid process, ventral quadrate process, and palatine wing merge at the medial process. The apex made by the ridges on the ectopterygoid and ventral quadrate processes is rather blunt, resulting a flat and triangular surface on the palatine wing ridge. The posterior end of this triangle is dorsoventrally thick. This is true in other *Edmontosaurus* specimens (*E. regalis,* CMN 2289; *E. annectens,* CMN 8509, and ROM 53539) but not in *Brachylophosaurus canadensis* (MOR 1071 7-23-98-387 and MOR 1071 8-98-cc), in which the corresponding part is dorsoventrally narrow.

2.3.4 Mandible

2.3.4.1 Predentary

Three predentaries (Figure 2-24) represent different growth stages of the Alaskan edmontosaur: one small and one large size class 1 specimen (Figure 2-24A-F, UAMES 4437 and UAMES 4947, UAMES 15621) and a size class 2 specimen (Figure 2-24G-I, UAMES 4928). UAMES 4928 is dorsoventrally compressed and its right lateral process has shifted medially from its original position. UAMES 4947 lacks its left half. UAMES 4437 differs from the other two in that it is not rounded at its anterolateral corner, but this is likely because the lateral sides of its lateral processes are missing. The anterior margin of the predentary is marked with sub-triangular denticles, which project anterodorsally. Although Prieto-Márquez [42] suggests that the number of denticles increases slightly through ontogeny, all the predentaries of the PCF materials have only three denticles lateral to the median denticle, and thus do not show ontogenetic variation in number within this size range. The size of the denticles does not increase proportionally to the

whole predentary size, and in larger specimens (UAMES 4947 and UAMES 4928) the spaces between these denticles is greater than in the smallest specimen (UAMES 4437). The anterior margin of the predentary is nearly straight in dorsal view, forming an angle of ~90° with the lateral borders of the lateral processes. In better-preserved specimens (UAMES 4437, UAMES 4947), the anterior margin forms a gentle curve dorsally in anterior view. The central denticle is largest and there are at least three denticles on both sides, which is fewer than the four or five found in adult saurolophines (e.g., *E. regalis*, CMN 2289; *Brachylophosaurus canadensis,* MOR 1071 7-28-98-299; *Maiasaura peeblesorum,* YPM-PU22405). Posterior to the denticles are five to six foramina that penetrate through the predentary. Among these, the medial-most foramina are the largest. The posterodorsal median process, which projects from the posterodorsal portion of the predentary along the midline, is robust for its size compared to adult saurolophines (see Chapter 1). On the ventral midline of the predentary are bilobed processes, which project posteroventrally (preserved in UAMES 15621). UAMES 4437 and UAMES 15621 preserve the bony lamina between the lobes, and the lobes and lamina project posteroventrally as a whole. Many saurolophines have a ridge on the lingual side and dorsal surface of the posterodorsal median process [42], and this ridge is also seen in PCF *Edmontosaurus* sp. nov., although it is not very conspicuous.

2.3.4.2 Dentary

The edentulous process of the dentary (Figure 2-25A-D) is relatively short and more strongly deflected ventrally than the dentary edentulous process of other *Edmontosaurus* species, which is an ontogenetically variable character in edmontosaurs (see Chapter 1). In particular, a size class 2 dentary (UAMES 4946) has a shorter edentulous process than that of a size class 2 dentary of *E. annectens* (BHI-6218) (see Chapter 1). On the lateral side, there is no shelf that supports the predentary lateral process. Laterally, the edentulous process has a row of several foramina that is nearly parallel to the dorsal margin of the dentary. The anterior-most foramen, located at the tip of the edentulous process, is the largest and opens anteriorly. Posteriorly on the main body of the dentary, several foramina are distributed randomly.

The occlusal plane of the dentary is straight and almost parallel to the ventral margin. The caudal end of the dental battery lies in the same transverse plane as the caudal margin of the coronoid process, as in a size class 2 *Edmontosaurus annectens* (AMNH 5046), which is shorter than subadult and adult specimens of *Edmontosaurus* species (*E. regalis,* CMN 2289, ROM 658; *E. annectens,* ROM 64084), suggesting ontogenic change of this character. No dentaries were preserved with a complete battery of teeth. A size class 2 specimen (UAMES 4946) has at least 27 tooth sulci, and size class 1 specimens have at least 26 tooth sulci.

The coronoid process is vertical to slightly tilted anteriorly, forming an angle of 81 ± 6° (n = 6, 78-90°). In comparison to the adult *Edmontosaurus* species listed above, it is relatively long, but this is a feature common to other juvenile saurolophine dinosaurs (e.g., juvenile *Brachylophosaurus canadensis*, MOR 1071-7-10-98-179, and juvenile *Maiasaura peeblesorum*, MOR 547-W-25-6). The apex of the coronoid process is expanded anteroposteriorly and is mediolaterally flattened. There are dorsoventrally-oriented sub-parallel ridges on the medial side. There is a sharp dorsal projection from the apex of the coronoid process in a size class 2 specimen (UAMES 4946), similar to *E. annectens* (ROM 53530 and ROM 64084), *Prosaurolophus maximus* (MOR 447-8-11-7-2, Horner [46]), *Brachylophosaurus canadensis* (CMN 8893), and possibly to *E. regalis* (CMN 2289), according to Lambe [52]. The coronoid process has a ridge which projects posteromedially and runs dorsoventrally. The ventral margin has a wide bulge rostral to the coronoid process.

2.3.4.3 Dentary tooth

Most dentaries of the PCF specimens lack dentary teeth (Figure 2-25E-G), but UAMES 13196 is preserved with one tooth in growth position. As in many other hadrosaurs, the lingual side of the tooth is rhomboid in outline. A straight primary ridge is located along the center of the lingual side of the teeth. It is 5 mm wide, and although the apical end is missing, its length is approximately 8-9 mm. Many larger teeth, ranging between 0.7-1.6 mm in width and 1.4- 2.2 mm in height, are also known from the LBB.

The height/width ratios of the PCF specimens are around 1.4-2.9, which is comparable to other *Edmontosaurus* specimens [42,52,69]. Although this ratio is a character used by Prieto-Márquez [42,60], this value would increase as the teeth elongate, suggesting it is not a valid character for juvenile specimens (see Chapter 1).

2.3.4.4 Surangular

The surangular (Figure 2-26) is nearly trapezoidal in dorsal view. The coronoid process (rostrodorsal process of Prieto-Márquez [42]) projects dorsally from near the anterolateral corner of the element. The medial sagittal ridge extends along the posteromedial border and is confluent with the posterior articular process (caudal process of Prieto-Márquez [42]), which extends further posterodorsally.

The anteromedial flange of the anteromedial side extends further anteriorly than the coronoid process, as seen in adult *Edmontosaurus* specimens (*E. regalis,* CMN 2289; *E. annectens*, ROM 64076). Whether this is true in other saurolophines is difficult to determine due to the fragile nature of this flange. Along the anteroventral surface, there is a shallow depression with low sub-radical ridges for articulation with the dentary. The articular surface of the dentary in both size class 1 and size class 3 of the PCF specimens is nearly equal in size and position to the medial concavity of the dorsal side, being much wider than that of *Prosaurolophus maximus* (MOR 447-3-8-5-86 [46]) and *Brachylophosaurus canadensis* (MOR 1071 8-98-DD, MOR 1071 7-25-98-405-A), but posteriorly less extensive than many juvenile to adult *Edmontosaurus* specimens (*E. regalis,* CMN 2289; *E. annectens,* ROM 64076, ROM 53535 and CMN 8509), except for one size class 2 specimen of *E. annectens* (ROM 53536), whose articular surface is as extensive as in the Alaskan edmontosaur. The anterior end of the dentary articular surface is not bifurcated. The coronoid process extends nearly vertical relative to the main body of the surangular in lateral view, but it is more laterally oriented than in *E. regalis* (CMN 2289), *P. maximus* (MOR 447-3-8-5-86 [46]), and a specimen of *B. canadensis* (MOR 1071 8-98-DD). In *B. canadensis* (TMP.90.104.1) and another specimen of *E. regalis* (CMN 8744) the coronoid process tilts laterally, as it does in the Alaskan edmontosaur.

However, in the case of CMN 8744 this is likely due to dorsoventral crushing. Such a tilt of the coronoid process would bring the convex (ventrolateral) side of the surangular to a more laterally oriented position when articulated with the dentary, which is closer to the plesiomorphic condition in basal hadrosauroids, where the convex side of the surangular faces more laterally than ventrally [42,60,66]. In the Alaskan edmontosaur, the convex side of the surangular still faces more ventrally than dorsally, as in other saurolophines and lambeosaurines. This feature is attributable to the immature growth stage of the PCF specimens (see Chapter 1). The medial sagittal ridge ends nearly perpendicularly at its anterior end (see Figure 2-26F) to form a flange, similar to *E. regalis* (CMN 2289 [52]) and likely to *E. annectens* (ROM 64076, ROM 53535) and *Brachylophosaurus canadensis* (MOR 1071 7-13-99-84, MOR 1071 8-98-DD, TMP 90.104.1). In contrast, the medial sagittal ridge of *Gryposaurus monumentalis* ends with an anterodorsally projecting process (RAM 6797 [51]). The anterior end of this medial sagittal process is often incomplete. Therefore, further comparison with other taxa is difficult. The lateral margin between the coronoid process and the lateral bulge (quadrate articular surface of Gates and Sampson [51]) is less concave medially in both size class 1 and 3 specimens than in specimens of other *Edmontosaurus* species (*E. regalis*, CMN 8744; *E. annectens*, ROM 53535, ROM 53536, CMN 8744) (See Chapter 1).

2.3.4.5 Angular

The angular (Figure 2-27A, B) of the Alaskan edmontosaur is mediolaterally thin, and anteroposteriorly elongated. It curves dorsally with a gentle curve. Its posterior one-third bends very weakly laterally. The medial surface is flat, but its lateral surface has articular facets for the dentary and splenial.

2.3.4.6 Splenial

The splenial (Figure 2-27C-D) is tongue-shaped, mediolaterally flat, and curves slightly medially. The anterior portion of the splenial is missing. As in other saurolophines, it is dorsoventrally deep anteriorly but abruptly narrows posteriorly. Anteromedially, there is a triangular indentation that receives the splenial process of the

dentary. This indentation is anteroposteriorly shorter than in *Prosaurolophus maximus* (MOR 447-3-8-5-86 [46]), *Brachylophosaurus canadensis* (MOR 1071-8-6-98-483 [61]), and *Edmontosaurus regalis* (CMN 2289). Both size class 3 (ROM 53532) and adult *E. annectens* (ROM 64076), however, have a short indentation, as in the Alaskan edmontosaur (see Chapter 1). Posterior to the apex of the dentary indentation is a slight depression that runs posteriorly, and its dorsal border is not marked by a conspicuous ridge, which is seen in *P. maximus* (MOR 447-3-8-5-86 [46]) and adult *E. annectens* (ROM 64076). The posterior half of the splenial, where it articulates with the articular, is marked with radial ridges. Ventrally, the splenial articulates with the angular. In UAMES 4246, the anterior two-thirds of the angular articular facet faces ventromedially and the posterior third faces ventrally. Accordingly, the anterior two-thirds of the reverse side face dorsolaterally, thus the medial surface of the splenial is concave. The same pattern is seen in *P. maximus* (MOR 447-3-8-5-86 [46]). However, In UAMES 4275, the whole angular articular surface faces ventrally and the medial surface of the splenial is flat.

2.3.5 Axial postcranium

2.3.5.1 Cervical vertebrae

Only the neural arches are known from the LBB (Figure 2-28). The neural spine is absent in UAMES 12334 (size class 1) and UAMES 19734 (size class 2?), but it is present in UAMES 21559, UAMES 19535 (size class 2?) and UAMES 12945 (size class 3). Because the neural spine is present or better developed in the posterior cervical vertebrae in other hadrosaurids [52,70], it is likely that UAMES 12334 and UAMES 19734 are anterior cervicals, while UAMES 21559 and UAMES 12945 are posterior cervicals.

Compared to other hadrosaurids, the postzygapophyseal processes of the Alaskan edmontosaur are generally straighter and dorsoventrally flatter. The dorsal outline of the postzygapophyseal processes show some convex curvature but are weaker than in other specimens, including *Edmontosaurus regalis* (CMN 2289). The postzygapophyseal processes of the posterior cervical vertebrae are flatter and straighter than in *Gryposaurus*

notabilis (ROM 768) and brachylophosaurines (*Brachylophosaurus canadensis*, CMN 8893; *Acristavus gagslarsoni*, MOR 1155; *Maiasaura peeblesorum*, ROM 44770), but a similar postzygapophyseal process is also seen in *E. regalis* (CMN 2289) and *Shantungosaurus giganteus* (GMV V.1780 [59]). The articular surface of the postzygapophysis appears less expanded than in subadult specimens (UAMES 12945) and other adult hadrosaurid specimens.

2.3.5.2 Dorsal vertebrae

Although most of the PCF specimens are of size class 1, three of the best preserved dorsal vertebrae (Figure 2-29) are from size class 3 (UAMES 23033, UAMES 12516, and UAMES 6646). All dorsal vertebrae specimens that are possibly of size class 1 are disarticulated from the neural arches (UAMES 18462, UAMES 18704) and centra (UAMES 7661 and UAMES 12704). These size class 1 neural arches do not differ from size class 3 specimens, except in size and minor differences attributable to their relative positions along the vertebral column.

In UAMES 23033, the transverse processes are horizontal and the prezygapophyses are located on the anterodorsal surface of the transverse processes, being dorsolaterally offset from the pedicle of the neural arch, as in the cervical neural arches. In contrast, the prezygapophyses of the dorsal vertebrae are located immediately dorsal to the pedicle. The postzygapophyseal processes of UAMES 23033, however, are much smaller than those of the cervical vertebrae, and they project laterally rather than posterolaterally, as in the postzygapophyses of more posterior dorsal vertebra. Therefore, UAMES 23033 is intermediate in shape between cervical and dorsal vertebrae and can be interpreted as the anterior-most dorsal vertebra. The other specimens are interpreted as middle and posterior dorsals: In *Brachylophosaurus canadensis* (CMN 8893), middle dorsal vertebrae (D4-D7) have transverse processes that project dorsolaterally, while posterior dorsal vertebrae (D8-9) have horizontal transverse processes [48]. Therefore, UAMES 18462 and UAMES 12516, which have steeply inclined transverse processes, are likely from the anterior and middle dorsal vertebrae respectively. Although more

anterior dorsal vertebrae (D3) of *B. canadensis* also have horizontal transverse processes, the transverse processes of UAMES 23033, 18462 and 12516 are dorsoventrally wider and more strongly excavated posteriorly than in UAMES 6646 and UAMES 18704. Therefore, UAMES 6646 and UAMES 18704 are interpreted to be posterior dorsals. The relative positions of the juvenile dorsal vertebral centra (UAMES 7661 and 12704) are determined by comparison with size class 3 dorsal vertebral centra, which is discussed below.

The transverse processes of the dorsal vertebrae are buttressed by a ridge ventrally. The transverse processes are triangular in cross section, with the apex pointing ventrally. The parapophyses are located ventromedially to the transverse process and dorsal to the pedicles. The posterior surfaces of the transverse processes are excavated. This excavation is deeper proximally, due to the laminae that extend posteriorly between the postzygapophyses and the dorsal edge of the transverse processes. In the posterior dorsal vertebrae, the transverse processes are so thin dorsoventrally that only slight excavations are observed at the posterior proximal portions of the transverse processes. In the anterior-most and middle dorsal vertebrae, the prezygapophyses and postzygapophyses face dorsoventrally and ventrolaterally, but in the posterior dorsal vertebra, the prezygapophyses and postzygapophyses face nearly dorsally and ventrally. In the anterior-most dorsal vertebra, the centrum is nearly as long as wide and dorsoventrally slightly shorter than mediolaterally wide. In the middle and posterior dorsal vertebrae, the centrum is heart-shaped in anterior view. In the middle dorsal vertebrae, the centrum is dorsoventrally taller than wide, but the centrum of the posterior dorsal vertebra is as tall as wide. In the centrum of the anterior-most vertebra, both the concave (anterior) and convex (posterior) surfaces are more pronounced than those of other dorsals, and the more posteriorly located centra are shorter than those of other dorsals. Using these criteria, UAMES 7661 represents an anterior dorsal vertebra and UAMES 12704 is a posterior dorsal.

When compared with other specimens, the neural spine of the Alaskan

edmontosaur is proportionally similar to other saurolophines but is anteroposteriorly wider than in *Shantungosaurus giganteus* (GMV V.1780 [59]).

2.3.5.3 Dorsal ribs

Although all are disarticulated, the relative positions of the dorsal ribs (Figure 2-30) are determined by the angle between the shaft and neck, as well as the dorsoventral width of the neck. In the anterior to middle dorsal ribs, there is a bony lamina on the neck, between the tuberculum and rib head, corresponding to the dorsoventrally wide transverse process of the anterior and middle dorsal vertebrae. In the posterior dorsal ribs, the angle between the neck and shaft is shallower than in more anterior ribs, and the transverse processes of the posterior dorsal ribs are horizontal. In the anterior-most dorsal ribs, the neck and shaft make nearly a right angle, because the parapophyses of the anterior-most dorsal vertebrae are located more ventrally than on more posterior dorsals. The mid-dorsal ribs are intermediate in this respect. Proximally, the shaft of the rib is buttressed by a ridge anterolaterally. This ridge extends both anteriorly and posteriorly and is posteriorly more extensive than anteriorly. This ridge is widest in the middle dorsal ribs, and in anterior and posterior ribs the shafts are more flattened anteroposteriorly. Distally, the shaft flattens mediolaterally.

2.3.5.4 Sacrum

A possible size class 3 sacrum (Figure 2-31) was recovered from the LBB. At least eight fused sacral vertebrae are present, although the exact number is hard to determine due to poor preservation. In comparison, *Edmontosaurus regalis* also has eight sacral vertebrae [52], but this is fewer than the 10 observed in *Shantungosaurus giganteus* [71]. The neural spines are as tall as the sacral centra, as in other *Edmontosaurus* species (e.g., *E. regalis*, ROM 801, ROM 867; *E. annectens*, YPM 2182), and shorter than in *Brachylophosaurus canadensis* [70], although the true length in the Alaskan edmontosaur is unknown due to damage. As preserved, the fourth (?) sacral vertebra is the tallest dorsoventrally, while more anteriorly and posteriorly positioned sacral vertebrae are shorter, possibly due to poor preservation. The sacral

vertebrae are mediolaterally narrow and only half as wide as the posterior dorsal vertebral centra (UAMES 6646). No transverse processes are preserved with the sacrum.

2.3.5.5 Caudal vertebrae

The relative positions of the caudal vertebrae (Figure 2-32) are determined by morphology and size within each size category, with larger ones located more anteriorly and smaller ones more posteriorly. The neural arch is attached to the centrum more vertically in the anterior caudal vertebrae than in posterior caudal vertebrae. The postzygapophysis is directly attached to the main shaft of the neural spine. The anterior caudal vertebral centrum is dorsoventrally taller than wide and keystone-shaped in outline in anterior or posterior view. Mid-caudal centra are more hexagonal in outline and anteroposteriorly longer than anterior caudal vertebral centra. The lateral surfaces of the centrum are concave. In posterior caudal vertebrae, the dorsal ends of the neural spines expand anteroposteriorly. As in other hadrosaurids, the chevron is Y-shaped and has expanded bifurcated heads to articulate with the centra. The chevron is nearly straight in lateral view and attains maximum width anteroposteriorly near its distal end. The chevron articulates with successive centra.

2.3.6 Appendicular skeleton

2.3.6.1 Sternal

Only one poorly preserved sternal (Figure 2-33) is known from the LBB, and both its proximal and distal ends are damaged. Its dorsolateral profile is more strongly curved dorsally than in other saurolophines, including adult *Edmontosaurus* species (*Edmontosaurus regalis*, CMN 2289; *E. annectens*, AMNH 5060, TMNH 00001, and DMNH 1493). The ridge on the ventrolateral side of the sternal, seen in *E. annectens* (AMNH 5060 [72]) and *Kundurosaurus nagornyi* (AENM 2/913 Godefroit et al. [49]), is absent in the Alaskan edmontosaur. The ventromedial profile of the ventral process appears less curved than in other saurolophines, although this may be attributable to post-mortem damage.

2.3.6.2 Scapula

The scapulae (Figure 2-34) of size class 1 specimens of the Alaskan edmontosaur show some features that are different from size class 3 specimens and other species of *Edmontosaurus*. In the PCF size class 1 specimens, the coracoid process is relatively well developed, being proximodistally longer than that of size class 2 specimens and most other *Edmontosaurus* [42,60]. In a size class 2 specimen (UAMES 22012), the relative size of the coracoid process is similar to those of other *Edmontosaurus* specimens. In both juvenile and size class 2 specimens, the glenoid fossa forms a very gentle concave curve in lateral view, lacking the sharp indentation often seen in other adult saurolophines (e.g., *E. regalis,* CMN 2289; *E. annectens,* CMN 8509; *Brachylophosaurus canadensis*, MOR 5-10-99-505a). This morphology is similar to a specimen of *E. regalis* (CMN 867 [73]), suggesting this character is variable among edmontosaurs. The coronoid surface is mediolaterally narrow and shows no sign of expansion, in contrast to *E. regalis* (CMN2289), and the caudal buttress is relatively small. The caudal buttress extends posteroventrally, but it is not curved laterally to any significant degree. These characters result in a wider and shallower glenoid fossa when compared to adult *E. annectens* (CMN 8509) and *E. regalis* (CMN 2289). The deltoid process extends over the scapular neck and reaches near the ventral border.

The scapular blade of the PCF juvenile specimens, including the size class 3 scapula of the Alaskan edmontosaur (UAMES 29996), is more strongly constricted at its scapular "neck" than in adult *Edmontosaurus* (e.g., *E. regalis*, CMN 2289; *E. annectens*, CMN 8509) and expands in its posterior region. The strong neck constriction is typically seen in juvenile hadrosaurids [74,See chapter 1]. Around the constriction, the size class 2 scapula curves ventrally more strongly than the size class 1 and adult scapulae, but this is not seen in size class 3 specimens. The size class 1 specimens also appear strongly curved at the neck, but this is attributable the strong degree of constriction at this point. Although damaged, the size class 3 specimens have a better developed pseudoacromion process.

2.3.6.3 Coracoid

The glenoid fossa of the coracoid (Figure 2-35) is mediolaterally narrow and its external outline is concave. It lies in nearly the same plane as the posterior surface of the coracoid ventral process. The coracoid foramen is entirely included in the main body of the coracoid, and the scapular surface and glenoid are not separated by a groove, as seen in *Gryposaurus incurvimanus* Parks, 1920 [75]. The scapular facet is damaged in all specimens, so the angle at the posteroventral margin of the coracoid, between the scapular fossa and glenoid fossa, cannot be determined. The opening of the coracoid fossa is oval. The biceps tubercle is well developed, so that its anterior margin is offset more anteriorly than the anterior curve of the ventral process. The ventral process is moderately curved so that its distal end points caudoventrally.

2.3.6.4 Humerus

The humerus (Figure 2-36) is somewhat robust, with its width across the deltopectoral crest being mediolaterally about 1.7 times wider than the mediolateral width of the distal part, which is not covered by the deltopectoral crest. This is comparable to other species of *Edmontosaurus*, but it is more robust than *Brachylophosaurus canadensis* (CMN 8893), *Maiasaura peeblesorum* (ROM 44771), and *Kudurosaurus nagornyi* (AENM 2/908 [49]), as documented by Prieto-Márquez [42, 60]. Both outer and inner tuberosities show little expansion, as is often observed in juvenile hadrosaurids [74]. The humerus attains its maximum width at its proximal end. Adult *Edmontosaurus regalis* (CMN 2289) and some *E. annectens* (AMNH 5730) have a boss on the ridge that buttresses the humeral head, but the PCF specimens lack this feature. The deltopectoral crest (radial crest of Lambe [52]) extends about 52 % of the whole humerus length, which is close to that of *E. annectens* but shorter than *E. regalis*. Size class 2 and 3 specimens have longer deltopectoral processes, suggesting that in adults the deltopectoral process is possibly as well developed as in *E. regalis* (see Chapter 1). The anterior border of the humerus, from the inner tuberosity to the deltopectoral crest, forms a weak sigmoidal curve in most saurolophine hadrosaurs, including *E. regalis* (CMN 2289), but in the PCF specimens this margin is nearly straight. Such a straight anterior border is also observed

in *E. annectens* (AMNH 5879, AMNH 5730, YPM 2182, TMNH 00001), *Acristavus gagslarsoni* (MOR 1155), and neonate *Maiasaura peeblesorum* (YPM-PU22400), but not in *B. canadensis* (CMN 8893, MOR 1071 7-20-98-325), and *Shantungosaurus giganteus* (GMV V.1780 [59]). The distal corner of the deltopectoral crest is less developed than it is in adult saurolophines, forming a rather obtuse angle of 115-125°. The deltopectoral crest is known to increase in prominence throughout ontogeny [53,76], and enlargement of the deltopectoral crest would result in an increasingly sigmoidal curve of the anterior border of the humerus. The humeral shaft bends approximately 30-40° near its midpoint. In distal view, the ulnar condyle is generally much larger than the radial condyle. In anterior view, the ulnar condyle is mediolaterally and proximodistally larger than the radial condyle, but the degree to which it is larger varies among dozens of specimens. This is unusual among saurolophines, but it is also observed in *Shantungosaurus giganteus* (GMV V.1780 [59]). There is little difference between size class 1 and size class 2 (UAMES 13093) specimens with respect to humeral morphology.

2.3.6.5 Ulna

The forelimb of hadrosaurids has been reconstructed in two different ways. Some specimens are reconstructed so that the ulna articulates with the radial condyle and the radius articulates with the ulnar condyle, with the palm facing posteriorly. Others are reconstructed so that the ulna articulates with the ulnar condyle and the radius with the radial condyle, with the palm facing posteromedially. Senter [77] examined the forelimbs of hadrosaurids and concluded that the latter reconstruction is correct. Following his study, I use his direction terms accordingly.

Among size class 1 specimens, the ulna (Figure 2-37A-D) is nearly equal to or slightly longer than the mean length of size class 1 humeri. The proximal border of the medial process is at nearly a right angle to the shaft of the ulna as seen in proximal view. Similar to other saurolophines, the lateral process is smaller than the medial process of the ulna. The olecranon process ridge is proportionally well developed in smaller specimens. Because of this, the juvenile ulnae of the Alaskan edmontosaur appear more

robust than ulnae of other adult *Edmontosaurus* specimens (see Chapter 1). In contrast, with respect to diaphyseal width, PCF juvenile ulnae are more gracile than those of adult *E. annectens*, and in this way they are similar to those of adult *E. regalis*. However, the diaphyseal width of the Alaskan edmontosaur shows positive allometric growth relative to length, and therefore the adult status of the Alaskan edmontosaur is expected to be more similar to *E. annectens* than to *E. regalis* (see Chapter 1). The distal condyle of the ulna is anteroposteriorly broad, resulting in the characteristic convex curve on the posterior outline. However, the distal condyle shows some expansion, unlike in *E. regalis* (CMN 2289) and cf. *Saurolophus* (AMNH 5271). The distal radial facet is located anteromedially and is marked with longitudinally elongate ridges.

2.3.6.6 Radius

The radius (Figure 2-37E, F) of the PCF specimen is robust compared to other saurolophines, as a result of its much-expanded proximal and distal ends. The robustness of the ulna and radius is likely attributable to immaturity, as has been reported in *Hypacrosaurus stebingeri* (MOR 548 [54]). The proximal end expands abruptly mediolaterally, resulting in a shape similar to the head of a nail in anterior or posterior views. The proximal end is egg-shaped in articular view. *Brachylophosaurus canadensis* (MOR 1071 7-15-98-217) and *Kundurosaurus nagornyi* (AENM 2/904) have a keel on the posterior surface where it faces the ulna [49,70]), but such a keel is very weakly developed or non-existent in the PCF material. The distal end expands gradually, both mediolaterally and to a lesser degree anteroposteriorly. On the posterolateral side of the distal end, the radius articulates with the ulna, where it has a slightly depressed surface with sub-parallel ridges and grooves. Medial to the depression is a small ridge that delineates the depression. In distal view, the radius is semi-square-shaped.

2.3.6.7 Metacarpals

Based on the reconstruction of hadrosaurid forelimbs by Senter [77], the palms of the manus are interpreted to face posteromedially. Hence, the dorsal side of the mani would face anterolaterally, and digit II would be located more anteromedially than digit

V. Thus, the term “dorsal” is used to mean anterolateral, and “ventral” to mean posteromedial.

Metacarpal II (Figure 2-38A, B) is mediolaterally flat. The proximal half is medially convex and laterally concave where it contacts with metacarpal III. Distally, both dorsal and ventral surfaces are rather flat. It expands dorsocaudally at the distal and proximal ends, unlike in *Edmontosaurus regalis* (CMN 2289).

Metacarpal III (Figure 2-38C-E, J, K) is triangular in proximal view and keystone-shaped in distal view. There are parallel ridges on both the medial and lateral surfaces where it contacts metacarpal II and IV, respectively. Ventrally, there is a deeper groove, probably for flexor musculature. Metacarpal III is much more robust than that of other saurolophines, as the ratio of length to mediolateral width at mid-shaft is 7 for both a size class 3 specimen (UAMES 16215) and size class 1 specimens. In contrast, this value ranges from 8 to 9 in most saurolophines [42,60]. No obvious ontogenetic change (besides an increase in overall size) is observed between size classes 1 and 3.

Metacarpal IV (Figure 2-38F, G) is nearly as large as metacarpal III. Its proximal end expands mediolaterally, and its distal end expands dorsoventrally. The medial surface is flat except for the distal and proximal regions, where it articulates with metacarpal III, which is marked by the presence of parallel ridges. Most of the distal end of the metacarpal is reflected laterally.

Metacarpal V shows considerable variation in overall morphology. In the smallest specimen (UAMES 16733, Figure 2-38H), its proximal half is considerably expanded mediolaterally compared to its distal end. The larger specimens (UAMES 29662, UAMES 13230, UAMES 29676, Figure 2-38I) are more typical of Hadrosauridae; proximally they are nearly as wide as it is tall, and the distal part is also relatively wide. Distally they narrows dorsoventrally, but only gradually, unlike in the small specimen (UAMES 16733). While this difference in morphology is likely due to ontogenetic variation, it is also possible that UAMES 16733 may belong to another ornithopod taxon

or be aberrant.

2.3.6.8 Ilium

The preacetabular process (Figure 2-39) is moderately deflected ventrally relative to the main body of the ilium (about 30°). The anterior end of the process is not preserved, and therefore the presence of an anterior thickening, such at that seen in *Brachylophosaurus canadensis* (MOR 1071 8-2-98-487 and MOR 794 [70]) is unknown. The process is dorsally buttressed by a lateral dorsal ridge and medial dorsal shelf. Laterally, the dorsal ridge extends between the anterior portion of the preacetabular process (where it merges to the main body of the preacetabular process) and the suprailiac crest, similar to other species of *Edmontosaurus* (*E. regalis*, ROM 867; *E. annectens*, AMNH 5730, YPM 2182, TMNH 00001). However, in some specimens of *Edmontosaurus* (*E. regalis*, CMN 2289, CMN 8399; *E. annectens,* DMNH 1493) this ridge begins near the posterior portion of the process, showing there is variation in this feature. The medial dorsal shelf projects medially more than the lateral dorsal ridge projects laterally. The medial dorsal shelf extends from the anterior half of the preacetabular process anteriorly to the proximal half of the postacetabular process posteriorly. This differs from some saurolophines, such as *B. canadensis* (MOR 1071 8-2-98-487) and *Kritosaurus* sp. (YPM PU 16970) in which the ridge is shorter posteriorly. The medial border of the medial dorsal shelf is located only slightly ventrally to the dorsal border of the preacetabular process, unlike in *E. regalis* (CMN 2288) in which the shelf occurs considerably more ventrally. This difference is also seen in juvenile and adult *B. canadensis* (MOR 1071 8-2-98-487) and juvenile (MOR 547) and adult (ROM 44770) *Maiasaura peeblesorum*, although in these genera the shelves of the adult specimens are more dorsally positioned than in the juveniles. Therefore, this feature may not be systematically and ontogenetically informative. The ventral surface of the shelf is smooth and shows little sign of articulation with the sacrum in the Alaskan edmontosaur, unlike in cf. *Kritosaurus* (YPM PU 16970). The pubic peduncle is stout and triangular in shape, unlike the more slender pubic peduncle in *Gryposaurus notabilis* (ROM 4514) and *M. peeblesorum* (MOR 1071). The suprailiac crest is less developed than that of most

other saurolophines, with the dorsoventral depth being only around 25 % of the depth of the ilial body. The ventrolateral border of the suprailiac crest is broadly U-shaped in lateral view. In line with the anterior end of the suprailiac crest, the ventral border is expanded to form the ischial peduncle. The dorsal border above the suprailiac crest and postacetabular process is weakly concave, as in most species of *Edmontosaurus*, except CMN 2289 (*E. regalis*), in which the concavity is stronger. The ventrolateral acetabular margin is smooth, unlike in most adult specimens of other species of *Edmontosaurus*, in which the ventral acetabular surface and the lateral surface of the ilium body are clearly divided by a well defined edge. The postacetabular process is only slightly shallower dorsoventrally than the main body of the ilium. The presence of a deep postacetabular process is also observed in some specimens of *E. annectens* (TMNH 000001, AMNH 5730) but contrasts with the shallow postacetabular process in others (CMN 2288, YPM 2182). The postacetabular process lies in the same vertical parasagittal plane with the main body of the ilium and without the dorsomedial twist seen in *Secernosaurus koerneri* (MACN-RN 2 [65]) and some lambeosaurines [42,60]. The posterodorsal region of the process is indented, as seen in *Shantungosaurus giganteus* (GMV V.1780 [59])*, E. regalis*, (CMN 2288), *E. annectens* (TMNH 00001), and *Prosaurolophus maximus* (ROM 787). Medial to the indentation is a ridge that presumably receives the transverse processes of the sacrum.

2.3.6.9 Pubis

The pubis (Figure 2-40) is very fragile and undamaged specimens are not known from the LBB. Even the most complete PCF specimen (UAMES 22058) has an abraded anterior part of the prepubic blade, and thus its exact shape is not clear. The prepubic neck is weakly constricted. The dorsoventral depth at its neck is deeper than in other *Edmontosaurus* species and is longer than that of *E. regalis* (see Chapter 1). The iliac peduncle is at least 40 % taller than it is wide, unlike other species of *Edmontosaurus* (e.g., *E. regalis*, CMN 2289, 8399; *E. annectens,* DMNH 1493) but similar to the condition observed in some saurolophines (e.g., *Acristavus gagslarsoni*, MOR 1155; *Prosaurolophus maximus*, ROM 787; *Brachylophosaurus canadensis*, MOR 1071). The

iliac peduncle is twisted 45° relative to the main body. The posterior border of the iliac peduncle shows a slight expansion in a better-preserved specimen (UAMES 6677). A similar expansion is also seen in *E. annectens* (AMNH 5730), *Kundurosaurus manakini* (AENM 2/922-5L), cf. *Kritosaurus* (AMNH 5465), juvenile *Maiasaura peeblesorum* (MOR 547) and *P. maximus* (TMP 83.64.3). The ischial peduncle is offset laterally relative to the postpubic process (postpubic rod of Godefroit et al., 2012), similar to other species of *Edmontosaurus* (CMN 2288, ROM 801, AMNH 5730) and *K. manakini* (AENM 2/922-5L). The cross-sectional shape of the ischial peduncle is similar to a narrow isosceles triangle, being ventrally wide and dorsally narrow. In UAMES 13683, the ischial peduncle is swollen proximally and tapers distally to some degree. In UAMES 22885 and 22058, such a bulge is absent. The postpubic process varies from straight (UAMES 6677) to dorsally curved (UAMES 13687, UAMES 22058). Because all specimens are damaged to some extent, it is not possible to establish whether this variation is due to polymorphism or is just a taphonomic artifact.

2.3.6.10 Ischium

The acetabular border of the ischium (Figure 2-41) is longer and dorsoventrally deeper than in other species of *Edmontosaurus* (*E. regalis,* CMN 2289; *E. annectens,* CMN 8509, YPM 2128, and AMNH 5730 [74]). The dorsal border of the pubic peduncle is located slightly more dorsally to the border of the proximal part of the ischium shaft. Because the anteroventral border of the pubic peduncle is not preserved, the exact height cannot be determined. The iliac peduncle is mediolaterally thicker than the pubic peduncle. Near its dorsal end, the iliac peduncle gradually expands mediolaterally, but it expands little posteriorly, resulting in a somewhat square shape in lateral view. The dorsal border of the iliac peduncle is broadly rounded and tilted anteriorly in the parasagittal plane. A large portion of the obturator process is missing. On the proximal portion of the dorsal surface on the ischial shaft is a shallow groove, and the shaft narrows ventrally, resulting in a cordiform cross section. Distally, the shaft curves gently dorsally, slightly more strongly than it does in *E. regalis* (CMN 2288) and *Kundurosaurus nagornyi* (AENM 2/922- 3L [49]). The Alaskan edmontosaur also differs

from *E. annectens* in that the shaft is nearly straight (CMN 8509 and AMNH 5730 [74]). The distal end of the ischium shaft is not preserved in any PCF specimen.

2.3.6.11 Femur

The hindlimb of the juvenile Alaskan edmontosaur is relatively long compared to that of other specimens of *Edmontosaurus*, but not significantly. The femur/humerus ratio is higher than other species of *Edmontosaurus*, but it is still within the 2 sigma range of other *Edmontosaurus* species. The femur/tibia ratio is close to the average ratio for other *Edmontosaurus* specimens (table 2).

The depression between the femoral head and the greater trochanter in anterior view is shallower in other species of *Edmontosaurus* (*E. regalis*, CMN 2289; *E. annectens,* AMNH 5730), including the Alaskan edmontosaur (Figure 2-42), and in *Shantungosaurus giganteus* (GMV 1780 [59]), compared to the depression seen in the femurs of brachylophosaurines specimens (juvenile *Maiasaura peeblesorum*, MOR 547; subadult *Prosaurolophus maximus,* MOR 454; *Brachylophosaurus canadensis,* MOR 1071 8-1-99-327). The femoral shaft of the Alaskan edmontosaur is subcylindrical and mediolaterally wider than anteroposteriorly broad. As in the depression between the femoral head and the greater trochanter, the femoral shaft of the *Edmontosaurus* specimens and *S. giganteus* is more robust than those of brachylophosaurines. The fourth trochanter in the Alaskan edmontosaur is proximodistally slightly less expanded and dorsoventrally low compared to adult saurolophines (e.g., CMN 2289). Like other juvenile hadrosaurid specimens [53,74], the fourth trochanter of the PCF material is anteroposteriorly relatively short compared to that of adult femora (*E. regalis*, CMN 2288; *E. annectens*, TMNH00001). On the medial side of the trochanter is a well-defined muscle scar. The anterior outline of the distal portion of the femur is nearly straight, as the medial and lateral condyles do not expand much anteriorly. The medial condyle is larger than the lateral condyle, especially mediolaterally. The lateral surface of the lateral condyle is uneven; the posterior half of the lateral condyle is mediolaterally thinner than the anterior half, resulting in an abrupt step between each half. This is a common

character in other saurolophines (e.g., *E. regalis,* CMN 2289; *S. giganteus*, GMV 1780; *B. canadensis*, MOR 1071). The medial and lateral condyles are anteroposteriorly less developed than most specimens of adult *Edmontosaurus* (*E. regalis,* CMN 2289, CMN 8399; *E. annectens,* CMN 8509) but are comparable to size class 2 of *E. annectens* (LACM 23504), indicating this is an ontogenetically variable character.

2.3.6.12 Tibia

The tibia (Figure 2-43) is more robust, in terms of the relative expansion of the proximal and distal ends compared to length, than for most saurolophines, although it is as robust as *Saurolophus* sp. (AMNH 5271), *Shantungosaurus giganteus* (GMV V.1780 [59]), and *Edmontosaurus regalis* (ROM 801). The lateral condyle is more closely located to the medial condyle than it is to the cnemial crest. The medial condyle is proximodistally and anteroposteriorly larger than the lateral condyle. The cnemial crest is triangular in lateral and medial views and anteroposteriorly thinner than the medial and lateral condyles. The distal end of the tibia is rotated 45 degrees counterclockwise relative to the proximal part. The lateral malleolus extends posteromedially, while the medial malleolus extends anteriodistally. In distal view, the lateral and medial malleoli form an angle of about 140°, producing a concave surface distally that faces medially. The lateral malleolus is generally more robust than the medial malleolus.

2.3.6.13 Fibula

In the Alaskan edmontosaur, the anterior border of the fibula head (Figure 2-44) shows more sudden expansion than in the other known saurolophines (*Saurolophus* sp., AMNH 5721; *Brachylophosaurus canadensis*, MOR 1071 7-23-98-374; *Acristavus gagslarsoni*, MOR 1155; *Shantungosaurus giganteus*, GMV 1780 [59]). In contrast, the posterior border of the fibular head in the Alaskan edmontosaur is less expanded from its narrowest portion, one-third of the way from the distal end. The lateral malleolus expands more gradually than the “club”-like expansion seen in *B. canadensis* (MOR 1071 7-23-98-374), *A. gagslarsoni* (MOR 1155) and *S. giganteus* (GMV 1780, [59]). As a result, the distal one-fifth of the fibula, where the distal tibiofibular joint surface is located, is more

massive than other adult saurolophines.

2.3.6.14 Astragalus

The astragalus (Figure 2-45) covers two-thirds of the distal articular facet of the tibia. It is plate-shaped with an anterior ascending process that projects from its anteromedial edge. The anterior ascending process is concave anteriorly and convex posteriorly. Contrary to Brett-Surman and Wagner [74], who found that the ascending process of juvenile hadrosaurs is high and triangular, the process of a size class 1 specimen of the PCF taxon is relatively just as high and triangular as that of adult *Edmontosaurus regalis* (CMN 2288) but less so than that of adult *Brachylophosaurus canadensis* (MOR 1071) or *Saurolophus* sp. (AMNH 5271). The medial half of the astragalus covers the medial malleolus of the tibia. In medial view, the medial margin is dorsally concave and ventrally convex. The astragalus is thickest at the medial margin. The lateral margin of the astragalus is thin where it articulates with the thickest point of the medial malleolus of the tibia. The lateral border of the astragalus has a slight indentation where it articulates with the calcaneum.

2.3.6.15 Calcaneum

The taxonomic significance of the calcaneum has seldom been discussed, except for the possible loss of this element in *Parasaurolophus cyrtocristatus* [74,78]. However, the calcaneum of the PCF material (Figure 2-46) shows some differences from other saurolophines. In a size class 1 calcaneum (UAMES 21884), the tibial and fibular articular facets are nearly equal in size (see Chapter 1). This is also likely true in size class 3 (UAMES 18059) specimens. In all saurolophine specimens (*Edmontosaurus annectens*, CMN 8509; *Brachylophosaurus canadensis*, MOR 1071; cf. *Saurolophus*, AMNH 5271), the fibular articulation facets are larger than the tibia articulation surface. The PCF size class 1 materials also differ from other saurolophine taxa in that the distal articular surface is mediolaterally much narrower. However, whether these differences are attributable to ontogenetic change is not certain.

Specimens of size class 1 (UAMES 21884) and 3 (UAMES 18059) of the

Alaskan edmontosaur show certain differences. The astragalar articulation surface is smoother in the size class 1 specimen than in the size the class 3 specimen. Also, in size class 1, the tibial and fibular surfaces are less deeply concave (see Chapter 1). Shallowly concave articular surfaces are also seen in juvenile specimens of *Bactrosaurus johnsoni* [79] and therefore are attributable to ontogenic variation (See Chapter 1).

2.3.6.16 Metatarsals

All metatarsals of the Alaskan edmontosaur and adult *Edmontosaurus* are stouter than those of other adult saurolophines. Generally, metatarsal III is the largest, and metatarsal II is thinner than metatarsal IV.

Metatarsal II – The proximal end of metatarsal II (Figure 2-47A-D) is mediolaterally flattened and rhomboid in proximal view. Its proximal half is fan-shaped in lateral view and splayed proximally so that its proximal end is anteroposteriorly much wider than the distal half. The distal half of metatarsal II is anteroposteriorly narrower, but mediolaterally thicker than the proximal half. This morphology contrasts with that of brachylophosaurines (*Brachylophosaurus canadensis*, MOR 1071; *Maiasaura peeblesorum*, ROM 44770, YPM-PU 22400; *Acristavus gagslarsoni*, MOR 1155), in which the proximal half of metatarsal II is relatively less expanded anteroposteriorly, and therefore the whole metatarsal II looks relatively elongated. Mediolaterally, metatarsal II of the Alaskan edmontosaur is thicker than that of other saurolophines (*Edmontosaurus regalis*, CMN 2289; *Maiasaura peeblesorum*, ROM 44770; *Acristavus gagslarsoni*, MOR 1155) but thinner than metatarsal III. In *Bactrosaurus johnsoni*, the dorsomedial flange enlarges during growth [53], but in the PCF taxon, the flange is as well developed as it is in other adult saurolophines. It appears that the development of the dorsomedial flange is not ontogenetically variable in saurolophines, because the flange in a juvenile *Brachylophosaurus canadensis* (MOR 1071) and subadult *Prosaurolophus* sp. (MOR 454) is equally developed compared to adult *B. canadensis* and *Prosaurolophus maximus* (MOR 1071, MOR 447). The distal part of metatarsal II, however, is relatively more developed in larger individuals, as a size class 2 specimen of the Alaskan edmontosaur

(UAMES 13012, Figure 2-49C, D) and adult *E. regalis* (CMN 2889) have progressively more developed distal ends than size class 1 specimens of the PCF taxa.

Metatarsal III – The medial surface of metatarsal III (Figure 2-47E-H) is concave where it articulates with metatarsal II. Posteromedially, metatarsal III has a well-developed ventromedial flange. Specimens of metatarsal III from size class 1 (Figure 2-47E, F) are stouter than those of many saurolophines (e.g., *Maiasaura peeblesorum*, ROM 44770; *Acristavus gagslarsoni*, MOR 1155). Size class 2 specimens (Figure 2-47G, H) are even more robust, indicating positive allometric growth in metatarsal width (see Chapter 1). Metatarsal III of *Edmontosaurus* (*E. regalis,* CMN 2289; *Edmontosaurus*. Sp., CMN 21922) is as robust as that of the Alaskan edmontosaur.

Metatarsal IV–Compared to metatarsal II, metatarsal IV (Figure 2-47I-N) is more robust and mediolaterally thicker, and the proximal part of metatarsal IV is anteroposteriorly narrower. From the LBB, specimens of size classes 1 to 3 are known. They do not show notable differences in proportions, except that in size class 3 specimens the medial tuberosity is more pronounced and the dorsal surface is more strongly concave than in size class 1 and 2 specimens (see Chapter 1).

2.4 Discussion

2.4.1 Biogeography of *Edmontosaurus*

In Chapter 1, I conducted a cladistic analysis both including and excluding potentially ontogenetically variable characters to determine the phylogenetic position of the new Alaskan edmontosaur. In the resulting cladograms, the Alaskan edmontosaur was consistently recovered as the sister taxon of *Edmontosaurus regalis* + *E. annectens* (Figure 2-48). Assuming this reflects the actual relationships among the species of *Edmontosaurus* and it is not biased by juvenile status, then this pattern is not wholly congruent with the stratigraphic distribution of species; the geologically oldest member of the genus, *E. regalis*, is late Campanian in age and *E. annectens* is late Maastrichtian, while the Alaskan edmontosaur is early Maastrichtian in age. However, it should be

noted that definitive, late Campanian dinosaur remains are currently not recognized on the North Slope of Alaska, so the complete stratigraphic range of the Alaskan edmontosaur is uncertain.

While the geographic range of edmontosaurs is restricted to Laramidia, basal, successive sister taxa, *Shantungosaurus* and *Kundurosaurus*, are known from eastern Eurasia. A close phylogenetic relationship between *Edmontosaurus* and *Kundurosaurus* was also recovered in the cladistics analysis by Godefroit [49]. These taxa are known from Late Campanian to Maastrichtian formations. *Shantungosaurus* is known from Late Campanian-aged rocks from Chuncheng, Shantung, China [59,80]. While the age of *Kundurosaurus* is not well constrained, it is possibly from late Maastrichtian-aged rocks of Kundur, Amur Region, far eastern Russia [49]. Thus, the two genera overlap in temporal distribution with *Edmontosaurus*. Combining stratigraphic and phylogenetic data suggests a possible biogeographic scenario in which the common ancestor of *Edmontosaurus* and *Shantungosaurus* originated in eastern Eurasia and then dispersed to North America by the Campanian via a land corridor in the area of present day Alaska. This corridor is commonly known as Beringia in Quaternary studies, and this concept has also been applied to the Cretaceous [34], although the timing of connectivity between the two landmasses is poorly constrained. A similar dispersion pattern has been proposed for other dinosaurian clades at various classification levels, such as Lambeosaurinae, Hadrosauria, Ceratopsia, Ceratopsidae, and Tyrannosauridae [60,81-83]. With respect to edmontosaurs, the Alaskan taxon or its immediate ancestor radiated in polar regions of Laramidia by the late Campanian, while *E. regalis* and *E. annectens* later diverged and occupied more southerly regions of North America. However, because the Alaskan edmontosaur was not recovered as the sister taxon to *E. annectens*, it does not support the idea of a single anagenetic lineage among all three recognized species of *Edmontosaurus*, as has been proposed by Horner et al. [68] for other Late Cretaceous ornithischians, such as *Hypacrosaurus* and *Pachyrhinosaurus*. This biogeographic scenario presented here can be falsified by discovery of additional adult Alaskan edmontosaur specimens providing new morphological data about the species that could change our understanding

of its phylogenetic position among Edmontosaurini.

2.4.2 Paaŋaqtat Province

The existence of a distinct, early Maastrichtian polar fauna, provisionally termed the Paaŋaqtat Province, has been proposed for the Prince Creek Formation [12,15]. The fauna is characterized by polar dinosaurian species that are either unique and endemic to the Prince Creek Formation, such as the pachycephalosaurid *Alaskacephale gangloffi* [7,8] and the centrosaurine ceratopsid *Pachyrhinosaurus perotorum* [13], orodromine and thescelosaurine thescelosaurids that cannot be referred to any currently described species from more southerly latitudes [15], a large-toothed species of *Troodon*, and potentially other theropod taxa [15]. In their descriptive paper on *P. perotorum*, Fiorillo and Tykoski [13] pointed out that the existence of *P. perotorum* cannot be considered strong evidence of a unique fauna in Alaska, as *P. perotorum* may represent a species on a lineage of other *Pachyrhinosaurus*. At any given time in the Campanian-Maastrichtian, there may have been a single species of *Pachyrhinosaurus* across northern and southern Laramidia. Such an argument, however, is not valid for *Edmontosaurus*. Although the Alaskan edmontosaur does not overlap in age with *E. annectens* and *E. regalis*, the pattern of relationships among species of *Edmontosaurus* falsifies the hypothesis of anagenetic evolution, whereby the Alaskan taxon originated from *E. regalis.* Thus, the most parsimonious explanation for the available evidence is that the Alaskan taxon originated and existed only in high latitude environments of Laramidia. It also suggests that the Alaskan taxon (or its unknown immediate ancestor) and *E. regalis* could have co-existed temporally, but not geographically, given that only *Edmontosaurus regalis* is known from Campanian-aged rocks of Alberta. A further test of this hypothesis could theoretically be based on the discovery and taxonomic assignment of other edmontosaur remains from Campanian-aged sediment of polar environments in Laramidia. Therefore, recognition of a new species from a separate lineage of *Edmontosaurus* from the Prince Creek Formation lends further support for the Paaŋaqtat Province.

2.5 Acknowledgements

This work was supported in part by an NSF award (EAR 1226730 to P. Druckenmiller and G. Erickson), the Geist Scholarship Fund (University of Alaska Museum), and the University of Alaska Fairbanks Graduate School. I kindly acknowledge the help of the Bureau of Land Management Arctic Field Office, particularly Mike Kunz, for logistical support in the excavation of the Alaskan material. I appreciate my graduate committee members, Patrick S. Druckenmiller, Sarah Fowell, Kris Hundertmark, and Matthew Wooller for their support. I thank Kevin May, Roland Gangloff, and the field crews who collected the specimens over many field seasons. I thank David Evans and Nicolás Campione for providing photos of *Edmontosaurus*, and Ron Blakey, Kieran Shepherd, Margaret Beckel, Kevin Seymour, Jack Horner, Alana Gihlick, Carl Mehling Dan Brinkman, and Hiroaki Kikkawa for their help in observing specimens housed in the museums. I also thank H. David Sheet, Daniel Falster, Davit Warton, Ian Wright, and Pablo A. Goloboff, James S. Farris, Kevin Nixon, and Willi Henning Society for their software (Coordgen, MorphoJ, SMATR, TNT).

2.6 Figures

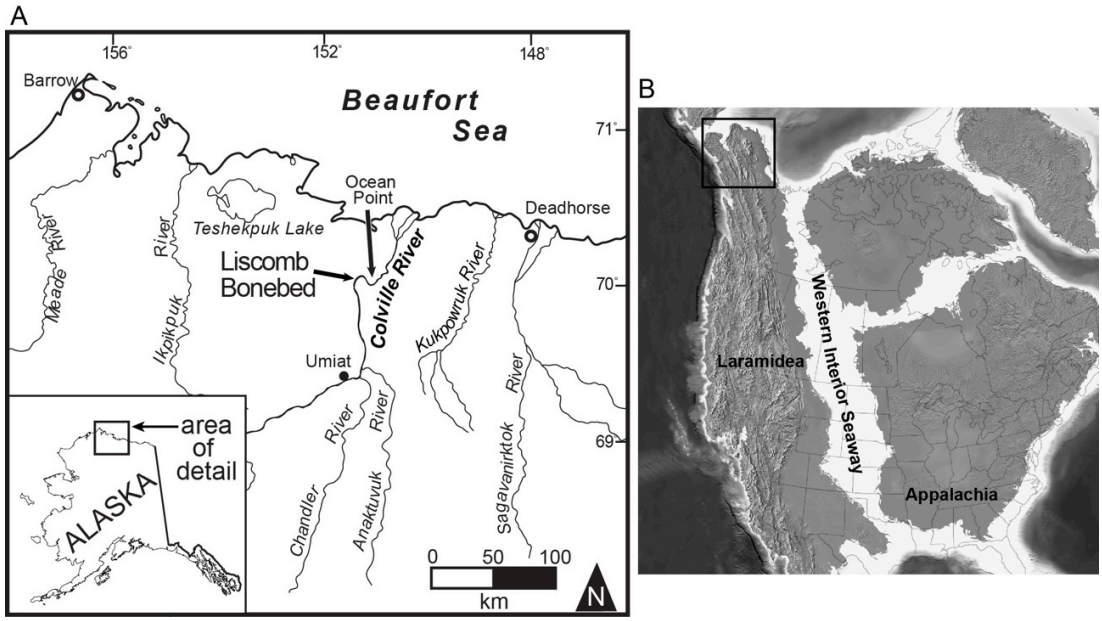

Figure 2-1. (A) Location of the Liscomb Bonebed, and (B) paleogeographic reconstruction map of North America at 70 Ma [84]. The inset box indicates the location of present-day Alaska.

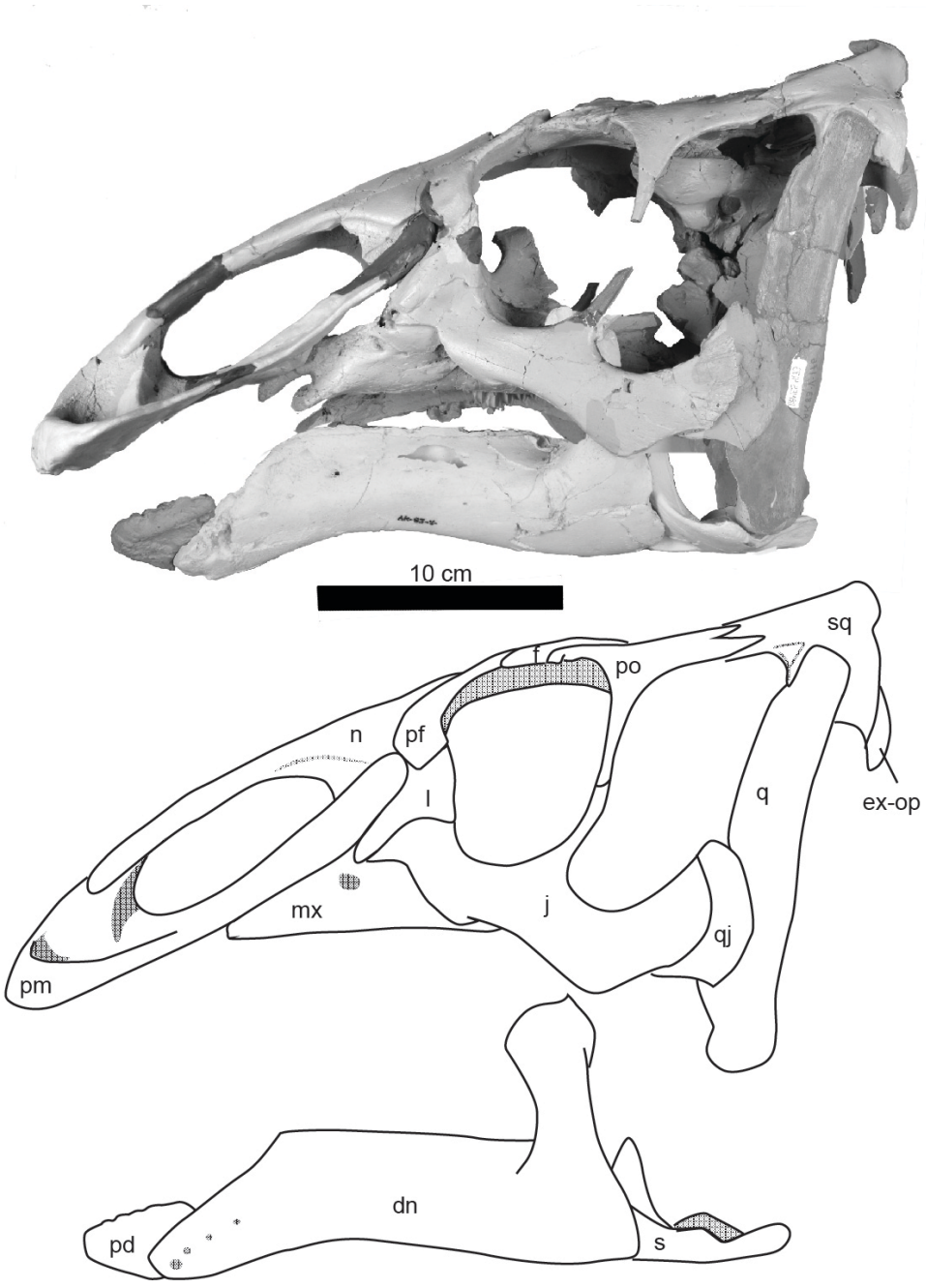

Figure 2-2. Composite cranial reconstruction of *Edmontosaurus* sp. nov. in left lateral view.

Figure 2-3 (facing page). Premaxilla. Composite images of right premaxillae (UAMES 4283, UAMES 12995) of size class 1 *Edmontosaurus* sp. nov. in lateral (A), dorsal (B), medial (C), and ventral views (D). Premaxilla (UAMES 12995) of size class 1 *Edmontosaurus* sp. nov. in anterior (E) and posterior views (G). Premaxilla (UAMES 4955) of size class 1 *Edmontosaurus* sp. nov. in posterior view (F). Premaxilla (UAMES 4184) of size class 2 *Edmontosaurus* sp. nov. in lateral (H) and medial (I) views. Abbreviations: adpf, anterodorsal premaxillary foramen; apc, anterior premaxillary cavity; apf, accessory premaxillary foramen; cnd, circumnarial depression; cns, cirucmnarial septum; pdpf, posterodorsal premaxillary foramen; ppdp, posterodorsal process; pplp, posterolateral process; pmfg, premaxillary foramen groove; vpf, ventra premaxillary foramen.

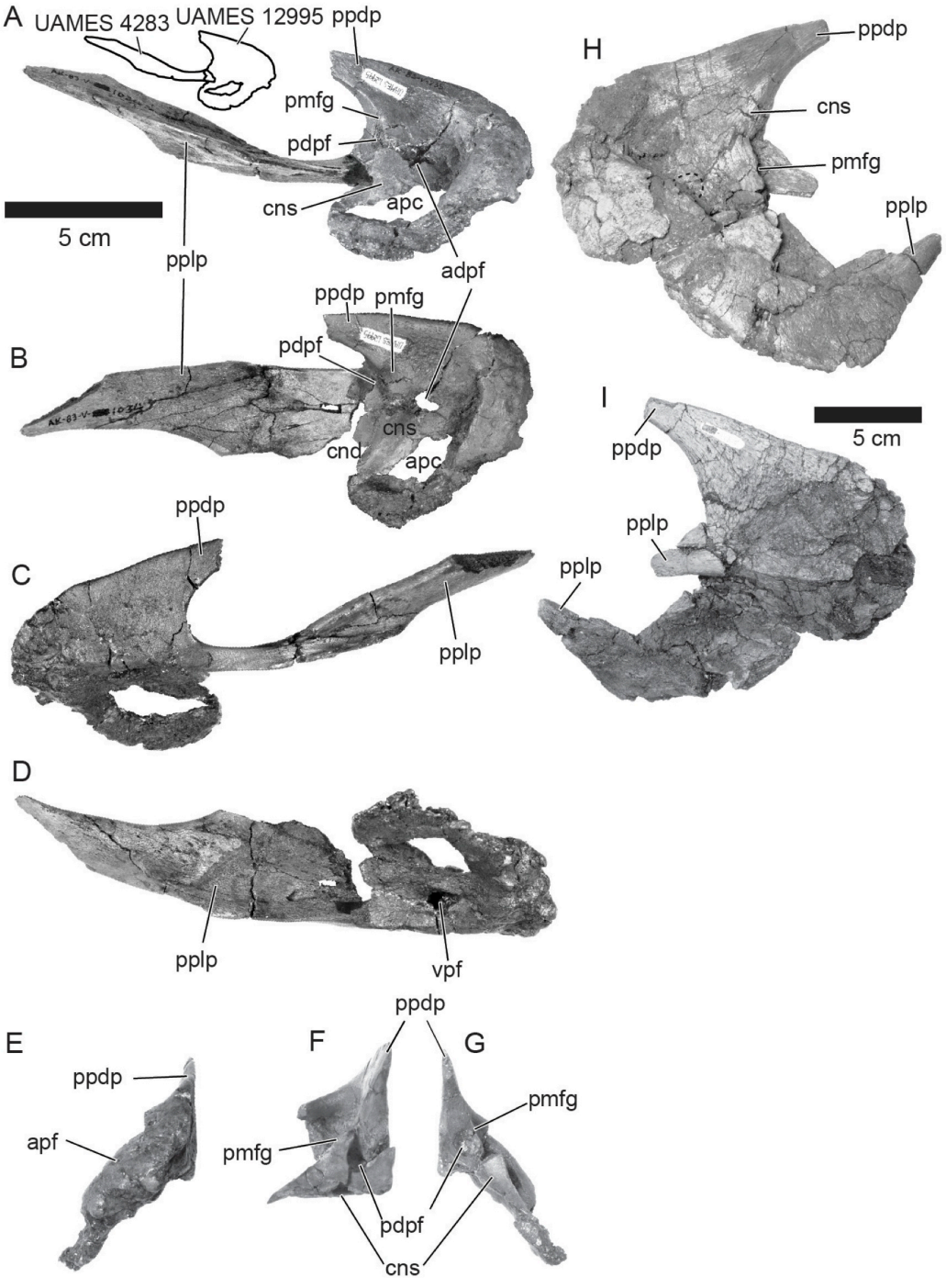
A
UAMES 4283
UAMES 12995
ppdp
pmfg
pdpf
cns
apc
5 cm
pplp
adpf
B
ppdp
pmfg
pdpf
cns
cnd
apc
C
ppdp
pplp
D
pplp
vpf
E
ppdp
apf
F
ppdp
pmfg
pdpf
cns
G
pmfg
H
ppdp
cns
pmfg
pplp
I
5 cm
ppdp
pplp
pplp

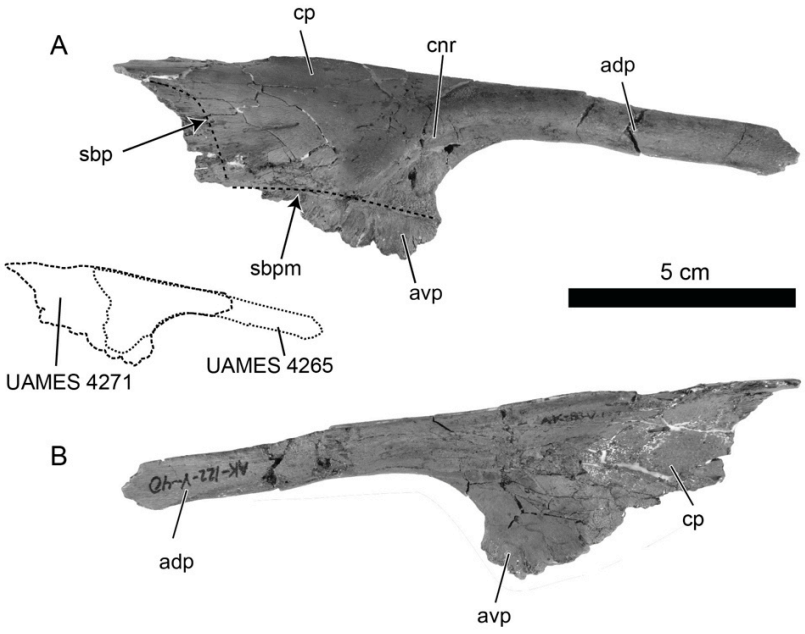

Figure 2-4. Nasal. Composite images of right nasals (UAMES 4271 and UAMES 4265) of size class 1 *Edmontosaurus* sp. nov. in lateral (A) and medial (B) views. Abbreviations: cnr, circumnarial ridge; cp, caudal plate; adp, anterodorsal process; avp, anteroventral process; sbp, sutural boundary for prefrontal; sbpm, sutural boundary for premaxilla.

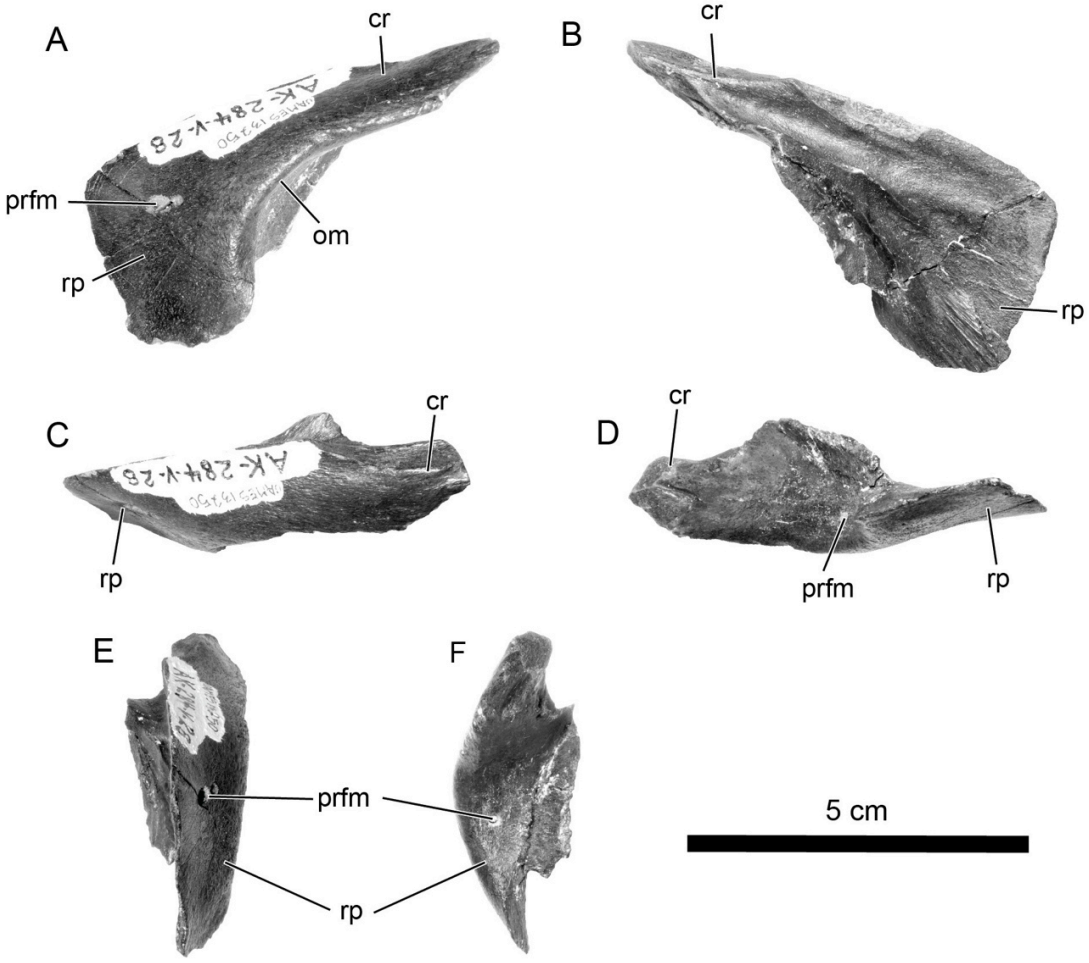

Figure 2-5. Prefrontal. Left prefrontal (UAMES 13250) of size class 1 *Edmontosaurus* sp. nov. in lateral (A), medial (B), dorsal (C), ventral (D), anterior (E) and posterior (F) views. Abbreviations: rp, rostral plate; cr, caudal ramus; om, orbital margin; prfm, prefrontal foramen; rp, rostral plate.

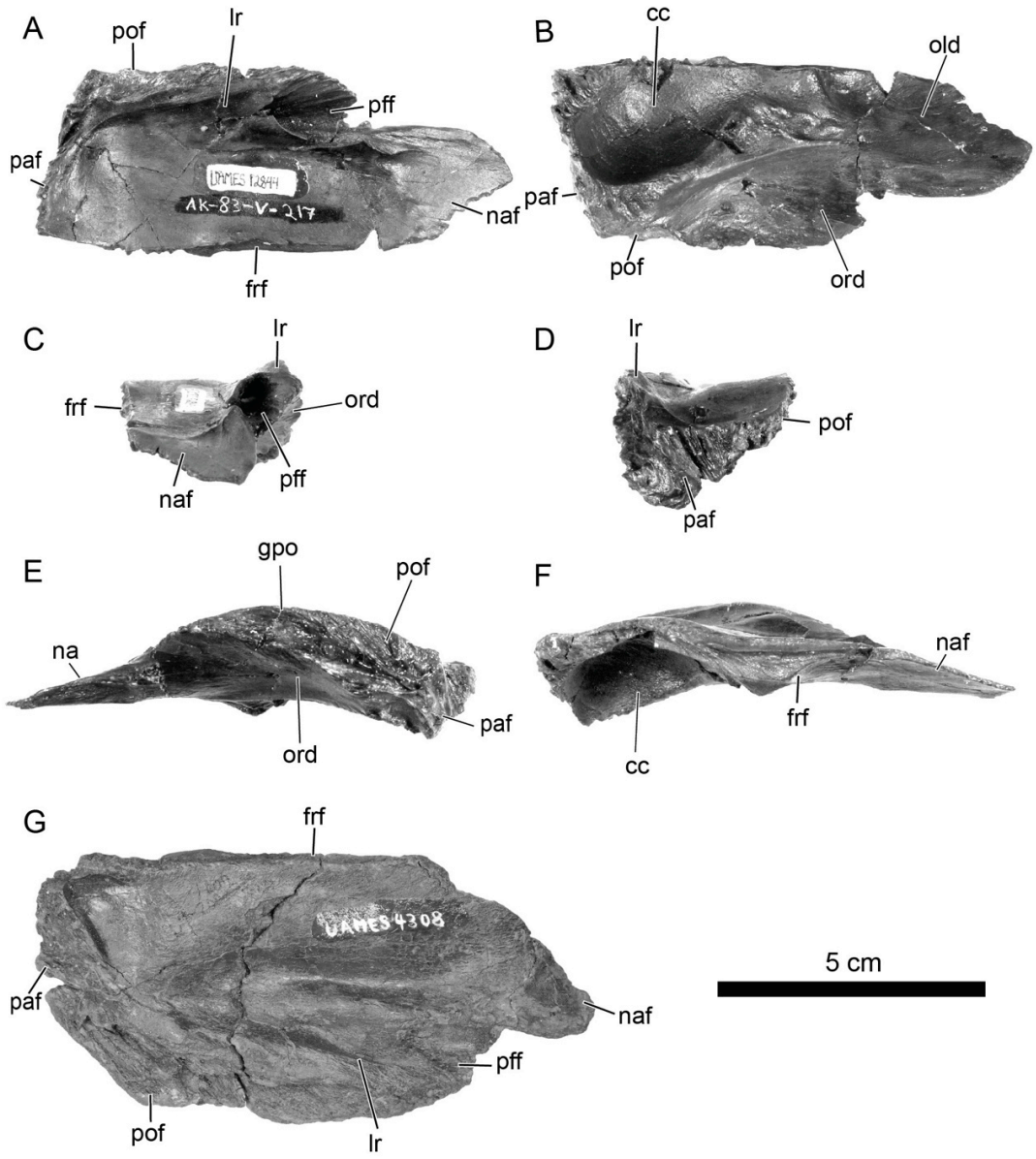

Figure 2-6. Frontal. Left frontal (UAMES 12844) of size class 1 *Edmontosaurus* sp. nov. in dorsal (A), ventral (B), anterior (C), posterior (D), lateral (E), and medial (F) views. Right frontal (UAMES 4308) of size class 3 *Edmontosaurus* sp. nov. in dorsal view (G). Abbreviations: cc, cerebral cavity; frf, frontal facet; lr, lateral ridge; old, olfactory depression; ord, orbital depression; gpo, groove for postorbital; naf facet, nasal facet; paf, parietal facet; pof, postorbital facet; pff, prefrontal facet.

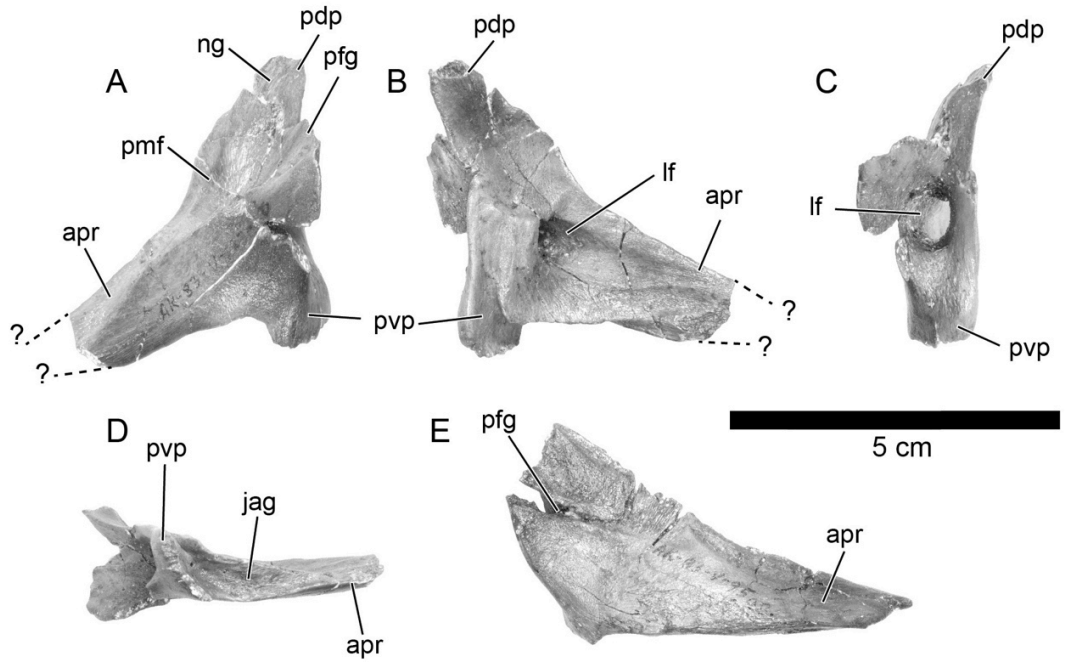

Figure 2-7. Lacrimal. Left lacrimal (UAMES 4245) of size class 1 *Edmontosaurus* sp. nov. in lateral (A), medial (B), posterior (C), and ventral (D) views. Right lacrimal with a narrow jugal articulation groove (UAMES4254, reversed) of size class 1 *Edmontosaurus* sp. nov. in lateral view (E). Abbreviations: apr, anterior process; jag, jugal articulation groove; lf, lacrimal foramen; ng, nasal groove; pfg, prefrontal groove, pdp; posterodorsal process; pmf, premaxilary facet; pvp, posteroventral process.

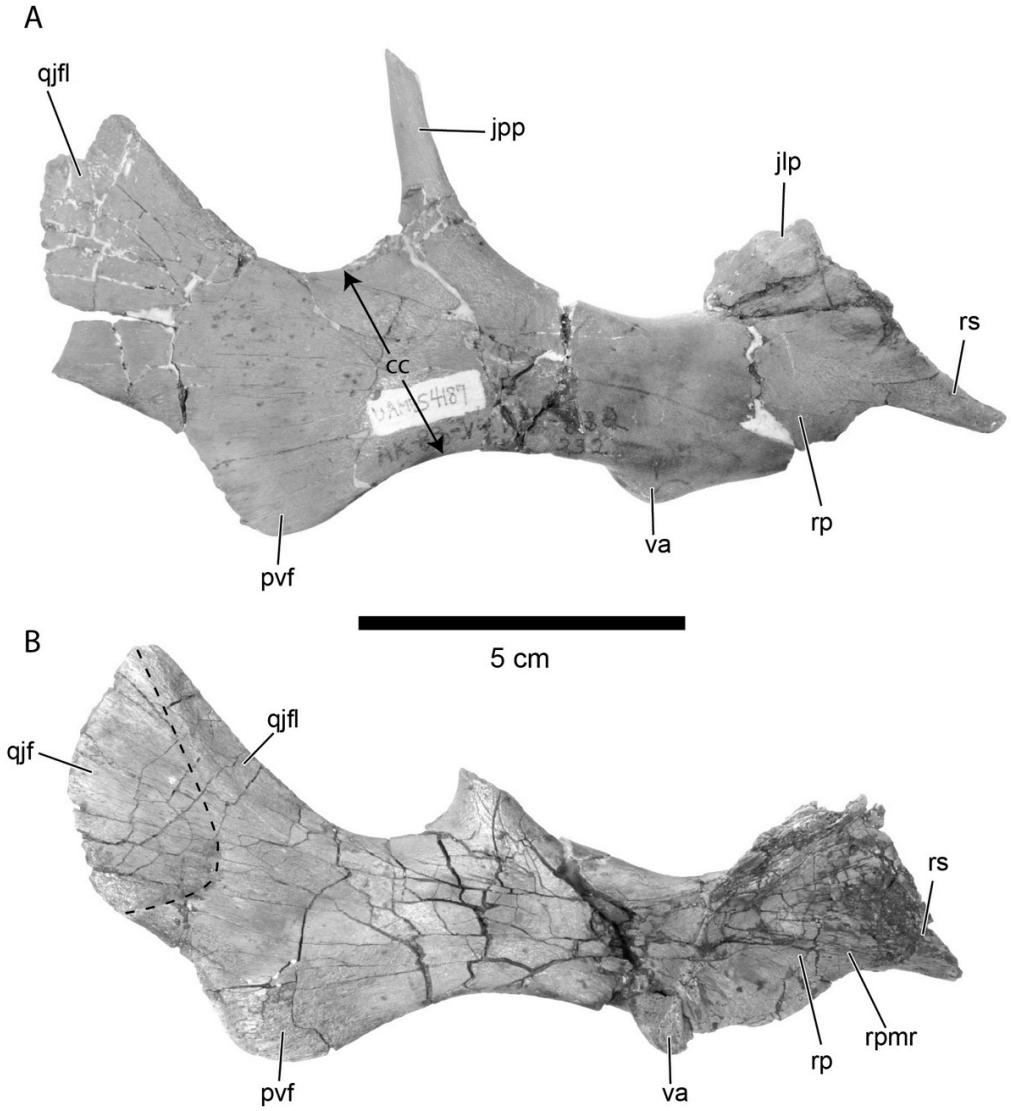

Figure 2-8. Jugal. Right jugal (UAMES 4187) of size class 1 *Edmontosaurus* sp. nov. in lateral view (A). Left jugal (UAMES 4213) of size class 1 *Edmontosaurus* sp. nov. in the medial view (B). Abbreviations: cc, caudal constriction; jlp, lacrimal process; jpp, postorbital process; pvf, posteroventral flange; qjf, quadratojugal facet (enclosed in the dashed line); qjfl, quadratojugal flange; rp, rostral process; rpmr, rostral process medial ridge; rs, rostral spur; va, ventral apex.

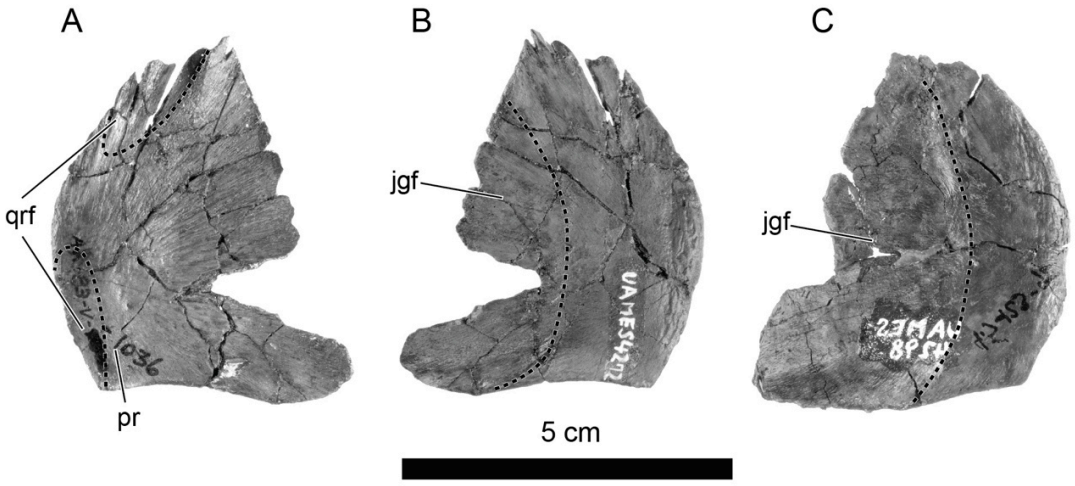

Figure 2-9. Quadratojugal. Left quadratojugal (UAMES 4272) of size class 1 *Edmontosaurus* sp. nov. in medial (A), and lateral (B) views. Right quadratojugal (UAMES 4298, reversed) of size class 1 *Edmontosaurus* sp. nov. in lateral view (C). UAMES 4272 (B) differs from UAMES 4298 (C) in that it has narrower jugal articulation surface. Abbreviations: jgf, jugal facet; pr, posterior ridge; qrf, quadrate.

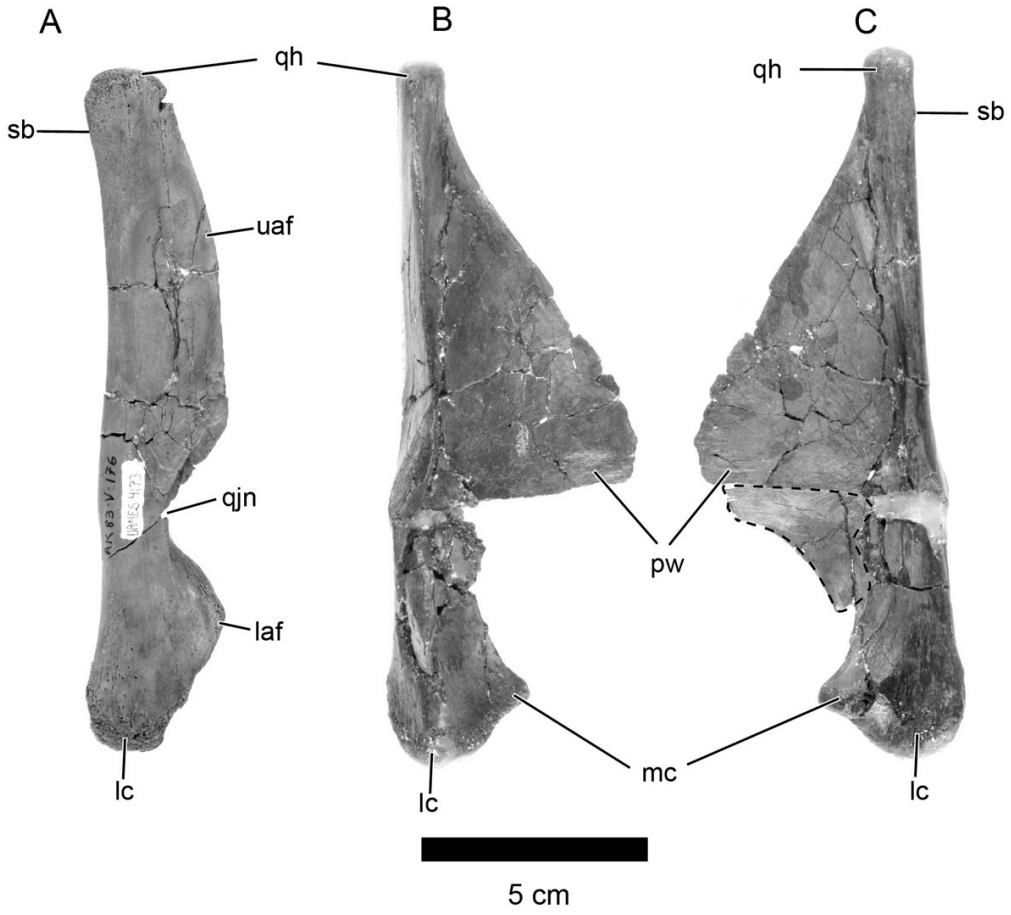

Figure 2-10. Quadrate. Right quadrate (UAMES 4173) of size class 1 *Edmontosaurus* sp. nov. in lateral view (A). Right quadrate (UAMES 4286) in anterior view (B), Composite reconstruction of the quadrates (UAMES 4286 and UAMES 4235) of size class 1 *Edmontosaurus* sp. nov. in posterior view (C). Portion enclosed in the dashed line is from UAMES 4235. Abbreviation: laf; lower anterior flange, lc; lateral condyle, mc; medial condyle, pw; pterygoid wing, qh; quadrate head, qjn; quadratojugal notch, sb; squamosal buttress, uaf; upper anterior flange.

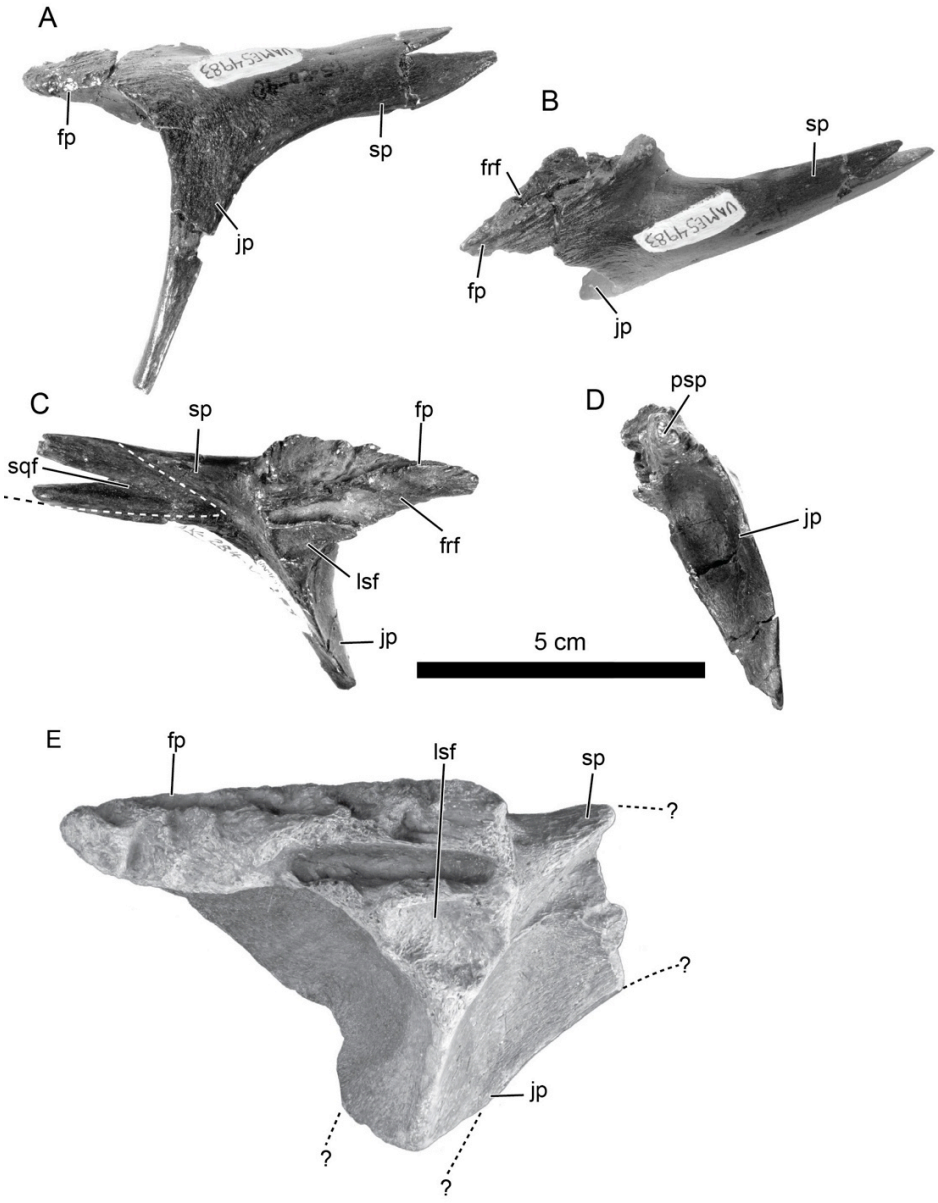

Figure 2-11. Postorbital. Left postorbital (UAMES 4983) of size class 1 *Edmontosaurus* sp. nov. in lateral (A) and dorsal (B) views. Left postorbital (UAMES 12965) of size class 1 *Edmontosaurus* sp. nov. in medial (C) and anterior (D) views. Incomplete right postorbital (UAMES 33308) of size class 3 of *Edmontosaurus* sp. nov. in medial view (E). Abbreviations: fp, frontal process; frf, frontal facet; jp, jugal process; lsf, laterosphenoid facet; sp, squamosal process; sqf, squamosal facet (enclosed in the dashed line).

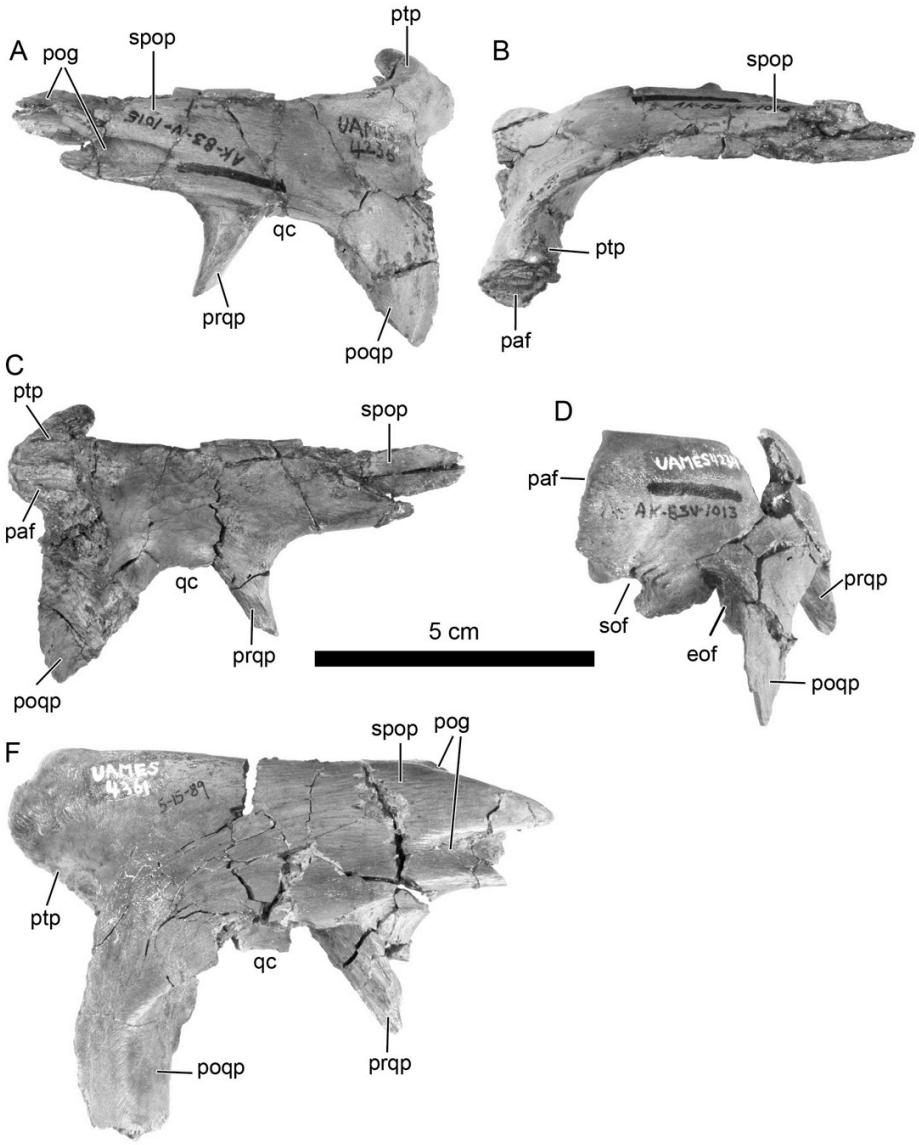

Figure 2-12. Squamosal. Left squamosal (UAMES 4236) of size class 1 *Edmontosaurus* sp. nov. in lateral (A), dorsal (B), and medial (C) views. Right squamosal (UAMES 4234) of size class 1 *Edmontosaurus* sp. nov. in posterior view (D). Right squamosal (UAMES 4361) of size class 2 *Edmontosaurus* sp. nov. in lateral view (F). Abbreviations: eof, exoccipital facet; paf, parietal facet; pog, postorbital groove; poqp, postquadratic process; prqp, prequadratic process; ptp, parietal process; qc, quadrate cotylus; sof, supraoccipital foramen; spop, postorbital process.

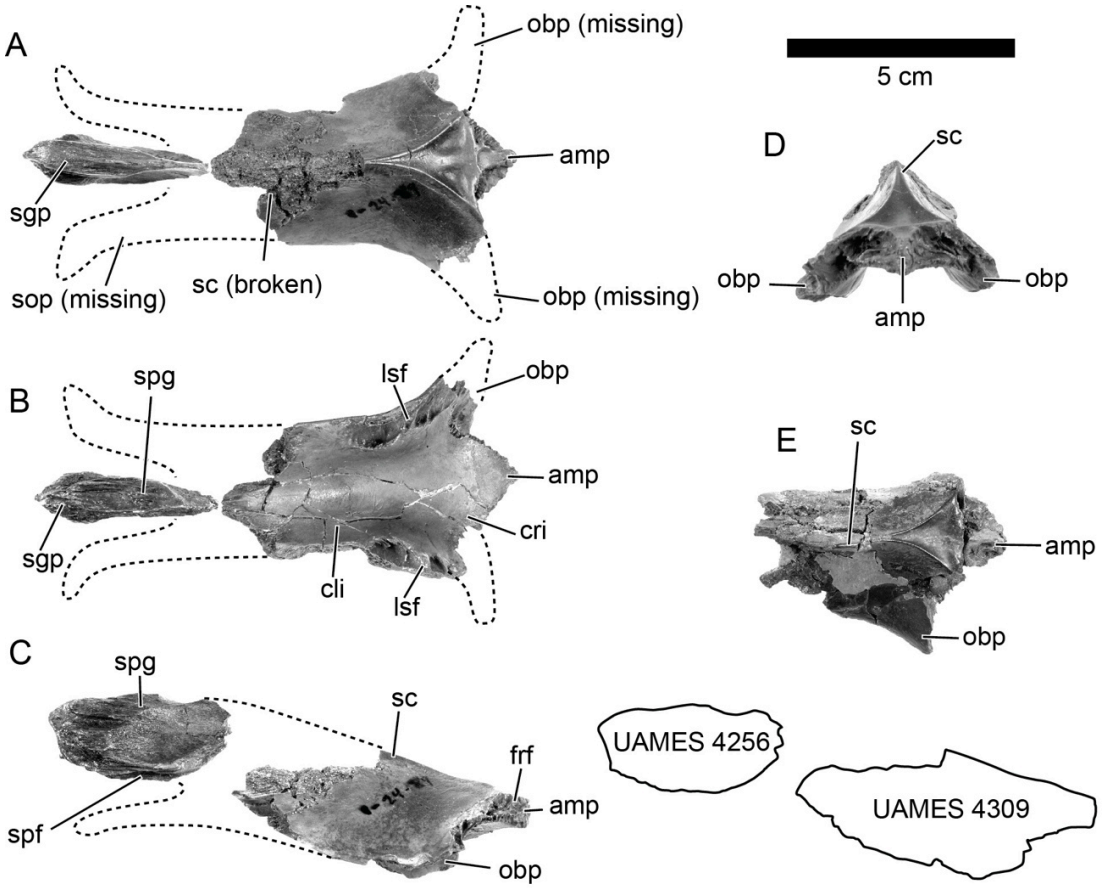

Figure 2-13. Parietal. Parietals (UAMES 4309 and 4256) of size class 1 *Edmontosaurus* sp. nov. in dorsal (A), ventral (B), lateral (C), and anterior (D) views. Parietal with a different indentation pattern in the triangular depression (UAMES 12957) of size class 1 *Edmontosaurus* sp. nov. in dorsal view (E). Abbreviations: amp, anteromedial process; cli, cerebellum impression; cri, cerebrum impression; frf, frontal facet; lsf, laterosphenoid facet; obp, postorbital process; sc, sagittal crest; sgp, sagittal process; sop, suporaoccipital process; spf, supraoccipital.

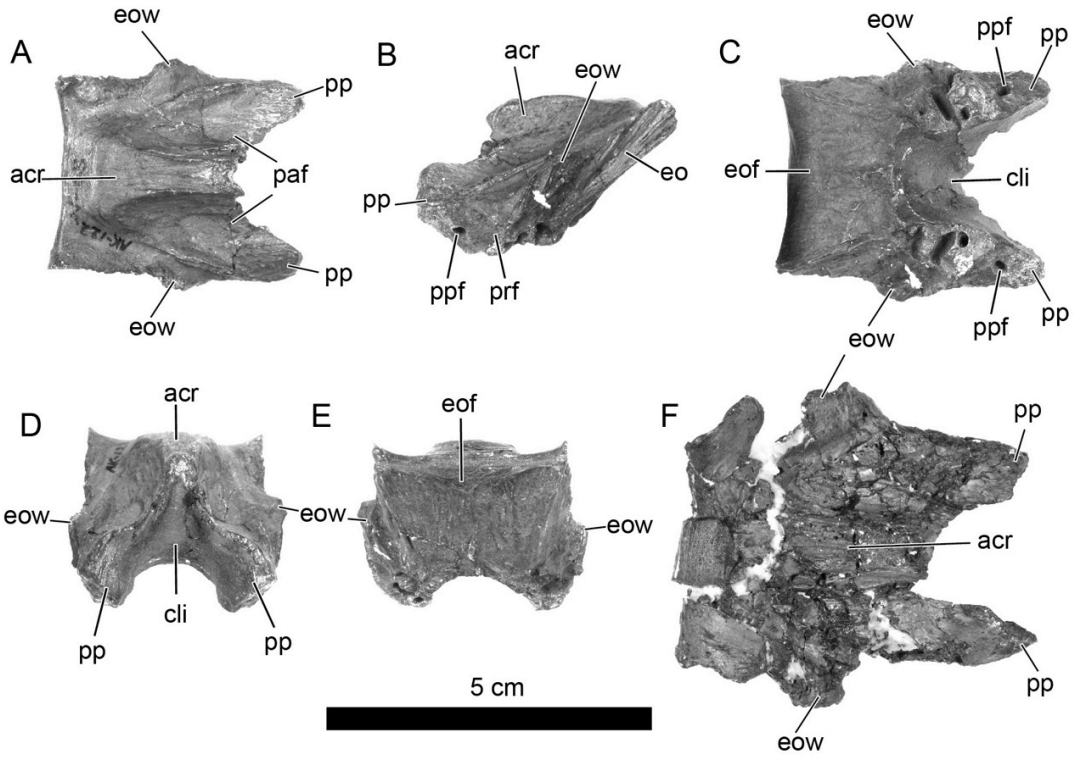

Figure 2-14. Supraoccipital. Supraoccipital (UAMES 4291) of size class 1 *Edmontosaurus* sp. nov. in dorsal (A), lateral (B), ventral (C), anterior (D), and posterior (E) views. Supraoccipital (UAMES 12727) of size class 2 *Edmontosaurus* sp. nov. in dorsal view (F). Abbreviations: acr, ascending ridge; cli, cerebellar impression; eof, exoccipital facet; eow, exoccipital wing; paf, parietal facet; pp, prootic process; ppf, prootic process foramen, prf; prootic facet.

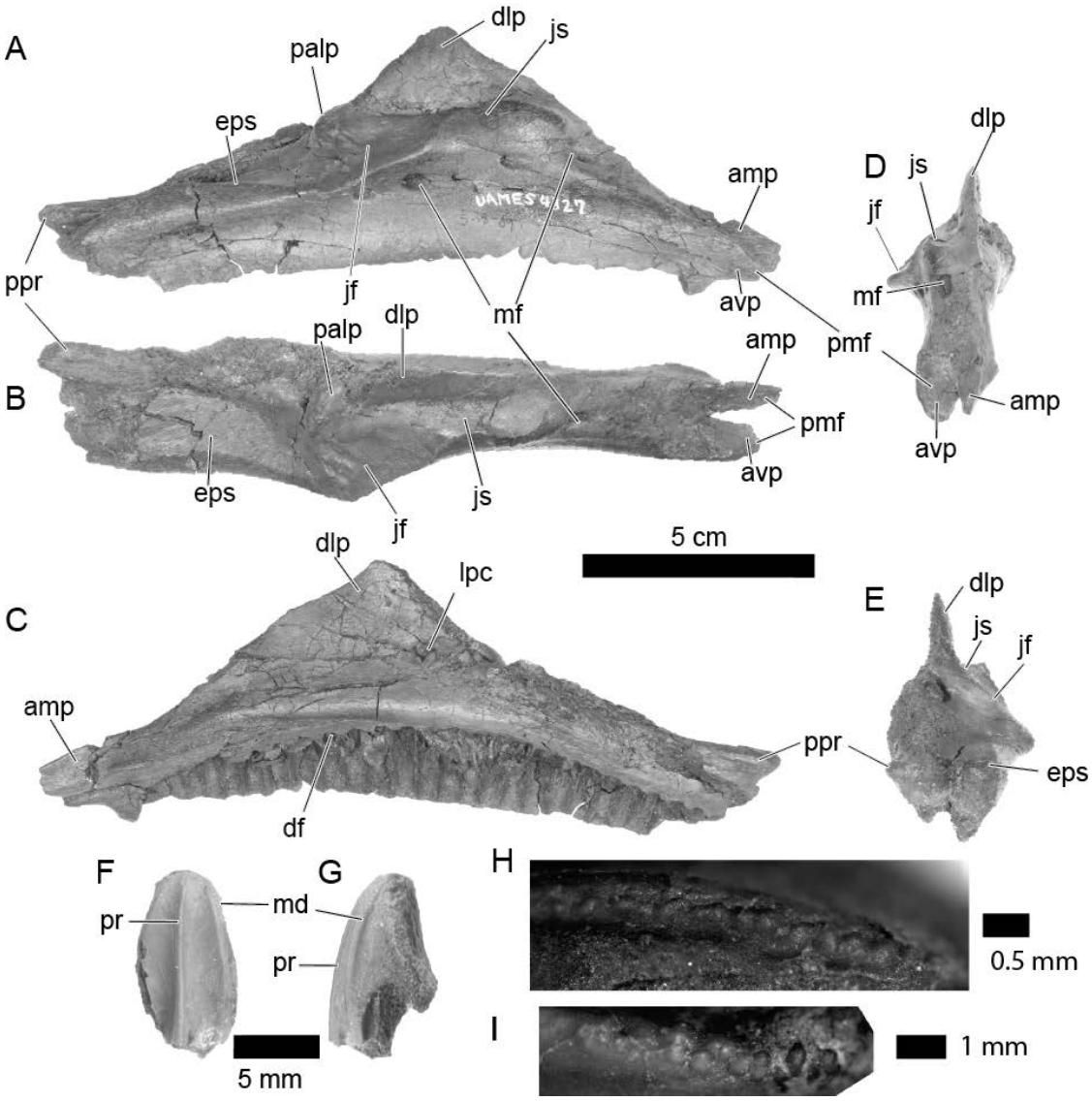

Figure 2-15. Maxilla. Right maxilla (UAMES 4327) of size class 1 *Edmontosaurus* sp. nov. in lateral (A), dorsal (B), medial (C), anterior (D), and posterior view (E). Maxillary tooth (extracted from UAMES 4185) of size class 1 *Edmontosaurus* sp. nov. in buccal (F) and side view (G). Magnified view of the marginal denticles of size class 1 *Edmontosaurus* sp. nov., UAMES 4185 (H) and UAMES 4250 (I). Abbreviations: amp, anteromedial process; avp, anteroventoral process; df, dental foramina; dlp, dorsal lacrimal process; eps, ectopterygoid shelf; jf, jugal facet; js, jugal shelf; lpc, lacrimal process canal; md, marginal denticle; mf, maxillary foramen; palp, palatine process; pmf, premaxilla facet; ppr, posterior process; pr, primary ridge.

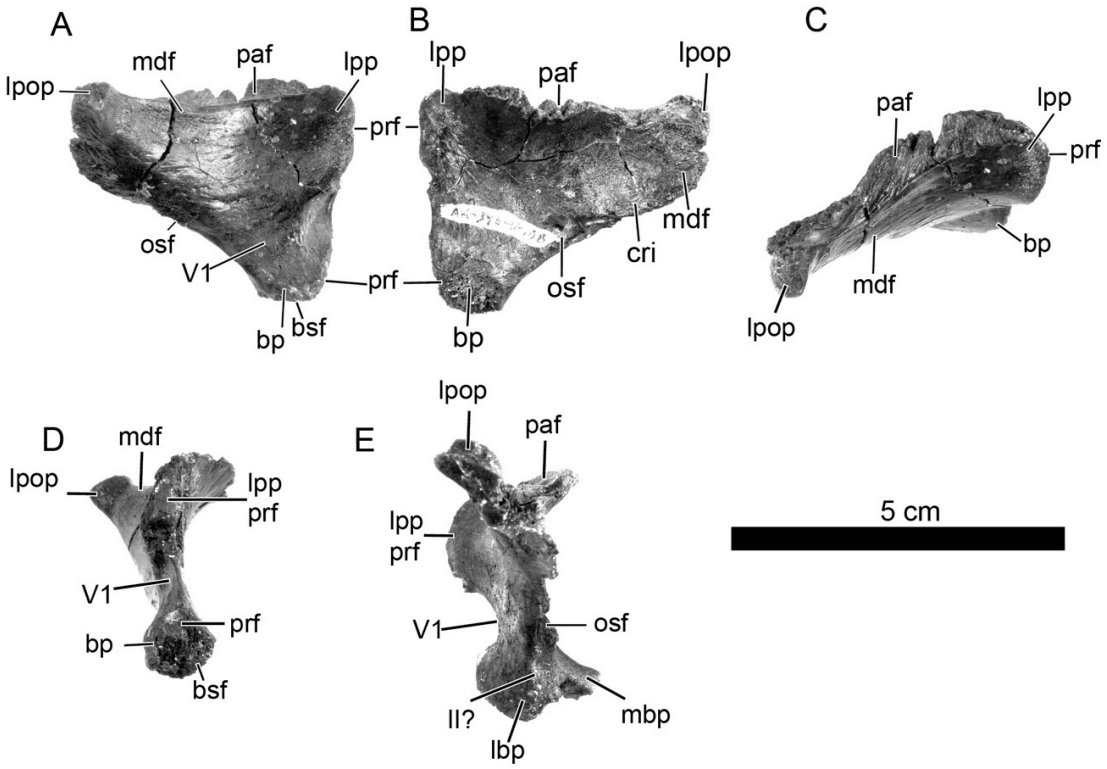

Figure 2-16. Laterosphenoid. Left laterosphenoid (UAMES 15284) of size class 1 *Edmontosaurus* sp. nov. in lateral (A), medial (B), dorsal (C), and posterior (D) views. Right laterosphenoid (UAMES 4352) of size class 1 *Edmontosaurus* sp. nov. in anterior view (E). Abbreviations: bp, basisphenoid process; bsf, basisphenoid facet; cri, cerebral impression; II, cranial nerve II; lbp, lateral basisphenoid process; lpop, postorbital process; lpp, prootic process; mbp, medial basisphenoid process; mdf, medial dorsal flange; osf, orbitosphenoid facet; paf, parietal facet; prf, prootic facet; V1, ophthalmic nerve.

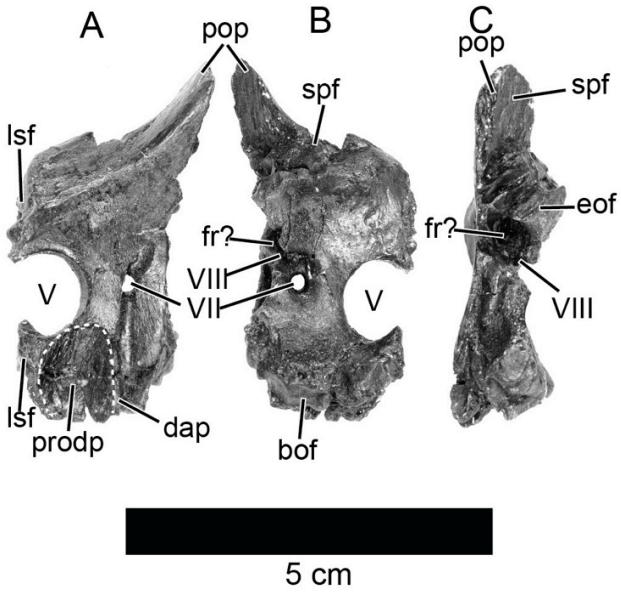

Figure 2-17. Prootic. Right prootic (UAMES 4357) of size class 1 *Edmontosaurus* sp. nov. in lateral (A), medial (B), and posterior (C) views. Abbreviations: bof, basioccipital facet; dap, dorsal part of the alar process; eof. exoccipital-opisthotic facet; fr, fenestra rotunda; lsf, laterosphenoid facet; pop, opisthotic process; prodp, prootic depression; spf, supraoccipital facet, VII, cranial nerve VII, VIII, cranial nerve VIII.

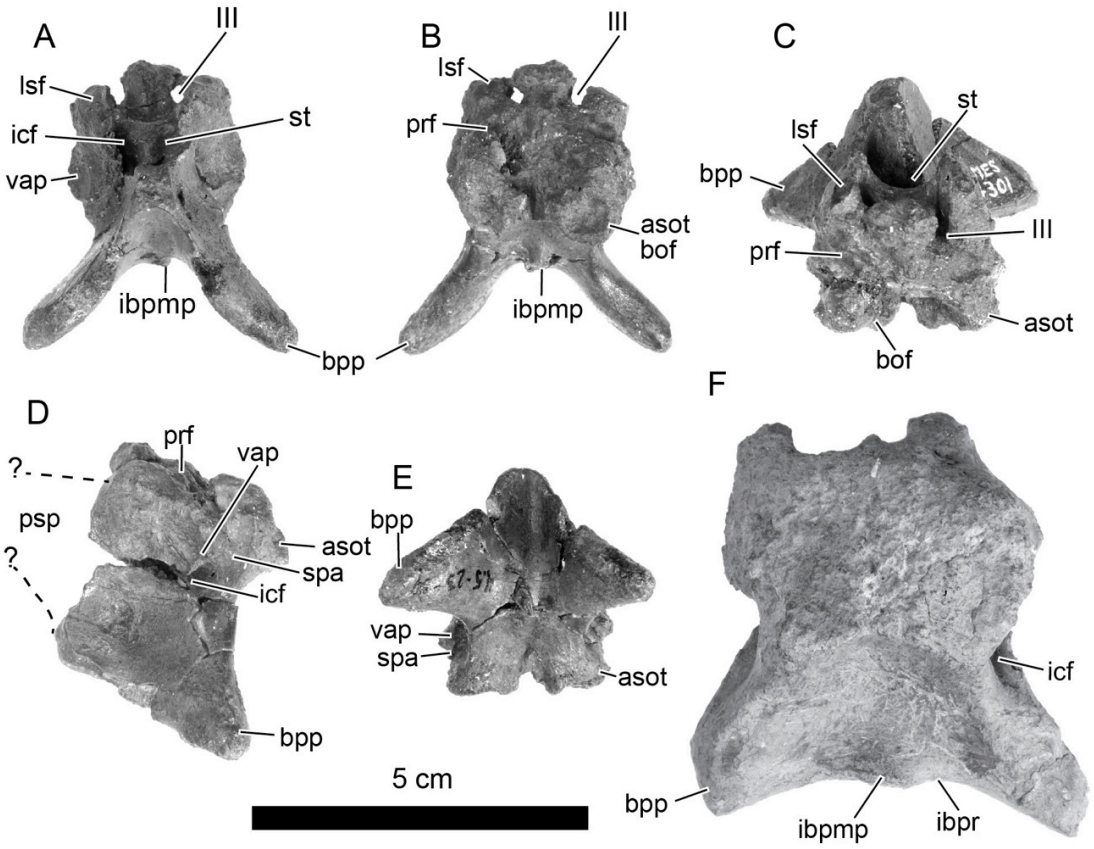

Figure 2-18. Basisphenoid. Basisphenoid (UAMES 4301) of size class 1 *Edmontosaurus* sp. nov. Anterior (A), posterior, dorsal (C), left lateral (D), ventral (E) views. Basisphenoid (UAMES 18882) of size class 3 *Edmontosaurus* sp. nov. in posterior view (F). Abbreviations: asot, anterior sphenooccipital tubera; bof, basioccipital facet; bpp, basipterygoid process; III, cranial nerve III; ibpr, interbasipterygoid ridge; ibpmp, interbasipterygoid ridge median process; icf, internal carotid foramen; lsf, laterosphenoid facet; prf, prootic facet; psp, parasphenoid process; spa, stapedial artery foramen; st, sella turcica; vap, ventral half of the alar process.

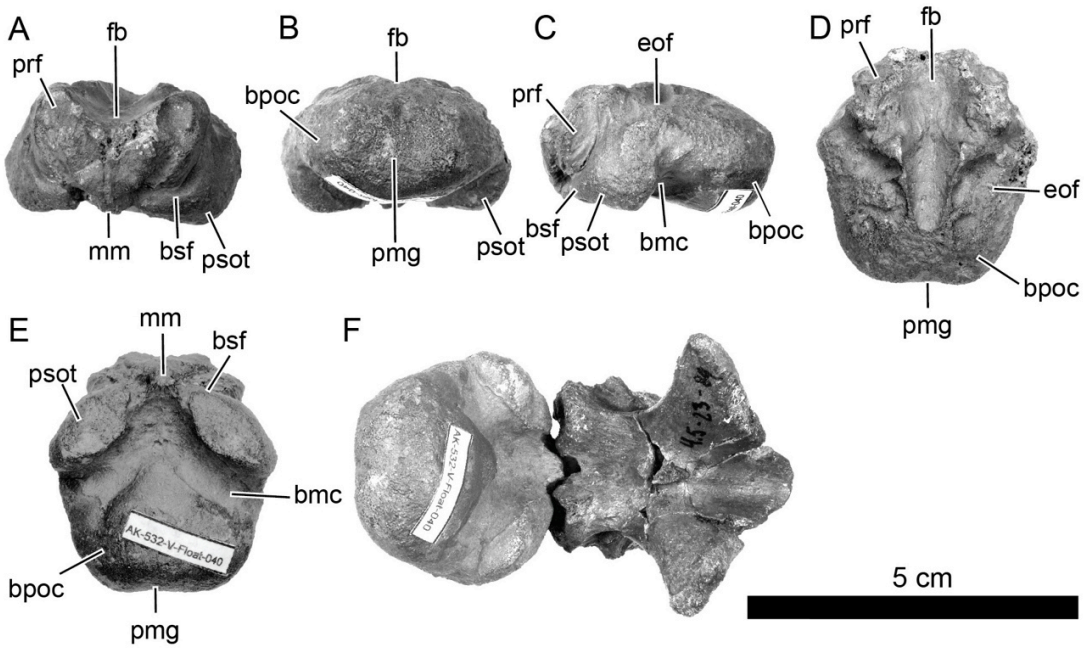

Figure 2-19. Basioccipital. Basioccipital (UAMES 4276) of size class 1 *Edmontosaurus* sp. nov. in anterior (A), posterior (B), left lateral (C), dorsal (D), and ventral (E) views. Articulation of the basioccipital with basisphenoid. Posteroventral view (F). Abbreviations: bmc, basioccipital medial cleft; bpoc, basal portion of occipital condyle; bsf, basisphenoid facet; eof, exoccipital facet; fb, floor of braincase; mm, median mound; psot, posterior sphenooccipital tubera; pmg, posterior medial groove; prf, prootic facet.

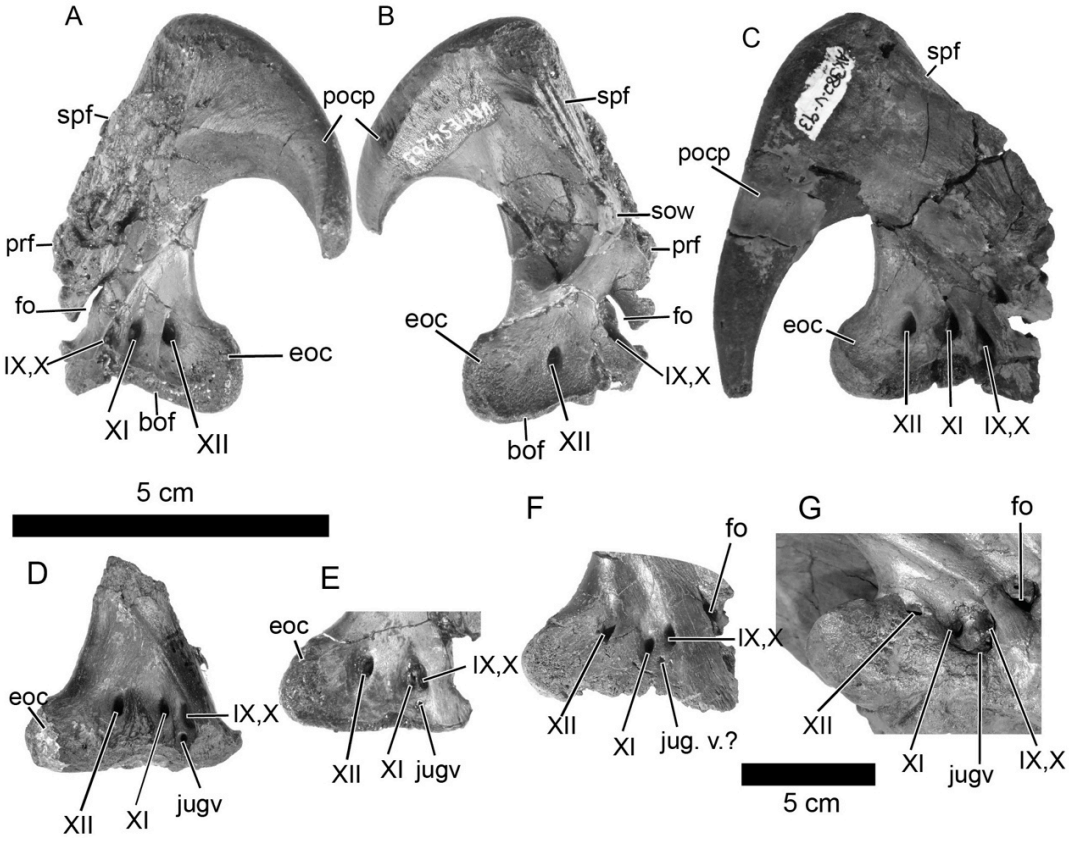

Figure 2-20. Exoccipital-ophisthotic. Left exoccipital-opisthotic (UAMES 4263) of size class 1 *Edmontosaurus* sp. nov. in lateral (A), and medial (B) views. Right exoccipital-opisthotic (UAMES 4095) of size class 1 *Edmontosaurus* sp. nov. in lateral view (C), left lateral views of the exoccipital condyloids; *Edmontosaurus* sp. nov. (UAMES 4378, D, reversed; UAMES 4279, E), *E. annectens* (ROM 64076, F), and *E. regalis* (CMN 2289, G). In D and G, the cranial nerve IX to X and the jugal vein are not included in a depression, and E and F, these cranial nerves and vein are included in a depression. Abbreviations: bof, basioccipital facet; eoc, exoccipital condyloid; fo, fenestra ovalis; jugv, jugal vein; pocp, paraoccipital process, prf; prootic facet, sow; supraoccipital wing, spf, supraoccipital facet; IX, cranial nerve IX; X, cranial nerve X; XI, cranial nerve XI; XII, cranial nerve

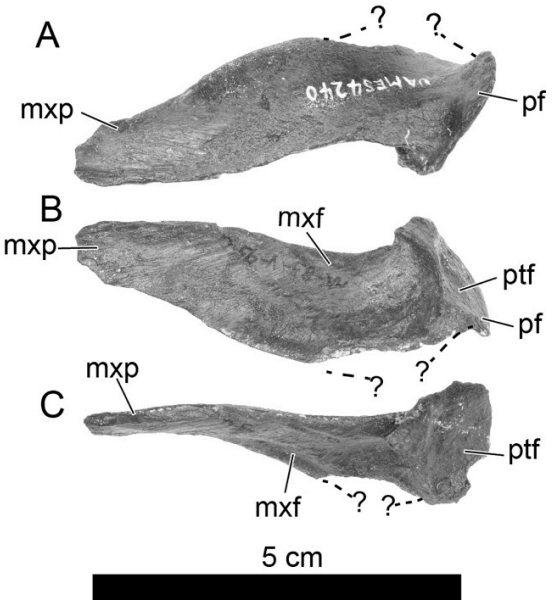

Figure 2-21. Ectopterygoid. Right ectopterygoid (UAMES 4240) of size class 1 *Edmontosaurus* sp. nov. in lateral (A), medial (B), and dorsal (C) views. Abbreviations: mxf, maxillary facet; mxp, maxillary process; pf, pterygoid flange; ptf, pterygoid facet.

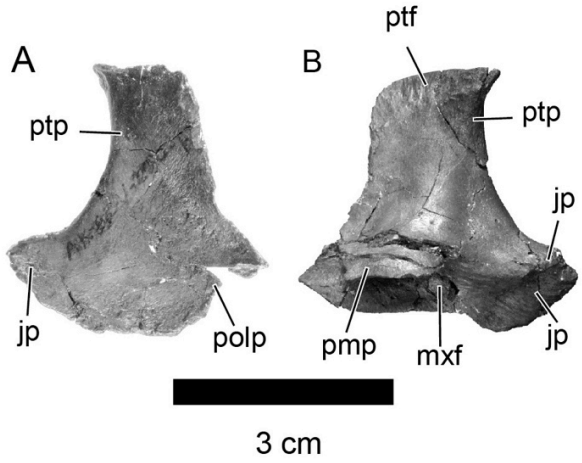

Figure 2-22. Palatine. Right palatine (UAMES 4257) of size class 1 *Edmontosaurus* sp. nov. in lateral view (A). Left palatine (UAMES 4331) of size class 1 *Edmontosaurus* sp. nov. in medial view (B). Abbreviations: jp, jugal process; mxf; maxilla facet; pmp, posterior medial process, polp; posterior lateral process, ptf; pterygoid facet, ptp; pterygoid process.

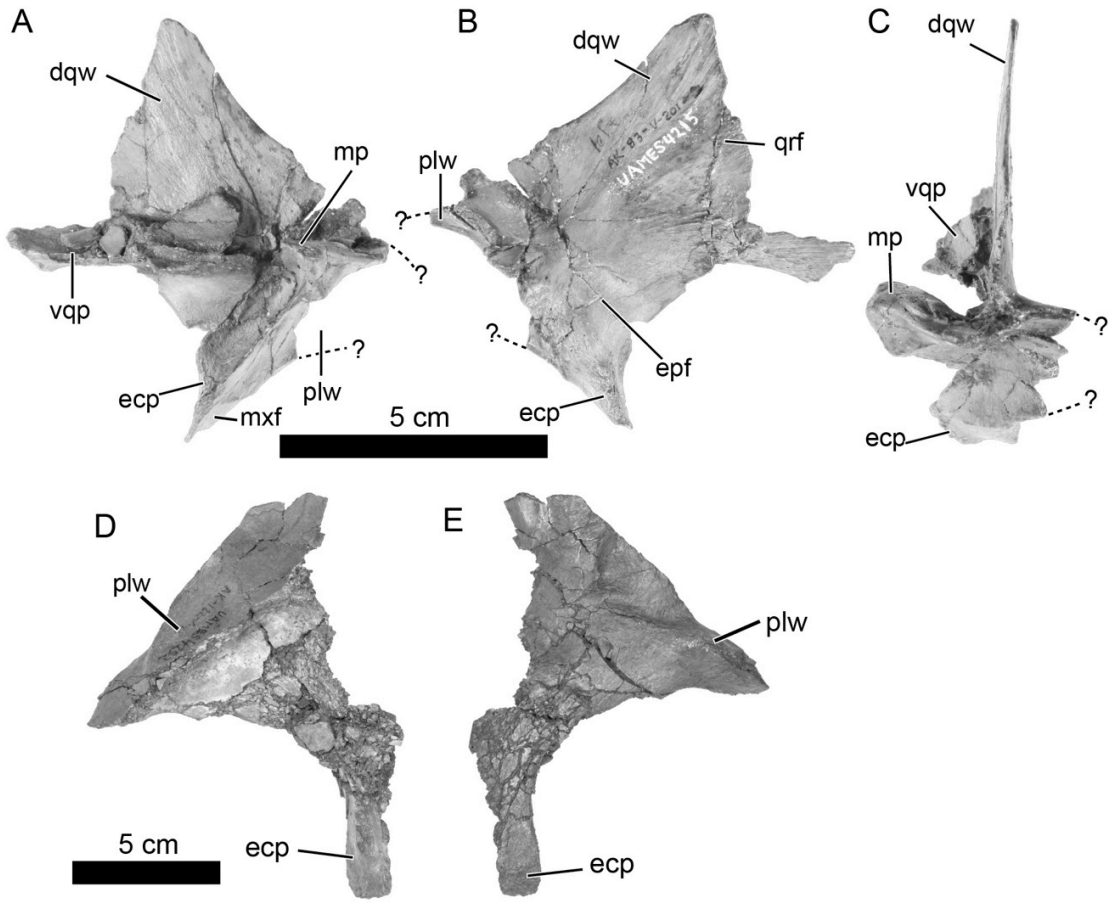

Figure 2-23. Pterygoid. Left pterygoid (UAMES 4215) of size class 1 *Edmontosaurus* sp. nov. in posteromedial (A), anterolateral (B), and anteromedial (C) views. Right pterygoid (UAMES 4252) of size class 3 *Edmontosaurus* sp. nov., posteromedial (D), anterolateral (E) views. Abbreviations: dqw, dorsal quadrate wing; ecp, ectopterygoid process; epf, epipterygoid facet; mp, medial process; mxf, maxilla facet; plw, palatine wing; qrf, quadrate face; vqp, ventral quadrate process.

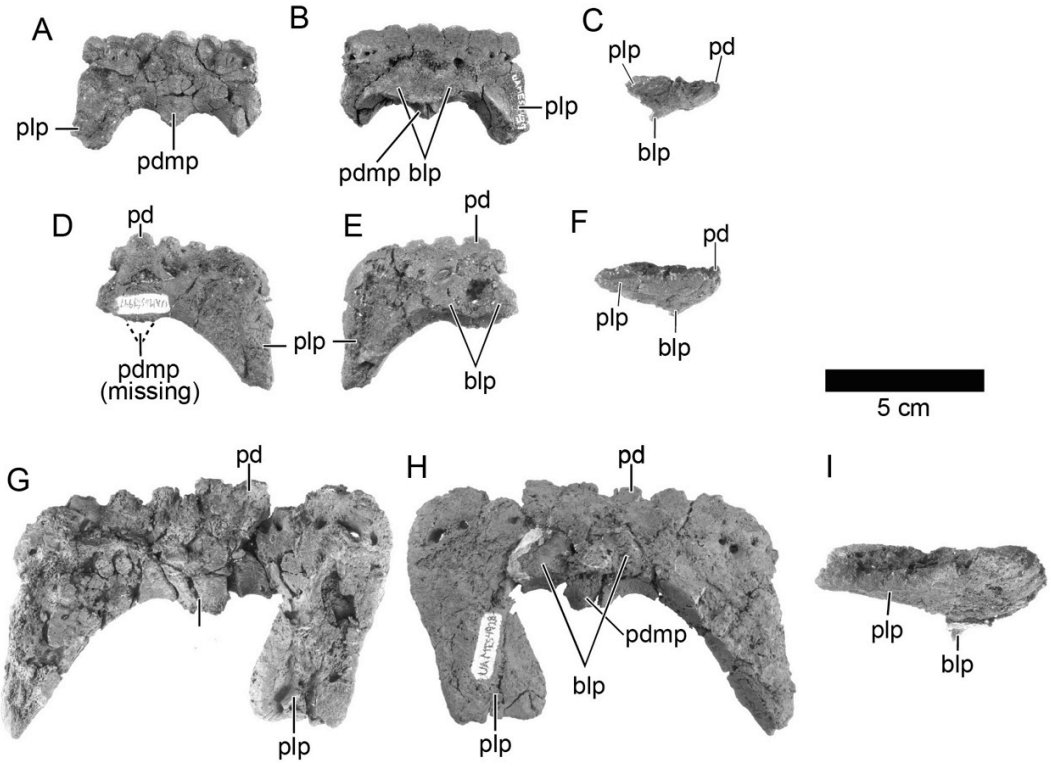

Figure 2-24. Predentary. Predentary (UAMES 4947) of a small size class 1 *Edmontosaurus* sp. nov. in dorsal (A), ventral (B), and right lateral (C) views. Predentary (UAMES 4437) of a large size class 1 *Edmontosaurus* sp. nov. in dorsal (D), ventral (E), and right lateral (F) views. Predentary (UAMES 4928) of size class 2 *Edmontosaurus* sp. nov. in dorsal (G), ventral (H), and right lateral (I) views. Abbreviations: blp, bilobed process; pd, primary denticle; pdmp, posterodorsal median process; plp, lateral process.

Figure 2-25. Dentary. Right dentary (UAMES 12941) of size class 1 *Edmontosaurus* sp. nov. in lateral (A), and medial (B) views. Left dentary (UAMES 4946) of size class 2 *Edmontosaurus* sp. nov. in medial (C) and lateral (D) views. Dentary tooth preserved with a dentary (UAMES 13196) of size class 1 *Edmontosaurus* sp. nov. in lingual view (E). Isolated dentary tooth (UAMES 7742) of size class 1 (?) *Edmontosaurus* sp. nov. in lingual (F) and side (G) views. Abbreviations: crp: coronoid process, db; dental battery, dsp; dentary splenial process; edp; edentulous process; md, marginal denticle; pr, primary ridge; saf; surangular facet.

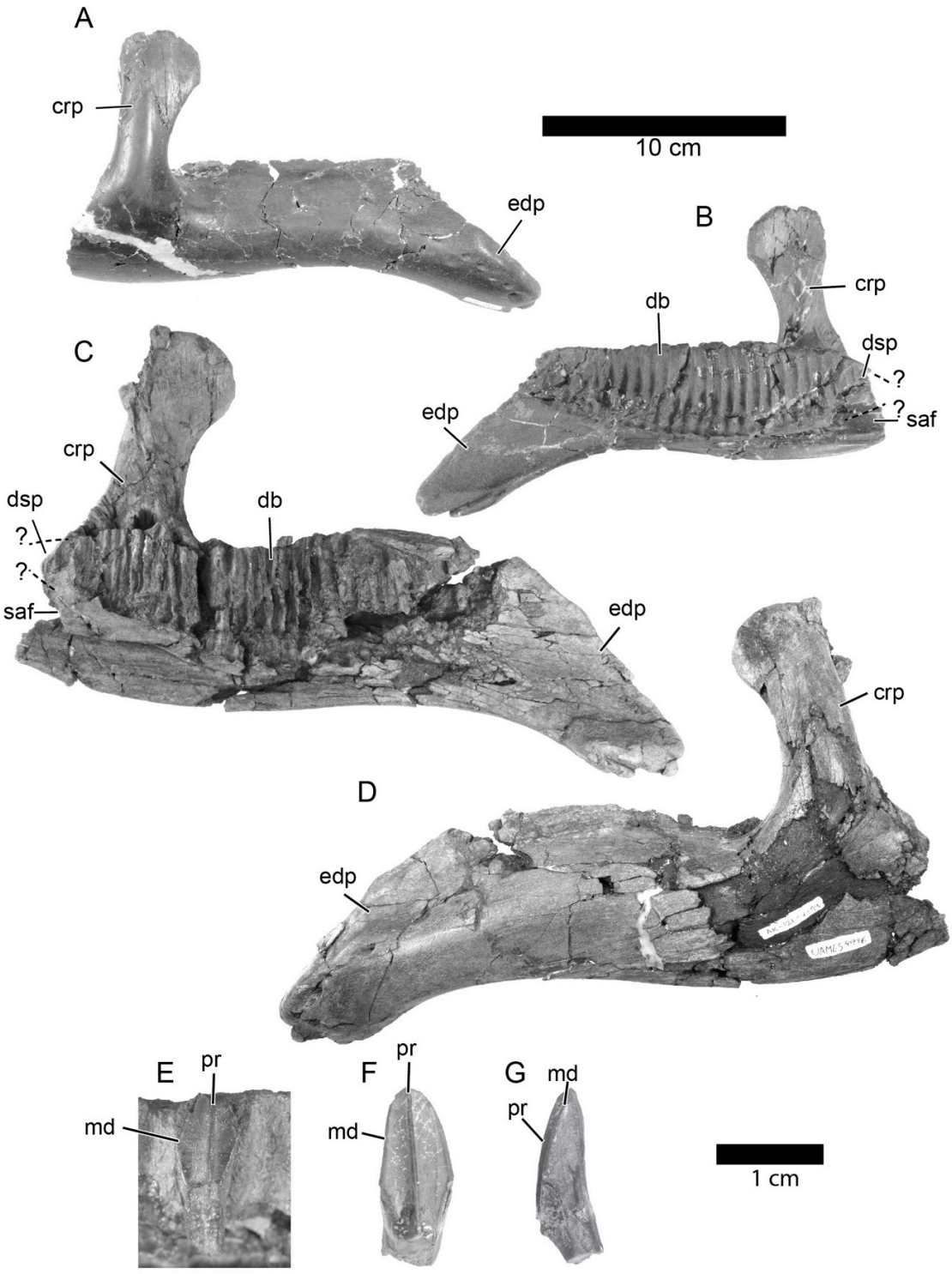
A
crp
edp
10 cm
B
crp
db
dsp
?
?
saf
edp
C
crp
dsp
?
?
saf
db
edp
D
crp
edp
E
pr
md
F
pr
md
G
md
pr
1 cm

Figure 2-26 (facing page). Surangular. Right surangular (UAMES 4457) of size class 1 *Edmontosaurus* sp. nov. in dorsal (A), lateral (B), ventral (C), anterior (D), and posterior (E) views. Left surangular that preserves the most complete medial sagittal flange (UAMES 4321) of size class 1 *Edmontosaurus* sp. nov. in medial view (F). Right surangular (UAMES 14132) of size class 3 *Edmontosaurus* sp. nov. in medial (G), ventral (H), and dorsal (I) views. Abbreviations: amf, anteromedial flange; anf, angular facet; dnf, dentary facet; msr, medial sagittal ridge; parp, posterior articular process; qrf, quadrate facet; sar, surface for articular; scp, coronoid process; slb, lateral bulge. The broken lines indicate the area of the dentary facet.

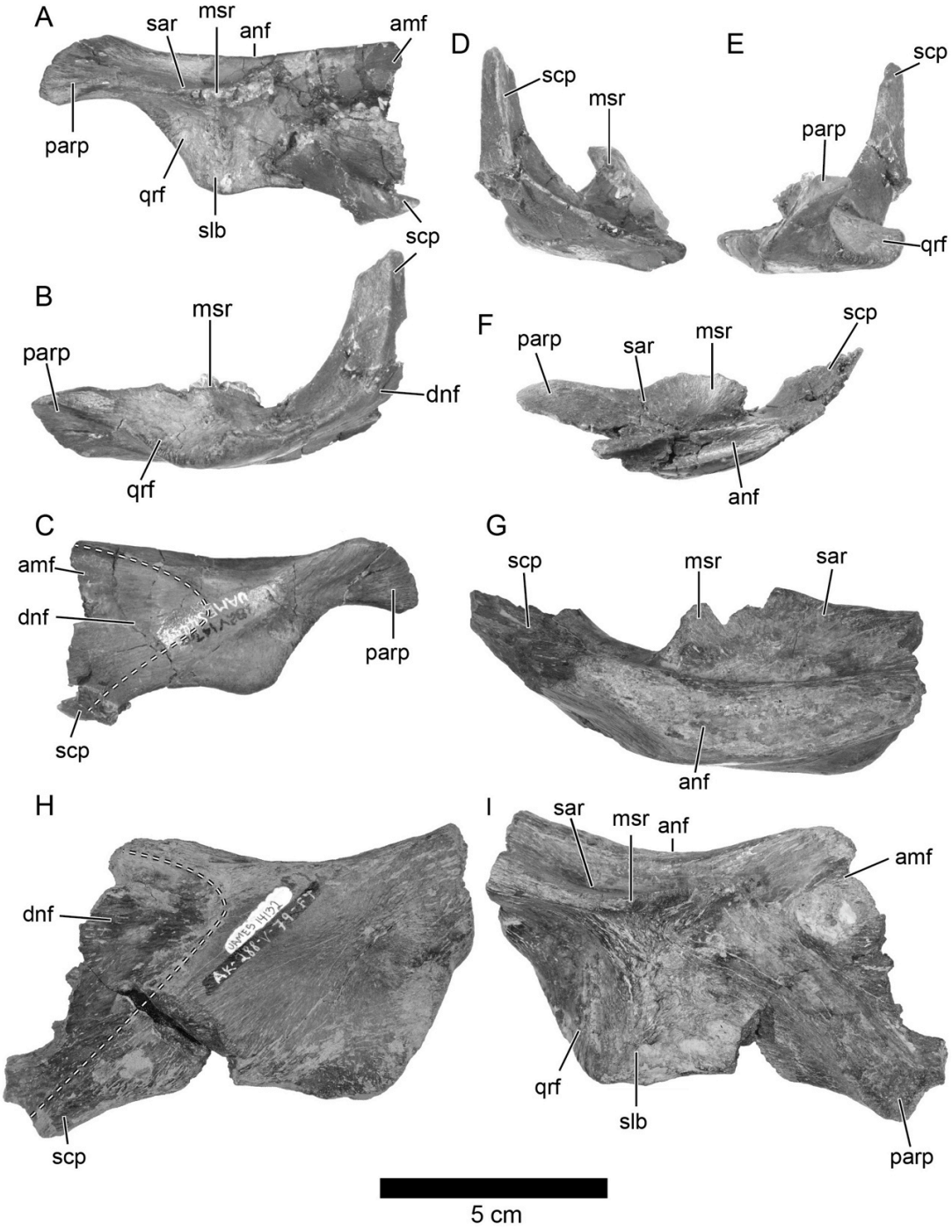
A
sar
msr
anf
amf
parp
qrf
slb
scp
B
msr
parp
dnf
qrf
C
amf
dnf
parp
scp
D
scp
msr
E
scp
parp
qrf
F
parp
sar
msr
scp
anf
G
scp
msr
sar
anf
H
dnf
scp
I
sar
msr
anf
amf
qrf
slb
parp
5 cm

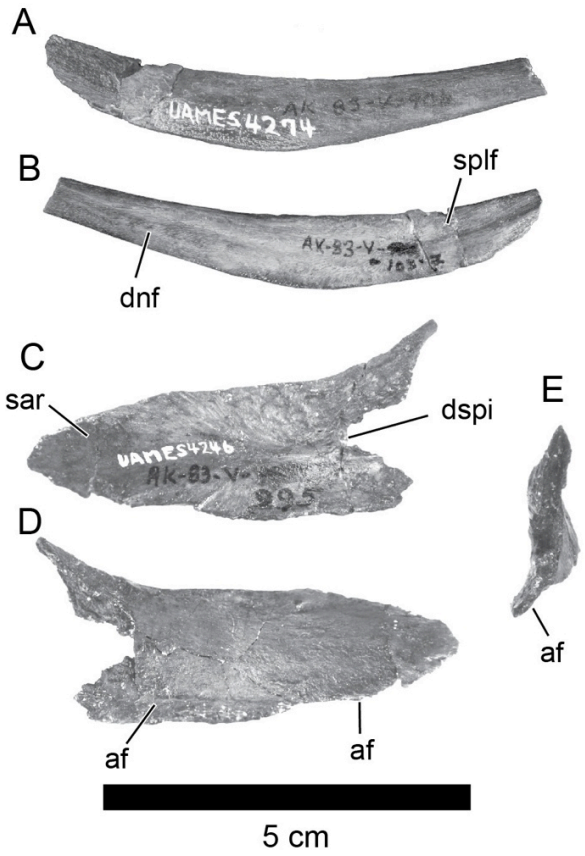

Figure 2-27. Angular. Left angular (UAMES 4274) of size class 1 *Edmontosaurus* sp. nov. in medial (A) and lateral (B) views. Right splenial (UAMES 4246) of size class 1 *Edmontosaurus* sp. nov. in lateral (C), medial (D), and anterior (E) views. Abbreviations: af; angular facet, dnf, dentary facet; dspi, dentary splenial process indentation; sar, surface for articular; splf, splenial facet.

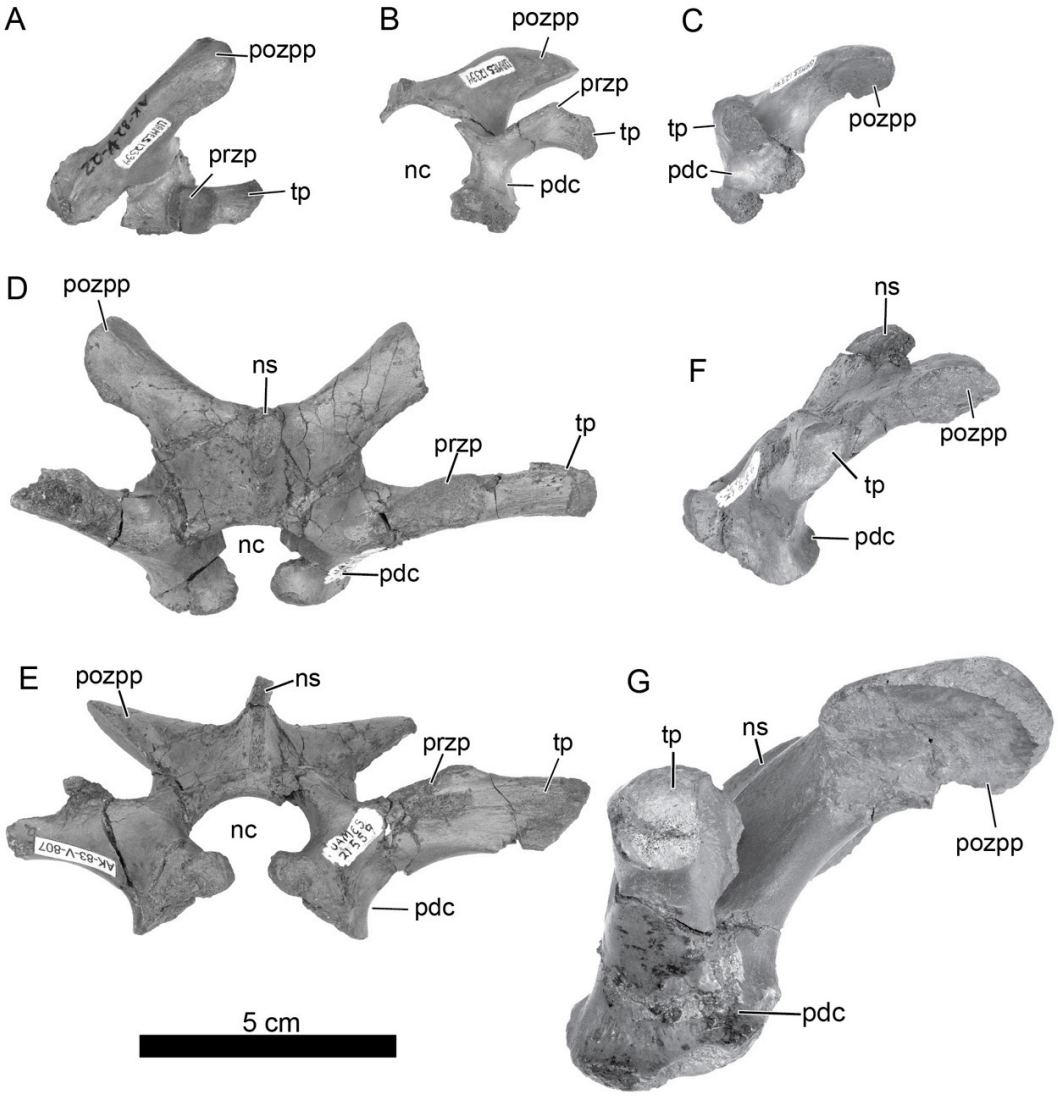

Figure 2-28. Cervical vertebral neural arch. Anterior cervical vertebral neural arch of size class 1 *Edmontosaurus* sp. nov., in dorsal (A), anterior (B), and left lateral (C) views. Posterior cervical vertebral neural arch of size class 2 (?) *Edmontosaurus* sp. nov. in dorsal (D), anterior (E), and left lateral (F) views. Posterior cervical vertebral neural arch of size class 3 (?) *Edmontosaurus* sp. nov. in left lateral view (G). Abbreviations: nc; neural canal, ns; neural spine, pdc, pedicle; pozpp; postzygapophyseal process, przp; prezygapophysis, tp; transverse process.

Figure 2-29 (facing page). Dorsal vertebra. Anterior-most dorsal vertebra (UAMES 23033) of the size class 3 *Edmontosaurus* sp. nov. in anterior (A), posterior (B), and right lateral (C) views. Anterior dorsal vertebral neural arch (UAMES 18462, D, E, and F) and centrum (UAMES 7661. G, H and I) of size class 1 *Edmontosaurus* sp. nov. in anterior (D, G), posterior (E, H), and right lateral (F, I) views. Middle dorsal vertebra (UAMES 12516) of size class 3 *Edmontosaurus* sp. nov. in anterior (J), posterior (K), and right lateral (L) views. Posterior dorsal vertebral neural arch (UAMES 18704 M, N, and O) and centrum (UAMES 12704. P, Q, and R) of size class *Edmontosaurus* sp.nov. in an terior (M, P), posterior (N, Q), and right lateral (O, R) views. Dorsal vertebra (UAMES 6 646) of size class 3 *Edmontosaurus* sp. nov. in anterior (S), posterior (T), and right latera l (U) views. Abbreviations: cnt, centrum; nc, neural canal; ns, neural spine; pdc, pedicle; pozp, postzygapophysis; pps, parapophysis; przp, prezygapophysis; tp, transverse process.

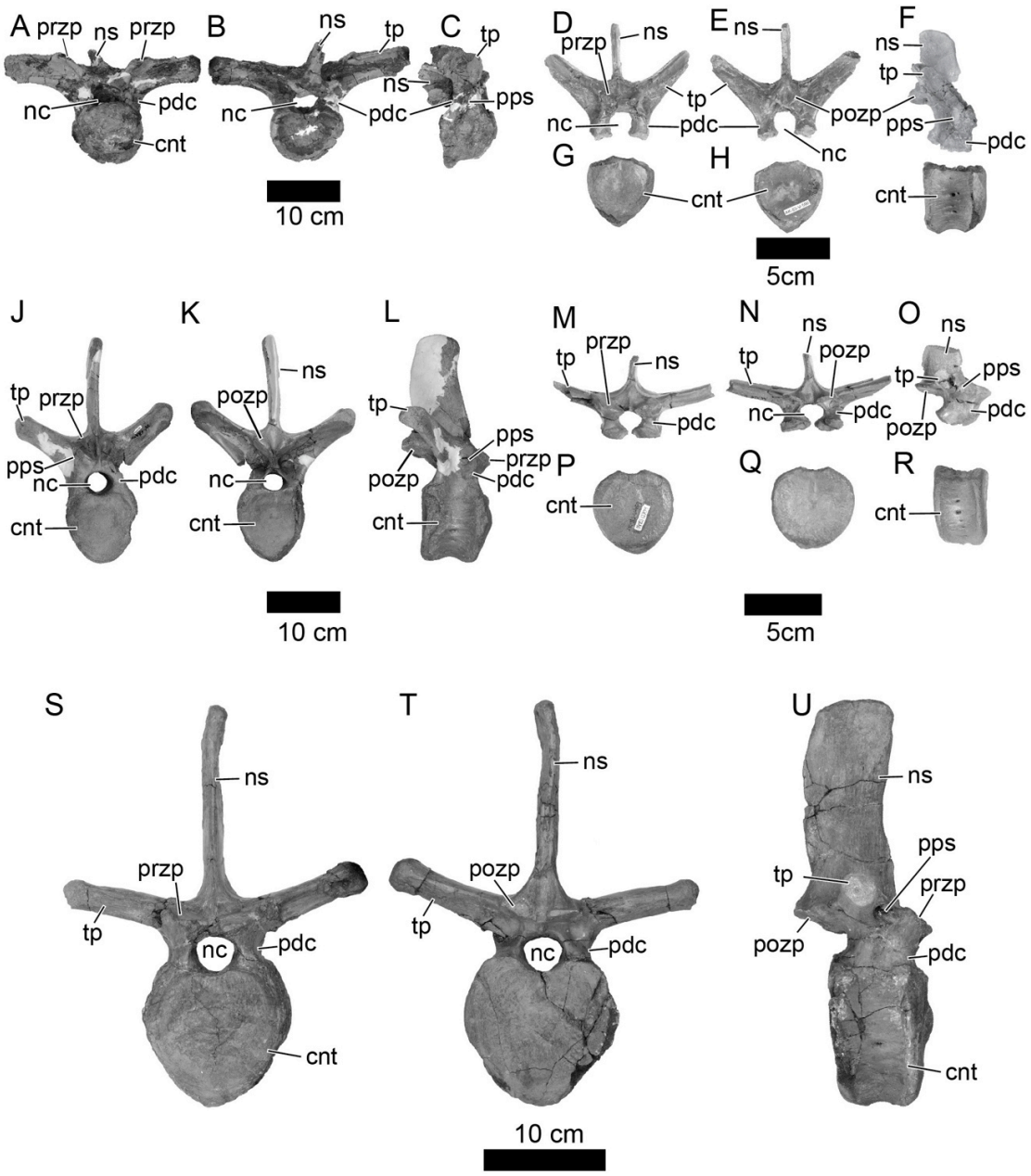
A
przp
ns
przp
nc
pdc
cnt
B
ns
tp
ns
nc
pdc
C
tp
pps
10 cm
D
przp
ns
tp
nc
pdc
E
ns
pozp
nc
F
ns
tp
pps
pdc
G
cnt
H
cnt
cnt
5cm
J
tp
przp
pps
nc
pdc
cnt
K
ns
pozp
nc
cnt
L
tp
pps
przp
pozp
pdc
cnt
M
tp
przp
ns
pdc
N
ns
tp
pozp
nc
pdc
O
ns
tp
pps
pdc
pozp
P
cnt
Q
R
cnt
10 cm
5cm
S
ns
przp
tp
nc
pdc
cnt
T
ns
pozp
tp
nc
pdc
U
ns
pps
tp
przp
pozp
pdc
cnt
10 cm

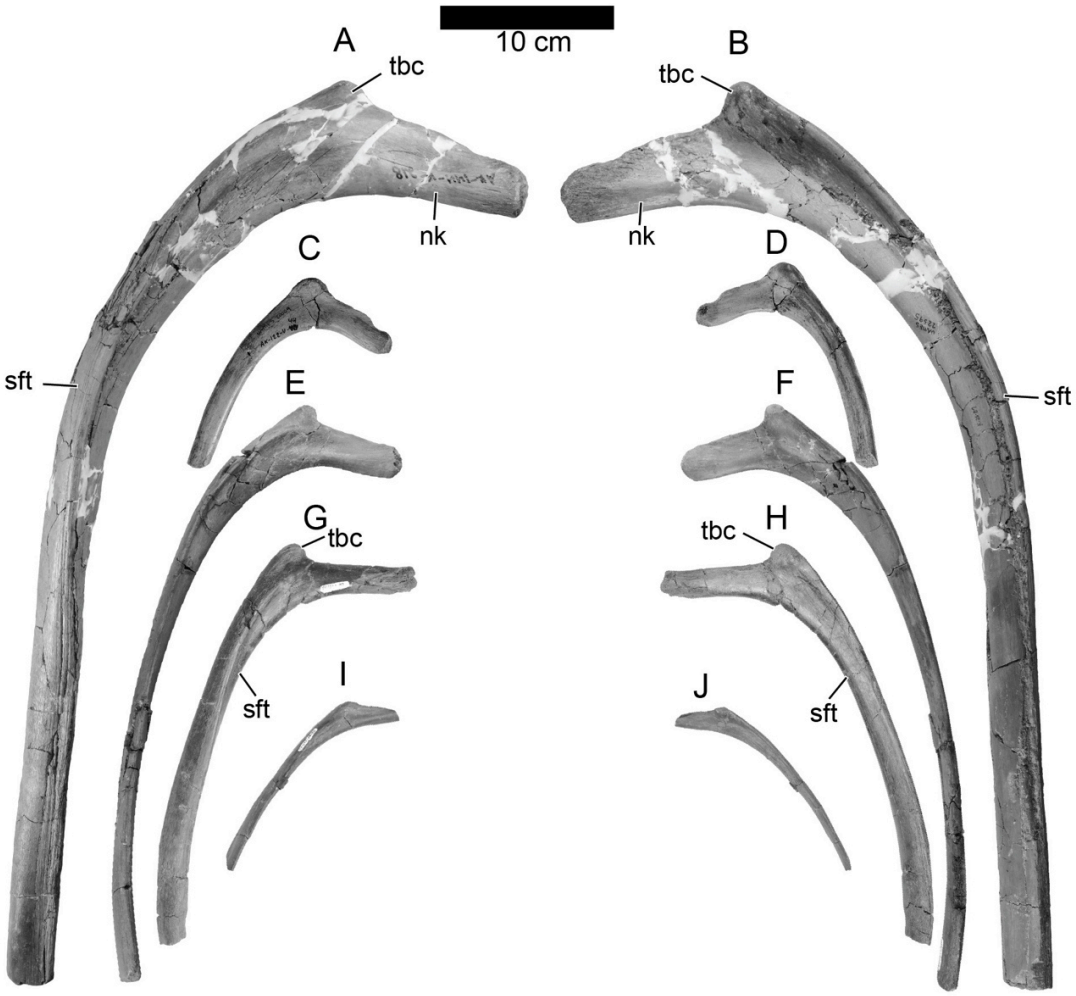

Figure 2-30. Dorsal ribs. Dorsal ribs (UAMES 22595) of size class 3 *Edmontosaurus* sp. nov. in anterior (A), and posterior (B) views. Dorsal ribs of anterior-most (UAMES 2009. C and D), anterior-middle (UAMES 13004. E and F), posterior-middle (UAMES 4473, reversed. G and H), and posterior (UAMES 13040, reversed. I and J) positions of the size class 1 of *Edmontosaurus* sp. nov. in anterior (C, E, G, and I) and posterior (D, F, H, and views. Abbreviations: nk, neck; sft, shaft; tbc, tubercle.

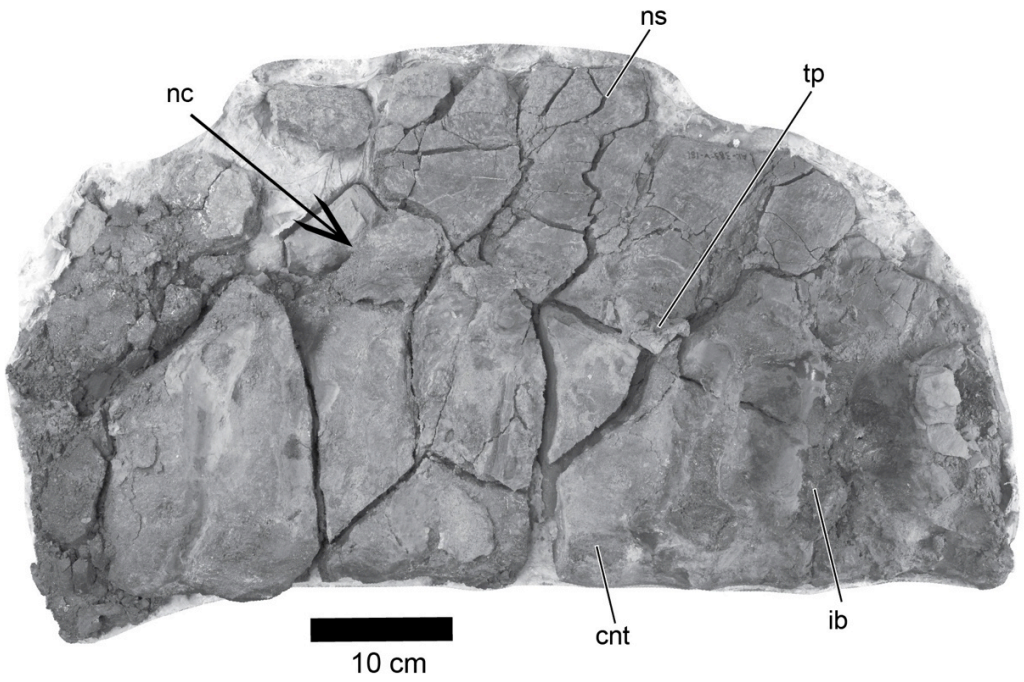

Figure 2-31. Sacrum. Sacrum (UAMES 23071) of size class 3 *Edmontosaurus* sp. nov.in lateral view. cnt, centrum; ib, iliac bade; nc, neural canal; ns, neural spine; tp, transverse process.

Figure 2-32 (facing page). Caudal vertebra. Anterior caudal vertebra (UAMES 18156) of size class 3 *Edmontosaurus* sp. nov. in anterior (A), posterior (B), and left lateral (C) views. Middle caudal vertebra (UAMES 17365) of size class 3 *Edmontosaurus* sp. nov. in anterior (D), posterior (E), and left lateral views (F). Mid-anterior caudal vertebral neural arch (UAMES 19877. G, H, and I), centrum (UAMES 14297. J, K, and L), and chevron (UAMES 29028. M, N, and O) of size class 1 *Edmontosaurus* sp. nov. in anterior (G, J, M), posterior (H, K, N), and left lateral (I, L, O) views. Mid-posterior caudal vertebra (UAMES 12709) of size class 1 *Edmontosaurus* sp. nov. in anterior (P), posterior (Q), and left lateral (R) views. Posterior caudal vertebra (UAMES 14411) of size class 1 *Edmontosaurus* sp. nov. in anterior (S), posterior (T), and left lateral (R) views. Abbreviations: ch, chevron head; cnt, centrum; nc, neural canal; ns, neural spine; pdc, pedicle; pozp, postzygapophysis; pozp, postzygapophyseal process; przp, prezygapophysis; tp, transverse process.

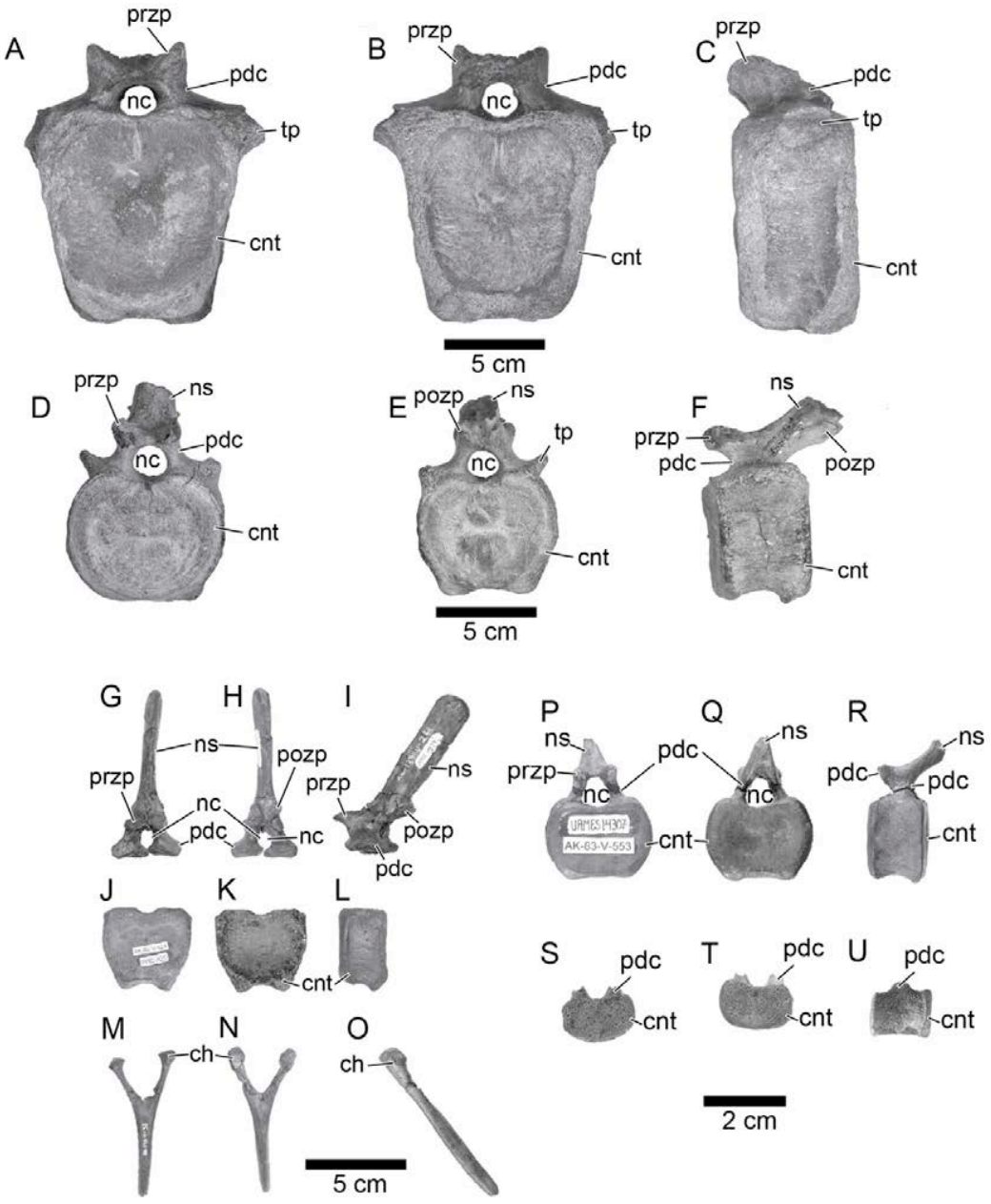
A
przp
pdc
nc
tp
cnt
B
przp
pdc
nc
tp
cnt
C
przp
pdc
tp
cnt
5 cm
D
przp
ns
pdc
nc
cnt
E
pozp
ns
tp
nc
cnt
F
ns
przp
pdc
pozp
cnt
5 cm
G
H
I
ns
pozp
przp
nc
pdc
nc
przp
ns
pozp
pdc
P
Q
R
ns
przp
pdc
nc
cnt
ns
nc
ns
pdc
pdc
cnt
J
K
L
cnt
S
pdc
cnt
T
pdc
cnt
U
pdc
cnt
M
N
O
ch
ch
5 cm
2 cm

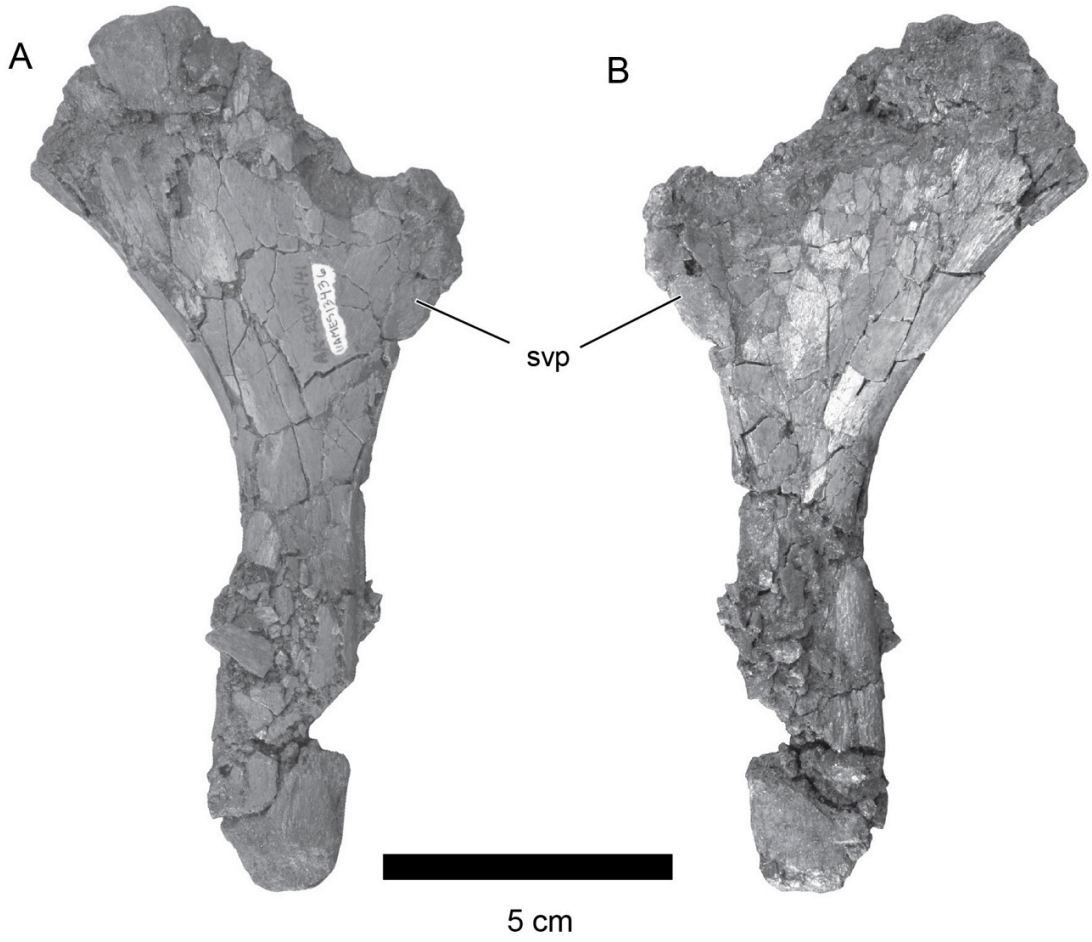

Fiugre 2-33. Sternal. Sternal (UAMES 13436) of size class 1 *Edmontosaurus* sp. nov. in ventrolateral (A) and dorsomedial (B) views. Abbreviations: svp, ventral process.

Figure 2-34 (Facing page). Scapula. Right scapula (UAMES 12711) of size class 1 *Edmontosaurus* sp. nov. in lateral (A), medial (B), and ventral (C) views. Left scapula (UAMES 22012) of size class 2 *Edmontosaurus* sp. nov. in lateral view (D). Left scapula (UAMES 29996) of size class 3 *Edmontosaurus* sp. nov. in lateral view (E). Abbreviations: cb, cudal buttress; cs, coronoid facet; cpr, coracoid process; dp, deltoid process; gf, glenoid fossa; pap, pseudoacromion process; scb, scapular blade.

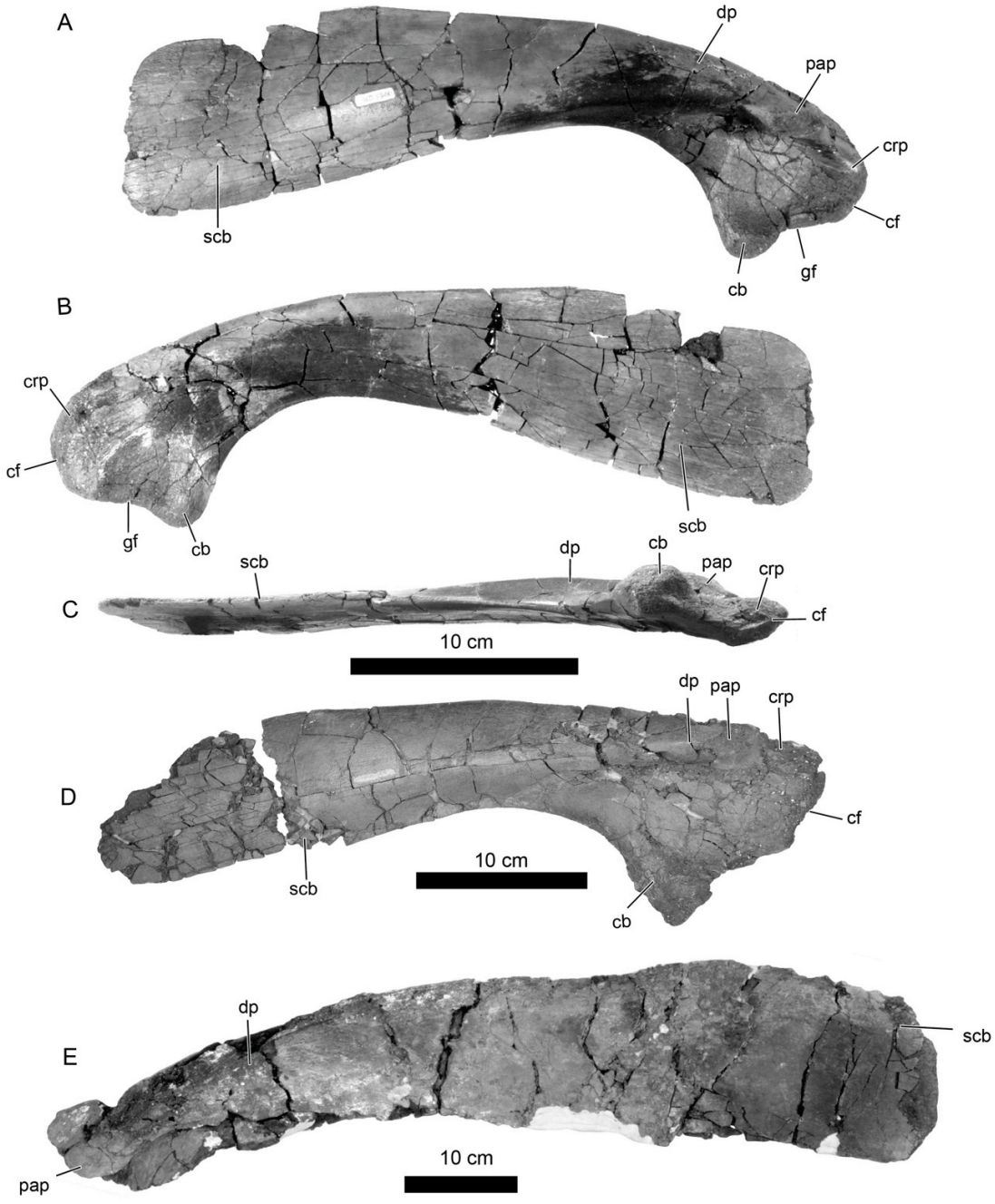
A
dp
pap
crp
cf
scb
cb
gf
B
crp
cf
gf
cb
scb
C
scb
dp
cb
pap
crp
cf
10 cm
D
dp
pap
crp
cf
scb
10 cm
cb
E
dp
scb
pap
10 cm

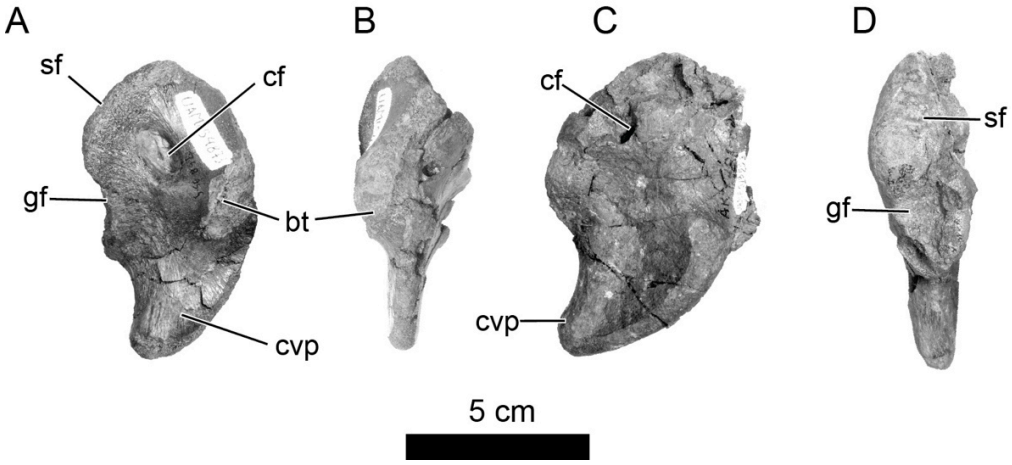

Figure 2-35. Coracoid. Right coracoid (UAMES 4873) of size class 1 *Edmontosaurus* sp. nov. in anterolateral (A) and anteromedial (B) views. Left coracoid (UAMES 13553) of size class 1 *Edmontosaurus* sp. nov. in posteromedial (C) and posterolateral views. Abbreviations: bt, biceps tubercle; cf, coracoid foramen; cvp, coracoid ventral process; gf, glenoid fossa, sf, scapular facet.

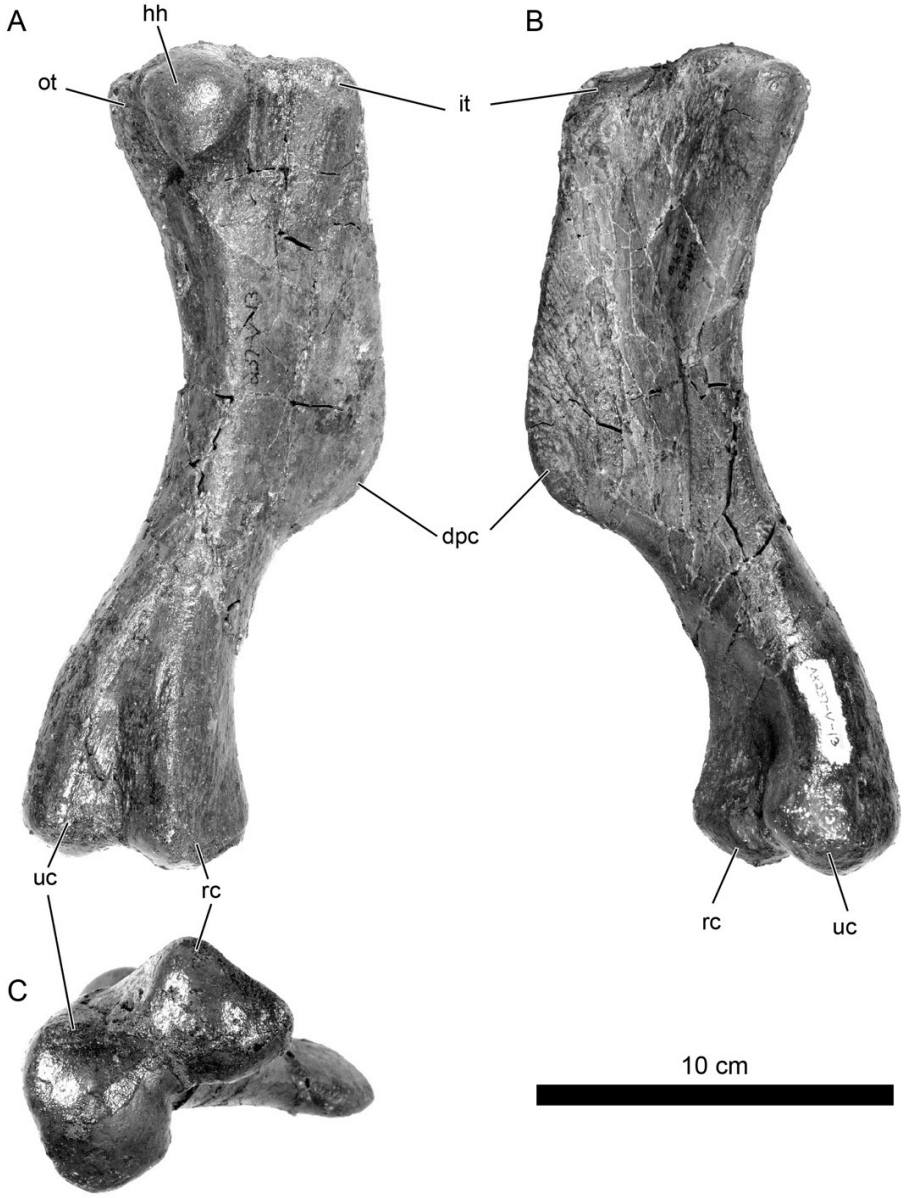

Figure 2-36. Humerus. Right humerus (UAMES 21596) of size class 1 *Edmontosaurus* sp. nov. in posterior (A), medial (B), and distal (C) views. Abbreviations: dpc, deltopectoral crest; hh, humeral head; it, inner tuberosity; ot, outer tuberosity; rc, radial condyle; uc, ulnar condyle.

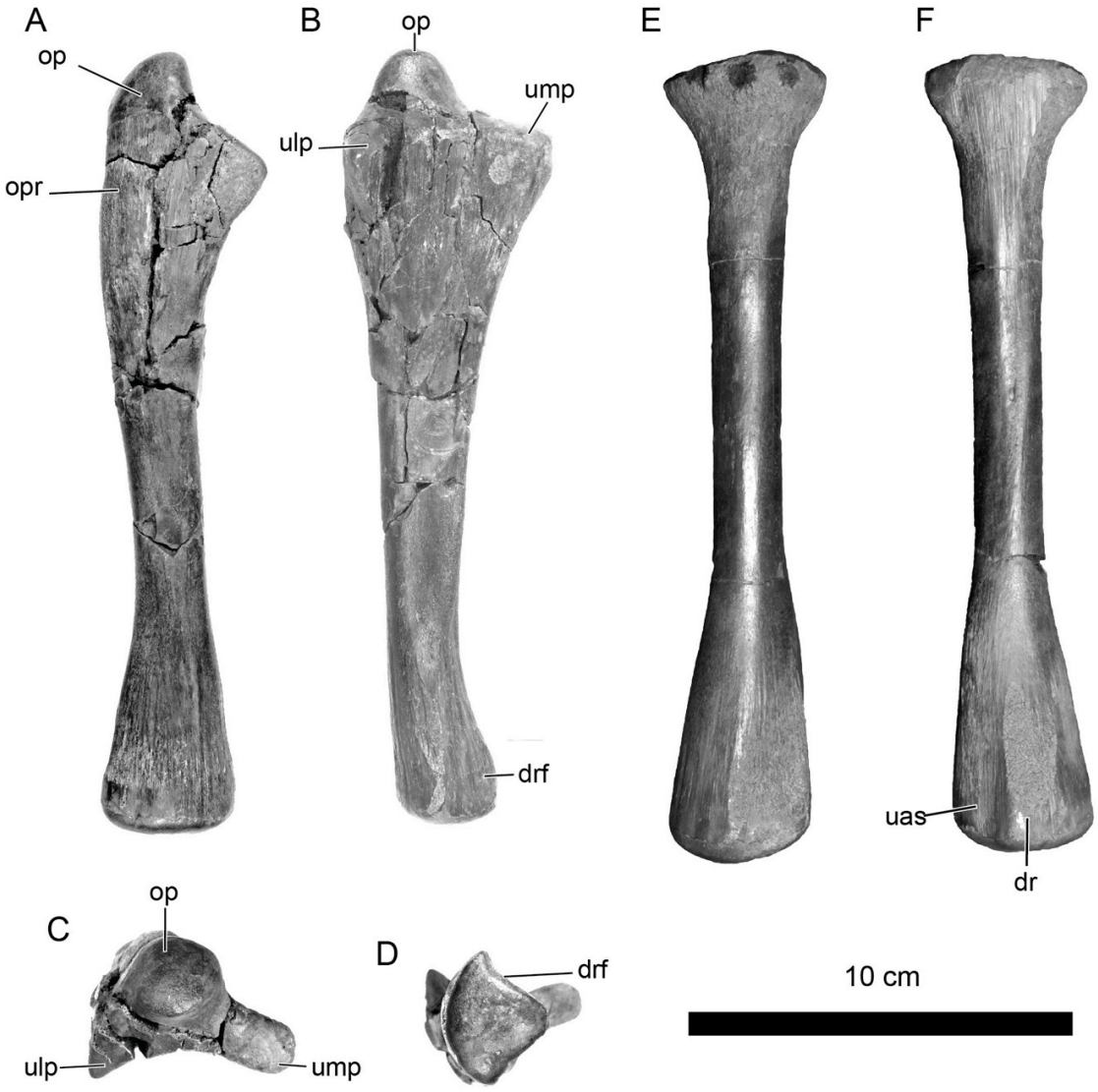

Figure 2-37. Ulna and radius. Right ulna (UAMES 12525) of size class 1 *Edmontosaurus* sp. nov. in lateral (A), anterior view (B), proximal view (C), and distal view (D). Left radius (UAMES 6272) of size class 1 *Edmontosaurus* sp. nov. in anterior (E) and posterior (F) views. Abbreviations: drf, distal radial facet; dr, distal ridge; op, olecranon process; opr, olecranon process ridge; ump, medial process; uas, ulnar articulation surface; ulp, lateral process.

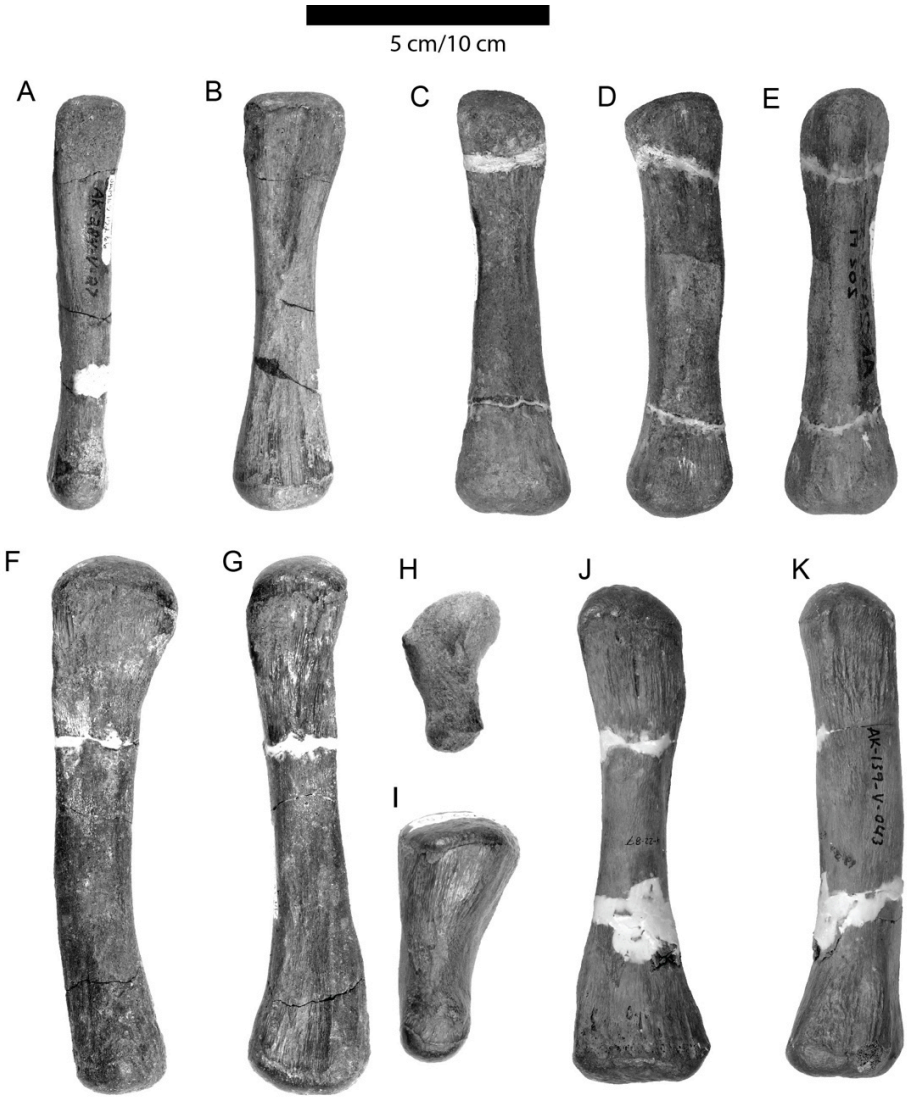

Figure 2-38. Metacarpals. Right metacarpal II (UAMES 13266) of size class 1 *Edmontosaurus* sp. nov. in dorsal (A), and lateral (B) views. Right metacarpal III (UAMES 13279, reversed) of size class 1 *Edmontosaurus* sp. nov. in dorsal (C), lateral (D), and ventral (E) views. Left metacarpal IV (UAMES 18068) of size class 1 *Edmontosaurus* sp. nov. in dorsal (F) and medial (G) views. Right metacarpal V (UAMES 16733) of a small size class 1 *Edmontosaurus* sp. nov. (?) in medial view (H). Right metacarpal V (UAMES 29676) of a small size class 1 *Edmontosaurus* sp. nov. (?) in medial view (I). Left metacarpal III
(UAMES 16215) of size class 3 *Edmontosaurus* sp. nov. in anterior (J), and lateral (K) views (K); Scale bar is 10 cm from (A) to (G), 5 cm for (I) and (J).

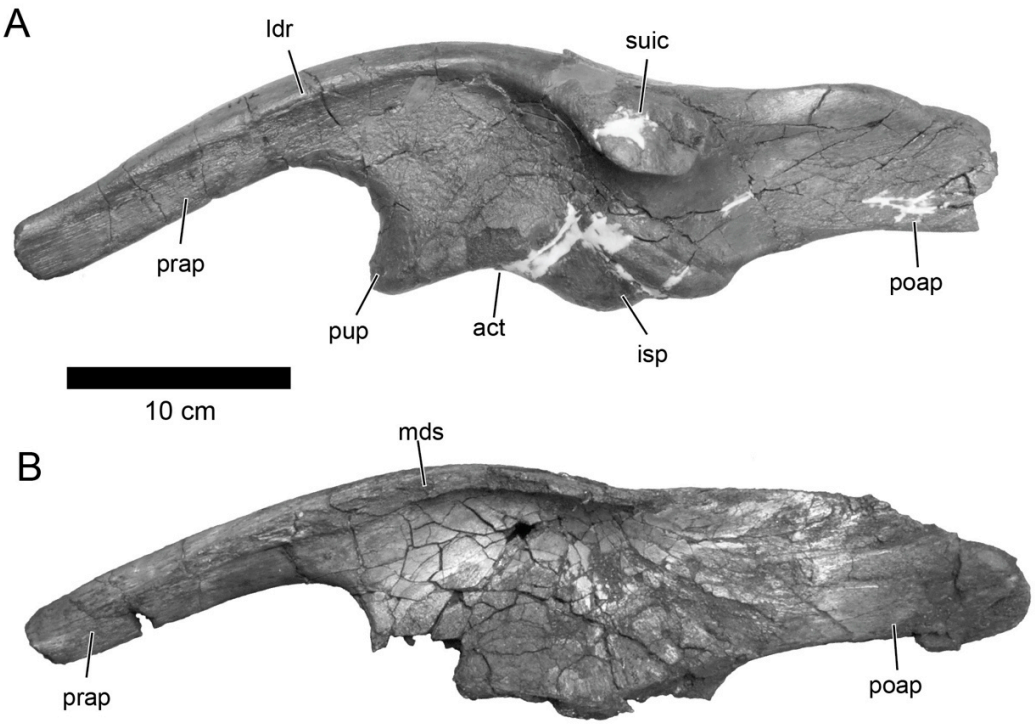

Figure 2-39. Ilium. Left ilium (UAMES 6637) of size class 1 *Edmontosaurus* sp. nov. in lateral view (A). Right ilium (UAMES 13293) of size class 1 *Edmontosaurus* sp. nov. in medial view (B). Abbreviations: act, acetabulum; isp, ischial peduncle; ldr, lateral dorsal ridge; mds, medial dorsal shelf; poap, postacetabular process; prap, preacetabular process; pup, pubic peduncle; suic, suprailiac crest.

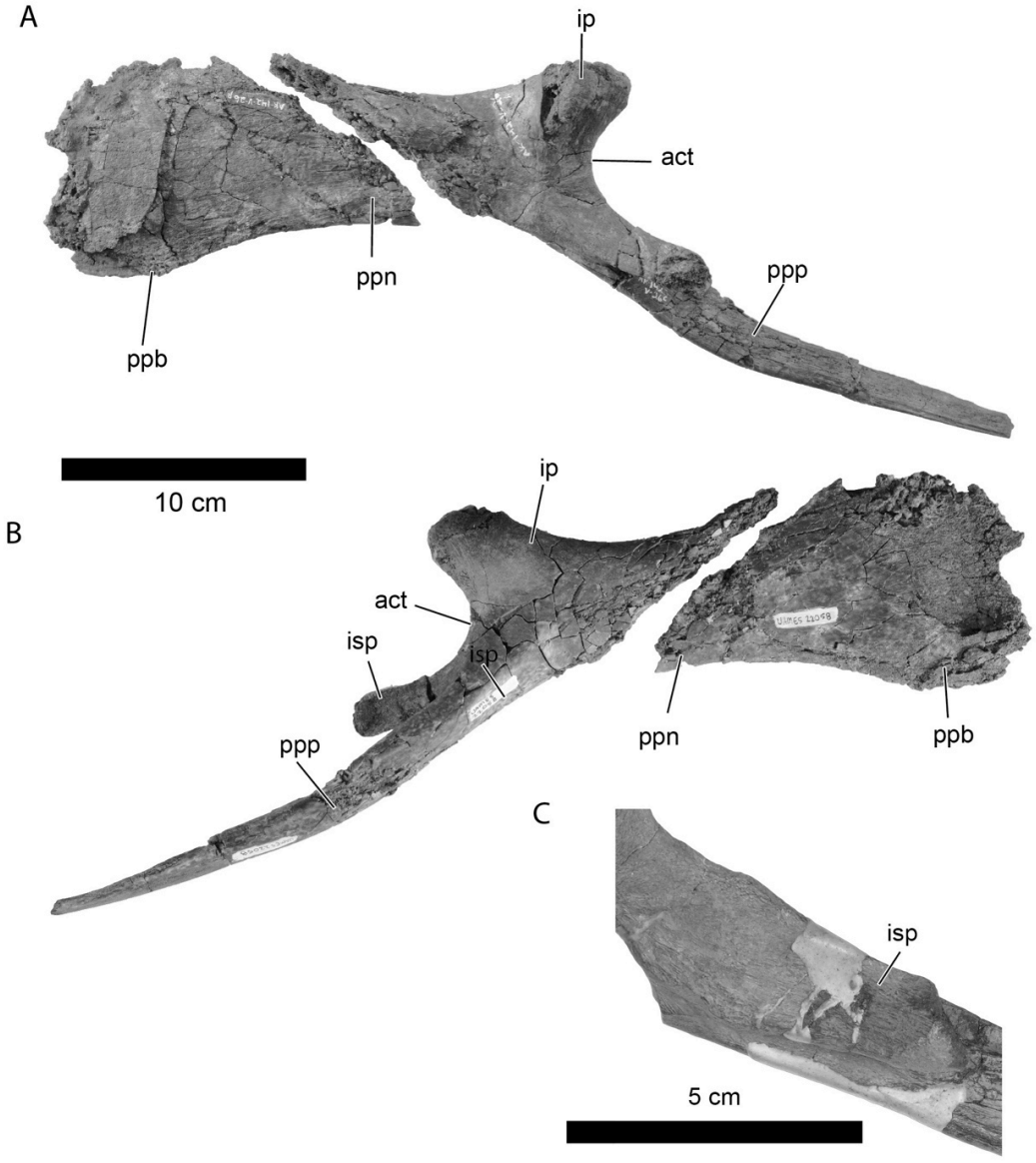

Figure 2-40. Pubis. Left pubis of size class 1 of *Edmontosaurus* sp. nov. in lateral (A) and medial (B) views (UAMES 22058). Close up of the ischial peduncle (C, UAMES 13683) of size class 1 *Edmontosaurus* sp. nov. Abbreviations: ip, iliac peduncle; isp, ischial peduncle; ppb, prepubic blade; ppn, prepubic neck; ppp, postpubic process.

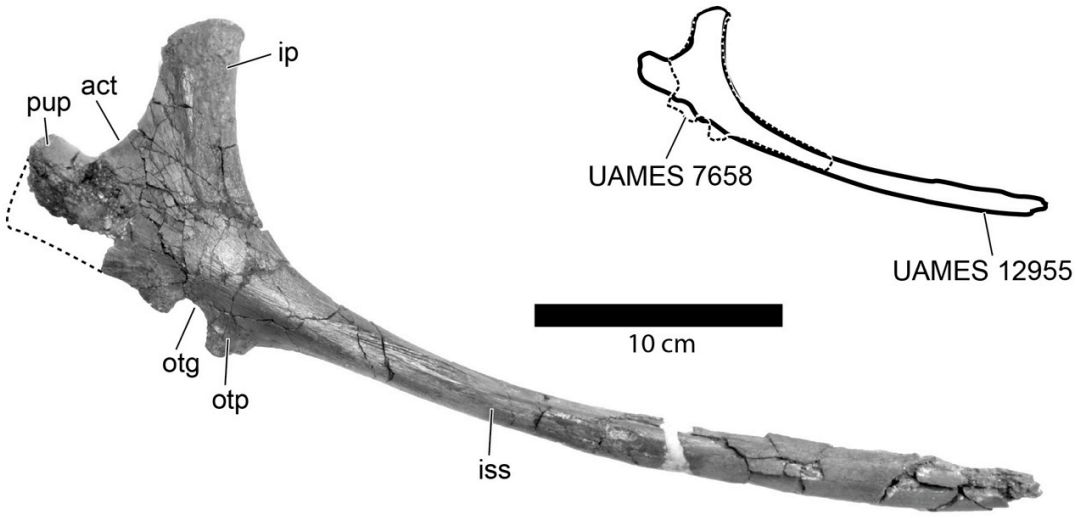

Figure 2-41. Ischium. Composite images of left ischia (UAMES 7658 and UAMES 12955) of size class 1 *Edmontosaurus* sp. nov. in lateral view. Abbreviations: act, acetabulum; ip, iliac peduncle; iss, ischium shaft; otg, obturator gutter; otp, obturator process; pup, pubic peduncle.

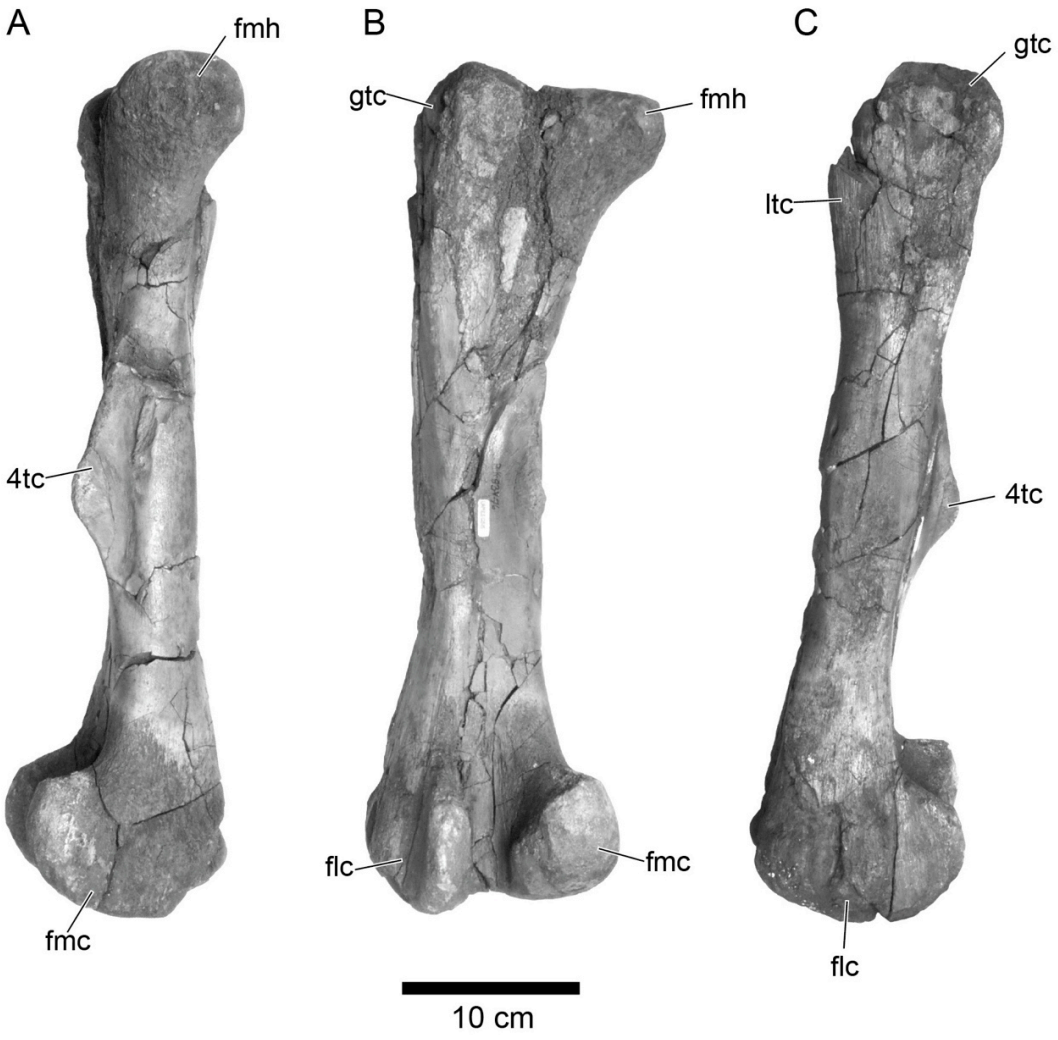

Figure 2-42. Femur. Femur (UAMES 12515) of size class 1 *Edmontosaurus* sp. nov. in medial (A), dorsal (B), and lateral (C) views. Abbreviations: fmh, femoral head; ltc, lessor trochanter; gtc, greater trochanter; 4tc, fourth trochanter; fmc, femur medial condyle; flc, femur lateral condyle.

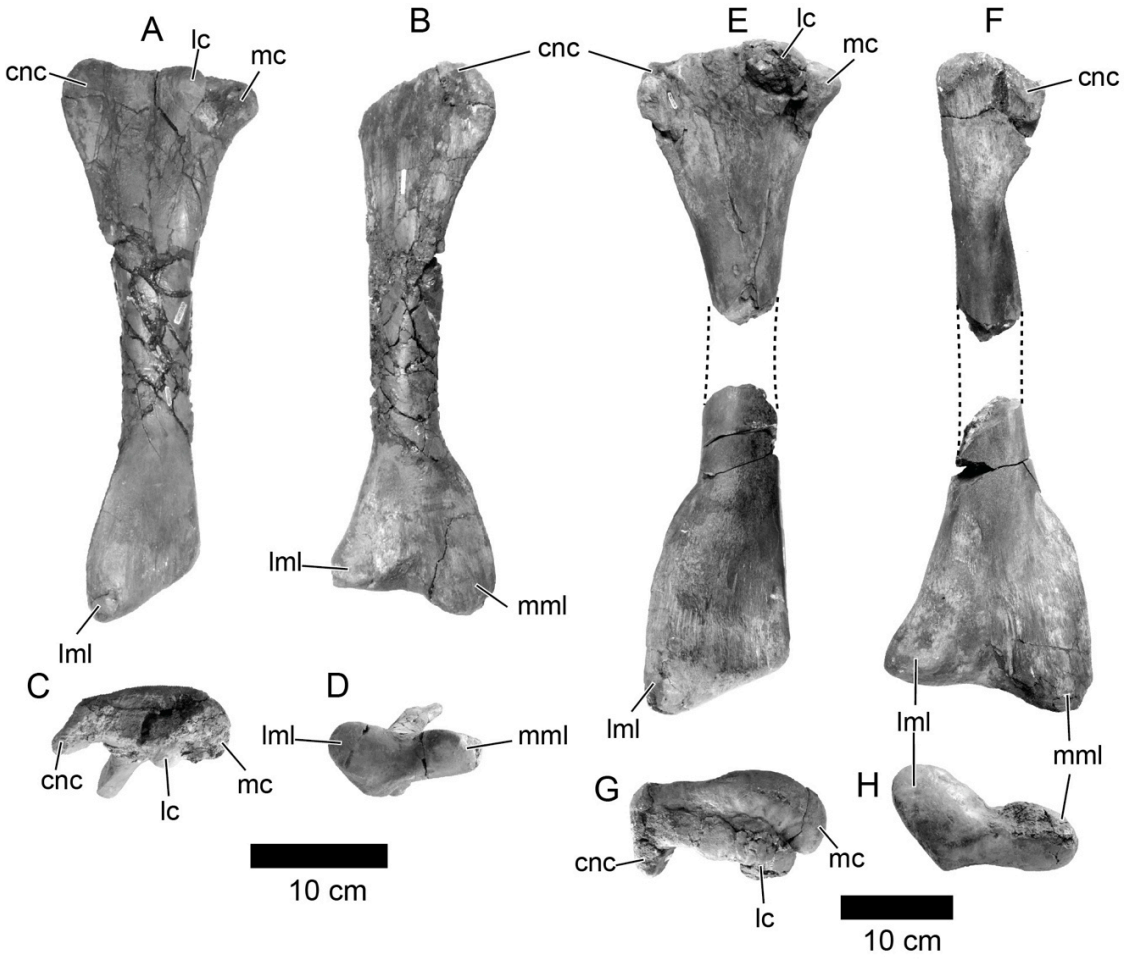

Figure 2-43. Tibia. Left tibia (UAMES 12715) of size class 1 *Edmontosaurus* sp. nov. in lateral (A), ventral (B), proximal (C), and distal (D) views. Right tibia (UAMES 12518, reversed) of size class 2 *Edmontosaurus* sp. nov. in lateral (E), ventral (F), proximal (G), and distal (H) views. Abbreviations: cnc, cnemial crest; lc, lateral condyle; lml, lateral malleolus; mc, medial condyle; mml, medial malleolus.

Figure 2-44. Fibular. Left fibula (UAMES 15553) of size class 1 *Edmontosaurus* sp. nov. in ventral (A), and dorsal (B) views. Left fibula (UAMES 13120) of size class 3 *Edmontosaurus* sp. nov. in dorsal view (C). Abbreviations: dtjf, distal tibiofibular joint facet (enclosed in the dashed line); fh, fibular head; lml, lateral malleolus; ptjf, proximal tibiofibular joint facet (enclosed in the dashed line).

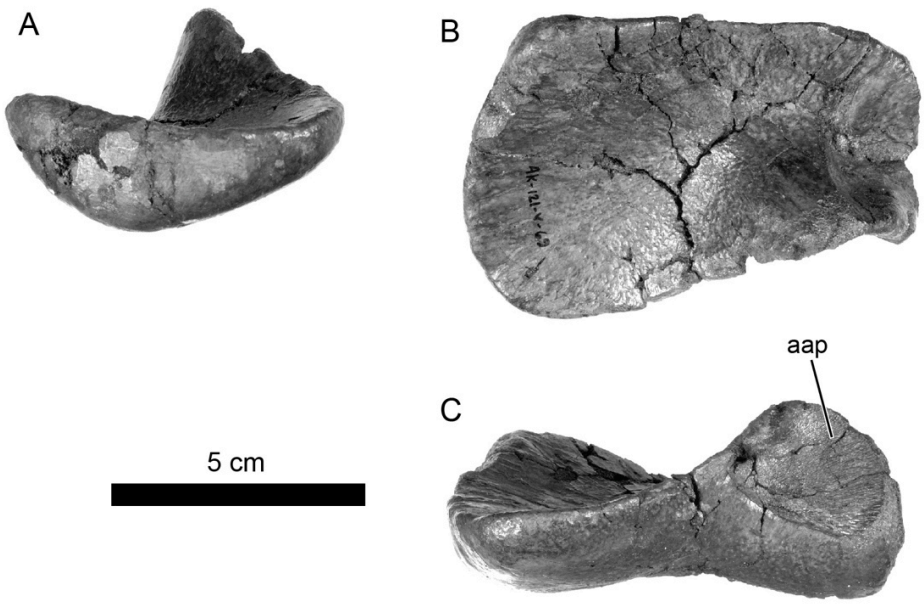

Figure 2-45. Astragalus. Right astragalus (UAMES 21950) of size class 1 *Edmontosaurus* sp. nov. in medial (A), proximal (B), and anterior (C) views. Abbreviations: aap, ascending anterior process.

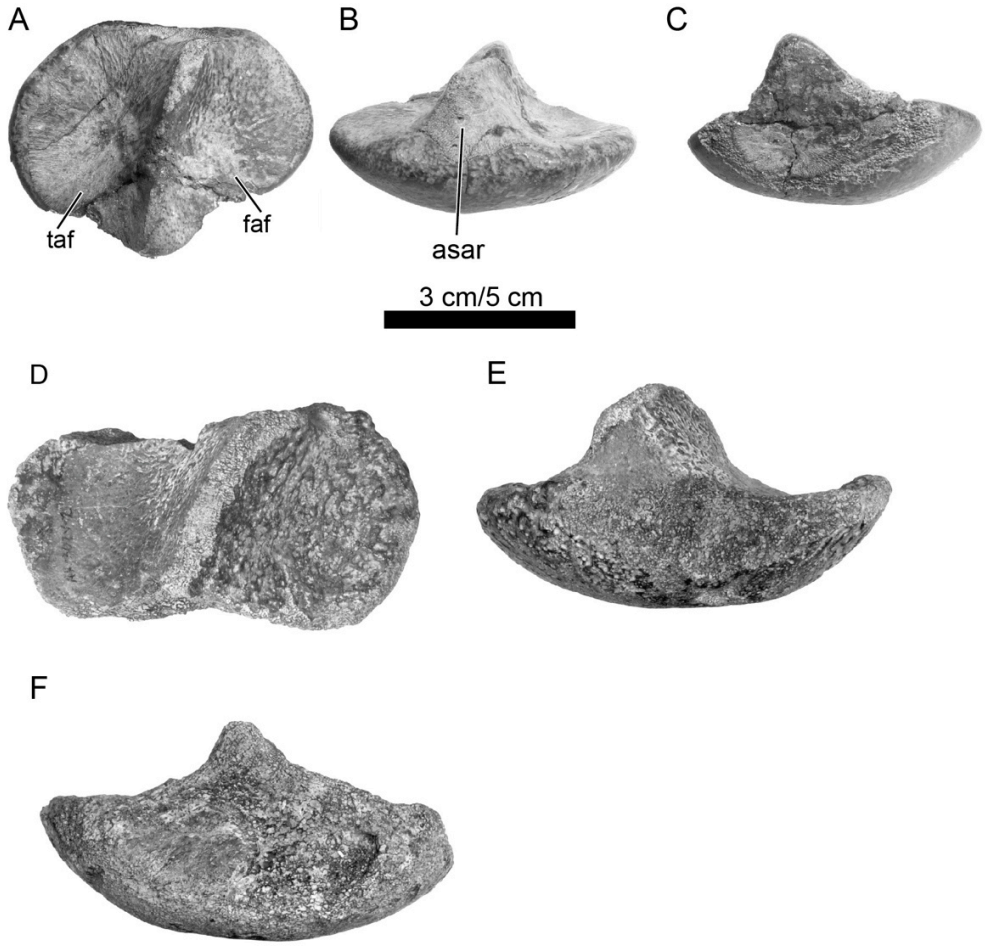

Figure 2-46. Calcaneum. Calcaneum (UAMES 21884) of size class 1 *Edmontosaurus* sp. nov. in proximal (A), medial (B), lateral (C) views. Calcaneum (UAMES 18059) of size class 3 *Edmontosaurus* sp. nov. in proximal (D), medial (E) and lateral (F) views. Abbreviations: asar, astragalar articular region; taf, tibia articular fact; faf, fibular articular facet. Scale bar equals 3 cm for A-C, and 5 cm for D-F.

Figure 2-47 (facing page). Metatarsals. Right metatarsal II (UAMES 19595, reversed) of size class 1 *Edmontosaurus* sp. nov. in medial (A) and dorsal (B) views. Left metatarsal II (UAMES 13012) of size class 2 *Edmontosaurus* sp. nov. in medial (C), and dorsal (D) views. Right metatarsal III (UAMES 12585) of size class 1 *Edmontosaurus* sp. nov. in dorsal (A), and medial (B) views. Right metatarsal III (UAMES 7652) of size class 2 *Edmontosaurus* sp. nov. in dorsal (C) and medial (D) views. Left metatarsal IV (UAMES 22374) of size class 1 *Edmontosaurus* sp. nov. in medial (I) view, and dorsal (J) views. Left metatarsal IV (UAMES 22629) of size class 2 *Edmontosaurus* sp. nov. in medial (K), and dorsal (L) views. Right metatarsal IV (UAMES 12545, reversed) of size class 3 *Edmontosaurus s*p. nov. in medial (M), and dorsal (N) views. Abbreviations: mfg, mediodrosal flange; mtb, medial tuberosity; vfg, medioventral flange.

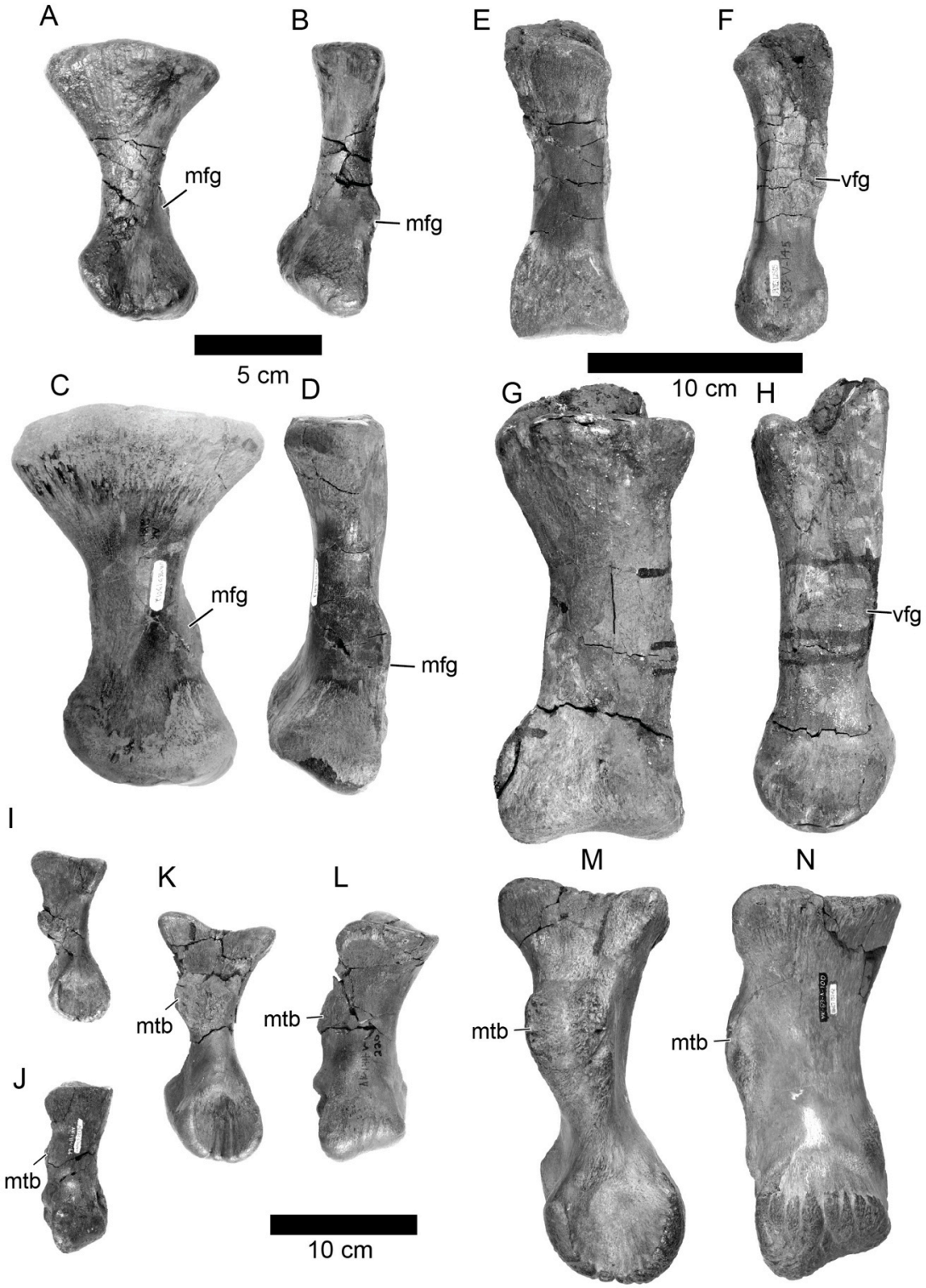
A
B
E
F
mfg
mfg
vfg
5 cm
10 cm
C
D
G
H
mfg
mfg
vfg
I
K
L
M
N
mtb
mtb
mtb
mtb
J
mtb
10 cm

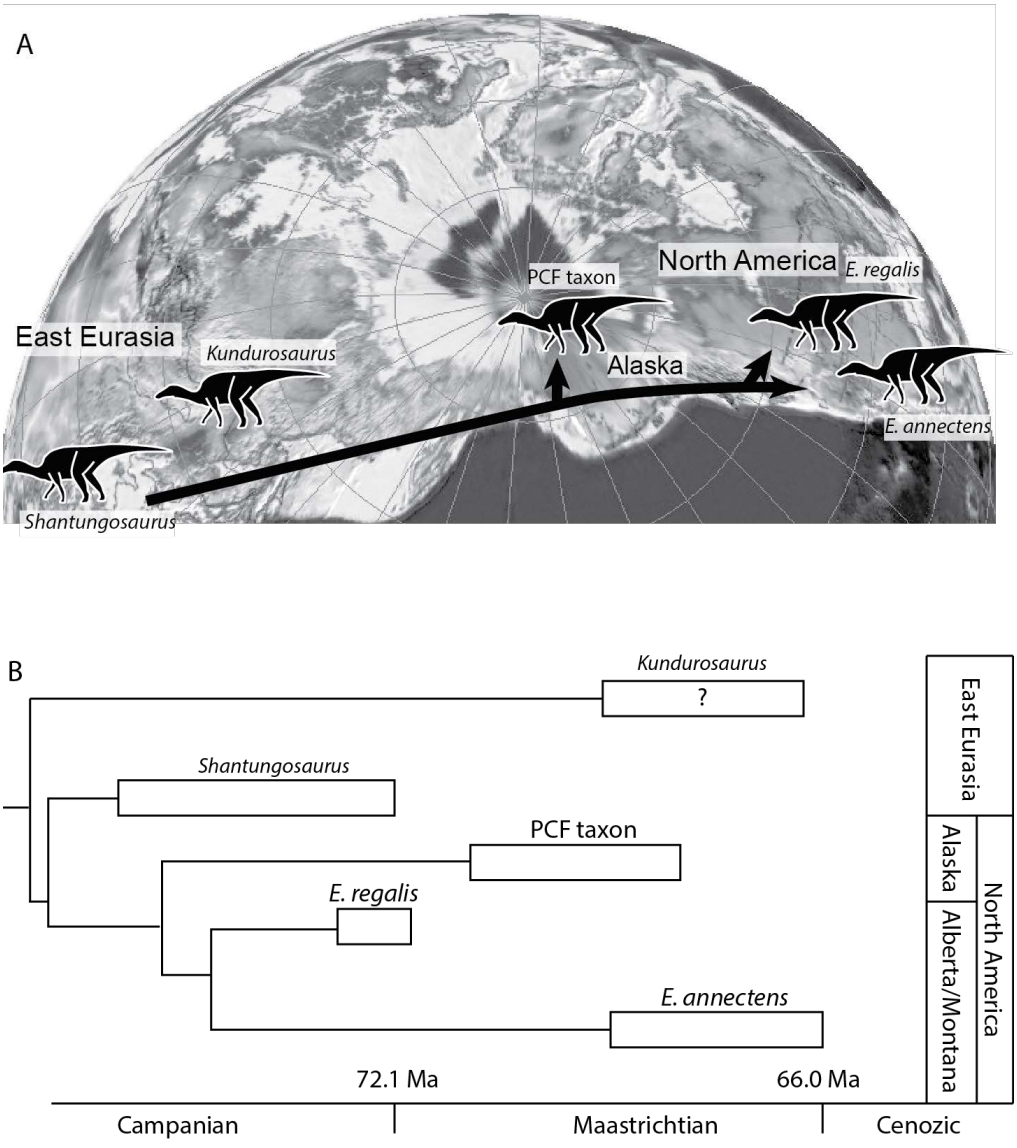

Figure 48. Paleobiogeography of Edmontosaurini. (A) Dispersion model of Edmontosaurini from Asia to North America. (B) Time calculated cladogram. The phylogenic position of the Alaskan edmontosaur is consistent with the location of Alaska. The map (polar view at 68 Ma) is after Moore and Scotese [85].

2.7 Tables

Table 2-1. Number of specimens examined in the study.

Element	Size class 1	Size class 2	Size class 3
Premaxilla	5	1	
Nasal	9		
Prefrontal	5		
Frontal	9	2	
Lacrimal	5		
Jugal	8		1
Quadratojugal	10		
Quadrate	6	2	
Postorbital	9		1
Squamosal	7	1	
Maxilla	6		
Laterosphenoid	6		
Prootic	3		
Basisphenoid	8	1	1
Basioccipital	5		
Parietal	7		
Supraoccipital	5	1	
Exoccipital-opisthotic	8	2	
Ectopterygoid	3	1	
Palatine	3		
Pterygoid	3		1
Predentary	3	1	
Dentary	11	2	
Surangular	10	1	1
Angular	2		
Splenial	2		
Cervical vertebrae	1	2 (?)	1
Dorsal vertebrae	7	2	2
Dorsal rib			
Sacrum			1
Caudal vertebrae	14	3	4
Dorsal rib	7		1
Sternum	1		
Scapula	5	3	1
Coracoid	5		
Humerus	23	3	1
Ulna	8	3	1
Radius	12	2	
Metacarpal II	2		
Metacarpal III	4		1
Metacarpal IV	3		
Metacarpal V	4		
Ilium	3		
Pubis	6	1	
Ischium	2		
Femur	6	2	
Tibia	9	2	
Fibula	6		
Calcaneum	5		1
Astragalus	4		
Metatarsal II	10	1	
Metatarsal III	13	3	
Metatarsal IV	7	3	2
Sum	325	43	21

Table 2-2. Comparison of the lengths of the femur, humerus, and fibula

Specimen	Femur (cm)	Femur/Humerus	Femur/Tibia
Alaskan edmontosaur size class 1 (average)	42.2 (n = 6)	1.94 (n = 13)	1.13 (n = 9)
E. regalis			
CMN 2288	119	1.73	1.08
CMN 8399	112	1.91	1.20
ROM 801	124	1.91;	1.24
ROM 867	116	1.76	1.02
E. annectens			
CMN 8509	100	n/a	1.27
AMNH 5730	114	1.69	1.20
YPM 2182	106	1.80	1.12
Average and 2 sigma of *E. regalis* and *E. annectens*			
		1.80 ± 0.18	1.16 ± 0.18

Except for the PCF specimen and the length of the tibia of CMN 2288, measurements are cited from Lull and Wright [72] and Brett-Surman [86] and calculated. The n values next to the Femur/Humerus and Femur/Tibia values for the PCF juvenile indicate the numbers of humeri and tibia measured respectively. Average and SD are based on specimens of both *E. regalis* and *E. annectens.*

2.8 References

1. Brouwers EM, Clemens, WA, Spicer, RA, Ager, TA, Carter LD, et al. (1987) Dinosaurs on the North Slope, Alaska: High latitude, latest Cretaceous environments. Science 237: 1608-1610.
2. Davies KL (1987) Duck-bill dinosaurs (Hadrosauridae, Ornithischia) from the North Slope of Alaska. Journal of Paleontology 61: 198-200.
3. Nelms LG (1989) Late Cretaceous dinosaurs from the North Slope of Alaska. Journal of Vertebrate Paleontology, Abstracts of Papers 9: 34A.
4. Gangloff RA (1998) Arctic dinosaurs with emphasis on the Cretaceous record of Alaska and the Eurasian-North American connection. New Mexico Museum of Natural History and Science Bulletin 14: 211-220.
5. Fiorillo AR, Gangloff RA (2000) Theropod teeth from the Prince Creek Formation (Cretaceous) of Northern Alaska, with speculations on Arctic dinosaur paleoecology. Journal of Vertebrate Paleontology 20: 675-682.
6. Fiorillo AR (2004) The dinosaur of arctic Alaska. Scientific American 291: 84-91.
7. Gangloff RA, Fiorillo AR, Norton DW (2005) The first pachycephalosaurine (Dinosauria) from the paleo-Arctic of Alaska and its paleogeographic implications. Journal of Paleontology 79: 997-1001.
8. Sullivan RM (2006) A taxonomic review of the Pachycephalosauridae (Dinosauria: Ornithischia). New Mexico Museum of Natural History and Science Bulletin 35: 347-365.
9. Fiorillo AR (2008) On the occurrence of exceptionally large teeth of *Troodon* (Dinosauria: Saurischia) from the Late Cretaceous of northern Alaska. Palaios 23: 322-328.
10. Fiorillo AR, Tykoski RS, Currie PJ, McCarthy PJ, Flaig P (2009) Description of two partial *Troodon* braincases from the Prince Creek Formation (Upper Cretaceous), North Slope Alaska. Journal of Vertebrate Paleontology 29: 178-187.

11. Brown CM, Druckenmiller P (2011) Basal ornithopod (Dinosauria: Ornithischia) teeth from the Prince Creek Formation (early Maastrichtian) of Alaska. Canadian Journal of Earth Sciences 48: 1342-1354.
12. Erickson GM, Druckenmiller PS (2011) Longevity and growth rate estimates for a polar dinosaur: a *Pachyrhinosaurus* (Dinosauria: Neoceratopsia) specimen from the North Slope of Alaska showing a complete developmental record. Historical Biology 23: 327-334.
13. Fiorillo AR, Tykoski RS (2012) A new Maastrichtian species of the centrosaurine ceratopsid *Pachyrhinosaurus* from the North Slope of Alaska. Acta Palaeontologica Polonica 57: 561-573.
14. Mannion PD, Benson RBJ, Upchurch P, Butler RJ, Carrano MT et al. (2012) A temperate palaeodiversity peak in Mesozoic dinosaurs and evidence for Late Cretaceous geographical partitioning. Global Ecology and Biogeography 21: 898-908.
15. Druckenmiller P, Erickson G, Brinkman D, Brown C, Mori H (2013) Evidence for a distinct, early Maastrichtian polar dinosaur fauna from the Prince Creek Formation of northern Alaska. Journal of Vertebrate Paleontology, Program and Abstracts 2013: 117.
16. Gryc G, Patton Jr WW, Payne TG (1951) Present Cretaceous stratigraphic nomenclature of northern Alaska. Journal of the Washington Academy of Sciences 41: 159-167.
17. Mull CG, Houseknecht DW, Bird KJ (2003) Revised Cretaceous and Tertiary stratigraphic nomenclature in the Colville Basin, northern Alaska. US Gelogical Survey Professional Paper 1673: 1-51.
18. Flaig PP, McCarthy PJ, Fiorillo AR (2011) A tidally influenced, high-latitude coastal-plain: The upper Cretaceous (Maastrichtian) Prince Creek Formation, North Slope, Alaska. In: Davidson SK, Leleu S, North. CP, editors. From river to rock record: The Preservation of fluvial sediments and their subsequent interpretation. pp. 233-264.

19. Frederiksen NO, Ager TA, Edwards LE (1988) Palynology of Maastrichtian and Paleocene rocks, lower Colville River region, North Slope of Alaska. Canadian Journal of Earth Sciences 25: 512-527.
20. Frederiksen NO (1991) Pollen zonation and correlation of Maastrichtian marine beds and associated strata, Ocean Point dinosaur locality, North Slope, Alaska. United States Geological Survey Bulletin 1990-E: E1-E24.
21. Frederiksen NO, Mclntyre DJ, Sheehan TP (2002) Palynological dating of some Upper Cretaceous to Eocene outcrop and well samples from the region extending from the easternmost part of NPRA in Alaska to the western part of Arctic National Wildlife Refuge, North Slope of Alaska. US Geological Survey Open-File Report 02-405: 1-37.
22. Brouwers EM, Deckker PD (1993) Late Maastrichtian and Danian ostracode faunas from Northern Alaska; reconstructions of environment and paleogeography. Palaios 8: 140-154.
23. McKee E, Conrad JE, Tuin BD (1989) Better dates for arctic dinosaurs. Eos 70: 74.
24. Conrad JE, Mackee EH, Turrin BD (1992) Age of tephra beds at the Ocean Point Dinosaur Locality, North Slope, Alaska, based on K-Ar and $^{40}Ar/^{39}Ar$ analyses. Washington DC: United States Government Printing Office. 12 p.
25. Flores RM, Myers MD, Houseknecht DW, Stricker GD, Brizzolara DW et al. (2007) Stratigraphy and facies of Cretaceous Schrader Bluff and Prince Creek Formations in Colville River Bluffs, North Slope, Alaska. United States Geological Survey Professional Paper 1747: 1-52.
26. Flaig PP (2010) Depositional environments of the Late Cretaceous (Maastrichtian) dinosaur-bearing Prince Creek Formation: Colville River region, North Slope, Alaska. Unpublished Ph.D. thesis. Fairbanks, AK: University of Alaska Fairbanks. 311 p.

27. Witte, WK, Stone, DB, Mull CG (1987) Paleomagnetism, paleobotany, and paleogeography of the Cretaceous, North Slope, Alaska. In: Tailleur, IL, Weimer P, editors. Alaska North Slope Geology. Bakersfield, CA: Pacific Section, Society of Economic Paleontologists and Mineralogists. pp. 571-579.
28. Fiorillo AR, McCarthy PJ, Brandlen E, Flaig PP, Norton D et al. (2007) Paleontology, sedimentology, paleopedology, and palynology of the Kikak-Tegoseak Quarry (Prince Creek Formation, Late Cretaceous), Northern Alaska. In: Braman DR, editor. Ceratopsian symposium: Short papers, abstracts and programs. Drumheller, AB: pp. 48-49.
29. Spicer RA, Parrish JT (1990) Late Cretaceous-early Tertiary palaeoclimates of northern high latitudes: a quantitative view. Journal of the Geological Society, London Journal of the Geological Society 147: 329-341.
30. Spicer RA, Herman AB (2010) The Late Cretaceous environment of the Arctic: A quantitative reassessment based on plant fossils. Palaeogeography, Palaeoclimatology, Palaeoecology 295: 423-442.
31. Flaig PP, McCarthy PJ, Fiorillo AR (2013) Anatomy, evolution, and paleoenvironmeltal interpretation of an ancient arctic coastal plain: integrated paleopedology and palynology from the Upper Cretaceous (Maastrichtian) Prince Creek Formation, North Slope, Alaska, USA. In: Driese SG, Nordt LC, editors. New frontiers in paleopedology and terrestrial paleoclimatology: Paleosols and soil surface analog systems. pp. 179-230.
32. Clemens WA, Nelms LG (1993) Paleoecological implications of Alaskan terrestrial vertebrate fauna in latest Cretaceous time at high paleolatitudes. Geology 21: 503-506.
33. Gangloff RA (1994) The record of Cretaceous dinosaurs in Alaska: an overview. In: Thurston DK, Fujita K, editors. Proceedings of the 1992 international conference on Arctic margins. Alaska Geological Society. pp. 399-404.

34. Fiorillo AR (2008) Dinosaurs of Alaska: Implications for the Cretaceous origin of Beringia. The terrane puzzle: New perspectives on paleontology and stratigraphy from the North American cordillera 442: 313-325.
35. Gangloff RA, Fiorillo AR (2010) Taphonomy and paleoecology of a bonebed from the Prince Creek Formation, North Slope, Alaska. Palaios 25: 299-317.
36. Fiorillo AR, McCarthy PJ, Flaig PP (2010) Taphonomic and sedimentologic interpretations of the dinosaur-bearing Upper Cretaceous Strata of the Prince Creek Formation, Northern Alaska: Insights from an ancient high-latitude terrestrial ecosystem. Palaeogeography, Palaeoclimatology, Palaeoecology 295: 376-388.
37. Horner JR, Weishampel DB, Forster CA (2004) Hadrosauridae. In: Weishampel DB, Dodson P, Osmølska H, editors. The dinosauria. Berkeley and Los Angels, California: University of California Press. pp. 438-463.
38. Seeley HG (1887) Researches on the structure, organization, and classification of the fossil reptilia. I. On *Protorosaurus Speneri* (von Meyer). Philosophical Transactions of the Royal Society of London B 178: 187-213.
39. Marsh OC (1881) Principal characters of American Jurassic dinosaurs, IV. American Journal of Science 3: 167-170.
40. Cope ED (1870) Synopsis of the extinct Batrachia and Reptilia of North America. Transactions of the American Philosophical Society, 2nd series 14: 252.
41. Brown B (1914) *Corythosaurus casuarius*, a new crested dinosaur from the Belly River Cretaceous; with provisional classification of the family Trachodontidae. Bulletin of the American Museum of Natural History 33: 559-565.
42. Prieto-Márquez A (2010) Global phylogeny of Hadrosauridae (Dinosauria: Ornithopoda) using parsimony and Bayesian methods. Zoological Journal of the Linnean Society 159: 435-502.
43. Lambe LM (1917) A new genus and species of crestless hadrosaur from the Edmonton Formation of Alberta. Ottawa Naturalist 31: 65-73.

44. Horner JR (1983) Cranial osteology and morphology of the type specimen of *Maiasaura peeblesorum* (Ornithischia: Hadrosauridae), with discussion of its phylogenetic position. Journal of Vertebrate Paleontology 3: 29-38.
45. Brown B (1916) A new crested trachodont dinosaur, *Prosaurolophus maximus*. Bulletin of the American Museum of Natural History 35: 701-708.
46. Horner JR (1992) Cranial morphology of *Prosaurolophus* (Ornithischia: Hadrosauridae) with descriptions of two new hadrosaurid species and an evaluation of hadrosaurid phylogenetic relationships. Museum of the Rockies Occasional paper 2: 1-119.
47. Sternberg CM (1953) A new hadrosaur from the Oldman Formation of Alberta: discussion of nomenclature. National Museum of Canada, Bulletin 128: 275-286.
48. Cuthbertson RS, Holmes RB (2010) The first complete description of the holotype of *Brachylophosaurus canadensis* Sternberg, 1953 (Dinosauria: Hadrosauridae) with comments on intraspecific variation. Zoological Journal of the Linnean Society 159: 373-397.
49. Godefroit P, Bolotsky YL, Lauters P (2012) A new saurolophine dinosaur from the Latest Cretaceous of far Eastern Russia. PLoS ONE 7: e36849.
50. Bolotsky YL, Godefroit P (2004) A new hadrosaurine dinosaur from the Late Cretaceous of Far Eastern Russia. Journal of Vertebrate Paleontology 24: 351-365.
51. Gates TA, Sampson SD (2007) A new species of *Gryposaurus* (Dinosauria: Hadrosauridae) from the late Campanian Kaiparowits Formation, southern Utah, USA. Zoological Journal of the Linnean Society 151: 351-376.
52. Lambe ML (1920) The hadrosaur *Edmontosaurus* from the Upper Cretaceous of Alberta. Canada Geological Survey Memoir 120: 1-79.
53. Prieto-Márquez A (2011) Cranial and appendicular ontogeny of *Bactrosaurus johnsoni*, a hadrosauroid dinosaur from the Late Cretaceous of northern China. Palaeontology 54: 773-792.

54. Horner JR, Currie PJ (1994) Embryonic and neonatal morphology and ontogeny of a new species of *Hypacrosaurus* (Ornithischia, Lambeosauridae) from Montana and Alberta. In: Carpenter KH, Karl F., Horner JR, editors. Dinosaur eggs and babies. Cambridge, UK: Cambridge University Press. pp. 312-336.
55. Bell PR (2010) Redescription of the skull of *Saurolophus osborni* Brown 1912 (Ornithischia: Hadrosauridae). Cretaceous Research 32: 30-44.
56. Horner JR, Makela R (1979) Nest of juveniles provides evidence of family structure among dinosaurs. Nature 282: 296-298.
57. Gates TA, Horner JR, Hanna RR, Nelson CR (2011) New unadorned hadrosaurine hadrosaurid (Dinosauria, Ornithopoda) from the Campanian of North America. Journal of Vertebrate Paleontology 31: 798-811.
58. Brown B (1912) A crested dinosaur from the Edmonton Cretaceous. Bulletin of the American Museum of Natural History 31: 131-136.
59. Hu C-C (1972) A new hadrosaur from the Cretaceous of Chucheng, Shantung. Peking, China: 29 p.
60. Prieto-Márquez A (2008) Phylogeny and historical biogeography of hadrosaurid dinosaurs. Unpublished Ph.D. thesis. Tallahassee: Florida State University. 861 p.
61. Prieto-Márquez A (2005) New information on the cranium of *Brachylophosaurus canadensis* (Dinosauria, Hadrosauridae); with a revision of its phylogenetic position. Journal of Vertebrate Paleontology 25: 144-156.
62. Campione NE, Evans DC (2011) Cranial growth and variation in edmontosaurs (Dinosauria: Hadrosauridae): Implications for Latest Cretaceous megaherbivore diversity in North America. PLoS ONE 6: e25186.
63. Prieto-Márquez A, Norell MA (2010) Anatomy and relationships of *Gilmoreosaurus mongoliensis* (Dinosauria: Hadrosauroidea) from the Late Cretaceous of Central Asia. American Museum Novitates 3694: 1-49.
64. Lambe LM (1914) On *Gryposaurus notabilis*, a new genus and species of trachodont dinosaur from the Belly River Formation of Alberta, with a description of the skull of *Chasmosaurus belli*. The Ottawa Naturalist 27: 145-155.

65. Prieto-Márquez A, Salinas GC (2010) A re-evaluation of *Secernosaurus koerneri* and *Kritosaurus australis* (Dinosauria, Hadrosauridae) from the Late Cretaceous of Argentina. Journal of Vertebrate Paleontology 30: 813-837.
66. Prieto-Márquez A (2013) Skeletal morphology of *Kritosaurus navajovius* (Dinosauria: Hadrosauridae) from the Late Cretaceous of the North American south-west, with an evaluation of the phylogenetic systematics and biogeography of Kritosaurini. Journal of Systematic Palaeontology 12: 133-175.
67. Ostrom JH (1961) Cranial morphology of the hadrosaurian dinosaurs of North America. Bulletin of the American Museum of Natural History 122: 37-186.
68. Horner JR, Varricchio DJ, Goodwin MB (1992) Marine transgressions and the evolution of Cretaceous dinosaurs. Nature 358: 59-61.
69. Sternberg CM (1926) A new species of *Thespesius* from the Lance Formation of Saskatchewan. Bulletin of Geological Survey Canada 44: 73-84.
70. Prieto-Márquez A (2006) Postcranial osteology of the hadrosaurid dinosaur *Brachylophosaurus canadensis* from the Late Cretaceous of Montana. In: Carpenter K, editor. Horns and Beaks: Ceratopsian and Ornithopod Dinosaurs. Bloomington, IN: Indiana University Press. pp. 91-155.
71. Yannan JI, Xuri W, Yongqing LIU, Qiang JI (2011) Systematics, behavior and living environment of *Shantungosaurus giganteus* (Dinosauria: Hadrosauridae). Acta Geologica Sinica-English Edition 85: 58-65.
72. Lull RS, Wright NE (1942) Hadrosaurian dinosaurs of North America. Geological Society of America Special Papers 40: 1-242.
73. Parks WA (1935) New species of trachodont dinosaurs from the Cretaceous formations of Alberta: With notes on other species. University of Toronto Studies: Geological Series 37: 1-45.

74. Brett-Surman M, Wagner JR (2007) Discussion of character analysis of the appendicular anatomy in Campanian and Maastrichtian North American hadrosaurids-variation and ontogeny. In: Carpenter K, editor. Horns and beaks: Ceratopsian and ornithopod dinosaurs. Bloomington, IN: Indiana University Press. pp. 135-169.
75. Parks WA (1920) The osteology of the trachodont dinosaur *Kritosaurus incurvimanus*. University of Toronto Studies: Geological Series 11: 1-76.
76. Dilkes DW (2001) An ontogenetic perspective on locomotion in the Late Cretaceous dinosaur *Maiasaura peeblesorum* (Ornithischia: Hadrosauridae). Canadian Journal of Earth Science 38: 1205-1227.
77. Senter P (2012) Forearm orientation in Hadrosauridae (Dinosauria: Ornithopoda) and implications for museum mounts. Palaeontologia Electronica 15: 1-10.
78. Ostrom JH (1961) A new species of hadrosaurian dinosaur from the Cretaceous of New Mexico. Journal of Paleontology 575-577.
79. Gilmore CW (1933) On the dinosaurian fauna of the Iren Dabasu Formation. Bulletin of the American Museum of Natural History 67: 23-78.
80. Liu, Yongqing, Kuang H, Peng N, Xu H, Liu, Y. (2011) Sedimentary facies of dinosaur trackways and bonebeds in the Cretaceous Jiaolai Basin, eastern Shandong, China, and their paleogeographical implications. Earth Science Frontiers 18: 9-24.
81. Sereno PC (1999) The evolution of dinosaurs. Science 284: 2137-2147.
82. Godefroit P, Bolotsky Y, Alifanov V (2003) A remarkable hollow-crested hadrosaur from Russia: an Asian origin for lambeosaurines. Comptes Rendus Palevol 2: 143-151.
83. Zanno LE, Makovicky PJ (2011) On the earliest record of Cretaceous tyrannosauroids in western North America: implications for an Early Cretaceous Laurasian interchange event. Historical Biology 23: 317-325.
84. Blakey RC (2009) Paleogeography and geologic evolution of North America Available: http://cpgeosystems.com/nam.html.

85. Moore TL, Scotese CR (2012) Ancient Earth: Breakup of Pangea. Ver. 1.6. Available: http://www.ancient-earth.com.
86. Brett-Surman MK (1989) A revision of the Hadrosauridae (Reptilia: Ornithischia) and their evolution during the Campanian and Maastrichtian. Unpublished Ph.D. thesis. Washington DC: George Washington University. 272 p.

Chapter 3

Testing the migratory hypothesis for Alaskan *Edmontosaurus* using strontium isotope analysis of their teeth[3]

3.1 Abstract

During the Late Cretaceous, the Arctic had a rich dinosaurian fauna despite challenging winter conditions that included sub-freezing temperatures and prolonged darkness. The discovery of abundant remains of the hadrosaurid dinosaur *Edmontosaurus* from such high latitudes has long been of interest to many researchers who hypothesize they were either year-round residents capable of enduring winter conditions or that they migrated to more southerly environments. To test the migration hypothesis, I analyzed and compared the strontium isotope ratio ($^{87}Sr/^{86}Sr$) of seven *Edmontosaurus* teeth, five of which were removed from two well-preserved maxillary dental batteries. Additionally, three teeth of a putative non-migratory species, in this case the small theropod *Troodon*, were also analyzed. Because dinosaur enamel is very thin (~30-90 μm), I used laser-ablation MC-ICP-MS to measure the strontium compositions of the teeth. The enamel preserved statistically different $^{87}Sr/^{86}Sr$ values compared with those from dentine and bone, suggesting the enamel retains its original strontium signal and has not been diagenetically altered to a significant degree. The $^{87}Sr/^{86}Sr$ values recorded for in situ *Edmontosaurus* teeth fell within a narrow range. There was also no statistical difference in the mean $^{87}Sr/^{86}Sr$ values between the *Edmontosaurus* and *Troodon* teeth. Based on age estimates of the in situ *Edmontosaurus* teeth derived from a histological analysis, I find that the hadrosaurs preserved in the Liscomb Bonebed were not migratory in their last four months of life. Although the temporal resolution of this analysis is limited to approximately one third of a year, this study is consistent with other recent work suggesting that the Prince Creek Formation *Edmontosaurus* were perennial residents of the Arctic.

[3]Mori H, Druckenmiller PS, and Erickson GM. Prepared for submission to PLoS One.

3.2 Introduction

3.2.1 Background

In the Late Cretaceous, Arctic latitudes hosted a rich terrestrial vertebrate fauna compared to today [1-10]. In particular, the Prince Creek Formation (PCF) of northern Alaska preserves a diverse assemblage of dinosaurs that is of great relevance to broader paleobiological questions such as dinosaur physiology, migration and biogeography, because these dinosaurs lived in polar environments. In fact, the PCF dinosaur fauna lived as far north as land existed (> 80°N) during the entire Mesozoic [8,9,11]. Three unique dinosaur species are currently known from the PCF, *Pachyrhinosaurus perotorum* [11,12], *Alaskacephale gangloffi* [9], and *Edmontosaurus* sp. nov. (see Chapter 1), along with several other undescribed forms currently under study [13].

Among various fossil localities discovered in the PCF, the Liscomb Bonebed (LBB) is the most productive and arguably the single most fossiliferous site for polar dinosaurs in either hemisphere [4]. The LBB is exposed along the lower Colville River in the upper portion of the formation and has been excavated for over two decades (Figure 3-1). To date, approximately five thousand disarticulated, mostly juvenile remains of a new species of *Edmontosaurus* have been discovered. The LBB also contains rare remains of other taxa, including teeth of the theropod *Troodon* sp., which are larger and morphologically distinct from the congeneric found at lower latitudes.

The PCF (formerly referred to as the Kogosukuruk Tongue of the PCF [14]) is characterized by nonmarine sandstone, conglomerate, coal and mudstone, and is interpreted to represent interbedded fluvial (meandering channels and floodplains) and marginal marine sediment deposited on a low gradient Arctic coastal plain [15,16]. The age of the entire PCF ranges from Upper Cretaceous to Eocene based on palynological [17-19] and biostratigraphic data [20]. The numerical age of the dinosaur-bearing section of the formation, including the LBB where it is exposed along the lower Colville River, was dated to 71-68 Ma using $^{40}Ar/^{39}Ar$ methods [21,22]. The age of the LBB is further

constrained by an $^{40}Ar/^{39}Ar$ age of 69.2 ± 0.5 Ma from a stratigraphically underlying tuff at Sling Point and palynological analyses [23] that are consistent with an early Maastrichtian age [24]. Taphonomically, the LBB occurs in a trunk channel on a distributary channel splay complex and floodplain [24, 25]. The bonebed is interpreted to represent a mass mortality event associated with overbank flood deposits [26], which might have resulted from rapid melting of snow in the ancient Brooks Range [25]. The remains are almost entirely disarticulated, but they show little evidence of weathering or trampling and are typically preserved in three dimensions without any permineralization [25,26].

Witte et al. [27] placed the paleolatitude of northern Alaska at 67-85°N; thus, northern Alaska was at, or more likely well above, the paleo-Arctic Circle in the Late Cretaceous. As a result, the organisms inhabiting this area would have experienced a light regime characterized by extended periods (3-4 months) of winter darkness. Roehler and Stricker [28] considered the Aptian to Cenomanian climate of northern Alaska to be temperate to subtropical based on accumulated peat that indicates dense vegetation. Paleobotanical evidence suggests this relatively warm climate deteriorated in the early Maastrichtian [29,30] and that the mean annual temperature during deposition of the PCF was approximately 5-6 °C, with the cold month mean warmer than -2.0 ± 3.9 °C [31-33]. Analyses of growth rings of fossil trees from the PCF show that they ceased growth after the growing seasons [30,31,34], indicating that northern Alaska experienced unfavorable condition for tree growth during the winter due to prolonged darkness or possibly frost. For all of these reasons, it is likely that cooler climatic conditions excluded most terrestrial ectotherms. Indeed, lissamphibians, testudines, squamates, crocodilians and champsosaurs, all of which are common components of age-equivalent strata from lower latitudes, have never been documented in the PCF [35].

The discovery of dinosaurs from such high latitudes has been of interest for many researchers. If dinosaurs existed year-round in Arctic latitudes, how did they endure freezing temperatures and prolonged darkness during the winter? Two major possibilities

have been proposed: they migrated south to warmer environments during the winter, or they were capable of surviving the winter climate at high latitudes, possibly because they were endothermic. Hotton [36] proposed that Arctic dinosaurs, such as those found in the Yukon Territory, Canada, could have migrated to lower latitudes during the winter to avoid challenging conditions and poor food resources. Spotila et al. [37] calculated that even ectothermic dinosaurs of ~500 kg could have migrated more than a thousand kilometers. In contrast, Parrish et al. [38] argued that hadrosaurs could have wintered in northern Alaska because of mild temperatures relative to today and the rich vegetation that existed, at least seasonally, during the Late Cretaceous. Additionally, hadrosaurs had a relatviely large body size to help maintain their body temperature and might have had a lower metabolic rate, which requires less food to sustain life compared to endotherms [38].

Most analyses of the Alaskan *Edmontosaurus* migration do not appear to support the migration hypothesis. Fiorillo and Gangloff [39] argue that because juveniles of the new Alaskan species of *Edmontosaurus* are only ~10 % of the adult weight, they could not have migrated with adults, as do modern caribou, whose juveniles undertake migration when they are about 50-70 % of adult size. This argument is not wholly accurate; while their weight is low compared to adults, their absolute body weight (~200 to 500 kg, estimated from a clay model and circumference of the femur and humerus, after Alexander [40]) was much larger than that of adult caribou (~100 kg). The lack of a well-developed olecranon process and a small calcaneal heel in hadrosaurs is cited as suboptimal for a long migration, but hadrosaurs might not have needed such structures due to their large size [41]. A histological study by Chinsamy et al. [42] reveals that the bones of the Alaskan *Edmontosaurus* showed alternating cycles of reticular and circumferential fibro-lamellar patterns, which is not seen in southern specimens of *Edmontosaurus*. They interpret the circumferential fibro-lamellar tissue to represent annual periods of stress, presumably the winter season. However, they also admit that this stress could have been a result of long-distance migration. Thus, the question of whether North Slope dinosaurs migrated remains unsolved.

3.2.2 Isotope analysis

In recent years, isotopic studies have been used to track migration of both modern and extinct animals, interpret physiology and reconstruct paleoenvironments. Barrick et al. [43] argued that dinosaurs were endothermic animals because of small $\Delta^{18}O$ values of various bones, but it was later pointed out that diagenetic alteration could also have been responsible for alteration of the bone's original isotopic signal [44-48]. In contrast, fossil tooth enamel is extremely durable. As the most chemically stable hard tissue in the body, it would be expected to preserve the original isotopic signal recorded in tissues of the living organism if little or no bacterial activity was involved [45,49,50]. For this reason, isotopic studies of vertebrate remains are now commonly conducted preferentially on tooth enamel tissue for a more reliable signal. For example, Fricke et al. [51,52] assessed the dinosaurian migration hypothesis using stable oxygen and carbon isotope signals of the tooth enamel. They argued that the lack of isotopic overlap in hadrosaur tooth enamel from different localities between Alberta and New Mexico suggests hadrosaurs were not migratory [51]. However, in another study, Fricke et al. reveal variations in $\delta^{18}O$ of sauropod teeth, suggesting a probable seasonal migration [52].

Recently, Suarez et al. [53] reported on an analysis of stable oxygen isotopes in dinosaur teeth from the PCF, including two hadrosaurids and three theropod teeth from the LBB. Using $\delta^{18}O$ values of siderite in the PCF and a temperature range estimated from paleobotanical proxies [33], they calculate the range of Late Cretaceous meteoric water $\delta^{18}O$ values that the dinosaurs must have ingested. Assuming a body temperature of 37 °C, they calculate that the $\delta^{18}O$ values of the meteoric water ingested by the dinosaurs ranged between -22.4 to -23.8 ‰. This value is close to their estimated $\delta^{18}O$ value of meteoric water during the winter months, and it suggests that the dinosaurs preserved in the LBB over-wintered in northern Laramidia, near where they were deposited. While this study provids evidence for non-migratory behavior in Alaskan dinosaurs, it is not without problems. Their calculations relied on paleotemperatures estimated from paleobotanical evidence, which is now under question [54], and they analyzed only five

teeth from the LBB. The time span captured by these teeth is not known. Given that these studies are the first to employ an isotopic approach to test migration hypotheses for dinosaurs, they need to be replicated and independently verified using other isotopic systems.

Strontium is another element that has the potential to provide insight into migratory behaviors in extinct vertebrates based on its isotopic composition. $^{87}Sr/^{86}Sr$ values from sediment increase due to the radioactive decay of ^{87}Rb into ^{87}Sr. Thus, $^{87}Sr/^{86}Sr$ values in the sediment are controlled by the age and the amount of ^{87}Rb in rocks [55-57]. The $^{87}Sr/^{86}Sr$ of an organism is largely influenced by local geology [58-60]. Therefore, $^{87}Sr/^{86}Sr$ in animal tissues such as teeth can be used to track migration patterns. For example, Britton et al. [61] measured stable oxygen and strontium isotope ratios of modern caribou (*Rangifer tarandus granti*) tooth enamel to test whether it reveals patterns of movement. Their results are consistent with the known migratory ranges of caribou, except for one individual that may have been a domesticated reindeer (*R. tarandus tarandus*). This individual experienced no $^{87}Sr/^{86}Sr$ fluctuation, presumably because it was not migratory. Hoppe et al. [62] compare the $^{87}Sr/^{86}Sr$ values from analyses of Florida mammoth (*Mammuthus* sp.) and mastodon (*Mammut americanum*) tooth enamels with a $^{87}Sr/^{86}Sr$ map developed from the bedrock geology of Florida and Georgia and conclude that mastodons were migratory, while mammoths were not.

When analyzing ancient samples, strontium studies often employ solution methods, in which the samples are chemically prepared to remove diagenetic strontium, as proposed by Koch [63]. Although this method is generally regarded as a reliable means to determine $^{87}Sr/^{86}Sr$ values [64], it requires a relatively large amount of enamel (~5 mg), and thus it is not easily applicable to small teeth or teeth with very thin enamel layers. Recently, laser ablation multi-collector inductively coupled plasma mass spectrometry (LA-MC-ICP-MS) was adapted for in-situ analysis of small samples, or samples which need to be measured with a high spatial resolution [65-71]. In these in-situ analyses, diagenetic strontium is not chemically removed. Hence, the degree of alteration

needs to be assessed by comparing the $^{87}Sr/^{86}Sr$ to that of dentine or bones, which are more susceptible to diagenesis. Some of these studies were successfully employed on fossil bones. Richards et al. [66] worked on 40 ka Neanderthal teeth, demonstrating that these hominies had a wide geographical range. Copeland et al. [67,69] also showed that enamel preserves its original signal in 1.5-2.5 Ma rodent and hominid fossils.

In this study, I use strontium isotope geochemistry of in situ teeth from hadrosaurid maxillary dental batteries to test for migratory behavior in *Edmontosaurus*. I compare the $^{87}Sr/^{86}Sr$ values of *Edmontosaurus* teeth to that of teeth belonging to the small theropod dinosaur *Troodon*, which I assume was non-migratory. In theory, if I could recover the isotopic signal from one complete year recorded in the teeth of an individual hadrosaur that migrated, I would expect considerable variation in its $^{87}Sr/^{86}Sr$ values compared to that of a non-migratory species. Alternatively, if I saw no variation it would suggest year-round residency. Although one other preliminary study attempted to analyze $^{87}Sr/^{86}Sr$ values in dinosaurs [72], this is the first time strontium isotopes have ever been used to study the migratory behaviors of dinosaurs. It also has the additional advantage of being an independent method to assess putative migration of the PCF dinosaurs compared to other approaches described above.

3.3 Material and methods

3.3.1 Tooth age

In order to use hadrosaurid teeth in an isotopic study, it is first necessary to understand the unique and sophisticated system of tooth organization and replacement found in hadrosaurids. Lambe [73] first described the tooth replacement mechanism in hadrosaurs. In each of the four jaw quadrants (right and left sides of the upper and lower jaws) the teeth of hadrosaurids are organized into a single large unit known as a dental battery. Within each maxillary and dentary battery, hadrosaurs had dozens of tooth alveoli, and in each alveolus were several teeth aligned in a vertical row. In the case of

the PCF specimens of juvenile *Edmontosaurus*, there are 26 tooth alveoli and two to three teeth in each tooth alveolus (see Chapter 2; Figure 2-15, 2-25). The oldest teeth in the alveoli are exposed on the occlusal plane, while the youngest teeth are located farthest from the occlusal plane (more dorsally located in the maxilla, more ventrally located in the dentary). As the oldest teeth on the occlusal plane are worn out, mature younger teeth slowly migrated toward the occlusal surface. Because the teeth of a given row are imbricated, often the two oldest teeth in each tooth row are exposed on the occlusal plane, although in the PCF juvenile specimens of *Edmontosaurus*, usually only one tooth was actively in use. Together, all of the teeth visible in the occlusal plane functioned as a single masticatory unit in each jaw quadrant. Because teeth were in a constant state of replacement, each tooth records the isotopic signature of the short span of time during which it developed. However, all of the teeth within a given alveolus collectively record the isotopic environment over a much longer time period spanning the age of the oldest and youngest teeth. Thus, the unique dental system of hadrosaurids provides an opportunity to regularly and sequentially sample the isotopic environments in which an individual lived for a much greater range of time than could be provided by only a single tooth.

In hadrosaurs, enamel formed more quickly than dentine, in approximately 30 days (Erickson, G.M., personal communication). The enamel only covers one side of the tooth (buccal side in the maxillary teeth, and lingual side in the dentary teeth), so that the occlusal surface of the teeth is mostly dentine. This is a self-sharpening mechanism analogous to that found in modern rodents. The dentine grows internally (from the pulp cavity) over a longer time than the enamel [74] and is laid down in daily layers called the lines of von Ebner [75]. These lines can be observed and counted by the use of thin sections. By counting these lines, the age of a tooth can be estimated in days [76]. By subtracting the age of the youngest tooth from the age of the second youngest tooth, tooth replacement rate can be estimated [77].

To assess the length of the time span captured by the teeth, one *Troodon* tooth

(UAMES 7760) and three teeth (R-8-1, R-8-2, R-8-3) from an *Edmontosaurus* maxilla (UAMES 4219) were sectioned and the incremental lines of von Ebner in the dentine were counted by Dr. Greg Erickson (Florida State University) who pioneered this technique in dinosaurs. The tooth replacement rate of *Edmontosaurus* was estimated by subtracting the age of R-8-3 (the youngest tooth) from R-8-2 (the second-youngest tooth).

3.3.2 Materials

Two *Edmontosaurus* maxillae from the LBB with nearly complete dental batteries were chosen for sampling. I extracted three teeth from a single row of one specimen (e1, e2, e3; UAMES 4219) and two teeth from the other (e4, e5; UAMES 4185; Figure 3-2). In addition to the teeth removed from the maxillae, I also analyzed two isolated and worn teeth from the LBB, one of which was collected after it had weathered out of the bonebed (e6; UAMES 29431) and one which was directly excavated out of the LBB (e7; UAMES 29405). Because these latter two teeth showed a high degree of wear along their occlusal surfaces, They may represent teeth that are as old or maybe even older than the teeth removed directly from the occlusal plane of the other two maxillae.

The $^{87}Sr/^{86}Sr$ values of the *Edmontosaurus* teeth were then compared to those of three *Troodon* teeth (probably a non-migratory species) also excavated from the LBB (t1, UAMES 25316; t2, UAMES 29391; t3, 29535). To increase the sample size, some of these tooth enamel samples were measured 2 to 4 times at different spots. Because all *Troodon* teeth collected from LBB are isolated, it was not possible to measure the isotopic environment over a time span greater the age of the tooth itself.

3.3.3 LA-MC-ICP-MS

The enamels of most dinosaur teeth are very thin. The enamel thickness of the LBB *Edmontosaurus* is < 100 μm, and that of *Troodon* is 20-30 μm [78]. Because the traditional solution-based strontium analysis requires relatively large amounts of enamel, preparing enough of the enamel and avoiding contamination from the dentine is often

difficult. Therefore, I used laser-ablation-MC-ICP-MS techniques to analyze the $^{87}Sr/^{86}Sr$ values of the tooth enamel.

Assessing the degree of diagenesis is an important factor when dealing with ancient fossils, especially for in-situ analyses like LA-MC-ICP-MS in which diagenetic strontium is not chemically removed. Since strontium is a relatively heavy element, isotopic fractuation between tissues will not occur [79,80]. Dentine and bone are more prone to diagenesis than tooth enamel. For these reasons, if no isotopic difference is found between these tissues, it means the original isotopic values are either preserved or completely erased. In other words, if different $^{87}Sr/^{86}Sr$ values are recorded in the enamel versus bone/dentine, it means the original isotopic value in enamel is not completely altered [51,66,81,82]. For these reasons, the $^{87}Sr/^{86}Sr$ values of tooth dentine (e3, e4, e6, e7, and t3) and bone fragments (b, extracted from UAMES 4185) were also measured.

The strontium analysis was conducted following the methods describe by Copeland [65,67,69]. The $^{87}Sr/^{86}Sr$ values of samples were measured using the laser ablation unit (New Wave UP213) with a Nu Plasma high-resolution multi-collector inductively coupled plasma mass spectrometer in the Department of Geological Sciences at the University of Cape Town, South Africa. The diameter of the laser spot was 200 μm, measured continuously along a 750 μm long line. Because the enamel layer of dinosaur teeth is so thin, the power of the laser was reduced to a fluence of approximately 2.25 J/cm^2, firing at 10 Hz and moving at 100 μm/sec, going back and forth along the line 10 times. The standards used in the analyses were modern rodent teeth, which are also described by Copeland [65, 67].

3.4 Results

3.4.1 Tooth age

For *Edmontosaurus* tooth R-8-3, the average thickness of one incremental line of von Ebner is 0.0222 mm/day. The total thickness of the dentine layer of R-8-3 is 1.6 mm,

and that of R-8-2 was 2.7 mm. Therefore, dividing 1.1 mm by 0.0222 mm, it is estimated that the tooth replacement rate for *Edmontosaurus* was 50 days. In UAMES 4219, tooth e1 was older by 50 days than tooth e2, e2 was older by 50 days than e3, and enamel was estimated to form in ~30 days; therefore, the oldest tooth in UAMES 4219 (e1) is interpreted to be 130 days older than the youngest tooth (e3; Figure 3-3). Similarly, in UAMES 4185, the oldest tooth (e4) is approximately 80 days older than the youngest tooth (e5). Assuming UAMES 4185 and UAMES 4219 died at the same time, e4 is likely younger than e1, but older than e2, because e4 was not yet fully exposed on the occlusal plane. The tooth age of *Troodon* was determined to be 96 days. The tooth replacement rate of the *Troodon* teeth could not be estimated, because no sets of teeth in their maxilla or dentary alveolus have been found.

3.4.2 LA-MC-ICP-MS measurements

Table 3-1 lists the results of $^{87}Sr/^{86}Sr$ measurements. The dentine of one *Troodon* tooth (t1) shows abnormally high two-sigma values. This is possibly because sediment on the tooth surface was not properly removed, because it was cleaned separately from the rest of the samples. For these reasons, t1 was excluded from the interpretations. Figure 3-4 presents box plots of the data from the other teeth. The $^{87}Sr/^{86}Sr$ values of dentine and bones fall within a narrow range, around 0.70850. The $^{87}Sr/^{86}Sr$ values of the enamel of all the samples, including teeth of both *Edmontosaurus* and *Troodon*, ranged from 0.7081 to 0.7098. *Edmontosaurus* teeth removed from maxillae show nearly the same mean $^{87}Sr/^{86}Sr$ value as the *Troodon* teeth. However, isolated *Edmontosaurus* teeth show lower $^{87}Sr/^{86}Sr$ values (0.70814, 0.70874) than the other *Edmontosaurus* teeth.

3.5 Discussion

3.5.1 Migration hypothesis

The $^{87}Sr/^{86}Sr$ values of in situ maxillary teeth from *Edmontosaurus*, representing a

time span of approximately 130 days, fall within a narrow range, suggesting that these individuals lived in an environment with relatively constant $^{87}Sr/^{86}Sr$ values. The mean $^{87}Sr/^{86}Sr$ value of *Troodon* teeth is statistically indistinguishable from those of *Edmontosaurus* teeth, as would be expected for animals living with a geographically restricted range. Thus, it is likely that individuals of *Edmontosaurus* and *Troodon* preserved in the LBB lived in approximately the same geographic area close to their eventual site of burial during at least their last four months of life.

The LBB has been interpreted as a mass mortality event among a herd of dominantly juvenile individuals [25,26] (see Chapter 1 and 2). Although the exact mechanism of death is not certain, due to a near-complete degree of disarticulation [25,26], it is clear that the bones were transported after death. Given that most of the bones are not extensively broken and/or rounded, they were probably not deposited far from where the animal lived. Thus, the LBB was deposited within the environment in which the dinosaurs lived, and they were not transported great distances (> 50 km and probably much less) after death.

A factor in interpreting these data and choosing between various migratory or non-migratory scenarios lies in the temporal resolution of the available data, which is limited to approximately the last 130 days (one third of a year) of life for the *Edmontosaurus* specimens. Thus, the question arises: in which season of the year did the LBB hadrosaurids perish? If they died in late summer, the hypothesis that dinosaurs migrated to southern latitude during winter cannot be rejected based on available data, as they would be expected to remain throughout the food-rich, warmer summer season. If they died in middle to late winter, then they clearly stayed in northern Alaska during the most challenging time of year in terms of light regime, temperatures and food availability, and therefore were probably not migratory. Finally, if they perished in the spring or early summer, then migratory species would probably have just completed their spring migration.

Independent evidence derived from sedimentological and taphonomic studies of

the LBB suggests that the LBB *Edmontosaurus* may have bee killed by a spring or early summer flood resulting from spring run-off of melting snow in the early Brooks Range to the south [26]. If these individuals had migrated south during the coldest and darkest months of winter, then they were likely elsewhere in the months immediately before they perished, and we would expect to see strong variation in the isotopic strontium signal as a result. The lack of such variation provides strong, but not conclusive evidence that *Edmontosaurus* was non-migratory.

An alternative but less likely scenario is that the two species migrated together, resulting in overlapping strontium values. Possible supporting evidence for this lies in the fact that *Troodon* teeth from Alaska are significantly larger than those from more southerly latitudes (Alberta and the Montana) [7]. This larger body size (possibly up to 400 kg in adult) might have better enabled *Troodon* to migrate with the even larger *Edmontosaurus* juveniles and adults. However, most extant carnivores do not migrate, although this behavior has been recorded in spotted hyena (*Crocuta crocuta*), which follow their prey [83]. Given the great distances they would have needed to travel to reach even the paleo-Arctic Circle in the late Cretaceous (~ 3200 km [36]), I consider this scenario unlikely.

The interpretation of the strontium signals of the two isolated *Edmontosaurus* teeth (0.70814 and 0.70850) is ambiguous, as the values lie mostly outside those of in situ maxillary teeth. It should be noted that only tooth e7 shows a significantly lower $^{87}Sr/^{86}Sr$ value than the in situ maxillary teeth (the value for tooth e6 nearly overlaps the in situ teeth). Because these teeth were isolated, their ages relative to those in the maxillae cannot be determined. That these teeth were highly worn on the occlusal surface indicates they were likely as old or older than the oldest teeth in the two maxillae. These teeth could have been formed in a different strontium environment than northern Alaska. However, it is possible that tooth e7 experienced a stronger diagenetic effect than the teeth within the maxillae, because its $^{87}Sr/^{86}Sr$ values are close to those of the dentine and bone. For these reasons, I do not think this is a compelling evidence of *Edmontosaurus*

migration.

Several potential sources of error may affect these results and interpretations. One question that remains unanswered concerns the degree of expected strontium variation within the environment(s) in ancient Alaska in which the dinosaurs lived. Without comparing $^{87}Sr/^{86}Sr$ values of early Maastrichtian fossil teeth of non-migratory species throughout much of the northern-most area of Laramidia (present day Alaska), it is not possible to determine more precisely where the *Edmontosaurus* teeth in the LBB formed. However, because one *Troodon* tooth (t2) shows low $^{87}Sr/^{86}Sr$ values similar to the isolated *Edmontosaurus* teeth, it is possible that the home range of *Edmontosaurus* was not significantly wider than the range inhabited by *Troodon.*

3.5.2 Diagenesis

LA-MC-ICP-MS is ideal for analysis of large number of samples because it is relatively cheap, but it is also ideal for analyses of small samples. The drawback of this method is that diagenetic strontium is not chemically removed, thus it could obscure the original isotopic signal, evrn though the degree of the diagenesis is much less severe in enamel than in dentine or bone [47,63,64]. To determine whether if the enamel retains its original values, the $^{87}Sr/^{86}Sr$ value of the enamel and dentine are compared. Both the enamel and dentine values passed a Shapiro-Wilk test ($p < 0.05$); therefore a normal distribution can be considered for these values. The T-test indicates that the mean $^{87}Sr/^{86}Sr$ difference between enamel and dentine is statistically significant ($T = -4.1433$, $p << 0.01$). If diagenesis altered the original strontium signal, then the $^{87}Sr/^{86}Sr$ would be the same for enamel, dentine and bone. However, the strontium signal of the enamel is statistically different from that of dentine and bone. Either the enamel preserves its original strontium isotopic signal, or it suffered less diagenetic alteration than dentine and bone.

A comparison of $\Delta_{enamel\text{-}dentine}\ ^{87}Sr/^{86}Sr$ and $_{enamel}\ ^{87}Sr/^{86}Sr$ supports the interpretation that the fossil enamel preserves the original isotopic value. The enamel

$^{87}Sr/^{86}Sr$ value (S_e) is a result of partial (P_{ed}) replacement of its original $^{87}Sr/^{86}Sr$ (S_0) by the local $^{87}Sr/^{86}Sr$ value (S_d). This relationship can be expressed in an equation as

$$S_e=P_{ed}S_d+(1-P_{ed})S_0 \quad (1)$$

The same relationship is true for dentine, as

$$S_d=P_{dd}S_d+(1-P_{dd})S_0 \quad (2)$$

By subtracting Equation 2 from Equation 1, I get

$$S_e- S_d=(P_{ed}-P_{dd})(S_d - S_0) \quad (3)$$

Since enamel is more resistant to alteration than dentine, $P_{ed}<P_{dd}$, and in this analysis, I expect S_0 to equal S_e, and P_{ed} to be nearly 0. Thus, Equation 3 becomes

$$S_e- S_d= P_{dd}\cdot S_e - P_{dd}\cdot S_d \quad (4)$$

Therefore, if $_{enamel}{}^{87}Sr/^{86}Sr$ (S_e) really equals $S_{0,\ enamel}{}^{87}Sr/^{86}Sr$ correlates with $\Delta_{enamel\text{-}dentine}{}^{87}Sr/^{86}Sr$ [67]. I assessed whether this is true for my samples. When these values are compared, (Figure 3-5) they show high correlation as expected. According to Equation 4, the slope of the regression line represents the degree of diagenesis of dentine. This slope value is 86 % for the current analyses, which is much higher than 26 % for the

2 Ma old fossil rodent teeth from Swartkrans and Sterkfontein in South Africa [69], probably because the LBB specimens are much older. Also, from the intercept of the slope (- P_{dd}· S_d), S_d can be estimated as 0.7063. This value is close to the soluble $^{87}Sr/^{86}Sr$ values in North Slope region of Alaska (0.709 to 0.716), reported from multiple rivers and modern caribou teeth enamels [61,84]. For these reasons, it is very likely that the measured tooth enamel preserves the original isotopic signal.

3.6 Conclusion

Based on the values obtained for teeth found in the dental batteries and comparison with a putative non-migratory species, the results suggest the Alaskan *Edmontosaurus* lived in the area of the present-day LBB for approximately their last four months of life. Future work will benefit from additional isotopic studies of hadrosaur tooth enamel using other methods for analyzing strontium as well as measurement of other isotopic systems such as oxygen. This study is consistent with most other studies in concluding that dinosaurs preserved in the PCF did not migrate to any significant degree, although many questions remain in regarding how they coped with challenging conditions experienced in Cretaceous polar environments.

3.7 Acknowledgements

This work was supported in part by NSF Award (EAR, 1226730 to P. Druckenmiller and G. Erickson), the Geist Fund, the University of Alaska Fairbanks Graduate School, and the Geological Society of America Research Grant. I appreciate my graduate committee members, Drs. Patrick Druckenmiller, Sarah Fowell, Kris Hundertmark, and Matthew Wooller for their support. I acknowledge Dr. Gregory Erickson for determining replacement ages of *Edmontosaurus* teeth from the PCF and Dr. Petrus le Roux for conducting the strontium isotope analysis.

3.8 Figures

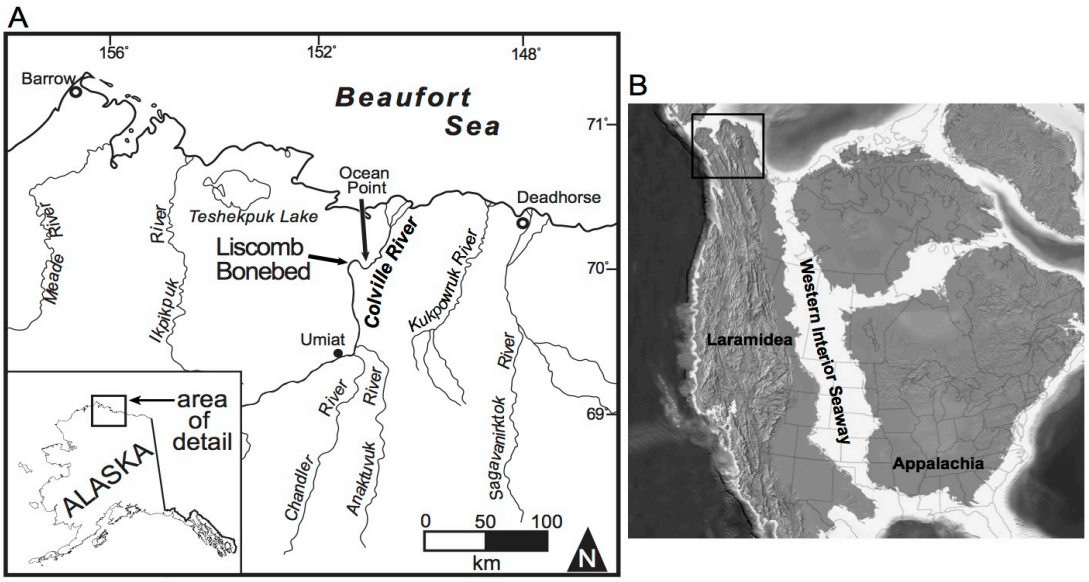

Figure 3-1. (A) Location of the Liscomb Bonebed and (B) paleogeographic reconstruction map of North America at 70 Ma [85]. The inset box indicates the location of present day Alaska.

Figure 3-2. Specimens sampled in this study. From two *Edmontosaurus* maxillae (UAMES 4219 and 4185), three (e1, e2, e3) and two (e4, e5) teeth are removed for analysis. Two isolated *Edmontosaurus* teeth (e6, e7), a bone fragment of UAMES 4185, and three teeth of *Troodon* are also measured for comparison. The black lines indicate where enamel was measured and the white lines show where dentine/bone was measured.

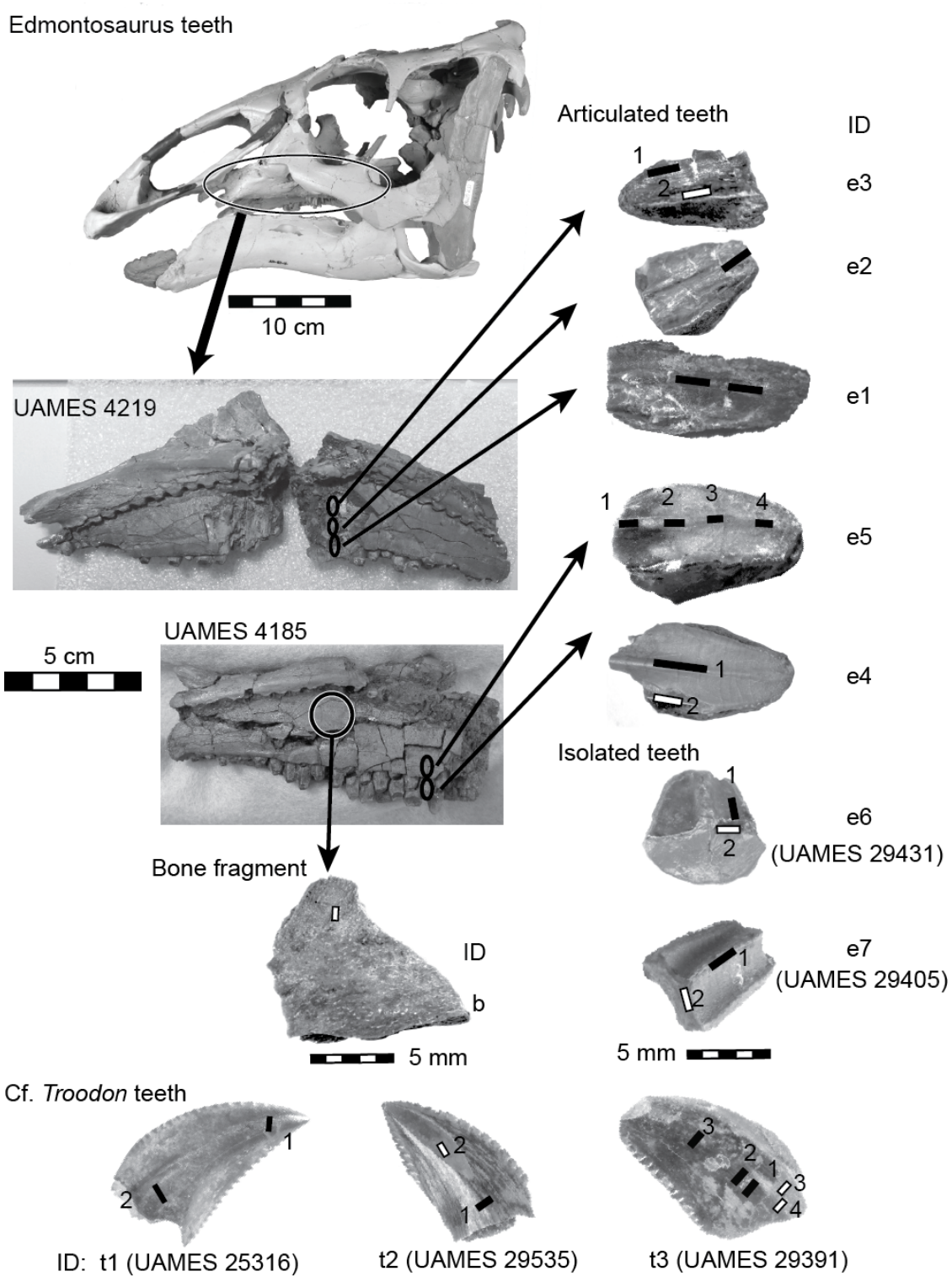
Edmontosaurus teeth
10 cm
UAMES 4219
5 cm
UAMES 4185
Bone fragment
ID
b
5 mm
Articulated teeth
ID
e3
e2
e1
e5
e4
Isolated teeth
e6
(UAMES 29431)
e7
(UAMES 29405)
5 mm
Cf. Troodon teeth
ID: t1 (UAMES 25316)
t2 (UAMES 29535)
t3 (UAMES 29391)

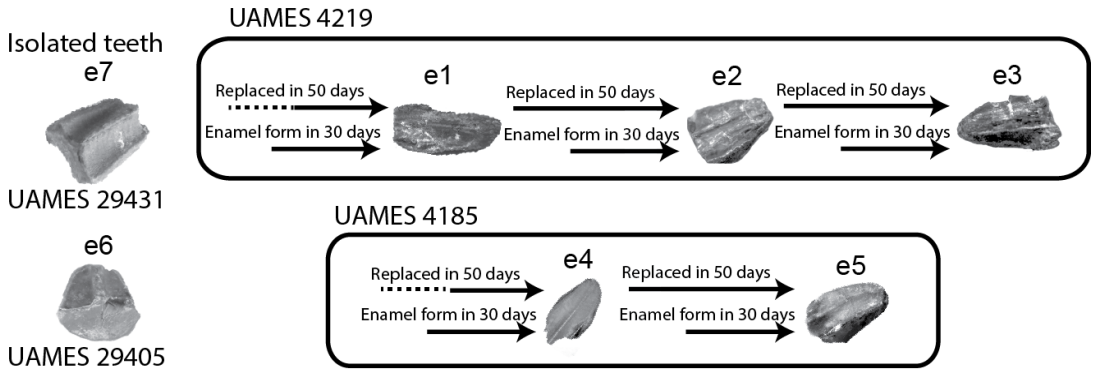

Figure 3-3. Temporal resolution and tooth replacement rates of *Edmontosaurus* teeth.

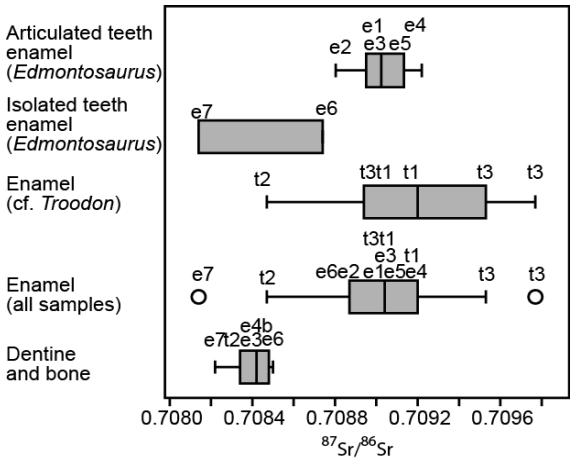

Figure 3-4. Box plots of $^{87}Sr/^{86}Sr$ values. The enamel preserves different $^{87}Sr/^{86}Sr$ values from dentine and bone. Tooth enamel of *Edmontosaurus* shows similar mean $^{87}Sr/^{86}Sr$ values to that of $^{87}Sr/^{86}Sr$ values of older *Edmontosaurus* and *Troodon* tooth enamels. Approximate $^{87}Sr/^{86}Sr$ values for each tooth are also represented by the sample numbers (see table 3-1).

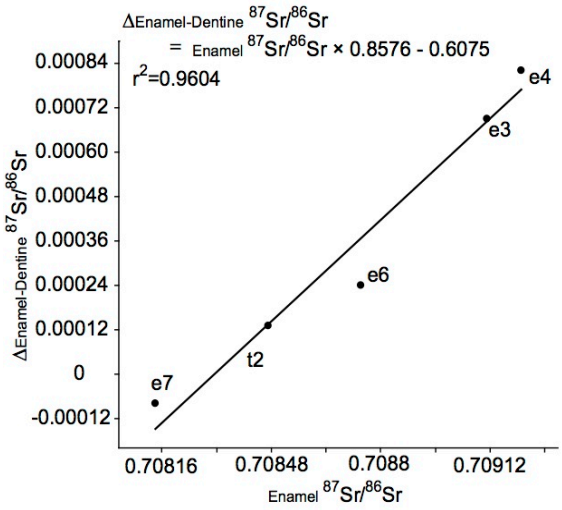

Figure 3-5. Biplots of $_{Enamel}{}^{87}Sr/^{86}Sr$ and $\Delta_{Enamel\ -\ Dentine}{}^{87}Sr/^{86}Sr$. Reduced major axis is employed to draw the regression line.

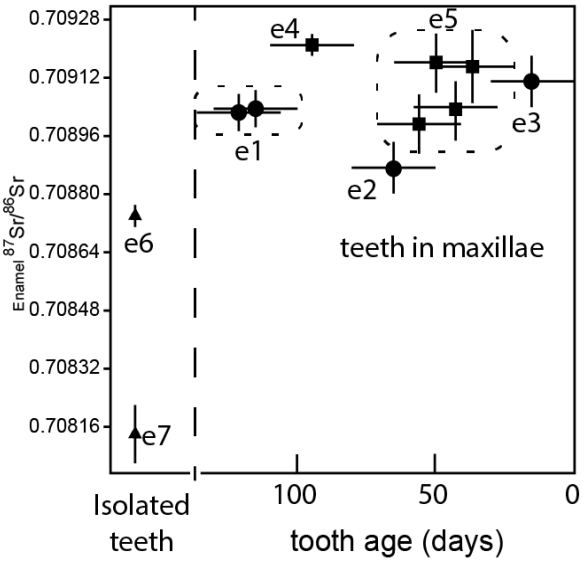

Figure 3-6. Change in $_{enamel}{}^{87}Sr/^{86}Sr$ values for *Edmontosaurus* over time. Teeth e1 and e5 are measured two and four times, and each analysis is shown. Tooth age is determined by their relative position within the maxillae. The ages of the isolated teeth are not known. Isolated teeth show a lower $^{87}Sr/^{86}Sr$ values than those of teeth removed from the maxillae. Black circles = analysis conducted on UAMES 4219; black squares = analysis conducted on UAMES 4185; black triangles =analysis conducted on isolated teeth. The vertical bars represent the 2-sigma range of each analysis, and the horizontal bars represent the time span in which each tooth formed (30 days).

3.9 Table

Table 3-1. Results of the $^{87}Sr/^{86}Sr$ measurements

Sample numbers	Tissue type	$^{87}Sr/^{86}Sr$ value	2-sigma error
e1 (1)	enamel	0.70905	0.00005
e1 (2)	enamel	0.70904	0.00006
e2	enamel	0.70887	0.00007
e3	enamel	0.70911	0.00003
e3	dentine	0.70842	0.00007
e4	enamel	0.70921	0.00003
e4	dentine	0.70839	0.00008
e5 (1)	enamel	0.70899	0.00008
e5 (2)	enamel	0.70914	0.00008
e5 (3)	enamel	0.70903	0.00008
e5 (4)	enamel	0.70913	0.00010
e6 (1)	enamel	0.70874	0.00003
e6 (2)	dentine	0.70850	0.00011
e7 (1)	enamel	0.70814	0.00008
e7 (2)	dentine	0.70822	0.00004
b	cortical bone	0.70848	0.00003
t1(1)	enamel	0.70904	0.00006
t1(2)	enamel	0.70920	0.00006
t2 (1)	enamel	0.70847	0.00012
t2 (2)	dentine	0.70834	0.00004
t3 (1)	enamel	0.70977	0.00016
t3 (2)	enamel	0.70953	0.00016
t3 (3)	enamel	0.70894	0.00009
t3 (4)	dentine	0.70976	0.00054
t3 (5)	dentine	0.71061	0.00082

3.10 References

1. Brouwers EM, Clemens, WA, Spicer, RA, Ager, TA, Carter LD, et al. (1987) Dinosaurs on the North Slope, Alaska: High latitude, latest Cretaceous environments. Science 237: 1608-1610.
2. Davies KL (1987) Duck-bill dinosaurs (Hadrosauridae, Ornithischia) from the North Slope of Alaska. Journal of Paleontology 61: 198-200.

3. Nelms LG (1989) Late Cretaceous dinosaurs from the North Slope of Alaska. Journal of Vertebrate Paleontology, Abstracts of Papers 9: 34A.
4. Gangloff RA (1998) Arctic dinosaurs with emphasis on the Cretaceous record of Alaska and the Eurasian-North American connection. New Mexico Museum of Natural History and Science Bulletin 14: 211-220.
5. Fiorillo AR, Gangloff RA (2000) Theropod teeth from the Prince Creek Formation (Cretaceous) of Northern Alaska, with speculations on Arctic dinosaur paleoecology. Journal of Vertebrate Paleontology 20: 675-682.
6. Fiorillo AR (2004) The dinosaur of arctic Alaska. Scientific American 291: 84-91.
7. Fiorillo AR, Tykoski RS, Currie PJ, McCarthy PJ, Flaig P (2009) Description of two partial *Troodon* braincases from the Prince Creek Formation (Upper Cretaceous), North Slope Alaska. Journal of Vertebrate Paleontology 29: 178-187.
8. Brown CM, Druckenmiller P (2011) Basal ornithopod (Dinosauria: Ornithischia) teeth from the Prince Creek Formation (early Maastrichtian) of Alaska. Canadian Journal of Earth Sciences 48: 1342-1354.
9. Fiorillo AR, Tykoski RS (2012) A new Maastrichtian species of the centrosaurine ceratopsid *Pachyrhinosaurus* from the North Slope of Alaska. Acta Palaeontologica Polonica 57: 561-573.
10. Mannion PD, Benson RBJ, Upchurch P, Butler RJ, Carrano MT et al. (2012) A temperate palaeodiversity peak in Mesozoic dinosaurs and evidence for Late Cretaceous geographical partitioning. Global Ecology and Biogeography 21: 898-908.
11. Sullivan RM (2006) A taxonomic review of the Pachycephalosauridae (Dinosauria: Ornithischia). New Mexico Museum of Natural History and Science Bulletin 35: 347-365.
12. Gangloff RA, Fiorillo AR, Norton DW (2005) The first pachycephalosaurine (Dinosauria) from the paleo-Arctic of Alaska and its paleogeographic implications. Journal of Paleontology 79: 997-1001.

13. Fiorillo AR (2008) On the occurrence of exceptionally large teeth of *Troodon* (Dinosauria: Saurischia) from the Late Cretaceous of northern Alaska. Palaios 23: 322-328.
14. Gryc G, Patton Jr WW, Payne TG (1951) Present Cretaceous stratigraphic nomenclature of northern Alaska. Journal of the Washington Academy of Sciences 41: 159-167.
15. Mull CG, Houseknecht DW, Bird KJ (2003) Revised Cretaceous and Tertiary stratigraphic nomenclature in the Colville Basin, northern Alaska. US Gelogical Survey Professional Paper 1673: 1-51.
16. Flaig PP, McCarthy PJ, Fiorillo AR (2011) A tidally influenced, high-latitude coastal-plain: The upper Cretaceous (Maastrichtian) Prince Creek Formation, North Slope, Alaska. In: Davidson SK, Leleu S, North. CP, editors. From river to rock record: The Preservation of fluvial sediments and their subsequent interpretation. pp. 233-264.
17. Frederiksen NO, Ager TA, Edwards LE (1988) Palynology of Maastrichtian and Paleocene rocks, lower Colville River region, North Slope of Alaska. Canadian Journal of Earth Sciences 25: 512-527.
18. Frederiksen NO (1991) Pollen zonation and correlation of Maastrichtian marine beds and associated strata, Ocean Point dinosaur locality, North Slope, Alaska. United States Geological Survey Bulletin 1990-E: E1-E24.
19. Frederiksen NO, Mclntyre DJ, Sheehan TP (2002) Palynological dating of some Upper Cretaceous to Eocene outcrop and well samples from the region extending from the easternmost part of NPRA in Alaska to the western part of Arctic National Wildlife Refuge, North Slope of Alaska. US Geological Survey Open-File Report 02-405: 1-37.
20. Brouwers EM, Deckker PD (1993) Late Maastrichtian and Danian ostracode faunas from Northern Alaska; reconstructions of environment and paleogeography. Palaios 8: 140-154.

21. McKee E, Conrad JE, Tuin BD (1989) Better dates for arctic dinosaurs. Eos 70: 74.
22. Conrad JE, Mackee EH, Turrin BD (1992) Age of tephra beds at the Ocean Point Dinosaur Locality, North Slope, Alaska, based on K-Ar and $^{40}Ar/^{39}Ar$ analyses. Washington DC: United States Government Printing Office. 12 p.
23. Flores RM, Myers MD, Houseknecht DW, Stricker GD, Brizzolara DW et al. (2007) Stratigraphy and facies of Cretaceous Schrader Bluff and Prince Creek Formations in Colville River Bluffs, North Slope, Alaska. United States Geological Survey Professional Paper 1747: 1-52.
24. Flaig PP (2010) Depositional environments of the Late Cretaceous (Maastrichtian) dinosaur-bearing Prince Creek Formation: Colville River region, North Slope, Alaska. Unpublished Ph.D. thesis. Fairbanks, AK: University of Alaska Fairbanks. 311 p.
25. Fiorillo AR, McCarthy PJ, Flaig PP (2010) Taphonomic and sedimentologic interpretations of the dinosaur-bearing Upper Cretaceous Strata of the Prince Creek Formation, Northern Alaska: Insights from an ancient high-latitude terrestrial ecosystem. Palaeogeography, Palaeoclimatology, Palaeoecology 295: 376-388.
26. Gangloff RA, Fiorillo AR (2010) Taphonomy and paleoecology of a bonebed from the Prince Creek Formation, North Slope, Alaska. Palaios 25: 299-317.
27. Witte, WK, Stone, DB, Mull CG (1987) Paleomagnetism, paleobotany, and paleogeography of the Cretaceous, North Slope, Alaska. In: Tailleur, IL, Weimer P, editors. Alaska North Slope geology. Bakersfield, CA: Pacific Section, Society of Economic Paleontologists and Mineralogists. pp. 571-579.
28. Roehler HW, Stricker GD (1984) Dinosaur and wood fossils from the Cretaceous Corwin Formation in the National Petroleum reserve, North Slope of Alaska. Alaskan Geological Society Journal 4: 35-41.
29. Parrish JT, Spicer RA (1988) Late Cretaceous terrestrial vegetation: A near-polar temperature curve. Geology 16: 22-25.

30. Spicer RA, Fairish JT, Grant PR (1992) Evolution of vegetation and coal-forming environments in the Late Cretaceous of the North Slope of Alaska. Geological Society of America Special Papers 267: 177-192.
31. Spicer RA, Parrish JT (1990) Late Cretaceous-early Tertiary palaeoclimates of northern high latitudes: a quantitative view. Journal of the Geological Society, London Journal of the Geological Society 147: 329-341.
32. Fiorillo AR, McCarthy PJ, Brandlen E, Flaig PP, Norton D et al. (2007) Paleontology, sedimentology, paleopedology, and palynology of the Kikak-Tegoseak Quarry (Prince Creek Formation, Late Cretaceous), Northern Alaska. In: Braman DR, editor. Ceratopsian symposium: Short papers, abstracts and programs. Drumheller, AB: pp. 48-49.
33. Spicer RA, Herman AB (2010) The Late Cretaceous environment of the Arctic: A quantitative reassessment based on plant fossils. Palaeogeography, Palaeoclimatology, Palaeoecology 295: 423-442.
34. Spicer RA, Parrish JT (1990) Latest Cretaceous woods of the central North Slope, Alaska. Palaeontology 33: 225-242.
35. Clemens WA, Nelms LG (1993) Paleoecological implications of Alaskan terrestrial vertebrate fauna in latest Cretaceous time at high paleolatitudes. Geology 21: 503-506.
36. Hotton III, N. (1980) An alternative to dinosaur endothermy. In: Thomas RDK, Olson EC, editors. A cold look at the warm-blooded dinosaurs. Boulder, CO.: Westview Press. pp. 311-350.
37. Spotila JR, O'connor MP, Dodson P, Paladino FV (1991) Hot and cold running dinosaurs: body size, metabolism and migration. Dinosaur Studies-Commemorating the 150th Anniversary of Richard Owen's Dinosauria: A Special Issue of the Journal Modern Geology 203-227.
38. Parrish JM, Parrish JT, Hutchison JH, Spicer RA (1987) Late Cretaceous vertebrate fossils from the North Slope of Alaska and implications for dinosaur ecology. Palaios 2: 377-389.

39. Fiorillo AR, Gangloff RA (2001) The caribou migration model for Arctic hadrosaurs (Dinosauria: Ornithischia): A reassessment. Historical Biology 15: 323-334.
40. Alexander RM (1989) Dynamics of dinosaurs and other extinct giants. New York: Columbia University Press. 167 p.
41. Bell PR, Snively E (2008) Polar dinosaurs on parade: a review of dinosaur migration. Alcheringa: An Australasian Journal of Palaeontology 32: 271-284.
42. Chinsamy A, Thomas DB, Tumarkin-Deratzian AR, Fiorillo AR (2012) Hadrosaurs were perennial polar residents. Evolutionary Biology 295: 610-614.
43. Barrick, R. E., Showers WJ, Fischer AG (1996) Comparison of thermoregulation of four ornithischian dinosaurs and a varanid lizard from the Cretaceous Two Medicine Formation: Evidence from oxygen isotopes. Palaios 11: 295-305.
44. Kolodny Y, Luz B, Sander M, Clemens WA (1996) Dinosaur bones: fossils or pseudomorphs? The pitfalls of physiology reconstruction from apatitic fossils. Palaeogeography, Palaeoclimatology, Palaeoecology 126: 161-171.
45. Sharp ZD, Atudorei V, Furrer H (2000) The effect of diagenesis on oxygen isotope ratios of biogenic phosphates. American Journal of Science 300: 222-237.
46. Chenery C, Trueman C, Spiro B, Eberth B (2001) Proof that stable isotope signals are altered during early diagenesis of bone apatite. Journal of Vertebrate Paleontology 21: 40A.
47. Hoppe KA, Koch PL, Furutani TT (2003) Assessing the preservation of biogenic strontium in fossil bones and tooth enamel. International Journal of Osteoarchaeology 13: 20-28.
48. Zazzo A, Lécuyer C, Mariotti A (2004) Experimentally-controlled carbon and oxygen isotope exchange between bioapatites and water under inorganic and microbially-mediated conditions. Geochimica et Cosmochimica Acta 68: 1-12.
49. Budd P, Montgomery J, Barreiro B, Thomas RG (2000) Differential diagenesis of strontium in archaeological human dental tissues. Applied Geochemistry 15: 687-694.

50. Zazzo A, Lécuyer C, Sheppard SMF, Grandjean P, Mariotti A (2004) Diagenesis and the reconstruction of paleoenvironments: A method to restore original ^{18}O values of carbonate and phosphate from fossil tooth enamel. Geochimica et Cosmochimica Acta 68: 2245-2258.
51. Fricke HC, Rogers RR, Gates TA (2009) Hadrosaurid migration: inferences based on stable isotope comparisons among Late Cretaceous dinosaur localities. Paleobiology 35: 270-288.
52. Fricke HC, Hencecroth J, ME. H (2011) Lowland-upland migration of sauropod dinosaurs during the Late Jurassic epoch. Nature 480: 513-515.
53. Suarez CA, Ludvigson GA, Gonzalez LA, Fiorillo AR, Flaig PP et al. (2013) Use of multiple oxygen isotope proxies for elucidating Arctic Cretaceous palaeo-hydrology. Geological Society, London, Special Publications 382: 185-202.
54. Little SA, Kembel SW, Wilf P (2010) Paleotemperature proxies from leaf fossils reinterpreted in light of evolutionary history. PLoS ONE 5: e15161.
55. Faure G, Powell JL (1972) Strontium isotope geology. New York: Springer-Verlag. 197 p.
56. Ericson JE (1985) Strontium isotope characterization in the study of prehistoric human ecology. Journal of Human Evolution 14: 503-514.
57. Bentley RA (2006) Strontium isotopes from the earth to the archaeological skeleton: a review. Journal of Archaeological Method and Theory 13: 135-187.
58. Hobson KA (1999) Tracing origins and migration of wildlife using stable isotopes: A review. Oecologia 120: 314-326.
59. Blum JD, Taliaferro EH, Weisse MT, Holmes RT (2000) Changes in Sr/Ca, Ba/Ca and $^{87}Sr/^{86}Sr$ ratios between trophic levels in two forest ecosystems in the northeastern U.S.A. Biogeochemistry 49: 87-101.
60. Hobson KA, Barnett-Johnson R, Cerling T (2010) Using isoscape to track animal migration. In: West JB, Bowen GJ, Dawson TE, Tu KP, editors. Isoscapes. Understanding Movement, Pattern, and Process on Earth through Isotope Mapping. New York: Springer. pp. 273-298.

61. Britton K, Grimes V, Dau J, Richards MP (2009) Reconstructing faunal migrations using intra-tooth sampling and strontium and oxygen isotope analyses: A case study of modern caribou (*Rangifer tarandus granti)*. Journal of Archaeological Science 36: 1163-1172.

62. Hoppe KA, Koch PL, Carlson RW, Webb SD (1999) Tracking mammoths and mastodons: Reconstruction of migratory behavior using strontium isotope ratios. Geology 27: 439-442.

63. Koch PL, Halliday AN, Wakter LM, Stearley RF, Huston TJ et al. (1992) Sr isotopic composition of hydroxyapatite from recent and fossil salmon: the record of lifetime migration and diagenesis. Earth and Planetary Science Letters 108: 277-287.

64. Simonetti A, Buzon MR, Creaser RA (2008) In-situ elemental and Sr isotope investigation of human tooth enamel by laser ablation-(MC)-ICP-MS: successes and pitfalls. Archaeometry 50: 371-385.

65. Copeland SR, Sponheimer M, Le Roux PJ, Grimes V, Lee-Thorp JA et al. (2008) Strontium isotope ratios ($^{87}Sr/^{86}Sr$) of tooth enamel: a comparison of solution and laser ablation multicollector inductively coupled plasma mass spectrometry methods. Rapid Communications in Mass Spectrometry 22: 3187-3194.

66. Richards M, Harvati K, Grimes V, Smith C, Smith T et al. (2008) Strontium isotope evidence of Neanderthal mobility at the site of Lakonis, Greece using laser-ablation PIMMS. Journal of Archaeological Science 35: 1251-1256.

67. Copeland SR, Sponheimer M, Lee-Thorp JA, Le Roux PJ, De Ruiter DJ et al. (2010) Strontium isotope ratios in fossil teeth from South Africa: Assessing laser ablation MC-ICP-MS analysis and the extent of diagenesis. Journal of Archaeological Science 37: 1437-1446.

68. Britton K, Grimes V, Niven L, Steele TE, McPherron S (2011) Strontium isotope evidence for migration in late Pleistocene *Rangifer*: Implications for Neanderthal hunting strategies at the Middle Palaeolithic site of Jonzac, France. Journal of human evolution 61: 176-185.

69. Copeland SR, Sponheimer M, de Ruiter DJ, Lee-Thorp JA, Codron D et al. (2011) Strontium isotope evidence for landscape use by early hominins. Nature 474: 76-78.
70. Irrgehera J, Teschler-Nicolab M, Katrin L, Christopher W, Daniela K et al. (2012) Migration and mobility in the latest Neolithic of the Traisen Valley, Lower Austria: Sr isotope analysis. In: Kaiser E, Burger J, Schier W, editors. Population Dynamics in Prehistory and Early History. New Approaches by Using Stable Isotopes and Genetics. Berlin, Germany: De Gruyter. pp. 199-211.
71. Cameron NE, Balks M, Littler RA, Manley-Harris M, Te Awekotuku N (2012) An investigation by LA-ICP-MS of possum tooth enamel as a model for identifying childhood geographical locations of historical and archaeological human from New Zealand. Journal of Pacific Archaeology 3: 49-58.
72. Heaman LM (2012) In situ geochemical, Sr isotope and U-Pb dating of dinosaur bone: A record of fossilization and fluid-flow history in the San Juan Basin, New Mexico. Geological Society of America Abstracts with Programs 44: 86.
73. Lambe ML (1920) The Hadrosaur *Edmontosaurus* from the Upper Cretaceous of Alberta. Canada Geological Survey Memoir 120: 1-79.
74. Horner JR (1983) Cranial osteology and morphology of the type specimen of *Maiasaura peeblesorum* (Ornithischia: Hadrosauridae), with discussion of its phylogenetic position. Journal of Vertebrate Paleontology 3: 29-38.
75. Cate T (1985) Oral histology: Development, structure and function. St. Louis, MO.: Mosby. 400 p.
76. Erickson GM (1996) Incremental lines of von Ebner in dinosaurs and the assessment of tooth replacement rates using growth line counts. Proceedings of the National Academy of Sciences of the United States of America 93: 1463-14627.
77. Erickson GM (1996) Daily deposition of dentine in juvenile *Alligator* and assessment of tooth replacement rates using incremental line counts. Journal of Morphology 228: 189-194.
78. Hwang SH (2009) The utility of tooth enamel microstructure in identifying isolated dinosaur teeth. Lethaia 43: 307-322.

79. Underwood EJ (1977) Trace elements in human and animal nutrition. fourth edition. London, UK: Academic Press. 545 p.
80. Montgomery J, Budd P, Cox A, Krause P, Thomas RG (1999) LA-ICP-MS evidence for the distribution of Pb and Sr in Romano-British, medieval and modern human teeth: implications for life history and exposure reconstruction. In: Young SMM, Pollard AM, Budd P, Ixer RA, editors. Metals in Antiquity: Proceedings of the International Symposium, Harvard University. Oxford, UK: Archaeopress. pp. 290-296.
81. Fricke HC, Pearson DA (2008) Stable isotope evidence for changes in dietary niche partitioning among hadrosaurian and ceratopsian dinosaurs of the Hell Creek Formation, North Dakota. Paleobiology 34: 534-552.
82. Fricke HC, Rogers RR, Backlund R, Dwyer CN, Echt S (2008) Preservation of primary stable isotope signals in dinosaur remains, and environmental gradients of the Late Cretaceous of Montana and Alberta. Palaeogeography, Palaeoclimatology, Palaeoecology 266: 13-27.
83. Trinkel M, Fleischmann PH, Steindorfer AF, Kastberger G (2004) Spotted hyenas (*Crocuta crocuta*) follow migratory prey. Seasonal expansion of a clan territory in Etosha, Namibia. Journal of Zoology 264: 125-133.
84. Keller K, Blum JD, Kling GW (2007) Geochemistry of soils and streams on surfaces of varying ages in arctic Alaska. Arctic, Antarctic, and Alpine Research 39: 84-98.
85. Blakey RC (2009) Paleogeography and geologic evolution of North America. Available: http://cpgeosystems.com/nam.html.

Conclusion

In this thesis, I studied the osteology and ecology of the most common dinosaur taxon from the Prince Creek Formation, *Edmontosaurus* sp. nov. and drew following conclusions:

1) The primary purpose of this research is to determine the taxonomic status of the PCF hadrosaurid. I tested this using three semi-independent methods and discovered it is not referable to other known species of *Edmontosaurus.* The methods used here will be employed in future studies of other juvenile materials. For example, this is the first time that hypothetical growth lines have been used. The reliability of this method should be tested in future studies.
2) The PCF hadrosaur represents a new species of *Edmontosaurus*. Notably, it differs from other species of *Edmontosaurus* in that its postorbital lacks a pocket, and the circumnarial septum projects posterolaterally, rather than being fan-shaped, as in other species of *Edmontosaurus*. No clear-cut autapomorphy of the new PCF *Edmontosaurus* is discovered, likely because it is too immature.
3) In the cladistic analyses, the Alaskan edmontosaur was consistently recovered as the sister taxon of *Edmontosaurus regalis* + *E. annectens*. *Shantungosaurus* and *Kundurosaurus* are recovered as the successive, basal sister taxa of *Edmontosaurus*, which are known from eastern Eurasia. This suggests a possible biogeographic scenario in which the common ancestor of *Edmontosaurus* and *Shantungosaurus* originated in eastern Eurasia and then dispersed by the Campanian to North America via a land corridor in the area of present day Alaska.
4) The recognition of a new Alaskan species from a separate lineage of *Edmontosaurus* lends further support for the occurrence of a unique, early Maastrichtian polar Alaskan fauna, known as the Paaŋaqtat Province.

5) The description of the PCF *Edmontosaurus* represents one of the most detailed descriptions of North American hadrosaurs known. It is also significant in that it describes the smallest individuals of *Edmontosaurus* known, which will benefit future ontogenetic studies of hadrosaurids in general.

6) LA-MC-ICP-MS measurement of PCF *Edmontosaurus* and *Troodon* tooth enamel shows reliable strontium signals. The values indicate that *Edmontosaurus* did not migrate during the last approximately four months prior to death. These results, coupled with the discovery that the Alaskan *Edmontosaurus* represents a new species that is not found at lower latitudes, provide strong support for the hypothesis that this taxon overwintered at the northern end of Laramidia. The oxygen isotope analysis of the PCF teeth materials is now underway and will be presented in a future paper.